University of London

Imperial College of Science, Technology and Medicine

THE ASSESSMENT OF WELD DEFECTS IN OFFSHORE STRUCTURES

by

IOANNIS SAVVAS KOUNTOURIS

A thesis submitted for the degree of Doctor of Philosophy in the Faculty of Engineering of the University of London and the Diploma of Imperial College

Engineering Structures Section

Civil Engineering Department

May 1989

With the exception of section 1.3, the entire work is dedicated to my wife

CORRECTIONS

Page no	Line no	Error	Correction
4	18	parametrs	parameters
7	31	frature	fracture
16	13	reliablity	reliability
18	21	parametr	parameter
20	12	3.1.20	1.3.20
20	16	α	a
21	12	3.1.20	1.3.20
21	14	3.1.20	1.3.20
22	21	of	or
23	29	meaurements	measurements
24	35	which it	which
27	8	varibles	variables
28	28	form	from
29	28	gien	given
30	5	accoustic	acoustic
31	1	shunts	shuts
34	12	reinspectd	reinspected
34	21	necesary	necessary
36	6	respeectively	respectively
40	15	diaxide	dioxide
42	3	Group W6	Group W5
43	6	Group W5	Group W6
53	3	is	are
60	6	ultronic	ultrasonic
85	33	conclusions	conclusion
86	19	defecct	defect
89	3	dfective	defective
89	17	SMAW position	Weld Type
109	7	numebr	number
110	2	Joing	Joint
113	3	dependance	dependence
141	27	appopriate	appropriate
147	11	Kilmogovov	Kolmogorov
160	3	parametrised	parameterised
161	26	rasonably	reasonably
174	middle table	LT	L1
188	4	distriutions	distributions
188	9	extrme	extreme
188	16	thw	the
191	4	ultrasonice	ultrasonics
233	24	efects	defects
236	7	n_i	r_i
257	22	3.2.4.1 to 3.2.4.5	6.2.2.1 to 6.2.2.5
270	5	105	10.5
275	11	respect	respects
279	20	effeciencies	efficiencies

TABLE OF CONTENTS

ABSTRACT 7

ACKNOWLEDGEMENTS 8

NOTATION 9

ABBREVIATIONS 10

CHAPTER 1: INTRODUCTION 12

1.1 General Remarks 12
1.2 Overview of Weld Defect Assessment 14
1.3 Reliability Methodology as Applied to Fracture Mechanics 16
1.4 Overview of Data Analysis and Statistical Problems 22
1.5 Layout of Thesis 28

CHAPTER 2: REVIEW OF METHODS OF NON-DESTRUCTIVE EXAMINATION FOR WELDS 29

2.1 General 29
2.2 Ultrasonic Testing 29
2.3 Magnetic Particle Inspection 31
2.4 Reliability of Non-Destructive Evaluation 32

CHAPTER 3: DESCRIPTION OF VARIOUS PARAMETRS USED IN THE ANALYSIS 34

3.1 Description of the Structure 35
3.2 Weld Joint Type 36
3.3 Defect Type 37
3.4 Welding Process 38
3.5 Original Welding Procedure 41
3.6 Other Parameters 41

CHAPTER 4: DEFECT OCCURRENCE 49

4.1 Statistical Theory 49
4.1.1 Analysis of Binary Data 49
4.1.2 Analysis of Ordered Categorical Data 51
4.1.3 Tests of Independence in rxs Frequency Tables 52
4.2 Defect Characteristics 53
4.3 Description of Analysis 54

4.4 Overall Two-way Analysis based on Global Location and Weld Joint Type 60
4.4.1 Defect Rates 60
4.4.2 Multiple Defects 63
4.4.3 Defect Types 74

4.5 Detailed Analysis According to Parameters of Influence 77
4.5.1 Defect Rates 77
4.5.2 Binary Analysis 87
4.5.2.1 Embedded Defects found by Ultrasonics 88
4.5.2.2 Surface-breaking Defects found by Magnetic Particle Testing 100
4.5.3 Multiple Defects 102
4.5.4 Defect Types 109
4.5.4.1 Cruciform and Tee Butt Joints 109
4.5.4.2 Plate Butt Joints 122
4.6 Conclusions 124

CHAPTER 5: DISTRIBUTION OF DEFECT SIZES 132

5.1 Statistical Theory 132
5.1.1 Choice of Distribution Models 132
5.1.1.1 Normal Distribution 132
5.1.1.2 Exponential Distribution 134
5.1.1.3 Gamma Distribution 135
5.1.1.4 Lognormal Distribution 137
5.1.1.5 Weibull Distribution 141
5.1.2 Distribution Fitting 143
5.1.2.1 Lognormal Distribution 144
5.1.2.2 Weibull Distribution 147
5.1.2.3 Uniform Distribution 150
5.1.2.4 Goodness-of-Fit Statistic 152
5.1.3 Correlation Coefficient 152
5.2 Literature Review 155
5.3 Surface-breaking Defects 158
5.3.1 Defect Location 159
5.3.2 Surface-breaking Toe Defects in Continuous Members 161
5.3.3 Surface-breaking Weld Defects 170
5.3.4 Surface-breaking Toe Defects in Abutting Members 178

5.3.5 Correlation between Defect Depth and Defect Length 178
5.3.6 Conclusions 186
5.3.7 Comparisons with other Published Data 187
5.4 Embedded Defects 191
5.4.1 Defect Characteristics 191
5.4.2 Defect Width 192
5.4.3 Defect Length 208
5.4.4 Defect Aspect Ratio 223
5.4.5 Correlations between Defect Width and Defect Length 229
5.4.6 Comparisons and Conclusions 229

CHAPTER 6: PROBABILISTIC MODELS FOR DEFECT DETECTION AND SIZING 236

6.1 Statistical Theory 236
6.1.1 Binomial Distribution 236
6.1.2 Binary Regression Models 238
6.2 Detection Efficiencies 241
6.2.1 Literature Review 242
6.2.2 Applications of Binary Regression Models 250
6.2.3 Discussion 257
6.2 Defect Sizing 268
6.3.1 Literature Review 268
6.3.2 Analysis of Data on Fatigue Cracks in Tubular Welded Joints 270
6.3.3 Discussion 273

CHAPTER 7: CONCLUSIONS 275

REFERENCES 282

ABSTRACT

The thesis provides a critical review of the occurrence and sizes of defects in welded joints in steel structures, and reviews the methods of non-destructive evaluation. In particular a detailed statistical analysis of the weld defect data base obtained from the Hutton tension leg platform has been undertaken. Suitable spatial and defect size distributions both for surface-breaking and embedded defects have been established and compared with distributions obtained from other structures. Special attention has been focussed on explaining variations in defect sizes under the influence of a number of factors such as the position of the welded joint in the structure, the position of the defect in the weld, the type of defect, the type of welded joint, the welding process, etc. Analysis has been undertaken of defect depth (or width), length, aspect ratio and in some cases defect orientation. Correlations between defect depth (or width) and length have also been examined. Suitable analyses were also undertaken to determine defect rates, the occurrence of multiple defects, the proportion of welds found defective and the frequency of occurrence of various defect types. In each case the contribution from various welding and location parameters has been established.

Also included in this thesis is an appraisal of the reliability of various non-destructive testing techniques. Current detection models and uncertainties in sizing are critically reviewed and new generalised models are proposed for use in up-dating defect size and occurrence distributions. Three new generalised models of sigmoidal shape have been proposed which have the capability of accommodating a large number of variables such as defect length, defect depth, defect width, defect area, plate thickness, recording level, etc. The three models are based on the binomial distribution and the methods of estimating the parameters are based on maximum likelihood estimation, for which the goodness-of-fit statistic (deviance) is completely determined. These models have been applied and compared with existing models currently in use, by using data derived from pressure vessel reliability programmes. Sizing errors using magnetic particle inspection have been assessed using data from surface-breaking fatigue cracks in tubular joints typical of offshore structures. It is anticipated that the results from the work will be of value in frature mechanics formulations, will serve as prior information on Bayesian quality control schemes for future inspections and finally will assist in the improvement of the performance of various NDE techniques currently in use in the offshore industry.

ACKNOWLEDGEMENTS

On completion of this work I would like to express my DEEPEST GRATITUDE equally to Professor A. Atchinson, Professor Sir D. Cox and Mrs. J. Snell for their constructive comments and advice on the statistical analysis of data.

My thanks go also to Mr. M.J. Baker who provided sufficient funds for the major part of my studies. I am also grateful to him for comments and advice throughout the entire work. His remarks on reading the first draft of the thesis are deeply appreciated.

I would also like to thank Conoco U.K. for funding part of the research and for their permission to make the data available for this study.

My thanks go also to Mrs. S. Wright for an exceptional typing work.

For the past few years I have enjoyed the company of many friends whom I wish to thank. Especially I would like to mention Mr. Wendy Aritenang with whom I had useful discussions over the past years.

NOTATION

As far as possible, where referenced relationships are quoted, the author's original notation has been retained. Many variables are therefore defined locally in the text to avoid confusion. The global notation used in this work is as follows:

a	defect length in the direction of welding
E[]	expected value of the random variable in brackets
D_n	deviance statistic with n degrees of freedom
$f_X(x)$	probability density function of random variable X at x
$F_X(x)$	cumulative distribution function of random variable evaluated at x
g_1	coefficient of skewness
g_2	coefficient of kurtosis
ℓn	natural logarithm
P[]	probability of the event in brackets
$P_{DN}(x)$	probability of detecting a defect of dimension x
$P_{ND}(x)$	probability of not detecting a defect of dimension x
r	correlation coefficient
r.m.s	root mean square value
SE	standard error
t_n	student's t distribution with n degrees of freedom
z	defect depth
α	scale parameter of Weibull distribution
β	shape parameter of Weibull distribution
γ	location parameter of Weibull distribution
ϵ	defect aspect ratio taken as the ratio of defect length to defect depth or defect width
μ	mean of normal distribution
σ^2	variance of normal distribution
χ^2_n	chi-square statistic with n degrees of freedom
$N(\mu,\sigma^2)$	normal distribution with parameters μ and σ^2
$\Lambda(\mu,\sigma^2)$	lognormal distribution with parameters μ and σ^2

ABBREVIATIONS

ASME	American Society of Mechanical Engineers
ASTM	American Society of Testing and Materials
B	Plate Butt Weld Joint
CDF	Cumulative Distribution Function
COV	Coefficient of Variation
CR	Crack-like Defect
DAC	Distance Amplitude Correction
GMAW	Gas Metal Arc Welding
IIW	International Institute of Welding
IP	Incomplete Penetration Defect
KST	Kolmogorov Smirnov Test
LI	Linear Indication Defect
L1	Depth of defect as measured at right angles to the surface of the continuous member
L3	Depth of defect as measured at right angles to the surface of the abutting member
LW	Depth of defect as measured at right angles to the surface of the weld surface
MPI	Magnetic Particle Inspection
NDE	Non-Destructive Examination
NF	Non-Fusion Defect
PDF	Probability Density Function
PISC	Plate Inspection Steering Committee
PO	Porosity Defect
PVRC	Pressure Vessel Research Committee
PWR	Pressurised Water Reactor
SAW	Submerged Arc Welding
SL	Slag Inclusion Defect
SMAW	Shielded Metal Arc Welding
ST(STC)	Surface-Breaking Toe Defect - Continuous Member
STA	Surface-Breaking Toe Defect - Abutting Member
SW(SWC)	Surface-Breaking Weld Defect
T	Tee Butt Weld Joint
TLP	Tension Leg Platform
UT	Ultrasonic Testing
UKAEA	United Kingdom Atomic Energy Authority
WI	Welding Institute
X	Cruciform Weld Joint

XT	Cruciform and Tee Butt Weld Joints taken together
1G	Flat Welding Position
2G	Horizontal Welding Position
3G	Vertical Welding Position
4G	Overhead Welding Position

CHAPTER 1

INTRODUCTION

1.1 General Remarks

The presence of both surface-breaking and embedded defects in the welds of offshore structures may lead to fatigue cracking and eventual fracture. Knowledge of the spatial and defect size distributions for defects of different types and sizes and in different positions in the weld are of importance in determining the probability of failure during the required design life of the structure. Thus the risk of failure of a welded structure by fatigue and fracture depends to a large extent on the number, size and type of weld defects which remain in the structure following fabrication. Other factors, such as the lifetime distributions of stress range, peak stresses, residual stresses, material toughness, etc., are also important but will not be discussed here.

The important regions of welded structures are generally subjected to some form of non-destructive evaluation (NDE) immediately following fabrication and, depending on the specification and design criteria, all or some of the weld defects that are found are repaired before the structure enters service. However, because NDE techniques and NDE operators are not 100% reliable, some defects escape detection and remain in the structure. Therefore of equal considerable interest is the effect of various standards of non-destructive evaluation on the final defect rates. Knowledge of likely defect occurrence for different types of welded joints and welding processes provides some of the information necessary to determine optimal strategies for NDE during fabrication.

The need for a rational procedure for the assessment of weld defects occurs with many types of structures but was very apparent during the fabrication of the Conoco Hutton Tension Leg Platform (TLP) (see Fig. 1.1), when weld defects of an unacceptable size were discovered at a late stage in the final assembly of the Lower Hull from its pre-fabricated components. Part of this thesis describes the work undertaken and the results obtained from the assessment of defect data relating to the welds in the Lower Hull of the Hutton TLP, for use in probabilistic fracture mechanics analysis. The remainder of this work concentrates on the reliability of non-destructive examination procedures, mainly ultrasonic testing (UT) and magnetic particle inspection (MPI). Both parts are important in the revision of NDE procedures for future structures.

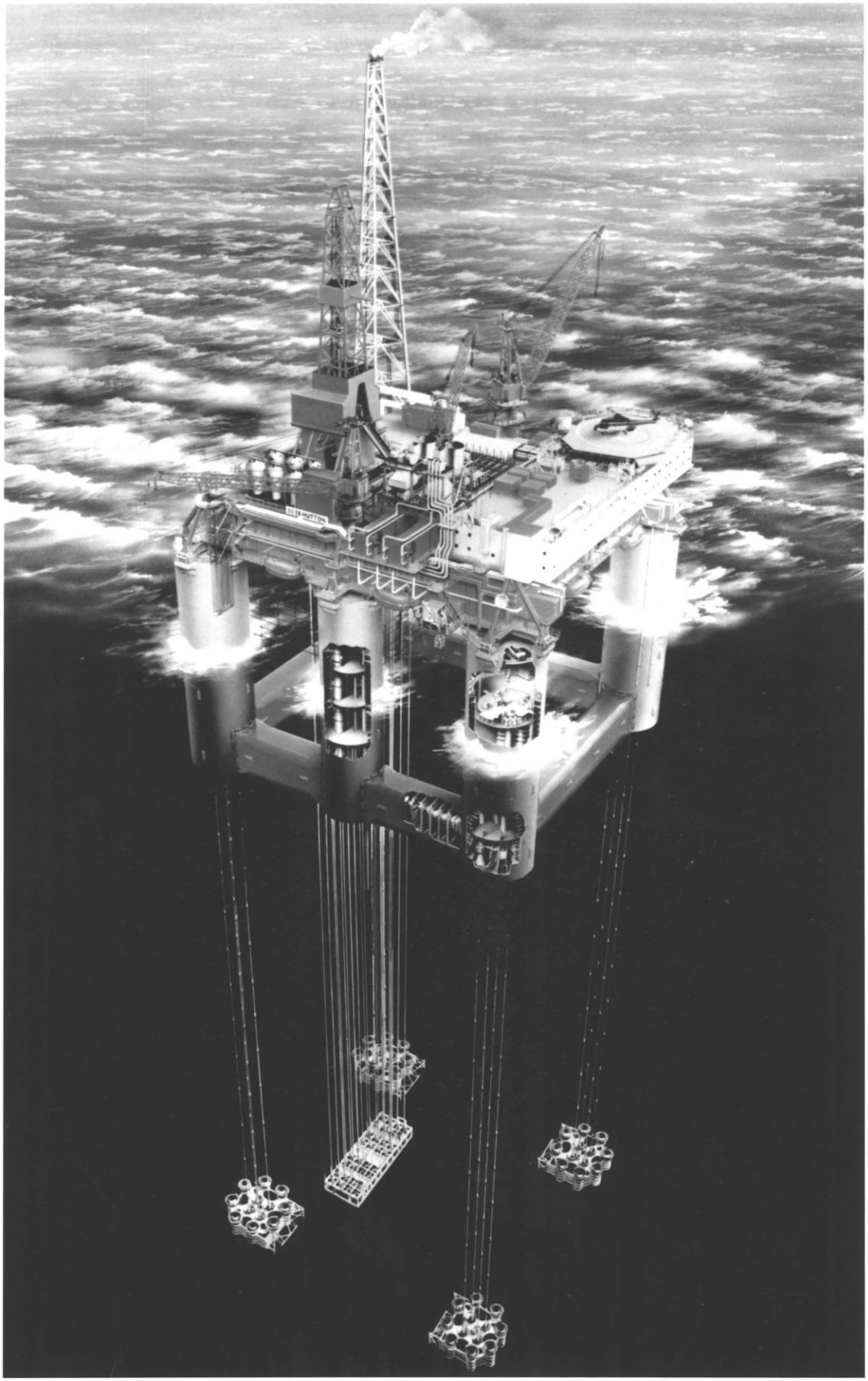


Fig 1.1 The Hutton Tension Leg Platform

1.2 Overview of Weld Defect Assessment

The significance of defects in welds depends on the function that the weld will perform and is governed by a number of parameters such as shape, size, type and their distribution and orientation within the weld. The actual sizes of defects are a function of the interaction of a large number of variables such as welding process, welding procedure, welding position, performance of individual welders, etc. Many of these quantities cannot be controlled to the desired extent and consequently exact predictions of defect sizes cannot be made. These uncertainties thus suggest a statistical approach to the expected sizes of defects.

The occurrence of defects in welds has received particular attention over the recent years in both the offshore and nuclear industries. Both the size and spatial distributions of defects are of primary importance in understanding the question of structural integrity. This is so because to be able to understand the question of structural integrity it is necessary to understand the factors which affect the occurrence and sizes of defects. These may include the type of welded joint, fabricator, welding process, welding position, welding procedure, individual welders, length of the weld etc. The relative contributions from many of these factors are very often unknown. Even when they are known, they often cannot be controlled as desired and their nature is sometimes too complicated to approach in a deterministic way. A probabilistic approach to the treatment of defect occurrence and sizing is therefore suggested.

Equally important is the reliability of non-destructive examination devices. This is assessed by the probability of correctly detecting and sizing defects. The better an NDE device is, the higher will be the probability that it will correctly detect defects and measure their sizes. To be able to estimate the number of defects present in a structure one must be able to model these detection and sizing uncertainties, and subsequently account for undetected defects and incorrect measurements. The probability distributions of measured sizes are then adjusted according to the calibration error and in turn weighted by the detection model to account for the possibility of missing existing defects.

Although the spatial distribution of defects in a structure entering service is important from the quality control point of view, the defect sizes are of importance in determining the probability of failure during the required design life of the structure. The methodology of undertaking an integrity analysis of a cracked structural component includes:

(1) fracture mechanics to determine the critical state of a cracked component

(2) fatigue crack growth using fracture mechanics to determine the crack size at any time

(3) random loading analysis to provide the input cyclic loading or extreme loading

(4) statistical modelling of each of the input variables from past experience and data

(5) efficient and accurate reliability analysis to determine the probability of failure.

When applying reliability theory to assess the significance of weld defects, one has to undertake at least the following tasks:

(a) to understand the concept of reliability theory for practical and theoretical problems

(b) to understand the physical phenomena of fatigue and fracture

(c) to identify basic statistical variables in the failure function

(d) to determine defect rates in welds depending on fabricator, type of welded joint, welding process, welding procedure, welding position and where possible individual welder

(e) to determine the occurrence of multiple defects in welds under the above conditions

(f) to perform an analysis on the relative frequency of different defect types

(g) to analyse the dimensions (length, depth, orientation and position) of defects and to fit probability distributions to these data

(h) to assess the reliability of individual NDE operators and the reliability of NDE techniques in general

(i) to apply the techniques of probabilistic fracture mechanics in order to assess the significance of different sizes of defects in terms of the probability of failure by fatigue and fracture for welds with different geometries. One way of

performing such an analysis would be to make use of the Paris Law with appropriate threshold effects in order to govern the growth of defects from their initial size. This could be followed by the application, for example, of the CEGB R6 procedure to assess the criticality of the enlarged defect to random peak stress [1].

1.3 Reliability Methodology as Applied to Fracture Mechanics

General

A general review of structural reliability theory is beyond the scope of the present work, and the reader who is unfamiliar with this field is referred to the general literature - for example see Thoft-Christensen and Baker [2] or Madsen et al [3]. Statistical reliability theory is not considered in depth in this thesis, but the data analysis that has been undertaken provides important information for later reliability studies. For this reason, the following information on reliablity methodology as applied to fracture mechanics is included. The remainder of this section is based on notes prepared by Mr. M.J. Baker for a short course given in 1985.

In principle, if the reliability problem is set up in terms of random variables then it is possible to define a safety margin M which is a deterministic function of the normal (design) input parameters $\underline{X}$ such that

$$M = g(\underline{X}) \leq 0 \qquad 1.3.1$$

corresponds to the unsafe state against which the structure is being designed. The reliability of the component is then defined as

$$P_s = 1 - P_f = 1 - P(M \leq 0) \qquad 1.3.2$$

where P_f is the failure probability in a specified reference period.

The assessment of the component reliability then consists of three steps:

- selecting a suitable form for the safety margin equation $g(\underline{X})$
- selecting suitable probability distributions for the input parameters $\underline{X}$
- evaluating the probability $P(g(\underline{X}) \leq 0)$

For many reliability problems, including those discussed here, the last step can be undertaken easily using so-called first order reliability methods [2] and will not be

discussed in detail here. In principle, the method works by mapping the (n-1) dimensional surface defined by setting $g(\underline{X}) = 0$ into an n-dimensional unit standard normal space (i.e. one in which the variables are all normally distributed with zero mean and unit standard deviation). The closest distance from the origin to this new surface is termed the reliability index β which is related to P_f by

$$P_f \approx \Phi(-\beta) \qquad 1.3.3$$

where Φ is the standard normal distribution function.

Furthermore, the coordinates of the closest point when mapped back to the space of the original variables give the values of the variables most likely to be associated with failure of the structure (this statement is only approximate for non-normal variables). The values are often referred to as the 'design values' of the variables and the point is referred to as the 'design point'.

The coordinates of the closest point in a standard normal space also allow a set of sensitivity factors $\underline{\alpha}$ to be defined which indicate the relative importance of each of the variables with regard to their influence on the probability of failure. The sensitivity factors are such that

$$\sum_{i=1}^{n} \alpha_i^2 = 1 \qquad 1.3.4$$

and with low α_i indicating low sensitivity.

The S-N Approach

The most commonly used model for fatigue behaviour under constant amplitude loading is the linear logarithmic model

$$N_i S_i^m = K \qquad 1.3.5$$

where N_i is the number of cycles to failure, S_i is the range of applied stress and m and K are selected constants. Hence, failure can be assumed to occur when the number of cycles n is such that the damage D defined by

$$D = nS_i^m/K \qquad 1.3.6$$

exceeds unity. Furthermore, using Miner's rule it is also assumed that the damage D_1 due to one cycle of stress range S_i is given by

$$D_1 = S_i^m/K \qquad 1.3.7$$

and the total damage is

$$D = \left[\frac{1}{K}\right] \sum_{i=1}^{N} S_i^m \qquad 1.3.8$$

For normal design purposes, m and K are chosen to give a curve which is a conservative lower bound on the relevant test data or a selected number of standard deviations below the mean curve. However, for the purposes of reliability assessment, m and K need to be considered as random variables to allow for the large scatter in the number of cycles to failure experienced in practice; and a model uncertainty needs to be introduced into equation 1.3.8 to allow for the fact that the Miner's rule summation is subject to uncertainty.

The safety margin M (equation 1.3.1) may now be expressed as

$$M_1 = N - N_0 \qquad 1.3.9$$

where N is the number of cycles of stress to cause failure and N_0 is the required number to achieve a given design life, or as

$$M_2 = (\text{actual life}) - (\text{required life}) = L_a - L_r \qquad 1.3.10$$

The reliability is thus

$$P_S = 1 - P(M_1 \leq 0) = 1 - P(M_2 \leq 0) \qquad 1.3.11$$

Provided that M can be expressed in a suitable form, the techniques of first order reliability analysis can be used to evaluate P_S.

For example, as shown by Wirsching [4], Manners [5] and others, for offshore structures where the long-term distribution of wave height can be assumed to have a two-parameter Weibull distribution

$$F_H(h) = 1 - \exp(-(h/c)^{\alpha}) \qquad 1.3.12$$

and when the stress spectrum is narrow-banded and the structure is dynamically insensitive so that the stress range is closely related to wave height by

$$S = bH \qquad 1.3.13$$

where b is a constant, then from equation 1.3.7 the damage caused by one cycle of random wave height H is given by

$$D_1 = (bH)^m/K \qquad 1.3.14$$

and the expected damage per cycle is

$$E[D_1] = \int_0^{\infty} (bh)^m/K \; f_H(h)\,dh$$

$$= (bc)^m/K \; \Gamma(1 + m/\alpha) \qquad 1.3.15$$

If n is the number of stress cycles per year and X_m is the model uncertainty in the operation of Miner's rule, the actual life will be

$$L_a = \frac{X_m K}{n(bc)^m \Gamma(1 + m/\alpha)} \qquad 1.3.16$$

and the safety margin is

$$M = \frac{X_m K}{n(bc)^m \Gamma(1 + m/\alpha)} - L_r \qquad 1.3.17$$

It should be noted that equation 1.3.15 gives the expected damage per cycle. However, because there are a large number of cycles per year, the scatter in the amount of damage from cycle to cycle does not affect the annual damage rate which can be obtained by multiplying the expected damage per cycle by the number of cycles per year. The uncertainty in the safety margin M results from uncertainties in the parameters X_m, K and m. In other words, the expected damage per cycle given by equation 1.3.15 is a conditional expectation.

No restrictions are placed on the distributions of X_m, K and m; but if it is assumed that they are lognormal, then a new safety margin M' may be defined as

$$M' = \frac{X_m K}{L_r^n (bc)^m \Gamma(1 + m/\alpha)} \qquad 1.3.18$$

where M' is also a lognormal variable so that

$$P_s = 1 - P(M' \leq 1) = 1 - P(\ell n\, M' \leq 0) \qquad 1.3.19$$

Analytical solutions can also be obtained for certain other long-term distributions of wave height.

In the case of dynamically sensitive offshore structures, some of the above assumptions do not apply and it is necessary to resort to spectral analysis of the structure's response to wave loading - see [6].

Crack Growth

Assuming the crack growth from a surface defect in a weld toe is governed by linear elastic fracture mechanics, the Paris law gives

$$\frac{da}{dN} = C(\Delta K)^m \qquad 1.3.20$$

where

$\frac{da}{dN}$ is the rate of crack growth

a is the current crack or defect size

ΔK is the range of stress intensity factor at the crack tip

C and m are crack growth parameters.

In normal fracture mechanics calculations C and m are taken to be constants but in a reliability analysis they need to be treated as uncertain quantities.

The range of stress factor, ΔK, is related to the normalised stress intensity factor, Y, by

$$\Delta K = Y\Delta\sigma\sqrt{\pi a} \qquad 1.3.21$$

where $\Delta\sigma$ is the range of applied stress.

Equation 3.1.20 may therefore be re-written as

$$\frac{da}{dN} = C(Y\Delta\sigma\sqrt{\pi a})^m \qquad 1.3.22$$

For the special conditions where

(i) the stress range $\Delta\sigma$ is constant

(ii) Y is independent of α

Equation 3.1.22 gives

$$\int_{\alpha_o}^{\alpha_N} a^{-m/2}da = \int_{o}^{N} CY^m(\Delta\sigma)^m\pi^{m/2}dn \qquad 1.3.23$$

Yielding, for $m \neq 2$

$$\alpha_N^{(2-m)/2} = \alpha_o^{(2-m)/2} + \frac{2-m}{2} CY^m(\Delta\sigma)^m\pi^{m/2}N \qquad 1.3.24$$

or

$$\alpha_N = \left[\alpha_o^{(2-m)/2} + \frac{2-m}{2} CY^m(\Delta\sigma)^m\pi^{m/2}N\right]^{2/(2-m)} \qquad 1.3.25$$

where α_o is the initial crack size

and α_N is the crack size after N cycles of applied stress.

However, in most situations neither of the above special conditions is met. The welded joints are subjected to a number of widely differing stress ranges, but more seriously, the normalised stress intensity factor varies considerably with crack size. Hence Y must be expressed as

$$Y = Y(\alpha) \qquad 1.3.26$$

with the result that α_N cannot be obtained in closed form. However, for each given weld geometry and joint type, $Y(\alpha)$ may be obtained for a range of normalised crack sizes α/b (where b is the plate thickness) by detailed finite element modelling of the weld region - see [8].

A further constraint is that crack growth does not occur, and hence equation 3.1.20 does not apply, below a threshold value of ΔK, ΔK_{th}. For example the threshold effect can be modelled by a variable high pass filter F such that equaiton 3.1.20 becomes

$$\frac{da}{dN} = FC(Y\Delta\sigma\sqrt{\pi\alpha})^m \qquad 1.3.27$$

with

$$\left.\begin{aligned} F &= 0 && \text{for } \Delta K \leq \Delta K_{th} \\ F &= \frac{(\Delta K-\Delta K_{th})}{(\Delta K_u-\Delta K_{th})} && \text{for } \Delta K_{th} \leq \Delta K \leq \Delta K_u \\ F &= 1 && \text{for } \Delta K_u \leq \Delta K \end{aligned}\right\} \qquad 1.3.28$$

and with $\Delta K_{th} = 50$ N/mm$^{3/2}$

and ΔK_u normally distributed with a mean of 90 N/mm$^{3/2}$.

For numerical calculations, an iterative algorithm is used - see [7].

1.4 Overview of Data Analysis and Statistical Problems

For the benefit of readers not familiar with statistical methodology the following section covering various aspects of statistical data analysis is included here. More detailed information is given in later chapters.

The first step in a statistical analysis is to examine the data for errors. Checks of data quality are of primary importance especially when dealing with a large data base. Such checks usually involve:

(1) Visual or computerised inspection of the data to check for values which are inconsistent with the ranges likely to occur for the various variables.

(2) Examination of frequency distributions of the major variables to look for inconsistent observations.

(3) Scatter plots are a good way to display unusual cases or outliers, for example to show whether or not the length of a defect is higher than the actual linear length of the weld. A scatter plot of these two variables will show if the data coding is mistakenly reversed for some cases.

(4) Very often the data recorded are not complete and some values may be missing. These missing values are usually left blank or coded by a special code. This is important because missing values and unusually extreme values that appear to be incorrect should be treated appropriately and not entered as real values in any analysis.

(5) Examination of the methods that have been used for collecting the data to discover whether or not certain sources give rise to biases in the measurements.

The raw material of all statistical investigations consists of individual observations, and these have to be summarized and screened in some way before any use can be made of them. It is understood that the aim of statistical methods goes beyond the simple presentation of data to include the drawing of inferences from them. However these two aspects – description and inference – cannot be separated.

It is important to distinguish between the two types of observation, that is qualitative and quantitative; the former being those which are not characterized by a numerical quantity. The problem is summarizing qualitative data is relatively simple. The main aim is to count the numbers of observations in the various categories of combination

of categories and probably express them as row, columns or overall percentages. This cross tabulation, as it is usually termed, helps in preliminary tests of whether rows are independent of columns. Multiway frequency tables with appropriate percentages usually provide useful information prior to formal fit of log-linear models. A particularly important type of qualitative observation is that in which a certain attribute is either absent or present. Such data are usually called binary data.

The problems of summarizing quantitative data in which the observations are numerical quantities are usually not straightforward. It is useful to subdivide such observations into discrete and continuous measurements. A useful initial step of summarizing a large collection of quantitative data is the formation of a frequency distribution. That is a table showing the number of observations, or frequency, at various values or ranges of values of the variable. Frequency distributions can be illustrated visually by means of histograms. Most frequency distributions met in practice have one peak and are described as unimodal. Nevertheless, occasionally distributions with more than one mode can be found, like the distribution of casual blood pressure in a large population, which is usually bimodal. Another characteristic of some interest is the symmetry or lack of symmetry of the distribution, i.e. the skewness of the distribution. Two other characteristics of a distribution are the location and the degree of variation of observations about the centre of the distribution. It is often important to give in a single figure some indication of the general level of a series of measurements, i.e. the mean or average of the variable. Other measures of location are the mode and median which are usually less important than the mean. Equally important for descriptive purposes are the statistics variance, range, maximum, minimum and coefficient of variation.

Histograms and descriptive statistics are even more important when grouping variables are introduced. A grouping variable can provide information about a variable not used as the plot axes. If for example defect depth is divided into groups of defect type, different lettering can be used to represent cases from each defect depth group. When meaurements of the subjects are plotted, slag inclusion defects, for example, may appear in a separate area of the plot with significantly different descriptive statistics, indicating that they should be analyzed separately in later analyses.

The grouping into strata or subpopulations is important and deserves more attention. Unusual data values that are masked in a total population may stand out when the data are separated into groups or strata. Printing histograms side by side for each group and descriptive statistics for each group coupled with preliminary one-way or two-way analysis of variance investigates the homogeneity of the various groups. From this one can identify extreme outliers, obtain an idea of the distribution of data

within groups, and examine whether the assumption of normality is reasonable. Lack of constant variance over groups can also be observed and tested and may give an indication that the input data should be transformed.

After screening and describing the data, one should be ready to make decisions regarding transformations. All statistical methods are based upon certain assumptions, for instance the forms of distributions or of relationships between variables. In realistic situations these assumptions are unlikely to be completely true. Very often the original data will present some elements which are incompatible with the theoretical model. In such cases it is advisable to try and look at the data in a rather different way, for example by using a different scale of measurement for one or more variables and then use standard methods of analysis. These procedures are appropriate at the very early stages of dealing with the data before formal and detailed analyses are carried out. This is helped a great deal by using simple descriptive tools like frequency distributions, histograms, bivariate scatter plots, mean values etc.

Looking at the data from a different angle implies in fact performing some kind of transformation to the data. There are two general types of transformations. Linear transformations involve the change of origin and can be useful in either performing arithmetic operations or in helping the investigator to display the results in a more readily understood and acceptable scale of measurement. More important however from the statistical point of view, are the non-linear transformation. There are three main reasons for performing such transformations:

(1) to stabilize the variance
(2) to linearize relationships
(3) to make distributions more normal

Variance-stabilizing transformations are very important because many of the available statistical methods rely on the strong assumption that the residual variance for various subgroups shoud be constant. If the variance of the observations is known to be a simple function of the mean, then a suitable transformation such as, for instance, taking the logarithm or the square root of the values will have the effect of stabilizing the variance.

Linearizing transformations are usually encountered in regression. For example, if a regression line, say of y on x is non-linear a satisfactory solution may be to fit a curvilinear function. The problem is particularly acute in the case where the dependent variable is a proportion which it is restricted between the values of 0 and

1 and where changes in any explanatory variable at the extreme ends are unlikely to produce much changes in the proportion. Furthermore, the variance of an observed proportion depends on the expected proportion as well as on the denominator of the fraction. Several transformations are used for proportions. These include the angular, probit, logit, complementary log-log transformations.

A similar point arises in normalizing transformations. Non-normal variation can be introduced into a theoretical model but the required methods of analysis are often very complex. Nevertheless many of the standard methods of analysis are insensitive to non-normality and this particular problem is less severe than the other two. Furthermore, it usually happens that the same transformation at the same time stabilizes the variance, produces linear relationships and provides more nearly normal distributions.

Returning now to those types of analyses where the probability element is more central; the objective being to assess the uncertainty in the conclusions. When the sample has been drawn the question which usually arises is what sort of inferences can be drawn about the population on the basis of the sample. A widely used device for this is the significance test. One might be interested in a certain hypothesis called the null hypothesis H_0 which specifies values of the parameters of the population. If H_0 specifies the mean and standard deviation of a normal distribution as μ_0 and σ_0 a test designed to detect departures of the population mean from μ_0 could reasonably be based on the examination of the sample mean $\bar{x}$. Similarly for the standard deviation σ_0 with the sample standard deviation s.

As an example, consider the problem of testing H_0 that the parameters of the normal distribution are $\mu = \mu_0$ and $\sigma = \sigma_0$ using the mean $\bar{x}$ of a sample size n. If H_0 is true the probability is 0.05 that a value of $\bar{x}$ will give

$$\mu = \frac{\bar{x} - \mu_0}{\sigma_0/\sqrt{n}}$$

greater than 1.96 in absolute value. If μ is numerically greater than 1.96 the difference between μ_0 and $\bar{x}$ is said to be significant at the 5% level. Similarly, an even more extreme difference giving a value of μ numerically greater than 2.58 is significant at the 1% level.

The significance test which has been considered above is two-sided in the sense that sufficiently large departures of $\bar{x}$ from μ_0 in either direction will be judged significant. If for any reason it was decided that interest lay in possible departures of μ from μ_0 only in one direction, say in excess of μ_0, it would be reasonable to

count as significant only those values of $\bar{x}$ which differed significantly from μ_0 in that direction. Such a test is called one–sided. The critical value for a one–sided test at level P is therefore the same as that for a two–sided test at level 2P.

Suppose now that one is interested in some component parameter θ in a model. To estimate the parameter θ an estimator $\hat{\theta}$ is determined according to some criterion. A random sample is taken and the estimate of θ, $\hat{\theta}$ is found. The result is a single number and there is no indication of how likely it is that this number $\hat{\theta}$ is close to θ, the unknown true value. The method of confidence intervals is an attempt to overcome this problem with point estimators. Here one constructs an interval whose endpoints are statistics of a random sample, and hence random variables, and gives a statement of the likelihood that the true value of the parameter lies in this interval.

With the same assumptions as before, that is $\bar{x}$ is the mean of a random sample size n, one might wish to construct a confidence interval for the population mean, μ, (with σ unknown) without concentrating on a single possible value μ_0. If we suppose that the distribution of x is normal, the probability is 0.95 that $\bar{x} - \mu$ lies between

$$-1.96\ \sigma/\sqrt{n} \text{ and } +1.96\ \sigma/\sqrt{n}; \quad \text{i.e. that } -1.96\ \sigma/\sqrt{n} < \bar{x}-\mu < 1.96\ \sigma/\sqrt{n}.$$

Or an equivalent statement by rearranging:

$$\bar{x} - 1.96\ \sigma/\sqrt{n} < \mu < \bar{x} + 1.96\ \sigma/\sqrt{n}$$

This statement, which is true with probability 0.95, asserts that μ lies in a certain interval called the 95% confidence interval. The ends of this interval, which are called the 95% confidence limits, are symmetrical about $\bar{x}$ and, since σ and n are known, can be calculated from the sample data.

No attempt will be made to cover here the full theory of confidence interval and significance test but it should be pointed out that there is a close formal relation between confidence intervals and significance tests. However, one thing which is very important to highlight, is to recognize the difference between practical and statistical significance. Just because two experimental conclusions produce mean responses that are statistically different, there is no assurance that this difference is large enough to have any practical value.

For example, an engineer may determine that the repair process of a structural component by a new procedure may produce a mean improvement in time spent of 0.5 h/m. This is a statistically significant result. However, if the additional cost of the new repair procedure is £1000 then 0.5 h/m difference is probably too small to be of any practical value.

Statistical procedures are usually based on a probabilistic model for the data and the model formulation is an essential issue. Very often the systematic relation between a response variable Y_i and the i^{th} observation and an explanatory variable x_i is such that $E[Y_i] = g(x_i ; \beta)$ where g is a known function and β a vector of unknown parameters. In some situations the distribution of Y_i may be defined by the mean, as for instance in Poisson, binomial and exponential distributions. In other situations it might be possible to express each Y_i in terms of a set of independent, identically distributed random varibles $\epsilon_1, \epsilon_2, \ldots, \epsilon_n$ of zero mean.

Whatever the form of the model, methods of examining its adequacy of fit are of primary importance. With large amounts of data, graphical analyses, summary statistics an inspection of suitable tables will usually lead to investigation of the adequacy of the proposed model. Residuals, i.e. the differences between the observed and the fitted transforms adjusted to have approximately unit variance are the major tools in assessing the adequacy of the proposed model. These can be plotted against regressor variables and against the fitted values. Further the distribution of residuals may indicate the presence of outliers whose inclusion or exclusion from the analyses will need further consideration.

1.5 Layout of Thesis

The work in this thesis is divided into five major chapters.

Chapter 2 contains an overall review on various methods of non-destructive evaluation, namely ultrasonic testing and magnetic particle inspection. Problems of detection and sizing of weld defects are discussed in depth.

Chapter 3 contains a detailed description of the Hutton TLP defect data base and the various fabrication and location parameters which have been used in the analysis of data.

In Chapter 4, a detailed analysis of the occurrence of defects in the welds of the Lower Hull of the TLP is included. This comprises a separate investigation of defect occurrence for both surface-breaking defects and embedded defects. For each category detailed analyses are included for defect rates, defined at the percentage of weld length found defective, frequency of occurrence of various defect types, multiple defect occurrence and binary analysis.

Chapter 5 contains criteria for choosing particular distributions in modelling defect sizes and investigates the variations of sizes in both surface-breaking and embedded defects. Special attention is focussed on explaining variations of defect sizes under the influence of a number of factors such as welding process, welding procedure, fabricator, type of welded joint, defect type and overall global and defect location. The results are compared with probability distributions of defect sizes in other offshore and nuclear structures.

Chapter 6 introduces the use of binary regression functions in modelling uncertainties in defect detection. Published data from several national and international programmes set up to determine the reliability of NDE procedures for the detection of weld defects are reviewed. Functions currently used in industry to model the probability on non-detection are critically examined and new generalised models are proposed. The proposed models can be used to update the defect occurrence and defect size distributions obtained form raw data. Furthermore, sizing errors using magnetic particle inspeciton are assessed using data from surface-breaking fatigue cracks in tubular joints typical of offshore structures.

Finally, Chapter 7 contains a brief summary of some of the main conclusions reached in the present study.

CHAPTER 2

REVIEW OF METHODS OF NON-DESTRUCTIVE EXAMINATION FOR WELDS

2.1 General

Non-destructive examination techniques have been in use extensively for a long time to assure the safety of structures. However, one can never be certain that any non-destructive examination system will successfully detect and size all defects in the specimen examined. When a part is subjected to inspection it is exposed to some kind of agent such as ultrasound, gamma or X-radiation, a magnetic field or liquid penetrant. Defects are then detected and sized by interpreting the response from the applied agent. Apart from the element of human uncertainty with respect to the application of the agent and the correct interpretation of the response, there are a number of factors which may influence the performance of the NDE system. These include, the length of time taken to make the inspection, local and access geometry, material and defect characteristics, material thickness, defect dimensions, defect orientation relative to the external surface and others associated with the particular inspection technique in use.

There are many different types of NDE systems which are in use today but the six major systems are:

1.	Ultrasonic testing	(UT)
2.	Radiographic testing	(RT)
3.	Time of flight testing	(TOF)
4.	Magnetic particle inspection	(MPI)
5.	Eddy current testing	(ET)
6.	Liquid penetrant testing	(PT)

Of these, two major types of NDE techniques will be examined, namely ultrasonic testing and magnetic particle inspection, which are suitable for the detection of embedded and surface breaking defects respectively. Details of the other NDE methods are gien by Gessop [9] together with a summary of recent developments and applications.

2.2 Ultrasonic Testing (UT)

Among various UT techniques the pulse-echo method is the most commonly used NDE tool in the detecting and sizing of through volume defects. This technique is

extensively discussed in the book by Krautkramer et al [10] and here only its main features will be given.

A piezo-electric transducer converts electrical pulses into ultrasonic pulses which are directed into the surface under inspection. A couplant is required between the face of the probe and the surface to permit transmission of the accoustic energy from the transducer to the material under test. The incident pulse is reflected from defects and the back face of the specimen and returns to the test set (probe) where it is converted into an electrical signal. The deflection of the spot on the receiver (cathode ray tube) shows the instant of the pulse launch. The spot moves steadily across the screen as the pulse travels through the work piece. The sequence is repeated many times per second to produce a continuous display on the screen. The receiver is calibrated according to the speed of sound in the material to give the distance to the flaw. The horizontal position on the screen indicates the time of the return and consequently the distance to the reflecting surface. The echo signal from the back wall indicates the thickness.

The determination of defect type is based on the inspector's experience in interpreting typical signal permutations of a succession of echo signals of varying height and range and in visualising the nature of surfaces which give rise to them.

For sizing defects, the ultrasonic pulses form a divergent beam with its maximum intensity at the centre and decreasing to the boundaries. The probe is moved away from the maximum signal position until the signal falls to a low value, generally 1/10 of the maximum height. The top and bottom edges of the defect are located in turn and the defect sizes are plotted.

In order to cover the range of possible defect orientations, ultrasonic beams are generated using angle probes (usually 0,45 and 60 degrees). Since ultrasonic waves do not interact with objects having dimensions less than the wavelength of the ultrasonic wave, very high frequencies are required to detect small discontinuities, usually in the range 1 - 6 MHz.

Ideally, any defect in a weld should be detected and sized correctly, but there are many reasons why defects are sized incorrectly, missed altogether or falsely recorded. These problems are discussed in Refs [10 - 21] and include:

- Laminations in the base material can cause dispersion and distortion of the sound beams.

- Cold shunts between individual weld beads having curved contours cause scattering of the sound beam.

- Metallurgical discontinuities such as cladding cause dispersion of the ultrasound beam.

- Planar and volumetric defects have differences in their reflecting properties which are governed by the angles of incidence and reflection.

- Rough surfaces can materially reduce the sensitivity of the method and sudden changes in metal sections can produce misleading images.

- Defects under compressive loading can produce reduction in the amplitude of the reflected ultrasonic signal.

Other factors affecting the detectability of flaws include:

- Probe misalignments and/or loss of coupling.
- Shape of the reflector and its orientation relative to the sound beam.
- Access to the appropriate part of the weld surface.
- Defect orientation relative to the inspection surface.

2.3 Magnetic Particle Inspection (MPI)

Magnetic particle inspection is used for detecting the presence of discontinuities in ferromagnetic metallic materials such as iron and magnetic metallic alloys of steel. The method can detect discontinuities which are open or slightly below the surface of the material. Detection of the latter depends on their orientation, size, shape and distance below the surface.

The principles of its operation are based on the properties of magnetic fields, the details of which will not be discussed here, see [22, 23]. The main features of the method involve the establishment of a suitable magnetic field within the surface, the application of magnetic particles to the surface under test and finally examination of the work piece for accumulations of the magnetic particles.

The generation of the magnetic field is usually done by either the use of high current flow from prods (typically up to 1000A) at a potential of 6V or less (DC current is generally preferred for use in detecting subsurface defects) or the use of an AC electromagnetic yoke. When the current flows through the surface a magnetic

field is generated in a direction perpendicular to the current flow and invisible distortion in the lines of the magnetic field occur due to the presence of discontinuities. When a magnetic medium (dry powder or liquid suspension) is applied to the surface the particles accumulate around the area of the leakage flux and make the flaws visible. A study of the various patterns is required to enable proper identification of the defects. The process is repeated to reveal cracks of all orientations.

A number of limitations are associated with the method and misleading indications are often produced. Sudden changes in physical dimensions such as sharp corners, changes in the magnetic properties of the surface, non-uniformity of the metal such as magnetic to non-magnetic welds and the presence of dirt on the testing surface usually give the same indication as defects. Furthermore, no defect indications are produced at all if, for example, dry powder (which is suitable for subsurface flaws and rough surfaces) is used as the detecting medium and the test surface is not first dried. Details of the current magnetizing source (AC, DC etc.), types of agents and powder used are well documented in [22].

With regard to the sizing of flaws, MPI provides visual information on the defect length only and no information on depth. Provided the defect dimensions are of sufficient size, measurements can be made using ultrasonic methods. In cases where the nature of indications are such that ultrasonic examination is not possible, exploratory grinding is required to remove the flaw and assess its depth [24]. Such excavation usually tends to over-estimate both defect length and depth.

2.4 Reliability of Non-Destructive Evaluation

It is clear from the preceeding sections that non-destructive examination devices are not ideal and their performance depends upon several factors many of which cannot be controlled to the extent which is desired. Because of this, certain defects may remain in the structure undetected and others which are successfully detected may be sized incorrectly. In statistical terms, these departures from ideal performance lead to errors in both the defect occurrence distributions and the defect size distributions when sample data from particular structures are analysed. Unless allowances are made for such effects, this could lead to either 'critical defects' being left in the structure with serious consequences, or to unnecessary repairs; both resulting in financial losses.

Probabilistic models for defect detection and sizing are investigated in section 6 where a review of published information from several national and international programmes

on detection probabilities and sizing errors is carried out. In addition, a number of functions which are currently used to define 'failure to detect' probabilities are critically reviewed and new generalised models are proposed for use in updating defect size and occurrence distributions.

CHAPTER 3

DESCRIPTION OF VARIOUS PARAMETERS USED IN THE ANALYSIS

The need for a rational procedure for the assessment of weld defects occurs with many types of structures but was very apparent during the fabrication of the Hutton TLP when weld defects of an unacceptable size were discovered at a late stage in the final assembly of the Lower Hull from its pre-fabricated components. This discovery led to what was termed phase III NDE, an extensive reinspection of a large proportion of all welds in the lower hull. It must be emphasized that this comprised an additional reinspection of the lower hull and was carried out independently of the non-destructive examination of welds which followed immediately after fabrication. The principal testing techniques used were ultrasonic testing (UT) and magnetic particle inspection (MPI). Approximately 30km of weld were reinspectd by ultrasonic testing and about 76km by magnetic particle inspection, a total of 121,270 UT and MPI examinations.

A detailed statistical analysis of the phase III NDE data has been undertaken to see whether detailed information could be gained about the occurrence of the defects and their relationships to the various welding parameters. During the phase III NDE, data from both ultrasonic and the magnetic particle investigations were transferred to a computer data base comprising 29 useful fields of data for each inspection record. In all the data base contained approximately 30 million characters of useful information, but before it could be used it was necesary to undertake as many checks on the records as possible to establish the validity of the information and to eliminate some of the inevitable errors in recording and transcribing the data. Some of the parameters could be independently checked since they were recorded in two different ways; for instance, the welding process was encoded directly as SMAW, GMAW etc., but could also be derived from the welding procedure which was encoded separately. Other parameters could not be checked directly and these were subjected to range checks to highlight gross abnormalities.

The checking of the data base had to be undertaken by computer because of the vast amount of information available, but even this was not straightforward because of anomalies which had been introduced at various stages in the creation of the data base. The most serious deficiency found was that a not insignificant proportion of some data fields were blank because the correct information was not available at the time the data base was created. These missing data made the analysis more difficult since missing information of a non-random nature could have introduced bias into the results.

An indication of the likely accuracy of the data base can be obtained from the parameter identifying the weld type joint which was found to be blank in 24 out of a total of 144,761 records and to contain meaningless characters in a further 15 records. Combining these two sets gives a lower bound on the error rate of 0.027% which is considered to be satisfactory. The actual error rate depends, of course, on the number of valid characters incorrectly and inadvertently substituted for correct characters during the creation of the data base.

The following sections contain a description of the various welding and fabrication parameters which have been used in the statistical analysis of the weld defect data base.

3.1 Description of the Structure

The Lower Hull of the Conoco Hutton Tension Leg Platform (TLP) was designed as a cellular structure providing the buoyancy which supports the Hutton platform and maintains its tethers in tension. The platform deck is supported on six stiffened cylindrical columns connected at their bases by rectangular pontoons (see Fig. 3.1.1). Individual buoyancy tanks are formed in the columns and pontoons by cross-sectional watertight bulkheads.

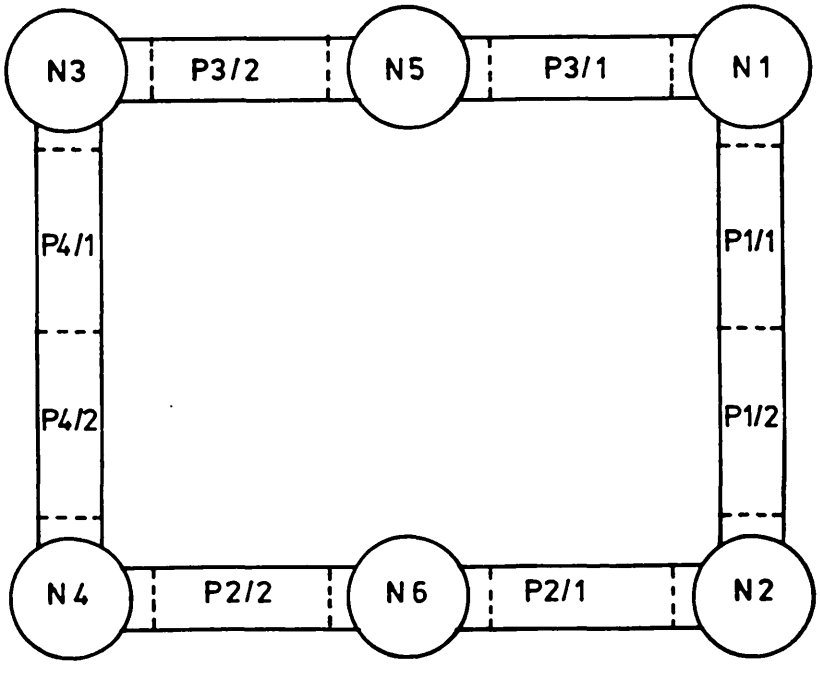


Fig. 3.1.1: Plan of the TLP Lower Hull

The lower hull is made up of 14 sections: the centre nodes N5 and N6; the eight pontoon sections; the corner nodes N1 and N4; and the corner nodes N2 and N3. These were fabricated in eight different yards all of which are known to have used a common set of welding procedures. Fabrication details of the various sub-assemblies are not given in this thesis but can be found in [25] (Volumes I - VI, relating to nodes 1 - 6 respeectively).

3.2 Weld Joint Type

A welded joint is considered to consist of all the parts involved in the welding and includes the weld metal, the heat affected zone and the unaffected base metal.

A welded joint is made by fusing the steel plates or sections along the line of the joint. The metal melted from each member of the joint, together with additional weld metal, unites in a pool of molten metal which bridges the interface. As the pool cools molten metal at the fusion boundary solidifies, forming a solid bond with the parent metal. When solidification is complete, there is a continuity of metal through the joint.

The types of welded joints which have been considered in the analysis are: tee butt weld (T), plate butt weld (B), cruciform joint (X) and fillet weld (F). The four joints are illustrated in Fig. 3.2.1 below.

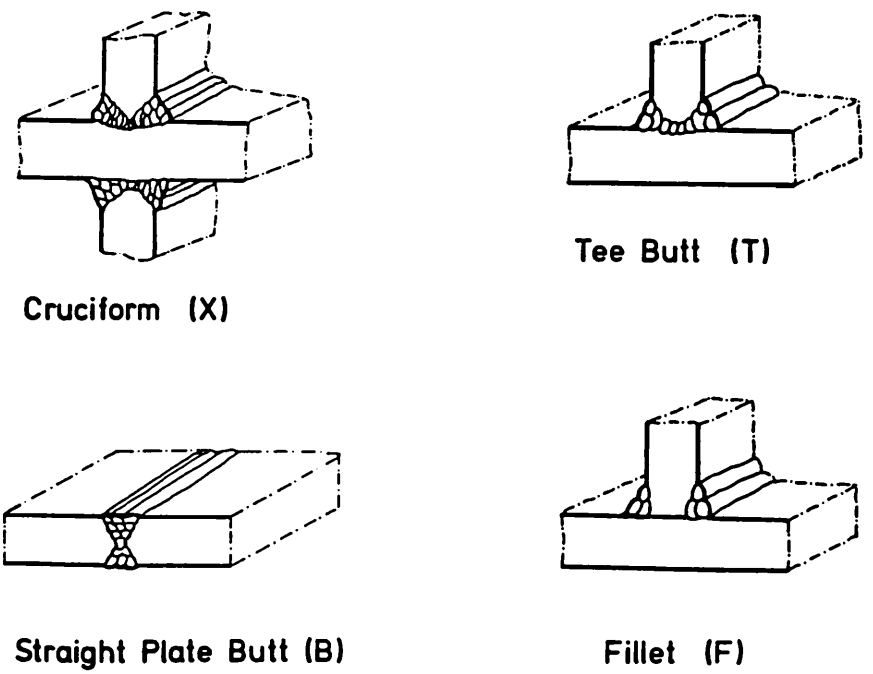


Fig. 3.2.1: Types of Welded Joint

3.3 Defect Type

Discontinuities are usually understood as interruptions of the normal physical structure of a weld but not all such interruptions affect the function that the weld will perform. The significance of discontinuities depends upon a number of factors such as size, shape, orientation and location within the weld. This leads to the definition of 'defect' which originates from discontinuities whose properties and characteristics are likely to damage the performance and usefulness of the part in which it occurs.

This section cannot cover all defects that may be found in a welded joint. There are many references which describe the various defects, see for example [26, 27], and discuss their causes and methods of prevention [28]. Some typical defect types are examined here, mainly non-fusion (NF), slag (SL), crack (CR), incomplete penetration (IP), porosity (PO) and linear indication (LI). The typical locations of some of these defects is illustrated in Fig. 3.3.1.

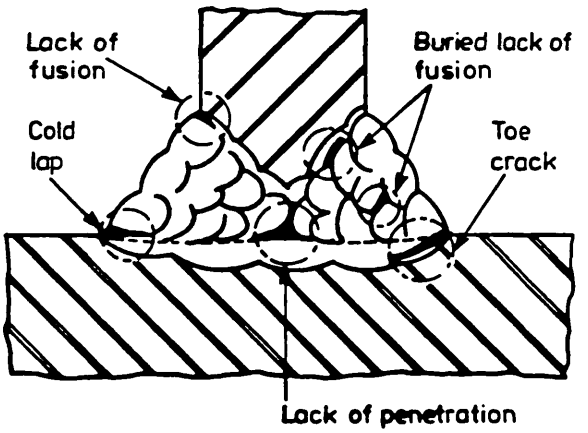


Fig. 3.3.1: Various Categories of Defect Types

Non-Fusion (NF)

Lack of fusion or non-fusion, as it is frequently termed, describes the failure of adjacent surfaces of the weld metal and the parent metal to fuse together, so producing a discontinuity between them. This type of defect may be caused by incorrect preheating, improper torch, improper electrode and/or metal manipulation and failure to remove slag or other material from the surface with which the deposited metal must fuse.

Overlaps and cold laps are non-fusion type defects which occur in regions near the weld toe. Overlaps usually form when low hydrogen type electrodes are used since they tend to produce weld profiles more convex than with other types of electrodes. When Gas Metal Arc Welding (GMAW) is used at a high production rate, welding arcs in the spray transfer mode travelling at a high speed are used and this procedure tends to produce cold laps. It is generally very difficult to distinguish these defects from toe cracks in the visual inspection and magnetic particle inspections and for this reason many overlaps and cold laps in the present study, were originally misjudged to be toe cracks.

Slag Inclusions (SL)

These are non-metallic solids produced by the welding process and entrapped in the weld deposit or between the weld metal and base metal. Slag inclusions may be formed by contamination of the weld metal by the atmosphere or incomplete removal of the slag from each weld run in multi-layer welds.

Crack (CR)

This is a general term used to describe defects of various types (e.g. solidification, reheat, hydrogen induced cracking) and can occur at any place in the weld and is caused by improper use of the heat source and by stresses being built up during the cooling process.

Incomplete Penetration (IP)

This describes the failure of the weld metal to penetrate and fill the root of the weld. Most frequently this type of defect arises because of improper groove design for the welding process used. It is a function of electrode manipulation and arc current or inadequate preparation of the joint surfaces.

Porosity (PO)

These types of defects are caused by gas entrapment in the weld metal and they are usually spherical in shape but can be elongated to produce piping or wormholes. Porosity may come from gases released by the cooling weldment since their solubility in the weld metal reduces as its temperature drops. Hydrogen is the most common gas and is supplied by the gas atmosphere surrounding the arc zone. Porosity may result from moisture, paint, oil or other contaminants on the plate, water in the area being welded, from damp electrodes or rusty electrode wire.

Linear Indication (LI)

The NDE operator cannot always distinguish between defects unless their characteristics are obvious. He will identify the defect based on its location and his experience. Consequently, usually MPI operators can give accurate defect classification but when in doubt may class the defect as a 'Linear Indication'. Such defects were frequently reported during non-destructive testing of the TLP structure.

3.4 Welding Process

Welding is used extensively for joining materials together and there are numerous methods for doing so, including arc welding, gas welding, laser beam welding, soldering etc. The data which are analysed in this thesis are known to have resulted from the use of three common welding processes, shielded metal arc welding (SMAW), gas metal arc welding (GMAW) and submerged arc welding (SAW). Full account of these processes will not be given here but are described in detail in Ref. [29]. A very brief description is given below.

Shielded Metal Arc Welding (SMAW)

This is one of the oldest and still the most widely used arc welding processes and is manually operated. It is also called manual metal arc (MMA) and requires considerable skill to produce good quality welds.

Coalescence is produced by heating with an electric arc between a coated metal rod called the electrode and the work. The electrode consists of a steel core wire normally ranging from 2 to 6mm in diameter and the flux covering it contains alloying elements (e.g. manganese and silicon). The operating characteristics of the electrode are controlled by these alloying elements. A variety of electrodes is available to suit different applications. SMAW electrodes are specified in [30]. The arc melts the parent metal and electrode. The flux melts with the core wire and flows over the surface of the pool to form a slag which must be removed after solidification.

A drawback of this process is that very frequently the welder has to stop and insert another electrode which becomes a problem on long welds especially when labour costs are high.

Gas Metal Arc Welding (GMAW)

This process is also termed as metal active gas (MAG) and sometimes metal inert gas (MIG), although the latter definition is limited to the use of pure argon as a shielding gas which is not used for steel.

GMAW is also manually operated. The arc and weld metal are shielded by a gas which does not react with molten steel. The electrode is solid and no flux is required to shield the pool (the alloying elements are in the electrode wire) but sometimes a flux-cored electrode is used to produce a slag which controls the weld profile. The arc length is controlled by the power supply unit.

The shielding gases have the purpose of protecting the arc and weld zone from air and providing the desired arc characteristics. Various gases are used depending on the metal reactivity and nature of the joint being welded. Usually the shielding gas is carbon diaxide or a mixture or argon and carbon dioxide.

Less skill is required to master this process as compared with the SMAW process but more skill is required to set up the correct welding conditions. If the welding is highly repetitive and the equipment is preset, a relatively shorter time is needed to train a welder. Overall times for productivity are better since there is no need to change electrode.

Submerged Arc Welding (SAW)

Submerged arc welding is used in both automatic and semi-automatic operations although the former is by far the more common. The electrode is a bare wire which is moved by a motor. The welding head is advanced along the joint by a tractor, gantry or boom. Both the current and voltage characteristics are preselected and are maintained that way by feed-back systems which vary in degree of complexity. The flux is in the form of granules and is placed on the surface of the joint. The arc works below the flux surface, melting a proportion of it to form a slag. Flux which is not fused is collected and used again for the next weld. Weld pools are large and can only be controlled in the flat and horizontal positions.

Current values can be set at high values providing substantial cost savings because of high metal deposition rates and low labour costs. The SAW process is considered for use in jobs which require repetition, high percentage arc time possible and consistent weld quality.

3.5 Original Welding Procedure

The term welding procedure is used to describe the complete operation of making a weld. It covers choice of electrode, edge preparation, preheat, welding parameters such as voltage, current and travel speed, welding position, number of weld passes to fill the groove and post-weld treatments, for example grinding or heat treatment.

A variety of welding procedures were used in the structure under study. For some analysis purposes the most commonly used procedures have been grouped into four major categories, namely W6, W8, W5 and W3, on the basis of weld preparation and detail of back gouging. These are illustrated in Figs. 3.5.1 to 3.5.4.

The grouping into these categories does not provide information on the welding position or welding process which have been used for welding. Each group, for example W8, comprises six different welding procedures.

i.e. W8-1 involving the SMAW process in the flat position
W8-2 involving the SMAW process in the horizontal position
W8-3 involving the SMAW process in the vertical position
W8-4 involving the SMAW process in the overhead position
W8-5 involving the GMAW process in the flat position
W8-6 involving the GMAW process in the horizontal position

Similar remarks apply for the other groups.

Although the number of passes used for welding are different for each component of the group, the procedures used under the W8 and W5 grouping involve fewer number of passes as compared with W6 and W3 respectively.

3.6 Other Parameters

Several other parameters were considered in the statistical analysis of the data, the most common of which are summarised below:

- Weld Line Identification Number.
  This was defined by contractors before fabrication.
  Various sub-block identification numbers are presented in Figs. 3.6.1 to 3.6.3.

- Fabricator.
  All sections were fabricated in eight different yards all of which are known to

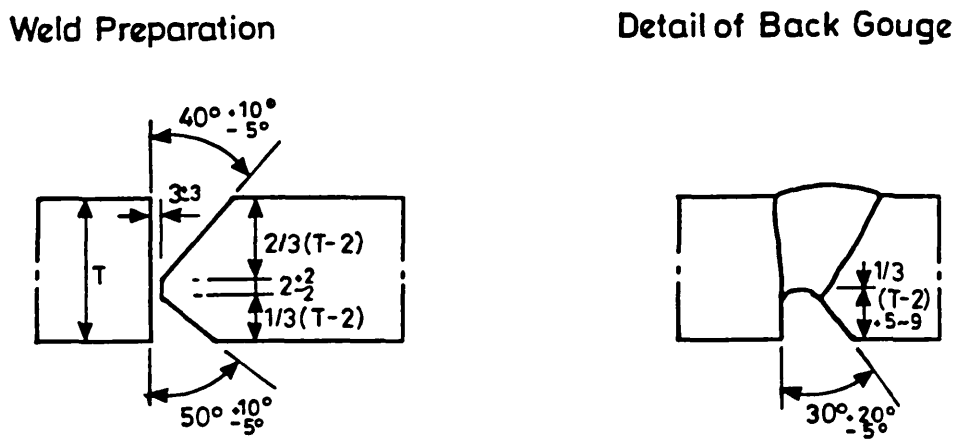


Fig. 3.5.1: Welding Procedures; Group W6

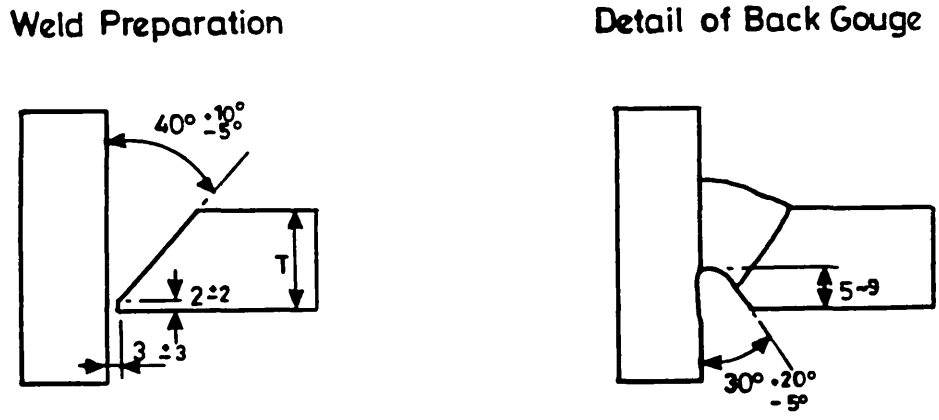


Fig. 3.5.2: Welding Procedures; Group W8

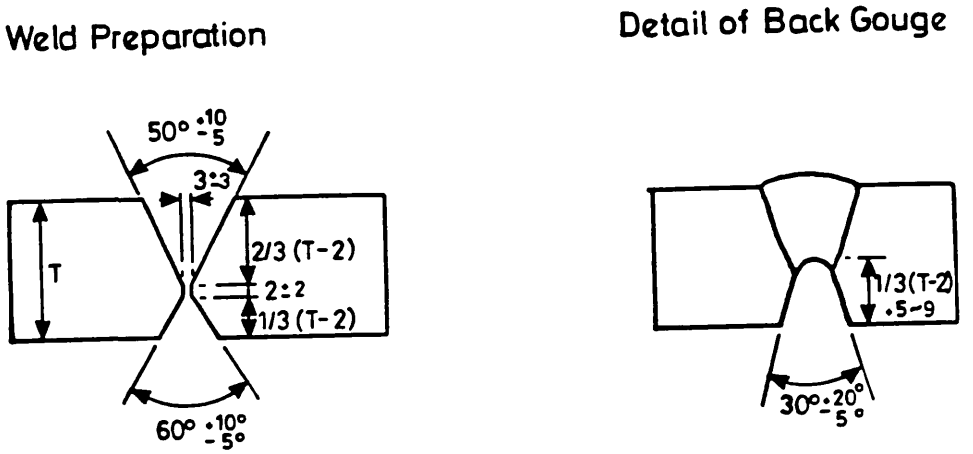


Fig. 3.5.3: Welding Procedures; Group W3

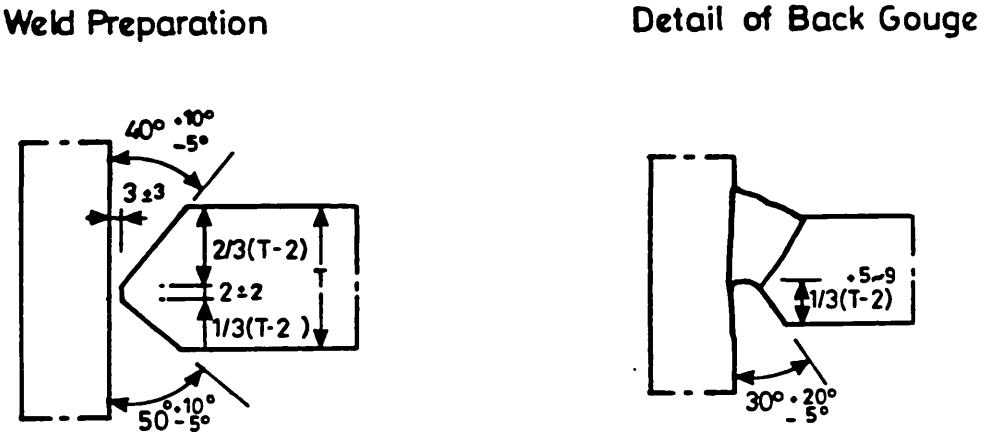


Fig. 3.5.4: Welding Procedures; Group W5

have used a common set of welding procedures.
Fabrication details of the various sub-assemblies have been kept confidential for the purpose of this thesis.

- Fatigue Zone.
  The lower hull structure was divided into a number of fatigue zones, A, B and C corresponding to different levels of defect tolerance, A being the most sensitive.

- NDE Operator.
  Given a weld was found defective, this parameter describes the multiple occurrence of defects on a single weld.

- Defect Location.
  This describes the location of defect within the welded joint. It specifies whether the defect is embedded (see Fig. 3.6.4) or surface breaking, whether it is a weld or toe defect and whether it is in a continuous or abutting member.

- NDE Type.
  It specifies whether ultrasonic testing or magnetic particle inspection was undertaken.

- Weld Length Tested.
  This parameter gives information on the amount of weld length that was inspected. It is measured in the direction of welding. The MPI weld length is approximately double the UT for the same weld number and type.

- Defect Length.
  This specifies the length of the defect measured in the direction of welding.

- Defect Position from Datum.
  It specifies the position of the defect relative to the measurement datum.

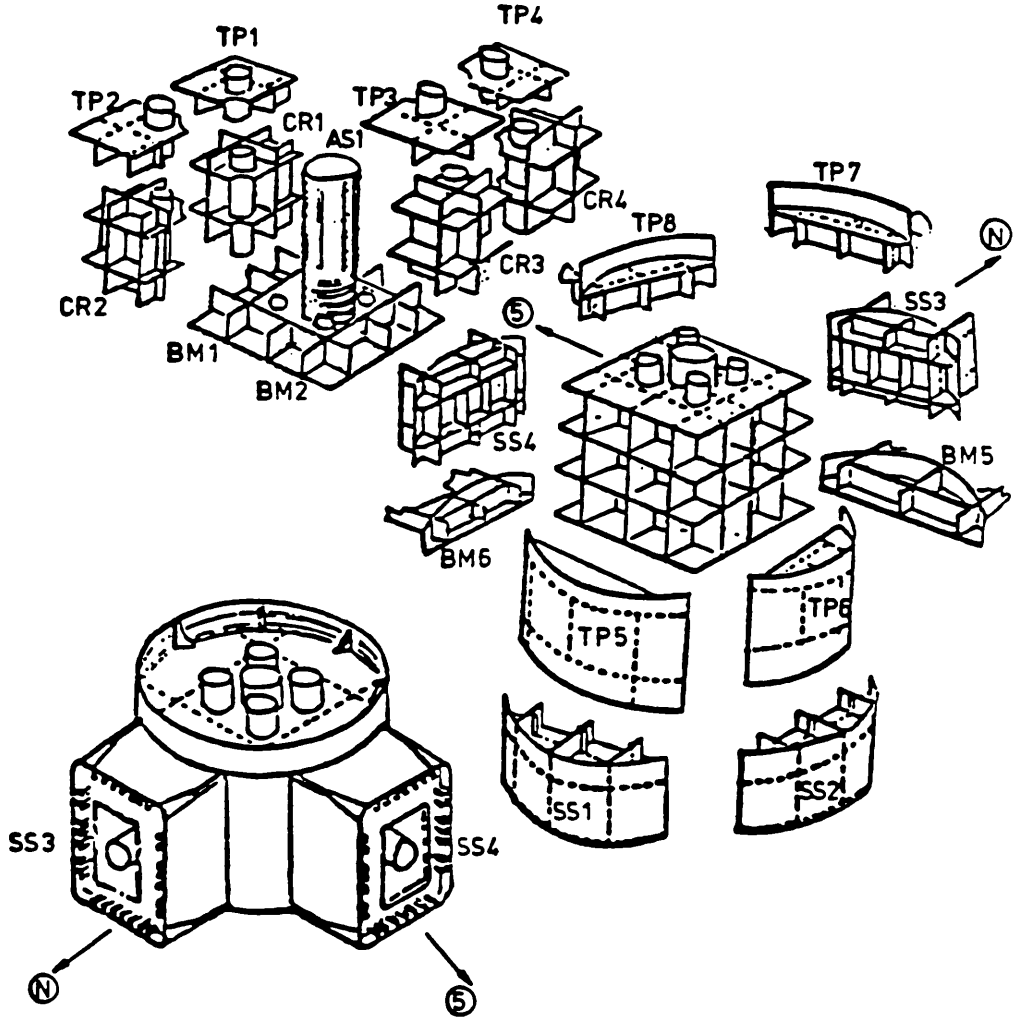


Fig. 3.6.1: Sub-Block Identification for Nodes 1 and 4

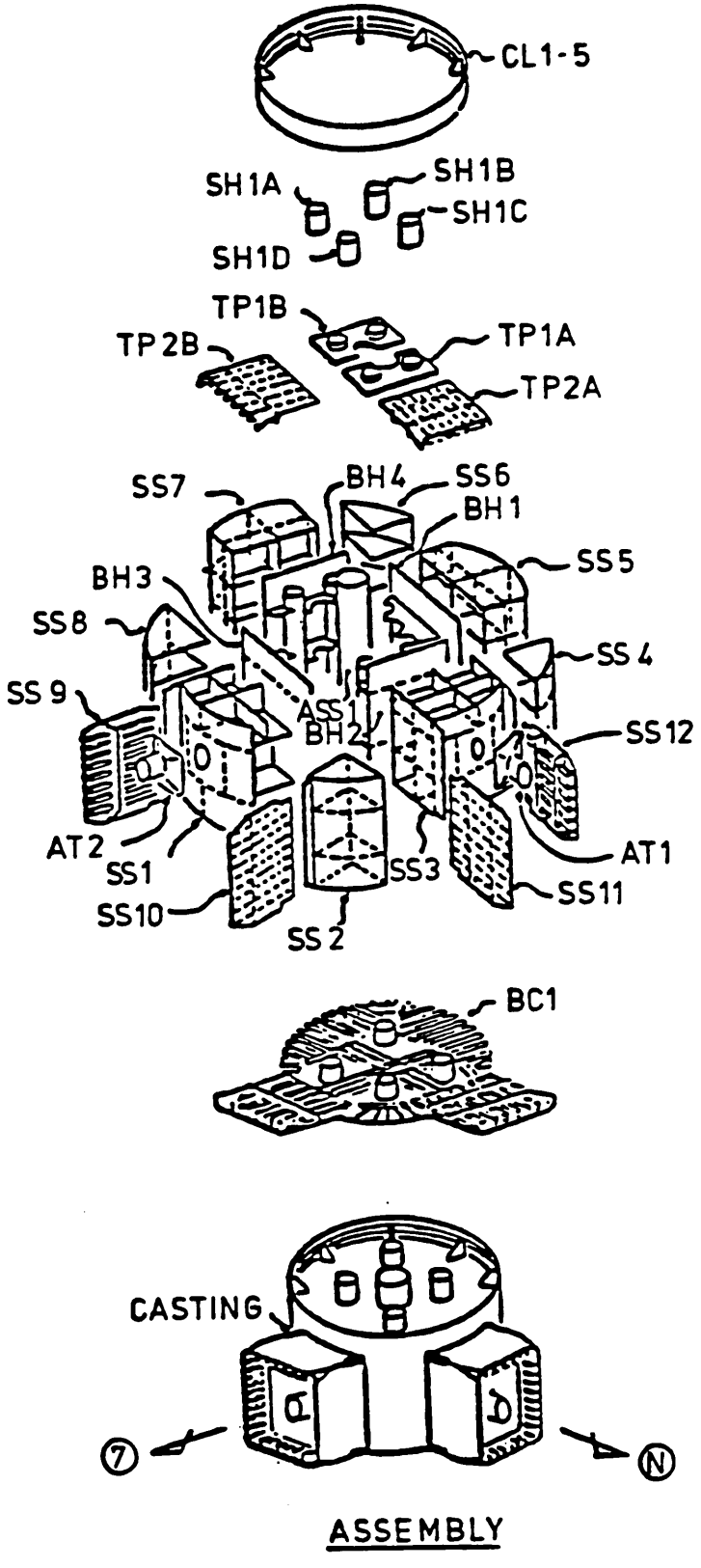


Fig. 3.6.2: Sub-Block Identification for Nodes 2 and 3

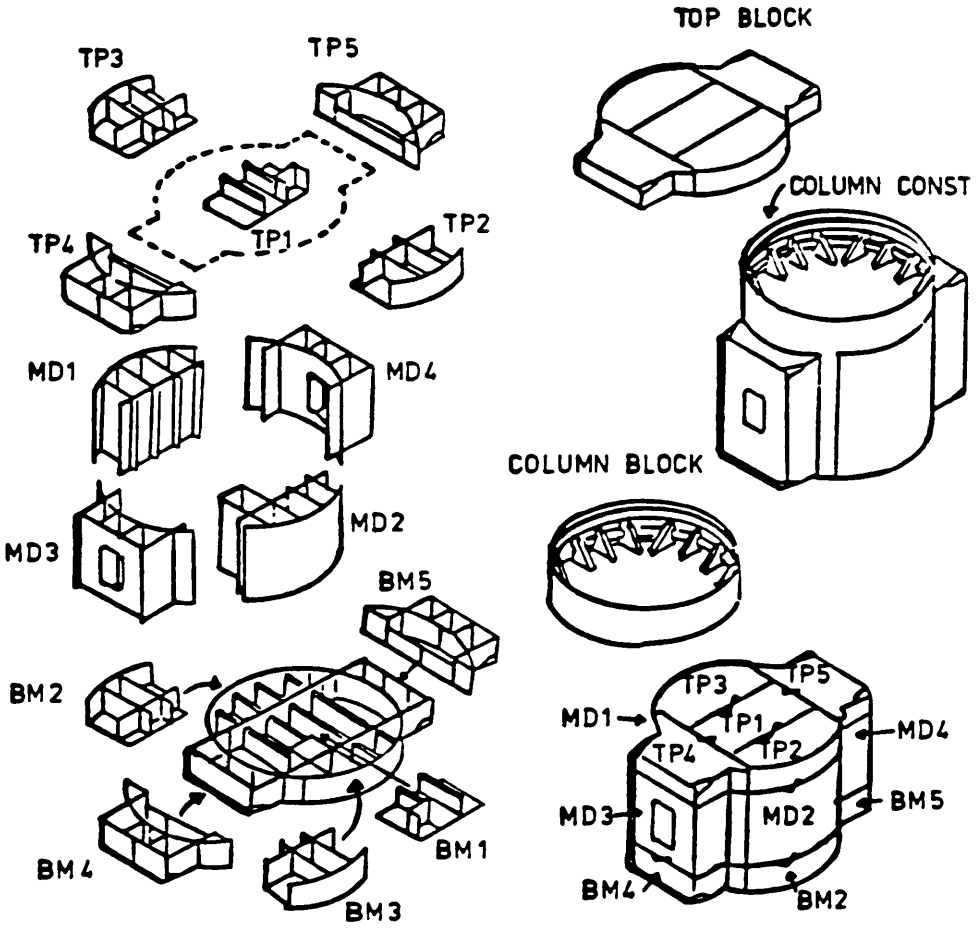


Fig. 3.6.3: Sub-Block Identification for Nodes 5 and 6

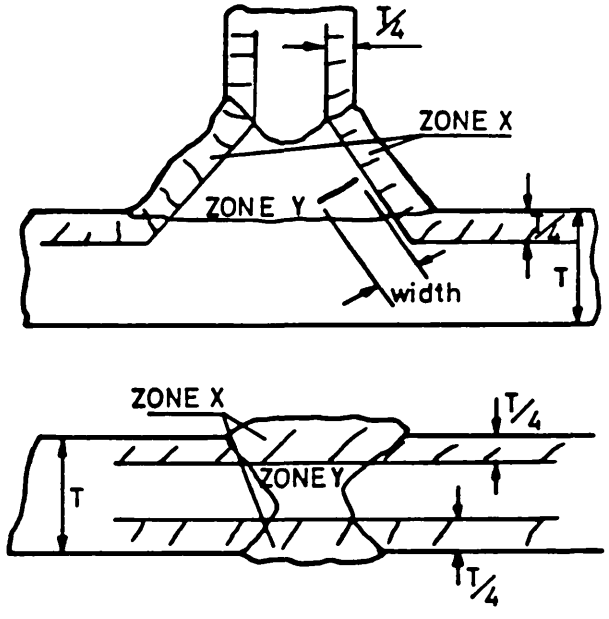


Fig. 3.6.4: Types of Defect Zone

CHAPTER 4

DEFECT OCCURRENCE

4.1 Statistical Theory

This section gives an outline of the theory which has been used in the analysis of occurrence of defects in the Hutton TLP, as recorded in the weld defect data base.

Differences in the proportions (e.g. number of defective welds/total number of welds inspected) can be analysed using the theory of binary data given in section 4.1.1. However, classification of the response (e.g. assessment of the NDE operator on the binary scale (e.g. defective weld and defect free weld) may sometimes not be sufficient to explore the complete variability in the data (e.g. a multiply-defective weld is not equivalent to a weld with a single defect). In such a case an analysis which takes account of the ordered response (e.g. a weld inspected is found to have 0 defects, 1 defect, 2 defects, 3 defects, 4 defects, 5 or more defects) is more informative. The theory of performing such analyses is given in section 4.1.2. A somewhat similar but less effective investigation can be undertaken by the theory described in section 4.1.3. The latter, however, is more suitable for analysing the frequency of occurrence of various defect types. For this type of data, the response is classified according to which category it belongs (e.g. a weld inspected belonging to the cruciform category may have a defect of the non-fusion type).

4.1.1 Analysis of Binary Data

With this category of data the response is measured on a binary scale, where the random variable Y is defined as:

$$Y = \begin{cases} 1 & \text{if the response is present (e.g. weld is defective)} \\ 0 & \text{if the response is absent (e.g. weld is defect free)} \end{cases}$$

If there are n independent identically distributed random variables (i.i.d r.v.)with $\pi = P[Y = 1]$, then the r.v. R denoting the number of outcomes with the attribute present, out of n trials, has a binomial distribution

$$R \sim B(n,\pi) \quad \text{i.e. } P[R=r] = \binom{n}{r} \pi^r (1-\pi)^{n-r} \qquad r = 0,1,\ldots,n$$

with $E[R] = n\pi$ and $Var[R] = n\pi(1-\pi)$.

Suppose we have k i.i.d. r.v. with $R_i \sim B(n_i, \pi_i)$ for i=1,...,k taken on p explanatory variables $x_{1\,1},\ldots,x_{1p}$. Many methods of analysing such data exist, depending on the nature of the investigation. A method which has been widely used here is the one which makes use of the empirical logistic transformation, for which a brief outline is given below. For further details see [31].

We write $\lambda_i = \ell n \left[\frac{\pi_i}{1-\pi_i}\right]$ and assume $\lambda_i = \sum_{j=1}^{p} x_{ij}\beta_j$

where β_j are unknown parameters and x_{ij} are known values (explanatory variables).

We look for a transformation of R_i that has mean approximately equal to λ_i, i.e. we linearise the observed proportions. Noting that $E[R_i/n_i] = \pi_i$, we might consider a transformation to a new random variable

$$z_i = \ell n \left[\frac{R_i}{n_i - R_i}\right]$$

This is known as the empirical logistic transformation with variance

$$Var[z_i] \approx \frac{1}{n_i \pi_i (1-\pi_i)}$$

We take as an estimate of $Var[z_i]$ to be

$$\frac{n_i}{R_i(n_i-R_i)} = \frac{1}{R_i} + \frac{1}{n_i - R_i}$$

To improve the approximation (z_i is undefined if $R_i = 0$), we take the modified transformation

$$z = \ell n \left[\frac{R+\frac{1}{2}}{n-R+\frac{1}{2}}\right],$$

and as an estimate of variance

$$est(Var[z]) = \frac{(n+1)(n+2)}{n(R+1)(n-R+1)}$$

which gives almost an unbiased estimate of Var[z].
In addition, it can be noted that $E[z-\lambda] = 0(1/n)$.

In this way:

(i) We transform the frequency of success R_i in n_i trials into a variable z_i which is approximately normally distributed with a known mean and variance.

(ii) Any differences and trends in the proportions can be tested and confidence intervals can be calculated.

(iii) A general factorial problem can be broken down to a number of single degree of freedom problems and individual contrasts can be constructed and compared.

(iv) Inspection of appropriate semi-normal probability plots can indicate additional sources of influence.

Furthermore, direct analysis in terms of the proportion π has the advantage of more direct interpretation:

(a) The proportion $P_i = R_i/n_i$ is approximately normally distributed with mean π_i and variance $\pi_i(1-\pi_i)/n_i$

(b) When the fundamental assumptions of analysis of variance are not violated, a least squares regression can be used with an average unbiased estimate of variance as an effective error mean square.

Further details on binary data with regression considerations are given in section 6. Numerous practical examples of such data analysis can be found in [85].

Calculations can be undertaken using the two statistical packages [34, 35].

4.1.2 Analysis of Ordered Categorical Data

Classification of the response on a binary scale (defective and defect free) may not always be sufficient to explore the complete variability in the data. In such a case, it will be more informative to expand the defect response into k categories assumed to be ordered in some way: e.g. 1 defect, 2 defects, 3 defects, $\geq$ 4 defects. Such consideration will explore differences, if any, in the distributions assumed to underlie the ordered continuum.

Consider two groups with k ordered categories and corresponding probabilities π_{1j} and π_{2j}, j=1,...k.

Define the cumulative probabilities:

$$\gamma_{1j} = \pi_{11} + \ldots + \pi_{1j} = P[\text{number in group 1} \leq j]$$
$$\gamma_{2j} = \pi_{21} + \ldots + \pi_{2j} = P[\text{number in group 2} \leq j]$$

We want to test the null hypothesis that the two distributions have the same shape but different location parameters.

i.e. $H_0 : \Delta = 0$
$H_1 : \Delta \neq 0$

where for the first group

$$\ell n \left[\frac{\gamma_{1j}}{1-\gamma_{1j}}\right] = \theta_j \qquad j = 1,\ldots,k-1$$

for the second group

$$\ell n \left[\frac{\gamma_{2j}}{1-\gamma_{2j}}\right] = \theta_j - \Delta \qquad \text{constant } \Delta \text{ for every } j$$

$$\text{i.e.} \qquad \frac{\gamma_{1j}}{1-\gamma_{1j}} = e^{\Delta}\ \frac{\gamma_{2j}}{1-\gamma_{2j}}$$

As a preliminary check, the empirical logistic transformation is used on the cumulative frequencies, and the corresponding differences for the two groups are checked to see whether they share the same sign and similar magnitude. A rough estimate on the factor exp(Δ) is then taken to be exp(unweighted average of the differences).

A more refined approach which provides a formal test on the null hypothesis is based on a weighted average, where the corresponding weights are chosen such that the variance of exp(Δ) or Δ is minimised. This results in a test on a Chi-squared component with 1 degree of freedom. The expected value and standard error of the estimate are easily obtained to enable one to construct confidence intervals on the parameter Δ. For details and derivations see [36] [37] [38].

4.1.3 Tests of Independence in r x s Frequency Tables

Consider s populations each one having r categories. Let P_{ij} be the probability by which a member from the j^{th} population is selected at random and placed in category i; for i = 1,...,r and j = 1,...,s. This may be termed the biovariate response (R,S) where $P[R=i, S=j] = P_{ij}$ and

$$\sum_{i,j} P_{ij} = 1$$

We are interested in finding whether differences, if any, exist between the distribution of R at different levels of S. We take a sample from each population and classify the units. Let n_{ij} be the frequency for the i^{th} category in the j^{th} population. Denote the marginal totals and overall total by:

$$n_{.j} = \sum_{i=1}^{r} n_{ij} \quad ; \quad n_{i.} = \sum_{j=1}^{s} n_{ij} \quad ; \quad n_{..} = \sum_{i,j} n_{ij}$$

Similarly for the probabilities (except p.. = 1)

Estimation of the probabilities from the data gives:

$$\hat{p}_{i.} = \frac{n_{i.}}{n_{..}} \quad ; \quad \hat{p}_{.j} = \frac{n_{.j}}{n_{..}}$$

When the probabilities are indepedent, the expected frequencies for each cell is

$$n_{..}\hat{p}_{ij} = n_{..}(\hat{p}_{i.})(\hat{p}_{.j})$$

The test for independence is the test for:

$$H_0 : p_{ij} = (p_{i.})(p_{.j}) \quad \text{against}$$
$$H_1 : H_A \neq H_0$$

by the statistic:

$$\chi^2 = \sum_{i,j} \left[n_{ij} - \frac{n_{i.}n_{.j}}{n_{..}} \right]^2 \Big/ \left[\frac{n_{i.}n_{.j}}{n_{..}} \right]$$

$$= \sum \frac{(\text{observed-expected})^2}{(\text{expected})}$$

which is a chi-squared distribution on (r-1)(s-1) degrees of freedom. For detailed description see [39]. Alternatively the likelihood-ratio chi-square statistic

$$L^2 = 2 \sum_i \sum_j n_{ij} \ell n \left[\frac{n_{ij}n_{..}}{n_{i.}n_{.j}} \right] = 2 \left[\sum_i \sum_j n_{ij}\ell n(n_{ij}) - \sum_i n_{i.}\ell n(n_{i.}) - \right.$$

$$\left. - \sum_j n_{.j}\ell n(n_{.j}) + n_{..}\ell n(n_{..}) \right] \quad \text{may be used}$$

4.2 Defect Characteristics

As it was pointed out at the introductory chapter of this work, the principal testing techniques used were ultrasonic testing (UT) and magnetic particle inspection (MPI). Approximately 30 km of weld were inspected by ultrasonic testing and about 76 km by magnetic particle inspection, a total of 121, 270 UT and MPI examinations.

The surface-breaking defects which are analysed in this work were detected by magnetic particle inspection in accordance with ASME section V using AC electromagnetic yoke equipment with a lifting power of 4.5 kgr. Sizing was subsequently performed by excavating or where appropriate by ultrasonics.

The embedded defects were detected and sized by manual ultrasonics. The probes had operating frequencies ranging between 2 to 5 MHz and scanning was done at angles 0°, 45°, 60° and 70° with maximum 6 dB drop.

The total amount of weld tested was defined as the length of the tested surface. The MPI weld length is approximately double the UT for the same weld number and type.

4.3 Description of the Analysis

The analysis of the data was far from straightforward, since there were both a large number of NDE records and a large number of possible parameters to be investigated. As with any statistical analysis, it was necessary to proceed in a sequential fashion, exploring possible sources of influence at a general level and then returning to examine the more important parameters in detail. One finding from the analysis is that whereas some parameters were found to be important for one fabricator they were less important for others, even for otherwise homogeneous sets of data. This is surprising since the lower hull was fabricated to a common specification throughout. Six particular fabrication yards are referred to in the present study as Aa, Bb, Cc, Dd, Ee and Ff.

In this study, the incidence of defects has been reported both in terms of defect rate defined as the ratio of the linear length of weld containing defects to the total length of weld inspected; and in terms of the occurrence of multiple defects, that is the number of NDE records reporting none, one, two and up to five or more defects. In addition, tables have been prepared showing in the finest detail the number of inspected welds and those found defective (possessing either 1 or more defects); also, in the cases of defective welds, the defect type category which has been assigned to them on detection. This detailed analysis in terms of defect rates, defective and defect free welds, multiple defects and defect types is presented in part of a nine volume report (see [40] and [25] Volumes I to VI relating to Nodes 1 to 6 respectively) which has been prepared for this purpose. Hereafter selective analyses on defect occurrence will be presented. Summaries of the raw data processed, the defect data analysed and the factors of influence examined are given in tables 4.3.1 to 4.3.3. The hierarchical nature of the defect data classification is illustrated in Fig. 4.3.1.

- Position in Lower Hull
- Length of weld examined
- Weld Type:
  - Cruciform (X)
  - Tee Butt (T)
  - Plate Butt (P)
  - Fillet (F)
- Type of NDE: MPI, UT
- Fabrication yard
- Amount of original NDE specified
- Original welding process
- Original welding procedure

Table 4.3.1

FOR EACH WELD:

- Number of defects
- Length of defect(s) in direction of welding

FOR EACH DEFECT:

- Type of defect
  - incomplete penetration
  - non—fusion, cold lap
  - slag inclusion
  - crack
  - linear indication
- Position of defect in weld body
- Depth, size and orientation of defect

Table 4.3.2

- Global location in structure: node, pontoon, etc.
- Detailed location in structure: sub—block
- Fabrication yard
- Type of welded joint
- Amount and type of NDE specified
- Welding process
- Welding procedure
- Welding position

Table 4.3.3

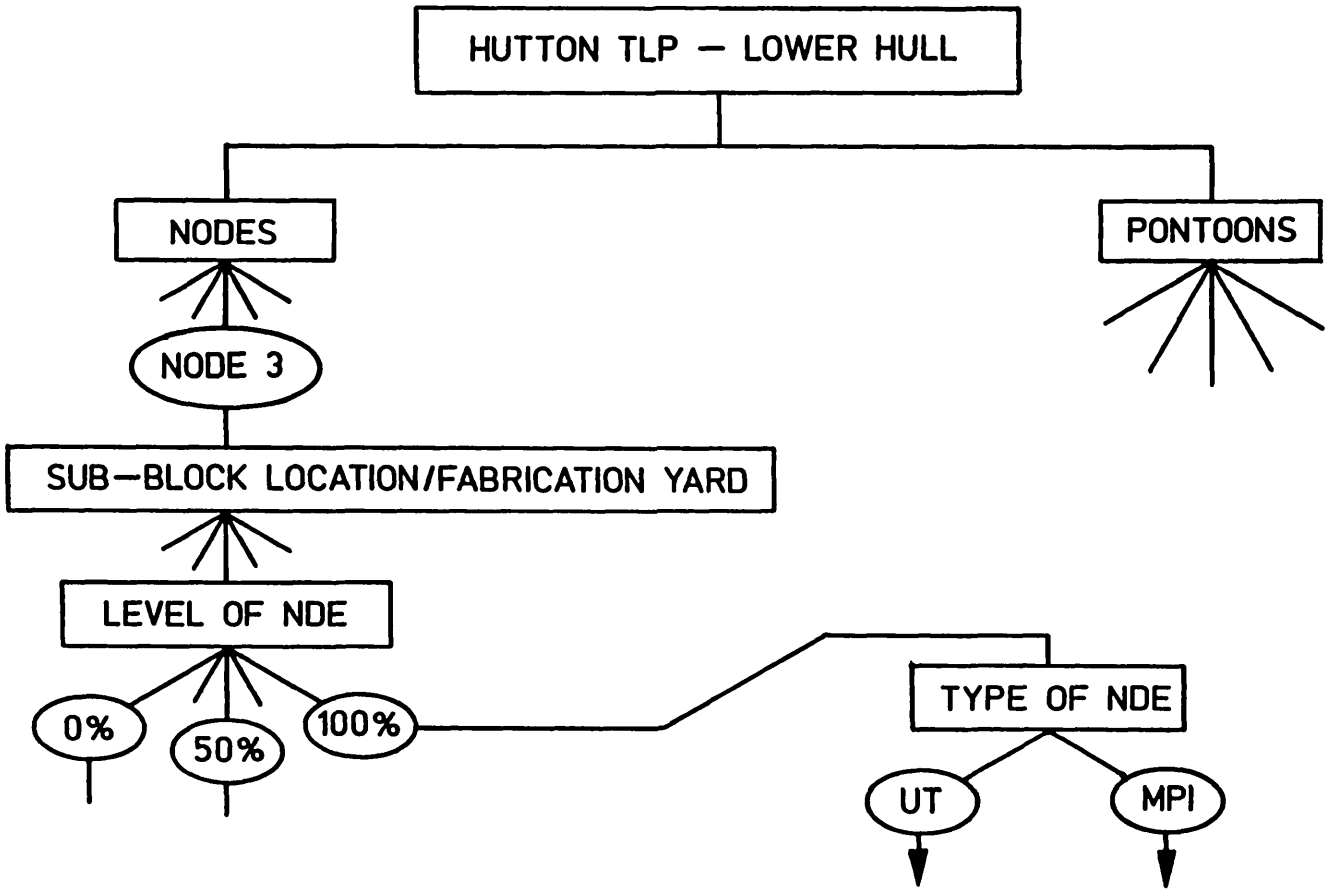


Fig. 4.3.1(a): Nature of Defect Data Classification

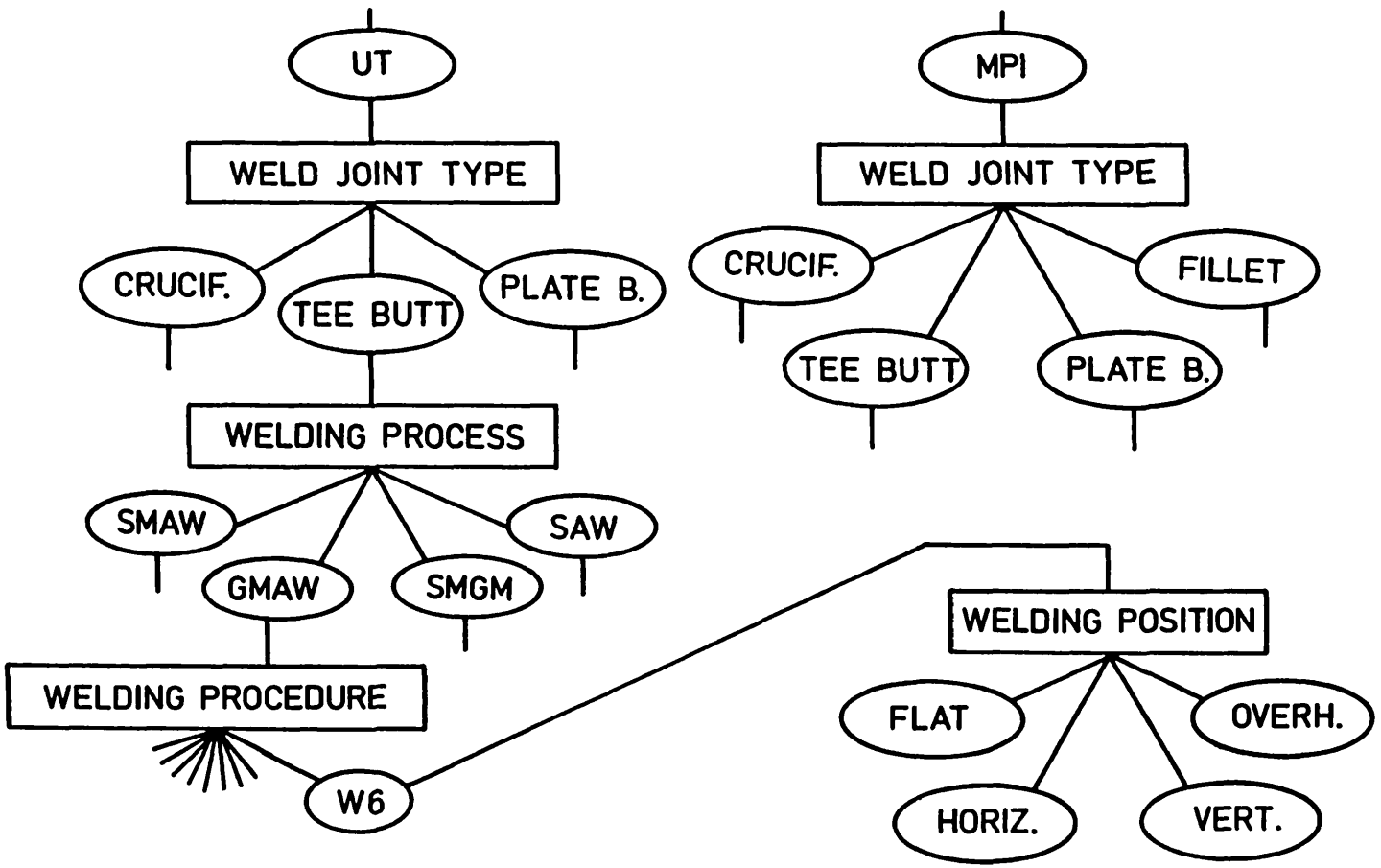


Fig. 4.3.1(b): Nature of Defect Data Classification

4.4 Overall Two-way Analysis based on Global Location and Weld Joint Type

The overall incidence of weld defects is of interest since it indicates the general standard of workmanship for the contract. However, as is discussed below, these global averages are of limited value since they mask other trends.

4.4.1 Defect Rates

The overall defect rates for embedded defects found by ultrsonic inspection (UT) are shown in table 4.4.1.1 for each of the six nodes (see fig. 3.1.1).

Weld Joint Type	Length of Weld Inspected and Percentage Defect Rate					
	Global Location - Node					
	1	2	3	4	5	6
Cruciform (m)	2152.0	2552.2	2393.7	2097.2	759.8	837.4
(%)	14.0	15.6	14.0	12.4	14.9	10.2
Tee Butt (m)	1888.7	1686.7	1587.7	2017.4	926.0	881.0
(%)	14.5	24.7	27.7	11.4	14.1	13.7
Plate Butt (m)	1649.0	1527.9	1327.3	1528.7	861.5	815.5
(%)	1.4	4.0	3.7	3.6	0.7	0.4

Table 4.4.1.1 : Overall defect rates for embedded defects found by UT

It can be seen that for tee butts and cruciforms the defect rate was rather high, and varied between 10% and 25%. The highest defect rate occurred for tee butt welds in Node 3 and was 27.7%; that is, for this category 27.7% of the total weld length inspected was found to contain defects of one type or another. The lowest defect rates were for straight plate butt welds, where the overall rate varied betwen 0.4% and 4.0%.

Similar trends are shown in table 4.4.1.2 for surface-breaking defects found by magnetic particle inspection.

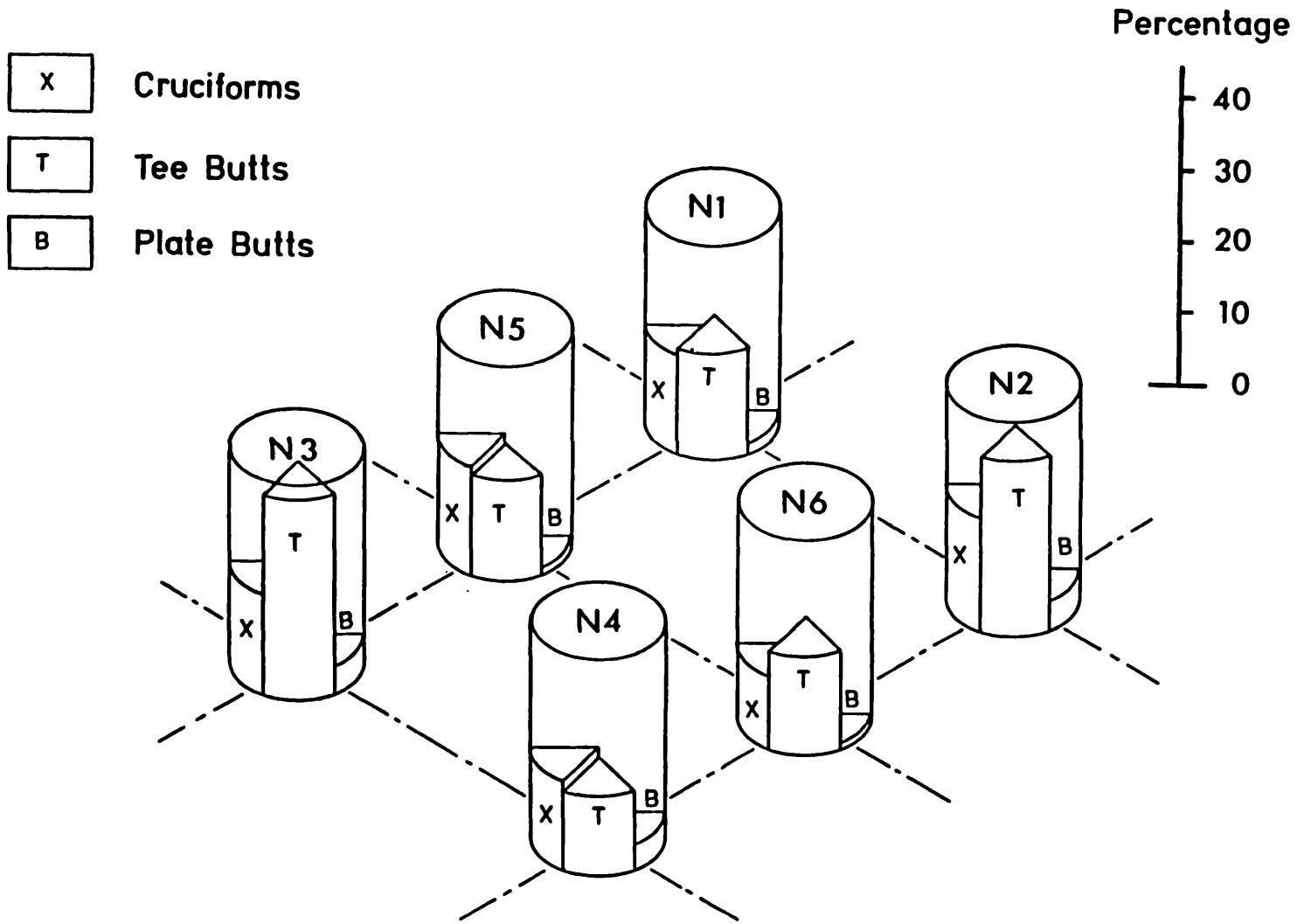


Fig. 4.4.1.1: Overall Defect Rates found by UT

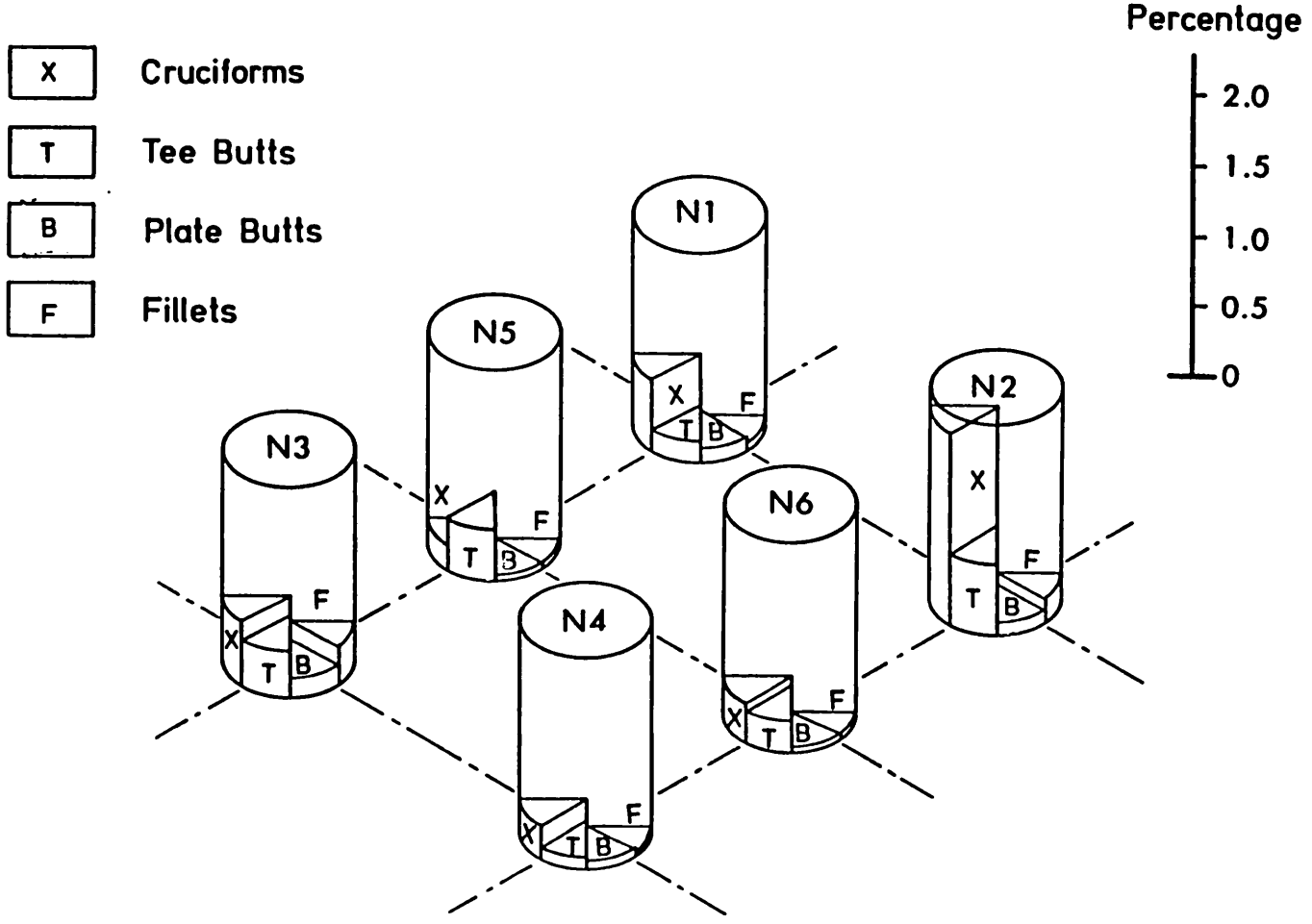


Fig. 4.4.1.2: Overall Defect Rates found by MPI

Weld Joint Type	Length of Weld Inspected and Percentage Defect Rate					
	Global Location - Node					
	1	2	3	4	5	6
Cruciform (m)	3950.0	4518.0	4013.7	3962.1	1271.1	1292.1
(%)	0.49	1.36	0.45	0.23	0.17	0.27
Tee Butt (m)	5215.2	4852.5	4363.3	4931.6	1544.3	1465.4
(%)	0.13	0.51	0.33	0.08	0.36	0.25
Plate Butt (m)	4140.7	3493.6	3356.5	3812.9	960.2	950.5
(%)	0.12	0.18	0.27	0.06	0.03	0.01
Fillet (m)	5812.7	3529.2	290.4	5563.2	1214.4	1526.3
(%)	0.06	0.18	0.27	0.06	0.03	0.01

Table 4.4.1.2 : Overall defect rates for surface defects found by MPI

In this case the defect rates were much lower, varying from 0.08% to 1.36% for cruciform and tee butt welds, and between 0.01% and 0.27% for plate butts and fillet welds.

Although tables 4.4.1.1 and 4.4.1.2 show some differences between nodes, these differences are the result of other parameters such as the amount of NDE following fabrication, welding process, welding position, fabricator, welding procedure as discussed in section 4.5.

The overall defect rates given in Tables 4.4.1.1 and 4.4.1.2 are presented graphically in Figures 4.4.1.1 and 4.4.1.2.

4.4.2 Multiple Defects

Tables 4.4.2.1 to 4.4.2.12 show the number of defective welds, for each type of welded joint and location, possessing 1, 2, 3, 4, 5 and more than 6 defects (6+). Row percentages for the frequency counts are also displayed. These row percentages in the form of three dimensional histograms are given in figures 4.4.2.1 to 4.4.2.6. Observation of row percentages across each weld type under UT, shows systematically higher proportions for defective welds having $\geq k$ defects ($k=2,\ldots,6$) for tee butts as compared with the cruciforms. Formal statistical tests in comparing the associated distributions are now performed.

Let j denote the possible number of defects in a defective weld. If two sets of such

welds are available, one being tee butts (T) and the other cruciforms (X), let θ be defined as:

$$\theta = \ell n \left[\frac{(P(T \text{ has } \leq i \text{ defects}))/(1-P(T \text{ has } \leq i \text{ defects}))}{(P(X \text{ has } \leq i \text{ defects}))/(1-P(X \text{ has } \leq i \text{ defects}))} \right]$$

Rearranging the above relationship gives:

$$\Delta = \exp(\theta) \left[\frac{(P(T \text{ has } \leq i \text{ defects}))/(1-P(T \text{ has } \leq i \text{ defects}))}{(P(X \text{ has } \leq i \text{ defects}))/(1-P(X \text{ has } \leq i \text{ defects}))} \right]$$

where, as before, i takes values from 1 to j-1.

A formal test can be performed to check whether the cumulative proportions are indeed related with the above equation, i.e. to test the hypothesis H_0 : $\theta=0$ (or $\Delta=1$) against the alternative hypothesis H_1 : $\theta\neq0$ (or $\Delta\neq1$). In the case of H_1 being true, a rough estimate of θ can be calculated using an unweighted average of the logistic transformation calculated for each value of i (see section 4.1.2). A better estimate can be found by a suitable choice of weights calculated from the data, such as to minimise the error of estimating θ. The resulting chi-square statistic (χ^2_1) on 1 degree of freedom can be checked against the 5% tabulated level (3.84) to check the validity of the test. A standard error can be attached to the estimate $\hat{\theta}$ and suitable confidence intervals can be constructed. The results can be interpreted more clearly if they are expressed in terms of $\Delta=\exp(\hat{\theta})$ known as the ratio of cumulative probabilities, or the ratio of odds.

As an example consider the data given in table 4.4.2.1. Application of the logistic transformation yields differences 0.454, 0.726, 0.941. Hence a rough estimate of θ is 1/3(0.454 + 0.726 + 0.941) = 0.707. Using weights calculated from the data gives $\hat{\theta}$=0.473, with a standard error of 0.134. The corresponding ratio of odds is $\Delta=\exp(\hat{\theta})$=1.605. Confidence intervals for $\hat{\theta}$ are 0.473 ± 0.134. The result is based on a chi-square statistic of 13.47 which compared with 3.84 suggests support of the alternative hypothesis H_1. Hence the following conclusion can be deduced: Given a weld is defective, the probability of it being multiply defective is higher for tee butts than for cruciforms. Alternatively, it can be stated that the odds of a weld being multiply defective are 1.6 times as large for tee butts as for cruciforms.

This test has been carried out for all nodes and the results are shown below in table 4.4.2.13.

Location	Unweighted θ	Weighted θ	Confidence Levels	Cumulative Ratio $\Delta=\exp(\theta)$	chi-square χ_1^2
Node 1	0.707	0.473	0.473±0.134	1.605	12.47
Node 2	0.074	0.040	0.040±0.105	1.041	0.15
Node 3	0.203	0.074	0.074±0.123	1.077	0.37
Node 4	0.910	0.435	0.435±0.156	1.55	7.82
Node 5	0.412	0.273	0.273±0.186	1.31	2.15
Node 6	1.756	1.649	1.649±0.218	5.20	57.14

Table 4.4.2.13 : Comparisons of UT defects in tee butts and cruciforms on the multiple scale

Weld Joint Type	Defect Number						
	1 Def	2 Def	3 Def	4 Def	5 Def	6+ Def	Total
X	688	118	21	7	0	5	839
T	408	98	23	6	3	11	549
B	74	16	2	0	0	1	93
F	23	1	0	0	1	0	25
Total	1193	233	46	13	4	17	1506

Table 4.4.2.1 : Multiple defects detected by UT in Node 1

Weld Joint Type	Defect Number						
	1 Def	2 Def	3 Def	4 Def	5 Def	6+ Def	Total
X	82.0	14.1	2.5	0.8	0.0	0.6	100.0
T	74.3	17.9	4.2	1.1	0.5	2.0	100.0
B	79.6	17.2	2.2	0.0	0.0	1.1	100.0
F	92.0	4.0	0.0	0.0	4.0	0.0	100.0
Total	79.2	15.5	3.1	0.9	0.3	1.1	100.0

Table 4.4.2.2 : Row percentages for defects detected by UT in Node 1

Weld Joint Type	Defect Number						
	1 Def	2 Def	3 Def	4 Def	5 Def	6+ Def	Total
X	945	183	60	37	21	23	1269
T	539	105	34	23	14	15	730
B	148	41	12	8	1	2	212
F	21	0	0	0	0	0	21
Total	1653	329	106	68	36	40	2232

Table 4.4.2.3 : Multiple defects detected by UT in Node 2

Weld Joint Type	Defect Number						
	1 Def	2 Def	3 Def	4 Def	5 Def	6+ Def	Total
X	74.5	14.4	4.7	2.9	1.7	1.8	100.0
T	73.8	14.4	4.7	3.2	1.9	2.1	100.0
B	69.8	19.3	5.7	3.8	0.5	0.9	100.0
F	100.0	0.0	0.0	0.0	0.0	0.0	100.0
Total	74.1	14.7	4.7	3.0	1.6	1.8	100.0

Table 4.4.2.4 : Row percentages for defects detected by UT in Node 2

Weld Joint Type	Defect Number						
	1 Def	2 Def	3 Def	4 Def	5 Def	6+ Def	Total
X	740	136	31	16	7	7	937
T	520	95	22	12	9	9	667
B	126	48	17	5	2	0	198
F	11	1	0	0	0	0	12
Total	1397	280	70	33	18	16	1814

Table 4.4.2.5 : Multiple defects detected by UT in Node 3

Weld Joint Type	Defect Number						
	1 Def	2 Def	3 Def	4 Def	5 Def	6+ Def	Total
X	79.0	14.5	3.3	1.7	0.7	0.7	100.0
T	78.0	14.2	3.3	1.8	1.3	1.3	100.0
B	63.6	24.2	8.6	2.5	1.0	0.0	100.0
F	91.7	8.3	0.0	0.0	0.0	0.0	100.0
Total	77.0	15.4	3.9	1.8	1.0	0.9	100.0

Table 4.4.2.6 : Row percentages for defects detected by UT in Node 3

Weld Joint Type	Defect Number						
	1 Def	2 Def	3 Def	4 Def	5 Def	6+ Def	Total
X	615	90	18	4	3	2	732
T	342	60	14	10	6	7	439
B	158	33	5	2	0	1	199
F	6	2	0	0	0	0	8
Total	1121	185	37	16	9	10	1378

Table 4.4.2.7 : Multiple defects detected by UT in Node 4

Weld Joint Type	Defect Number						
	1 Def	2 Def	3 Def	4 Def	5 Def	6+ Def	Total
X	84.0	12.3	2.5	0.5	0.4	0.3	100.0
T	77.9	13.7	3.2	2.3	1.4	1.6	100.0
B	79.4	16.6	2.5	1.0	0.0	0.5	100.0
F	75.0	25.0	0.0	0.0	0.0	0.0	100.0
Total	81.3	13.4	2.7	1.2	0.7	0.7	100.0

Table 4.4.2.8 : Row percentages for defects detected by UT in Node 4

Weld Joint Type	Defect Number						
	1 Def	2 Def	3 Def	4 Def	5 Def	6+ Def	Total
X	282	51	15	7	2	0	357
T	215	46	15	6	5	2	289
B	32	4	0	0	0	0	36
F	0	0	0	0	0	0	0
Total	529	101	30	13	7	2	682

Table 4.4.2.9 : Multiple defects detected by UT in Node 5

Weld Joint Type	Defect Number						
	1 Def	2 Def	3 Def	4 Def	5 Def	6+ Def	Total
X	79.0	14.3	4.2	2.0	0.6	0.0	100.0
T	74.4	15.9	5.2	2.1	1.7	0.7	100.0
B	88.9	11.1	0.0	0.0	0.0	0.0	100.0
F	0.0	0.0	0.0	0.0	0.0	0.0	0.0
Total	77.6	14.8	4.4	1.9	1.0	0.3	100.0

Table 4.4.2.10 : Row percentages for defects detected by UT in Node 5

Weld Joint Type	Defect Number						
	1 Def	2 Def	3 Def	4 Def	5 Def	6+ Def	Total
X	262	30	7	2	1	1	303
T	97	40	24	6	2	5	174
B	22	6	0	0	0	0	28
F	0	0	0	0	0	0	0
Total	381	76	31	8	3	6	505

Table 4.4.2.11 : Multiple defects detected by UT in Node 6

Weld Joint Type	Defect Number						
	1 Def	2 Def	3 Def	4 Def	5 Def	6+ Def	Total
X	86.5	9.9	2.3	0.7	0.3	0.3	100.0
T	55.7	23.0	13.8	3.4	1.1	2.9	100.0
B	78.6	21.4	0.0	0.0	0.0	0.0	100.0
F	0.0	0.0	0.0	0.0	0.0	0.0	0.0
Total	75.4	15.0	6.1	1.6	0.6	1.2	100.0

Table 4.4.2.12 : Row percentages for defects detected by UT in Node 6

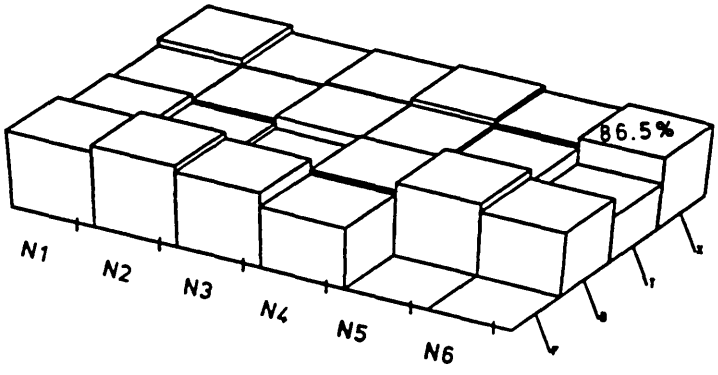


Fig. 4.4.2.1: Row Percentages for Welds Possessing 1 Defect

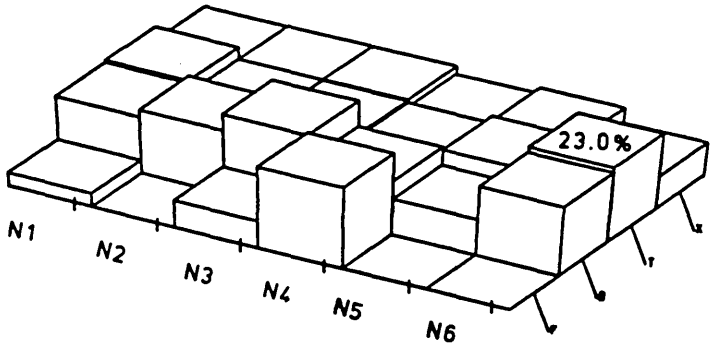


Fig. 4.4.2.2: Row Percentages for Welds Possessing 2 Defects

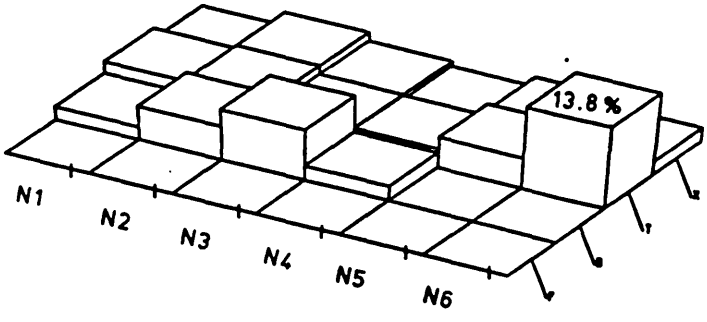


Fig. 4.4.2.3: Row Percentages for Welds Possessing 3 Defects

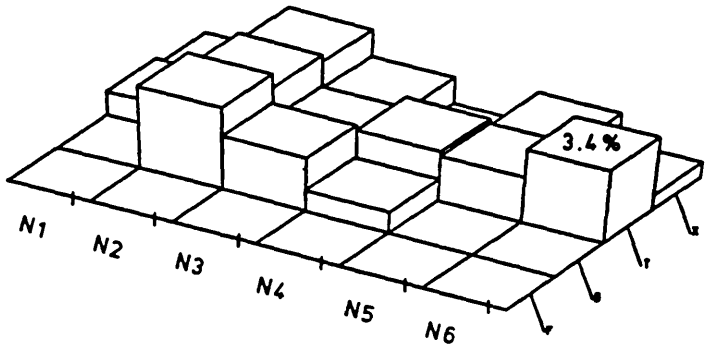


Fig. 4.4.2.4 : Row Percentages for Welds Possessing 4 Defects

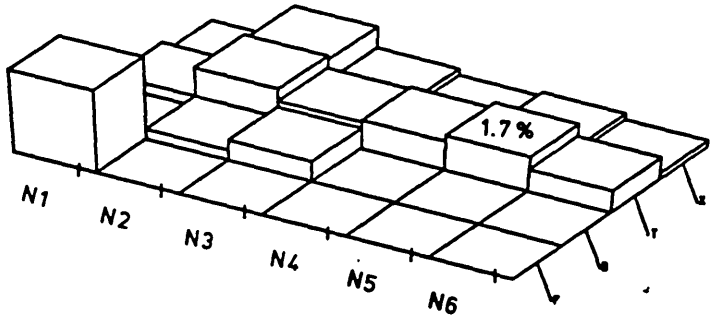


Fig.4.4.2.5 : Row Percentages for Welds Possessing 5 Defects

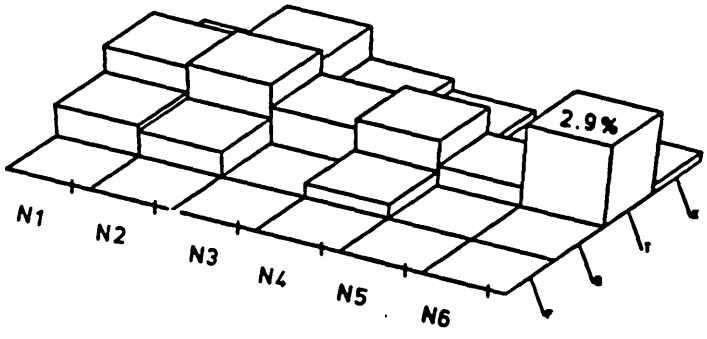


Fig. 4.4.2.6 : Row Percentages for Welds Possessing 6 or more Defects

The table shows that the same result was found in all the nodes, namely that tee butts are more likely to be multiply defective than cruciform welds. In all cases, except nodes 2 and 3, these findings are statistically significant. This conclusion from the data analysis is examined in more detail in following sections of this chapter.

4.4.3 Defect Types

Irrespective of the type of welded joint, the defects detected by UT were found to be mainly of the non-fusion type (NF). The percentages of NF defects as proportions of all defects are shown in table 4.4.3.1, for the various nodes.

Weld Joint Type	Node 1	Node 2	Node 3	Node 4	Node 5	Node 6
X	79.5	70.0	73.8	73.7	73.3	68.7
T	76.5	73.1	77.5	73.2	78.5	73.5
B	67.2	63.8	54.0	59.0	73.7	79.4

Table 4.4.3.1 : Percentage proportion of non-fusion defects (UT)

The percentage of non-fusion defects are typically between 60% and 80% of all embedded defects with the majority of the remainder being reported as slag inclusions. The percentages in table 4.4.3.1 show a high degree of consistency between nodes for any given type of welded joint, with only a few exceptions. Averaged over Nodes 1 to 4, the percentage of non-fusion defects is approximately 60% for plate butt welds compared with about 75% for both cruciforms and tee butts. However, in Nodes 5 and 6 the percentage of non-fusion defects is about 75% for all weld types.

A similar analysis for crack-like defects (CR) within the body of the weld is shown in table 4.4.3.2. The percentage proportion of crack-like defects is small, ranging from about 2% to 8%.

Weld Joint Type	Node 1	Node 2	Node 3	Node 4	Node 5	Node 6
X	3.1	3.7	5.8	2.9	3.1	5.6
T	5.3	4.3	4.8	4.4	3.0	2.2
B	2.6	2.3	3.3	1.6	7.9	5.9

Table 4.4.3.2 : Percentage proportion of crack-like defects (UT)

Considering all defect types and locations, the types in order of decreasing frequency of occurrence are: non-fusion (NF) 73%, slag (SL) 22%, crack (CR) 4% and porosity (PO) 1%.

A further analysis has been undertaken to check whether the differences in the frequency of occurrence of different defect types, between types of welded joint, discussed above, is statistically significant. The results have shown that the differences between X and T welds are not significant but the differences between B welds and the other two types are highly significant. The χ^2 statistic on observed differences between X, T and B welds taken over all defect types is 15.97 on 4 degrees of freedom for Node 1. A similar analysis for Nodes 2, 3 and 4 give statistics of 13.94, 93.04 and 30.69 respectively on 4 degrees of freedom - all highly significant. However for Nodes 5 and 6 these differences do not exist.

The differences reported above are likely to be real and to be associated with the different welding procedures used for plate butt welds.

Turning now to surface-breaking defects found by MPI, the statistics in each location and across every type of welded joint are dominated by defects of the linear indication type (LI) with the exception of cruciform joints in Nodes 1, 2 and 5. Table 4.4.3.3 shows the percentage of LI defects as a proportion of all defects.

Weld Joint Type	Node 1	Node 2	Node 3	Node 4	Node 5	Node 6
X	39.1	41.8	97.8	88.7	32.4	76.5
T	71.1	76.0	94.1	65.9	75.0	89.4
B	83.3	94.0	95.8	96.7	77.8	66.7
F	92.9	95.7	95.4	98.6	85.7	100

Table 4.4.3.3 : Percentage of proportion of linear indication defects (LI)

The percentages in table 4.4.3.3 show a high degree of relative consistency between nodes for the three weld types T, B and F. The average percentages of LI defects for all nodes are respectively 78.6, 85.6 and 94.7. In cruciform welds there is an apparent dependence on location with an average occurrence of 37.8% for Nodes 1, 2, 5 and 87.7% for Nodes 3, 4, 6. Comparisons between X and T have shown these differences to be highly significant with associated chi-square statistics χ^2_2=101.38, χ^2_2=139.11, χ^2_2=12.75 respectively for Nodes 1, 2 and 5.

The remainder of the defects are mostly crack-like defects (CR) as indicated in table 4.4.3.4.

Weld Joint Type	Node 1	Node 2	Node 3	Node 4	Node 5	Node 6
X	48.4	46.4	0.7	5.6	44.1	9.8
T	10.3	18.0	1.5	7.7	12.5	2.1
B	1.9	2.4	2.8	0.0	22.2	33.3
F	3.6	2.2	4.6	0.0	14.3	0.0

Table 4.4.3.4 : Percentage of proportion of crack-like defects (CR)

The results given above show a high degree of consistency with the exception of cruciform welds in Nodes 1, 2 and 5. However, since Nodes 1 and 4, 2 and 3, and 5 and 6 were fabricated by the same groups of fabricators and show great similarities in defect rates, it is very unlikely that the differences in defect type reported above are real. It must be presumed that NDE inspectors in Nodes 1, 2 and 5 were more likely to use the term 'crack' than 'linear indication' when first observing a linear type of surface-breaking defect. However, this mis-classification is relatively unimportant and had no effect on any of the other results.

4.5 Detailed Analysis According to Parameters of Influence

4.5.1 Defect Rates

The specification for fabrication of the lower hull provided for varying amounts of NDE. In areas which were considered to be of critical importance from the point of view of fatigue, 100% UT and 100% MPI was specified for all welds. Conversely, in structurally unimportant and fatigue insensitive areas 0% NDE was required. In other regions amounts varying between 20% and 60% were called for. In the analysis described here, only the two extreme categories of 0% and 100% are considered. These categories referred to the inspection of welds following fabrication (see introductory section of chapter 3).

Global Location	Welding Process	Weld Type	0% NDE		100% NDE	
Node 1	SMAW		Aa	Bb	Aa	Bb
		Cruciform	28.63	26.88	0.93	2.08
		Tee Butt	23.37	69.00	0.34	0.00
		Plate Butt	11.13	-	0.14	0.00
	GMAW	Cruciform	34.71	0.00	0.72	0.00
		Tee Butt	12.52	1.73	0.61	-
		Plate Butt	1.19	-	0.02	0.00
Node 2	SMAW		Cc	Dd	Cc	Dd
		Cruciform	6.63	33.44	1.06	10.62
		Tee Butt	5.49	51.20	0.88	14.25
		Plate Butt	1.93	16.96	0.00	3.50
	GMAW	Cruciform	3.46	33.19	1.14	35.03
		Tee Butt	3.80	37.44	6.41	22.18
		Plate Butt	0.00	51.84	-	4.07
Node 6	SMAW		Ee	Ff	Ee	Ff
		Cruciform	11.31	8.84	3.09	8.81
		Tee Butt	2.69	6.49	1.91	-
		Plate Butt	0.63	0.00	0.29	3.63
	GMAW	Cruciform	-	30.70	-	20.81
		Tee Butt	-	39.67	-	-
		Plate Butt	-	6.43	-	-

Table 4.5.1.1 : Percentage defect rates for embedded defects – for various parameters

Table 4.5.1.1 shows the defect rates for embedded defects for Nodes 1, 2 and 6, classified according to welding process, type of welded joint, fabricator and the specified amount of original NDE.

For Node 1, it can be seen that for both fabrication yards (Aa and Bb), the effect of NDE has produced a dramatic fall in the defect rate for all three weld types and for both welding processes (GMAW and SMAW). For fabricator Aa, the highest defect rates were for the cruciform welds with 5% NDE (28.63% and 34.71% welded by SMAW and GMAW respectively), but these rates both fell to less than 1% under conditions of 100% NDE. For plate butt welds the defect rates are lower, but nevertheless the effect of 100% NDE has been to reduce the rates by a factor of between 50 and 100. This very significant reduction for plate butt welds probably reflects the relative ease with which such joints can be checked by ultrasonic methods.

For Node 2 a somewhat different pattern emerged. It can be seen from table 4.5.1.1 that both for welds subjected to 100% NDE and for welds not subjected to NDE, the defect rates for fabricator Dd were much higher than for Cc. Indeed, the defect rates for fabricator Dd after 100% NDE were higher than the rates for fabricator Cc with no NDE. However, for any one fabrication yard and weld parameter, the defect rates for welds subjected to NDE were lower than for welds not subjected to NDE in all but two cases.

For Node 6 the pattern is again different with the defect rates for welds subjected to 100% NDE being a factor of only three or less than the rates for welds with 0% NDE (see Fig. 4.5.1.1).

Turning now to surface-breaking defects found by MPI, some statistics for Node 2 are given in table 4.5.1.2, see also Fig. 4.5.1.2. These results are reasonably representative of the other nodes and are interesting for three main reasons.

- Comparison between fabricators shows that the defect rate was significantly different.

- The average defect rate for surface-breaking defects can be seen to be very much lower than for embedded defects.

- The defect rate for welds subjected to 100% NDE was greater than for welds with no NDE.

Global Location	Welding Process	Weld Type	0% NDE		100% NDE	
			Cc	Dd	Cc	Dd
Node 2	SMAW	Cruciform	0.74	1.10	1.45	1.23
		Tee Butt	0.04	1.10	0.18	1.19
		Plate Butt	0.00	0.17	0.03	0.27
		Fillet	0.00	1.15	0.00	2.30
	GMAW	Cruciform	1.38	2.39	3.09	4.00
		Tee Butt	0.00	1.46	0.30	4.67
		Plate Butt	0.00	0.41	0.00	0.20
		Fillet	0.00	1.91	0.00	-

Table 4.5.1.2 : Percentage defect rates for surface-breaking defects - for various parameters

This last finding can be explained by reference to table 4.5.1.3, see also Fig. 4.5.1.3. Table 4.5.1.3 shows the overall defect rates for both embedded and surface-breaking defects for various weld types, welding processes and NDE rates, together with two other statistics - the average defect length (ADL) and the average distance between defects (ADBD). This shows that for embedded defects the average defect length in welds which had no NDE was, on average, about four times that for welds which had been subjected to NDE.

Defect Type	Welding Process	Weld Type	0% NDE			100% NDE		
			DR (%)	ADL (mm)	ADBD (m)	DR (%)	ADL (mm)	ADBD (m)
Embedded Defects	SMAW	Cruciform	28.50	276	0.97	1.07	103	9.65
		Tee Butt	29.78	430	1.45	0.31	84	27.29
		Plate Butt	11.13	240	2.16	0.13	69	54.21
	GMAW	Cruciform	28.72	391	1.36	0.72	91	12.55
		Tee Butt	12.15	298	2.45	0.61	81	13.31
		Plate Butt	1.19	121	10.16	0.02	25	110.85
Surface Breaking Defects	SMAW	Cruciform	0.316	33	10.4	0.715	61	8.5
		Tee Butt	0.112	13	11.8	0.165	30	18.3
		Plate Butt	0.099	23	23.6	0.185	270	145.8
		Fillet	0.144	112	77.3	0.083	60	72.0
	GMAW	Cruciform	0.159	31	19.5	0.344	47	13.6
		Tee Butt	0.026	11	41.0	0.047	13	28.5
		Plate Butt	0.062	9	14.2	0.0	-	-
		Fillet	0.023	34	150.5	0.050	48	94.9

DR – Defect rate (%)

ADL – Average defect length (mm), measured along the weld

ADBD – Average distance between defects (m), in the direction of welding

Table 4.5.1.3 : Effect of amount of NDE on defect statistics for embedded and surface-breaking defects in Node 1

However, in the case of surface-breaking defects the average defect length was typically twice as long as for welds which were subjected to 100% NDE than for those with no NDE. Although table 4.5.1.3 shows results just for Node 1, similar trends were shown by the other nodes. Comparison of all the ADBD statistics showed that for cruciform and tee butt welds the average distance between surface-breaking defects did not differ markedly between 0% NDE and the 100% NDE categories. This shows that the number of surface-breaking defects detected per metre run during the reinspection was the same, irrespective of the original level of NDE, in this case, MPI, indicating that the original NDE was ineffectual. This

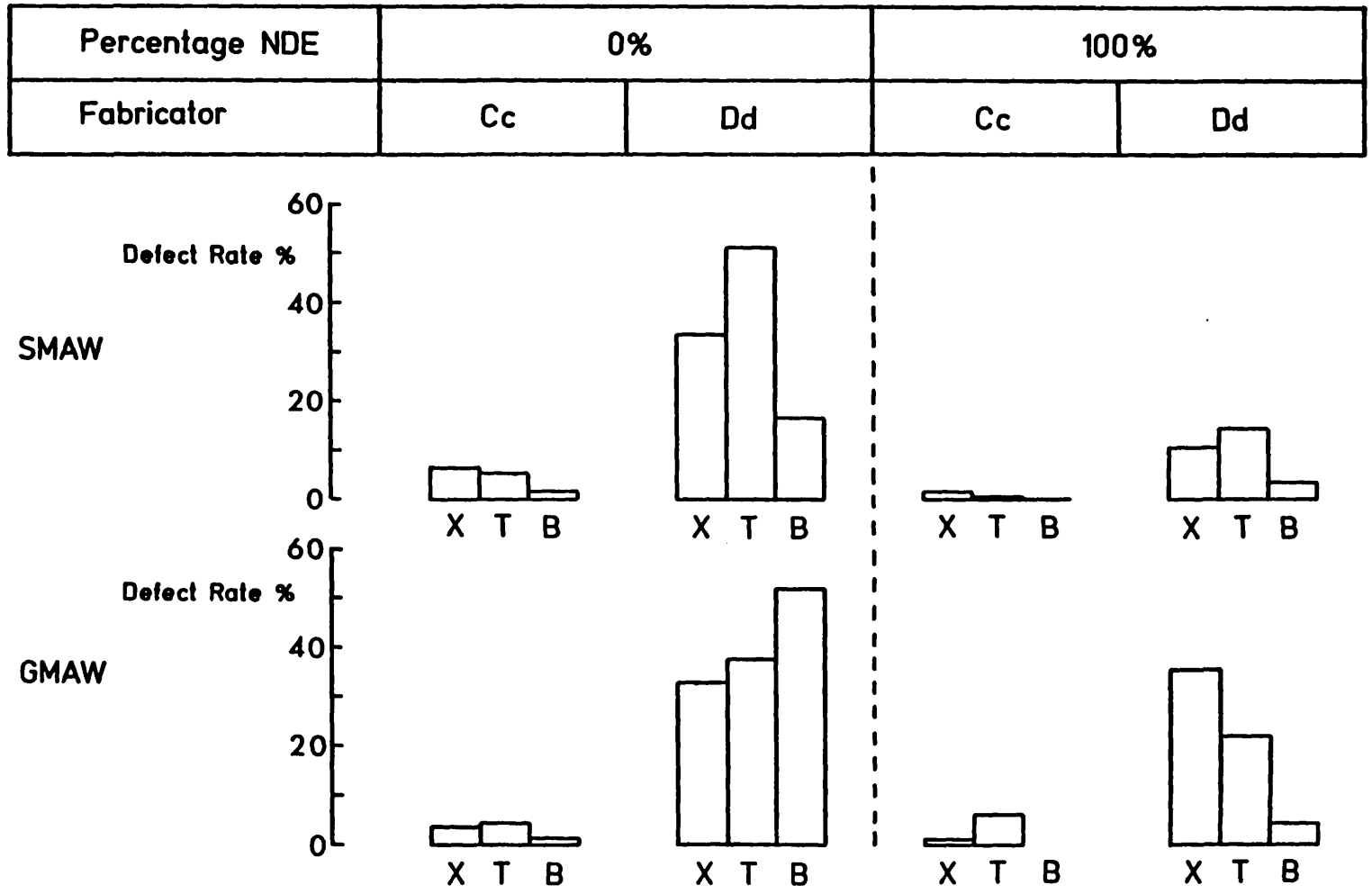


Fig. 4.5.1.1: Percentage Defect Rates for Embedded Defects

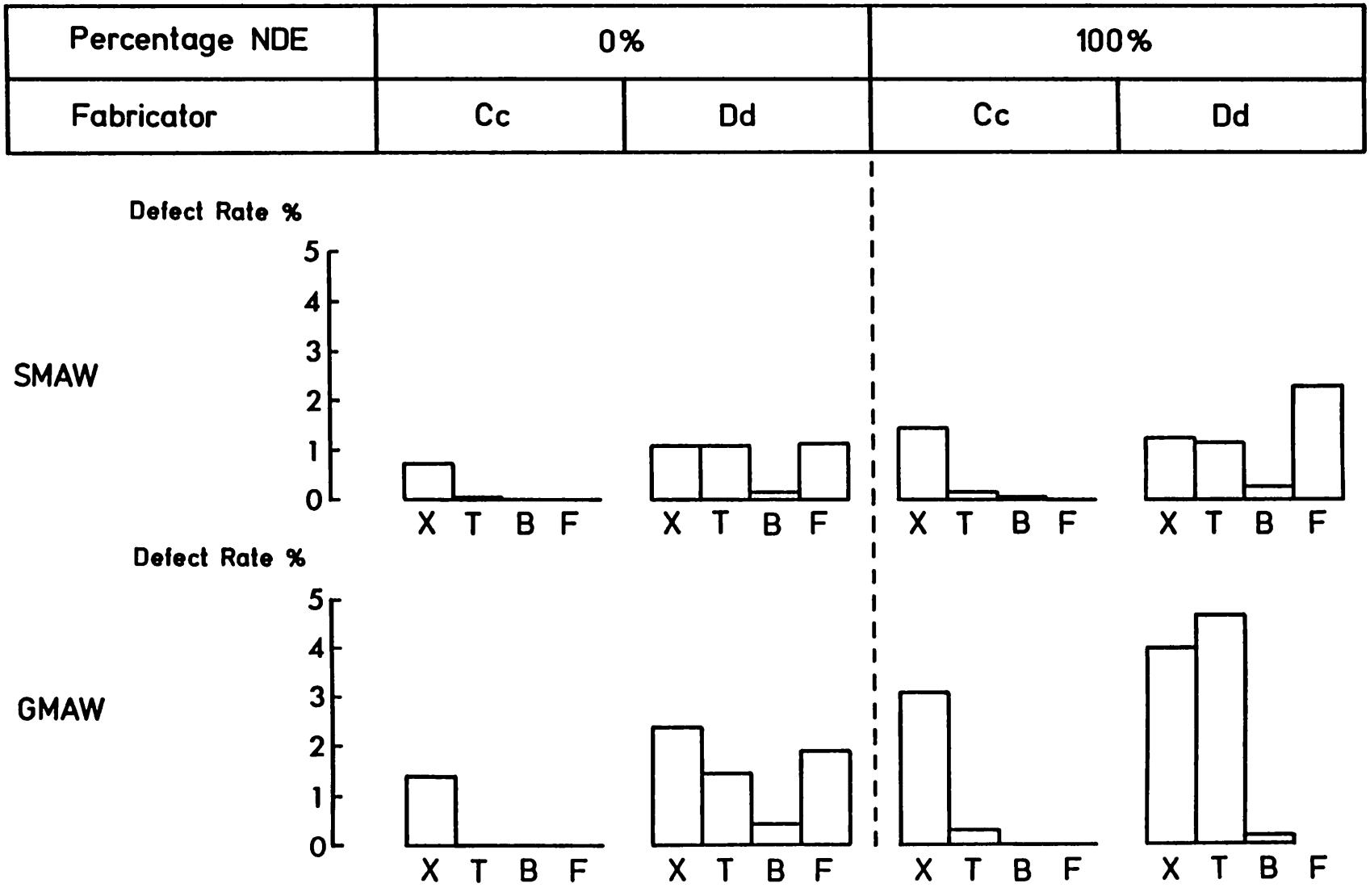


Fig. 4.5.1.2: Percentage Defect Rates for Surface-Breaking Defects

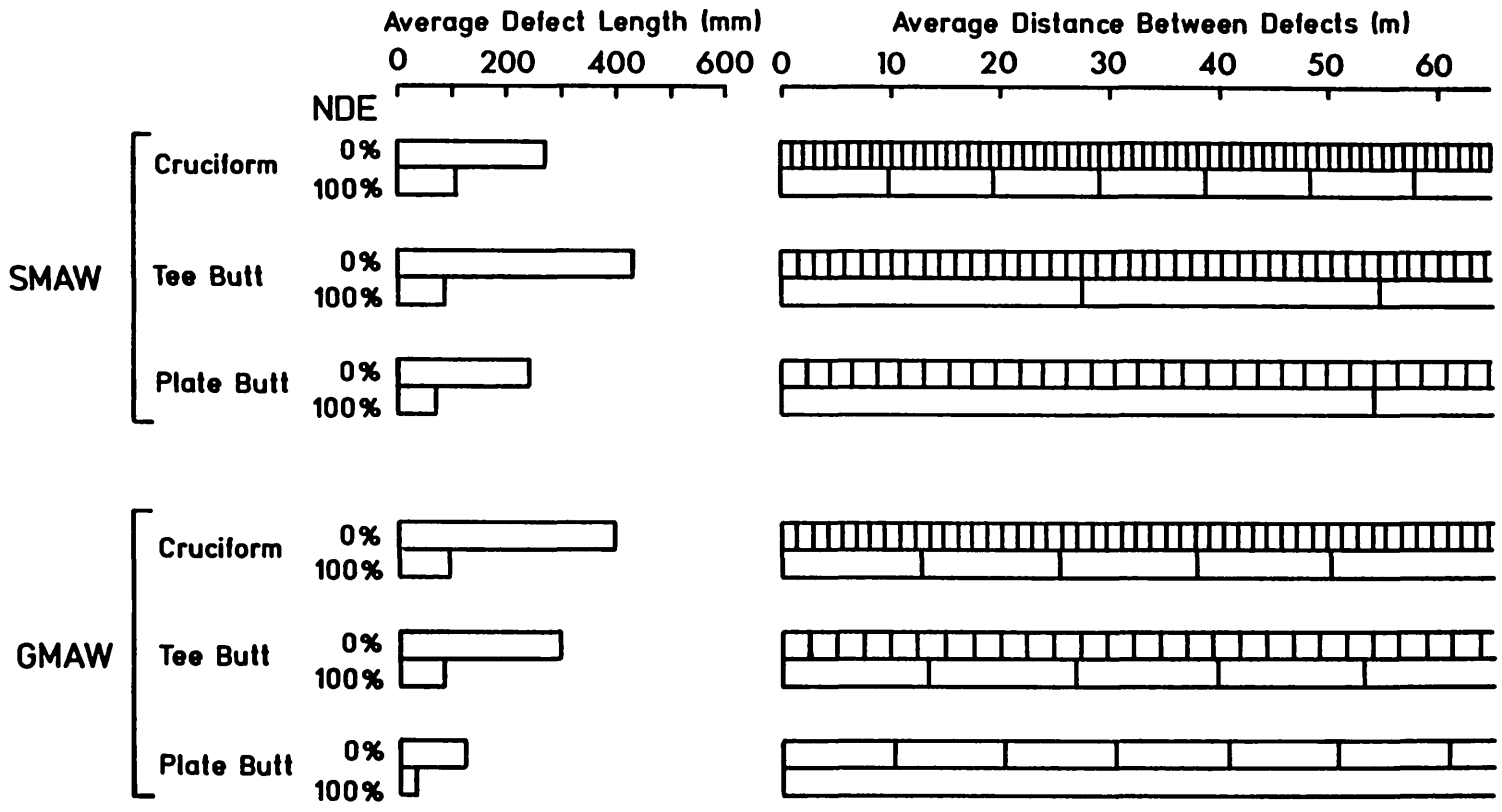


Fig. 4.5.1.3: Effect of Amount of Specified NDE on Defect Statistics for Embedded Defects in Node 1

combined with the fact that on average the defects in the zones which had been selected for 100% NDE were longer than elsewhere, has produced the initially surprising result mentioned above, that the defect rate in regions subjected to 100% MPI was higher than elsewhere.

Influence of Fabricator

Examination of tables 4.5.1.1 and 4.5.1.2 shows that the overall defect rates differed appreciably between nodes. These differences are due in part to varying effectiveness of the NDE procedures at the different fabrication yards, as discussed above, and in part to other factors such as the welding process used (see below). However, detailed analysis of the data, sub-divided according to fabricator, has shown that there were nevertheless marked differences in defect rates between fabricators, even when other sources of influence had been taken into account (see for example tables 4.5.1.1 and 4.5.1.2). In the case of fabricators Cc and Dd, the defect rates differed by a factor of about 10.

Influence of Type of Welded Joint

This was found to be one of the most important parameters in governing the occurrence of weld defects in the initial weld before any repair. The overall defect rates for embedded defects were found to be in the ranges 10% to 16% for cruciform welds, 11% to 28% for tee butts and 0.4% to 4% for plate butts. The corresponding figures for surface-breaking defects were 0.17% to 1.4% for cruciforms, 0.08% to 0.52% for tee butts, 0.01% to 0.12% for plate butts and 0.01% to 0.19% for fillet welds. However, these within-weld type and between-weld type differences were affected by other factors such as the welding process used and the amount of NDE applied. As discussed above, these latter factors did not have a consistent influence and it was found that the defect rates for certain combinations of weld type and welding process were significantly higher for some fabricators than for others.

Influence of Welding Process

The three main welding processes that were used in the fabrication of the lower hull were SMAW, GMAW and SAW (see section 3.4). The type of welding process used in the fabrication has been found to be an important factor affecting the defect rates. Some conclusions apply regardless of fabricator and weld type, whilst others are fabricator and weld type dependent.

A general conclusions was that the SAW process, which was used only for plate butt

welds welded in the flat position, was extremely reliable, being associated with very low defect rates. For Nodes 1 and 4, there were practically no defects found in welds made by this process, either surface or embedded. In Nodes 5 and 6, there were no surface-breaking defects and the embedded defect rate was low. In Nodes 2 and 3, welds made by fabricator Cc were very low and only welds made by fabricator Dd showed an appreciable defect rate.

For the welding processes SMAW and GMAW, very much higher defect rates were found, together with significant differences between fabricators. A brief summary is as follows:

(1) For fabricators Ee and Ff the overall defect rates were between 2 and 3 times greater for the GMAW process than for SMAW, for both cruciform and tee butt joints. This was true for both surface and embedded defects. For welds which were not originally subjected to NDE, the GMAW defect rate was 4 times that for SMAW (8% and 35% for SMAW and GMAW respectively for embedded defects, and 0.1% and 0.5% for surface-breaking defects).

(2) For fabricators Ee and Ff the rates for the SMAW and GMAW processes in plate butt welds differed by a factor of 10, GMAW giving the higher rate.

(3) In general the defect rate for the GMAW process was poor in comparison with that for the SMAW process. However, even in cases where the defecct rate was approximately the same, it was found that the chances of having a weld with multiple defects was much higher for the GMAW process than for the SMAW process. This will be discussed in detail in section 4.5.3.

Influence of Welding Positions

Because of the relatively large influence of weld type, welding process and fabricator on defect rates, the influence of welding position was only noticeable when examining otherwise homogeneous sets of data. Statistical tables have been produced which give information on defect rate and the proportion of defective welds for welds made in the flat (1G), horizontal (2G), vertical (3G) and overhead (4G) position. Detailed numerical results are given in [25, 40]. The general conclusion that can be drawn is that there is an increase in defect rate with increased difficulty of welding in the order given above. A number of examples are now given:

(1) For tee butt welds made by fabricator Ee using the manual SMAW process, the defect rates for embedded defects for the 1G, 2G, 3G positions were 0.4%,

2.6% and 5.6% respectively. The corresponding rates for fabricators Ff were 8.1%, 14.4% and 39.0%.

(2) Examining cruciform welds produced by fabricator Ff using welding procedure W6-SMAW, the defect rates for surface-breaking defects were found to be 0%, 0.14%, 0.36% and 0.61% for the 1G, 2G, 3G and 4G positions, respectively.

(3) The above results are quoted for welds subjected to varying amounts of original NDE and unknown amounts of repair before phase III NDE, and could therefore be subject to bias. However, a detailed analysis of the welds in Nodes 1 and 4 for various levels of original NDE has shown that this is not the case and that the differences in defect rates between welding positions are highly significant.

It should be noted that these conclusions apply only for defect rates. When multiple defects are taken into account a more complex pattern emerges, with welds made in the horizontal position showing a high frequency of defects. This will further be discussed in section 4.5.3.

Influence of Welding Procedure

A large number of different welding procedures were used in the fabrication of the lower hull and it was not possible to examine them all because of relatively small sample sizes. However, a general and not altogether surprising conclusion that is strongly supported by the data, is that welding procedures involving large numbers of passes tend to produce welds with higher defect rates than procedures requiring only a small number of passes.

4.5.2 Binary Analysis

This section contains a selective analysis of data related to untrasonic inspection and magnetic particle testing in Nodes 1 and 4. This pair of nodes had been fabricated by the same fabricators and they are of the same structural detail in terms of sub-block identification. Similar results to the ones presented in this section were observed in the two other pairs of nodes i.e. Nodes 2 and 3, and Nodes 5 and 6. Special attention here is focussed on the binary observations, i.e. a weld inspected constitutes a trial and if one defect or more is found the outcome of the trial takes the value 1, otherwise the value of 0. The statistical theory of analysing this type of data was presented earlier in section 4.1.1.

4.5.2.1 Embedded Defects found by Ultrasonics

Table 4.5.2.1.1 shows the number of defective welds r_i out of n_i welds inspected, classified according to type of welded joint (cruciform and tee butts), SMAW welding position (1G, 2G, 3G) and node location (Nodes 1 and 4).

		Node 1		Node 2, 4	
position		Weld Joint Type		Weld Joint Type	
		X	T	X	T
1G	r_i	77	53	51	28
	n_i	296	180	257	107
	p_i	0.2601	0.2044	0.1984	0.2617
	v_i	0.00065	0.00116	0.00062	0.00182
2G	r_i	143	185	84	98
	n_i	567	454	432	346
	p_i	0.2522	0.4075	0.1944	0.2832
	v_i	0.00033	0.00053	0.00036	0.00059
3G	r_i	192	57	203	50
	n_i	952	185	932	171
	p_i	0.2017	0.3081	0.2178	0.2924
	v_i	0.00097	0.00116	0.00018	0.00122

Table 4.5.2.1.1 : Number of defective welds r_i out of n_i inspected

The table is a 3 x 2 x 2 factorial system with the outcome of each weld inspection being a binary variable.

For the purpose of investigating the effect of welding position (1G – flat, 2G–horizontal, 3G–vertical), the positions have been ranked according to the assumed degree of difficulty in welding (i.e. 1G → 2G → 3G).

An unbiased estimate of the variance of the proportions p_i has been calculated as $v_i=(r_i(n_i-r_i))/(n_i^2(n_i-1))$ and is shown in each cell of table 4.5.2.1.1. It can be seen that the variances of tee butts are greater than for cruciforms because of the smaller number of inspected tee butt welds. The estimate of variance is based on the

binomial distribution and any violation of the independence assumption between welds of the same type would tend to inflate v_i.

To investigate the various factors which influence the proportion of defective welds the various cells in table 4.5.2.1.1 have been combined to make three further tables by unweighted averaging (table 4.5.2.1.2).

SMAW Position	Weld Type		
	X	T	X+T
1G	0.2293	0.2781	0.2537
2G	0.2233	0.3453	0.2843
3G	0.2098	0.3003	0.2551
1G+2G+3G	0.2208	0.3079	0.2644

SMAW Position	Global Location		
	N1	N4	N1+N4
1G	0.2773	0.2301	0.2537
2G	0.3299	0.2388	0.2843
3G	0.2549	0.2551	0.2551
1G+2G+3G	0.2870	0.241	0.2644

SMAW Position	Global Location		
	N1	N4	N1+N4
X	0.2380	0.2035	0.2208
T	0.3367	0.2791	0.3079
X+T	0.2874	0.2413	0.2543

Table 4.5.2.1.2 : Two-way and marginal proportions

Table 4.5.2.1.2 shows:

- the proportions of defective welds are higher for tee butts than for cruciforms in both Nodes 1 and 4.

- the proportion of defective welds is higher in Node 1 than Node 4 for both tee butts and cruciforms.

- the horizontal 2G position is the most dominant in being associated with a high percentage of defective welds.

To investigate the precision with which these conclusions can be stated the usual factorial contrasts are calculated and displayed in table 4.5.2.1.3. The values of the mean square values which exceed 3.84 times the mean square for the theoretical error indicate sources of influence which are significant at the 5% significance level.

The influence of weld type (source Y in table 4.5.2.1.3, part (i)) in affecting the proportion of defective welds is seen to be overwhelmingly significant and the location effect (L) is also highly significant. The quadratic position effect (P_Q) is not quite significant at the 5% level but the L X P_Q interaction is (probably because of the importance of L). None of the other interactions is seen to be important.

Because of the importance of the type of welded joint, part (ii) of table 4.5.2.1.3 has been prepared to show the importance of the various sources of influence for the two weld types separately. The location effect is significant for both weld types. The P_Q component, demonstrating the importance of the 2G welding position on the proportion of defective welds in tee butts is on the borderline of significance.

(i) Full Data

Source	Degrees of Freedom	Mean Square
Location L (N1 or N2)	1	0.00635
Type Y (X or T)	1	0.02277
Position (Linear) P_L	1	0.000004
Position (Quadr.) P_Q	1	0.00240
L x Y	1	0.00040
L x P_L	1	0.001123
L x P_Q	1	0.00304
Y x P_L	1	0.00087
Y x P_Q	1	0.00183
Y x L x P_L	1	0.00046
Y x L x P_Q	1	0.00071
Total	11	
Theoretical Error	∞	0.00073

(ii) Separate Data

Source	D F	X M.S	T M.S
Location L	1	0.00178	0.00497
Position (Linear) P_L	1	0.00038	0.00049
Position (Quad) P_Q	1	0.00002	0.00421
L x P_L	1	0.00151	0.00007
L x P_Q	1	0.00041	0.00334
Total	5		
Theoretical Error	∞	0.00039	0.00108

Table 4.5.2.1.3 : Analysis of variance table

Turning now to plate butt joints, table 4.5.2.1.4 shows the proportion of defective welds P_i for different welding processes and welding positions in Nodes 1 and 4. Also shown are the transformed proportions z_i (empirical logistic transformation, see section 4.1.1) together with their variances v_i. These figures allow comparisons to be made between any pair of welding positions or node locations. The main conclusions emerging from the table are as follows:

- The lowest proportion of defective welds occurs for the GMAW process used in the flat (1G) position in Node 1 (2.9%). Although this proportion is numerically less than for 1G-SMAW and 2G-SMAW, the difference is not statistically significant. Similarly in Node 4, no statistically significant differences exist among these three components.

- The highest proportion of defective welds occurs for the SMAW process used in the overhead position (4G-SMAW) (21.7% in Node 4 and 13.5% in Node 1). These results are highly significant in a statistical sense. Vertical welds in Node 4 also exhibit a high percentage of defectives.

- Comparisons between Nodes 1 and 4 show systematically higher proportions of defective welds in Node 4 for all five welding position components. The most significant difference lies in the 3G-SMAW component. Here the difference $\Delta Z=2.847-1.288=1.559$ corresponds to a standardised normal deviate of

  $1.559/\sqrt{(0.006 + 0.019)} = 9.86$, which is very highly significant.

(i) Plate Butts in Node 1

	Welding Position - Process				
	1G-SMAW	2G-SMAW	3G-SMAW	4G-SMAW	1G-GMAW
Defective Welds	6	5	16	52	8
Defect Free	154	133	284	332	270
All Welds	160	138	300	384	278
Prop of Def	0.038	0.036	0.053	0.135	0.029
Z_i	-3.168	-3.189	-2.847	-1.846	-3.460
V_i	0.150	0.175	0.006	0.022	0.115

(ii) Plate Butts in Node 4

	Welding Position - Process				
	1G-SMAW	2G-SMAW	3G-SMAW	4G-SMAW	1G-GMAW
Defective Welds	8	7	65	89	25
Defect Free	117	104	237	322	245
All Welds	125	111	302	411	270
Prop of Def	0.064	0.067	0.215	0.217	0.093
Z_i	-2.626	-2.634	-1.288	-1.282	-2.265
V_i	0.121	0.136	0.019	0.014	0.043

Table 4.5.2.1.4 : Statistics for plate butt welds in Nodes 1 and 4

The preceeding analyses were performed irrespective of the original level of NDE which was specified immediately after fabrication and could thus be criticised for introducing bias into the conclusions. The same analyses have then been undertaken for data obtained from regions of the structure in which 0% NDE was originally specified. The results are given below in tables 4.5.2.1.5 to 4.5.2.1.8. The purpose of these analyses was not to compare the performance of various levels of NDE since this was done in earlier sections for defect rates but to check whether the conclusions are valid irrespectively of original level of NDE. The results from these analyses indicate that this is indeed the case.

		Node 1		Node 4	
SMAW position		Weld Type		Weld Type	
		X	T	X	T
1G	r_i	77	52	44	24
	n_i	233	143	182	78
	p_i	0.3305	0.3636	0.2418	0.3077
	v_i	0.00095	0.00163	0.00101	0.00277
2G	r_i	103	136	70	64
	n_i	246	191	194	129
	p_i	0.4187	0.7120	0.3608	0.4961
	v_i	0.00099	0.00108	0.00120	0.00195
3G	r_i	162	48	193	44
	n_i	484	110	489	111
	p_i	0.3347	0.4364	0.3947	0.2964
	v_i	0.00046	0.00226	0.00049	0.00218

Table 4.5.2.1.5 : Number of defective welds r_i out of n_i inspected – 0% original NDE

SMAW Position	Weld Type		
	X	T	X+T
1G	0.2862	0.3357	0.3110
2G	0.3898	0.6041	0.4970
3G	0.3647	0.4164	0.3906
1G+2G+3G	0.3469	0.4521	0.3995

SMAW Position	Global Location		
	N1	N4	N1+N4
1G	0.3471	0.2748	0.3110
2G	0.5654	0.4285	0.4970
3G	0.3856	0.3663	0.3906
1G+2G+3G	0.4327	0.3662	0.3995

SMAW Position	Global Location		
	N1	N4	N1+N4
X	0.3613	0.3324	0.3469
T	0.5040	0.4000	0.4520
X + T	0.4327	0.3662	0.3995

Table 4.5.2.1.6 : Two-way and marginal proportions

(i) Full Data

Source	Degrees of Freedom	Mean Square
Location L (N1 or N2)	1	0.013227
Type Y (X or T)	1	0.033180
Position (Linear) P_L	1	0.012688
Position (Quadr.) P_Q	1	0.056979
L x Y	1	0.004226
L x P_L	1	0.338670
L x P_Q	1	0.007455
Y x P_L	1	0.000002
Y x P_Q	1	0.017865
Y x L x P_L	1	0.002205
Y x L x P_Q	1	0.002579
Total	11	
Theoretical Error	∞	0.001414

(ii) Separate Data

Source	D F	X M.S	T M.S
Location L	1	0.001250	0.016203
Position (Linear) P_L	1	0.006170	0.006521
Position (Quad) P_Q	1	0.005517	0.069327
L x P_L	1	0.005528	0.000063
L x P_Q	1	0.000632	0.009402
Total	5		
Theoretical Error	∞	0.000850	0.001978

Table 4.5.2.1.7 : Analysis of variance table

Tables 4.5.2.1.5 to 4.5.2.1.7 relating to cruciforms and tee butts confirm the earlier findings, namely:

- The proportion of defective welds is higher for tee butts than it is for

cruciforms in both Nodes 1 and 4.

- The proportion of defective welds is higher in Node 1 than in Node 4 for both tee butts and cruciforms.

- The 2G (horizontal) position is the most dominant in being associated with a high percentage of defective welds. This is particularly significant for tee butts where 60.4% of such welds are seen to be defective, compared with 41.6% in the vertical position and 33.6% in the flat position.

A similar analysis was undertaken for plate butts. This repeats the analysis in table 4.5.2.1.4 for those welds for which 0% NDE was specified. It can be concluded that from table 4.5.2.1.8 that:

- The lowest proportions of defective welds occur in welds made by GMAW in the flat (1G) position (0.033 and 0.103 for Nodes 1 and 4 respectively.

- There are very significant differences between the proportion of defective welds between Nodes 1 and 4 for all welding positions/processes.

- Welds made in the overhead position (4G) by the SMAW process show a particularly high proportion of defectives (18.7% in Node 1 and 33.6% in Node 4).

(i) Plate Butts in Node 1

	Welding Position - Process				
	1G-SMAW	2G-SMAW	3G-SMAW	4G-SMAW	1G-GMAW
Defective Welds	4	4	15	43	7
Defect Free	46	29	154	187	202
All Welds	50	33	169	230	209
Prop of Def	0.080	0.121	0.089	0.187	0.033
Z_i	-2.335	-1.880	-2.299	-1.461	-3.296
V_i	0.226	0.240	0.069	0.028	0.131

(ii) Plate Butts in Node 4

	Welding Position - Process				
	1G-SMAW	2G-SMAW	3G-SMAW	4G-SMAW	1G-GMAW
Defective Welds	5	6	64	84	23
Defect Free	18	33	108	166	201
All Welds	23	39	172	250	224
Prop of Def	0.217	0.154	0.372	0.336	0.103
Z_i	-1.213	-1.640	-0.520	-0.678	-2.149
V_i	0.229	0.177	0.025	0.017	0.047

Table 4.5.2.1.8 : Statistics for plate butts in Nodes 1 and 4 - 0% original NDE

4.5.2.2 Surface-breaking Defects found by Magnetic Particle Testing

Detailed comparisons between cruciform and tee butt joints for Nodes 1 and 4 are made in table 4.5.2.2.1 for the three welding positions 1G (flat), 2G (horizontal) and 3G (vertical). The table shows the number of defective welds r_i and the number of inspected welds n_i as well as the quantities z_i and v_i as defined in section 4.1.1.

		Node 1		Node 2	
SMAW position		Weld Type		Weld Type	
		X	T	X	T
1G	r_i	13	17	8	3
	n_i	308	395	309	230
	z_i	-3.086	-3.074	-3.569	-4.217
	v_i	0.0750	0.0583	0.1148	0.2553
2G	r_i	70	67	20	17
	n_i	712	785	562	671
	z_i	-2.210	-2.365	-3.276	-3.622
	v_i	0.0157	0.0161	0.049	0.0572
3G	r_i	65	16	27	10
	n_i	1447	444	1381	478
	z_i	-3.050	-3.257	-3.897	-3.798
	v_i	0.0159	0.0613	0.0365	0.0932

Table 4.5.2.2.1 : Number of defective welds r_i, out of n_i welds inspected

To construct single degree of freedom components, it is assumed that the three levels of welding position are in some fashion equally spaced. Then all contrasts involving welding position are divided into linear and quadratic components. Finally standarised contrasts are computed which have approximately unit theoretical variance. These are shown in table 4.5.2.2.2.

Weld-type Y (X or T)	-1.352
Location L (N1 or N4)	-5.795
Position (linear) P_L	0.066
Position (quadratic) P_Q	4.452
Y x L	-0.869
L x P_L	0.282
L x P_Q	1.453
Y x P_L	-0.626
Y x P_Q	0.230
Y x L x P_L	-1.146
Y x L x P_Q	0.025

Table 4.5.2.2.2 : Logistic factorial standardised contrasts

Inspection of table 4.5.2.2.2 shows that the location effect L and the quadratic position effect P_Q are highly significant. These effects can also be seen from the semi-normal probability plot (not shown here). The latter also demonstrates that there are no other significant sources of influence in governing the variability of the proportions of defective welds.

The highly significant location effect reflects the systematic differences between Nodes. In particular, the proportions of defective welds are higher in Node 1 than in Node 4 for each weld type joint and welding position. The significant location L component suggests splitting the data according to the factor L.

To do this the two halves of table 4.5.2.2.1 corresponding to Node 1 and Node 4, are analysed separately. For both locations, there is no systematic change with type of welded joint but an increase in the proportion of defective welds for the hotizontal 2G-SMAW position is very apparent. For Node 1, the average difference in Z_i between the 2G and 1G positions is 0.793 ± 0.203 (i.e. the approximate standard error estimated from the v_i's is 0.203). For the 2G and 3G components this difference is 0.866 ± 0.165. The corresponding effects for Node 4 are respectively 0.444 ± 0.345 and 0.399 ± 0.243.

A similar analysis to the above has been undertaken for plate butt and fillet joints. Again statistically significant differences are detectable in the proportion of defective welds, for welds made by SMAW in the 2G horizontal position.

4.5.3 Multiple Defects

This section contains an analysis of multiple defects from selective data from Nodes 5 and 6 found by ultrasonic testing. The analysis described here is limited to Nodes 5 and 6 but similar results apply for the other pairs of nodes, i.e. Nodes 2 and 3 and Nodes 1 and 4. As discussed in section 4.4.2, a number of welds were found to have multiple defects, particularly of the embedded type. Welds with multiple surface-breaking defects were found to be far less common.

The subset of data which is analysed here is from a specific fabrication yard and relates to the two welding positions in which multiple defects were found to be most common, that is the horizontal position 2G under the SMAW and GMAW processes.

Table 4.5.3.1 shows details of multiply defective welds possessing up to 4 or more defects in the two horizontal positions for three types of welded joint, namely cruciforms X, tee butts T and plate butts B. Appropriate row percentages for cruciforms and tee butts in the form of three dimensional histograms are given in figures 4.5.3.1 to 4.5.3.5.

Position	0 DEF	1 DEF	2 DEF	3 DEF	4+ DEF	Location	Joint	Case
2G-SMAW	378	55	10	2	1	Node 5	X	A1
2G-GMAW	261	101	24	9	6			
2G-SMAW	562	72	2	3	1	Node 6	X	A2
2G-GMAW	245	103	18	3	3			
2G-SMAW	554	81	13	4	1	Node 5	T	A3
2G-GMAW	195	101	24	6	11			
2G-SMAW	489	36	14	6	4	Node 6	T	A4
2G-GMAW	176	45	21	14	8			
1G-SMAW	143	11	0	0	0	Node 5	B	A5
1G-GMAW	46	3	2	0	0			
1G-SMAW	178	5	1	0	0	Node 6	B	A6
1G-GMAW	46	4	3	0	0			

Table 4.5.3.1 : Multiple defects in Nodes 5 and 6

Let j denote the possible number of defects in a weld. If two sets of welds are available, one corresponding to category C1 and the other to category C2, let θ be defined as:

$$\theta = \ln \left[\frac{(P(C_1 \text{ has} \leq i \text{ defects}))/(1-P(C_1 \text{ has} \leq i \text{ defects}))}{(P(C_2 \text{ has} \leq i \text{ defects}))/(1-P(C_2 \text{ has} \leq i \text{ defects}))} \right]$$

Rearranging the above relationship gives:

$$\Delta = \exp(\theta) \left[\frac{(P(C_1 \text{ has} \leq i \text{ defects}))/(1-P(C_1 \text{ has} \leq i \text{ defects}))}{(P(C_2 \text{ has} \leq i \text{ defects}))/(1-P(C_2 \text{ has} \leq i \text{ defects}))} \right]$$

where as before i takes values from 0 to j-1.

The aim of the analysis is to perform a formal test to determine whether the cumulative proportions are indeed related with the above relation, i.e. to test the hypothesis H_0: $\theta=0$ (or $\Delta=1$) against H_1 : $\theta\neq0$ (or $\Delta\neq1$). This is done according to

the theory of section 4.1.2 (see also section 4.4.2).

As an example consider the data of the first cell, related to cruciform joints in Node 5, given in table 4.5.3.1. Application of the logistic transformation yields differences −1.088, −1.252, −1.626, −1.585. Hence a rough estimate of θ is $\frac{1}{4}(-1.088-1.252-1.626-1.585)=-1.388$. Using weights calculated from the data given $\hat{\theta}=-1.103$, with a standard error of 0.159. The corresponding ratio of odds is $\Delta=\exp(\hat{\theta})=0.332$. Confidence intervals for $\hat{\theta}$ are -1.103 ± 0.159. The result is based on a chi-square statistic of 48.33 compared with $3.84(\chi_1^2\ 5\%)$ suggests support of the alternative hypothesis H_1. Hence it can be concluded that the odds of a weld being multiply defective are 0.332 times as large for the 2G-SMAW position as for the 2G-GMAW position.

This test has been carried out for all cells of table 4.5.3.1 and the results are shown in table 4.5.3.2.

Case	Unweighted θ	Weighted θ	Confidence Levels	Cumulative Ratio $\Delta=\exp(\theta)$	Chi-square χ_1^2
A1	-1.388	-1.103	-1.103±0.159	0.332	48.33
A2	-1.389	-1.334	-1.334±0.162	0.263	68.10
A3	-1.891	-1.417	-1.417±0.155	0.242	83.45
A4	-1.448	-1.407	-1.407±0.193	0.245	53.04
A5	-1.568	-0.414	-0.414±0.602	0.661	0.47
A6	-1.813	-1.500	-1.500±0.684	0.223	4.80

Table 4.5.3.2 : Comparisons of multiple defects between processes GMAW and SMAW

From table 4.5.3.2 it can be seen that the occurrence of multiple defects in the flat 1G and horizontal 2G positions is characteristic of the GMAW welding process. Another interesting feature emerging from table 4.5.3.1 is the very large number of welds with multiple defects for tee butts welded using 2G-GMAW as compared with the corresponding cruciform joints in the same node. This explains the general conclusions reached earlier in section 4.4.2, namely that, given a weld is defective, the probability of it being multiply defective is higher for tee butts than it is for cruciforms.

Further to the preceeding analysis, it would have been interesting to examine the

poor performance of the GMAW and SMAW procedures in the horizontal 2G position and check whether such performance could be attributed to specific components. At this stage we recall earlier remarks made in section 3.5 relating to the various original welding procedures. It has been stated that the SMAW and GMAW processes are mainly composed of two welding procedure groups, the W6-1 to W6-6 and W8-1 to W8-6. The horizontal SMAW position (2G) is made up from the W6-2 and W8-2 procedures while the corresponding GMAW position from the W6-6 and W8-6 procedures. The main difference between the W6-2 and W8-2 (similarly for W6-6 and W8-6) is the number of weld passes. The W6 being associated with more passes than the corresponding W8 group.

Procedure	1 DEF	2 DEF	3 DEF	4+ DEF	Location	Joint	Case
W6-2	8	1	0	0	Node 5	X	B1
W8-2	7	2	0	0			
W6-6	45	13	7	5	Node 5	X	B2
W8-6	56	11	2	1			
W6-2	7	1	2	1	Node 6	X	B3
W8-2	11	1	0	0			
W6-6	51	10	3	3	Node 6	X	B4
W8-6	47	6	0	0			
W6-2	25	6	0	0	Node 5	T	B5
W8-2	-	-	-	-			
W6-6	47	20	5	11	Node 5	T	B6
W8-6	54	4	1	0			
W6-2	13	4	3	3	Node 6	T	B7
W8-2	-	-	-	-			
W6-6	37	20	12	7	Node 6	T	B8
W8-6	8	1	1	0			

Table 4.5.3.3 : Multiple defects for various welding procedures - Nodes 5 & 6

Table 4.5.3.3 shows information in terms of multiply defective welds welded according to the W6–2, W8–2, W6–6 and W8–6 procedures for both cruciforms and .tee butts in Nodes 5 and 6. Pair comparisons for these procedures in the multiple scale has shown that the poor performance of the 2G–GMAW component (procedures W6–6 and W8–6) is due to the W6–6 procedure alone rather than the W8–6. It can therefore be stated that the increase in the number of passes used for welding increases the probability of the weld being multiply defective. Analytical details of the statistical tests are shown in table 4.5.3.4.

Case	Unweighted θ	Weighted θ	Confidence Levels	Cumulative Ratio $\Delta=\exp\theta$	Chi-square χ^2_1
B1	-0.212	-0.636	-0.636±1.265	0.529	0.25
B2	1.185	0.863	0.863±0.372	2.370	5.38
B3	1.710	1.610	1.610±1.003	5.002	2.58
B4	1.678	0.936	0.936±0.473	2.551	3.92
B5	-	-	-	-	-
B6	2.408	2.090	2.090±0.370	8.088	31.89
B7	-	-	-	-	-
B8	0.953	1.118	1.118±0.636	3.059	3.09

Table 4.5.3.4 : Comparisons of multiple defects for different welding procedures – Nodes 5 and 6

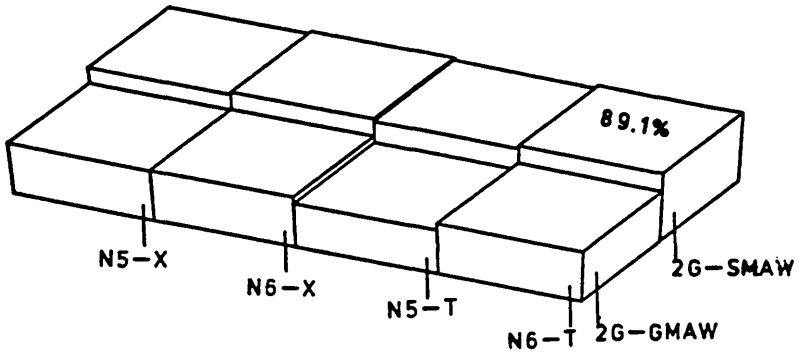


Fig. 4.5.3.1: Row Percentages for Welds Possessing 0 Defects

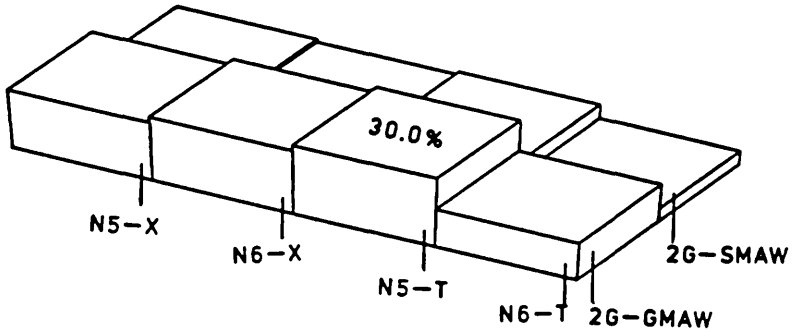


Fig. 4.5.3.2: Row Percentages for Welds Possessing 1 Defect

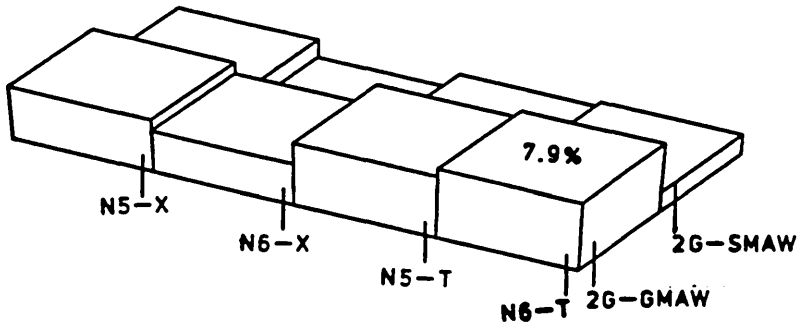


Fig. 4.5.3.3: Row Percentages for Welds Possessing 2 Defects

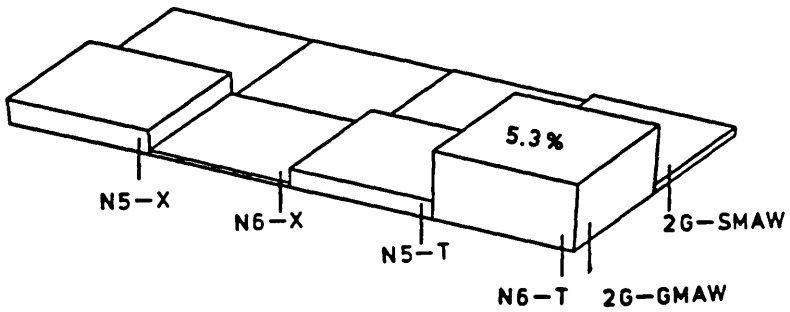


Fig. 4.5.3.4: Row Percentages for Welds Possessing 3 Defects

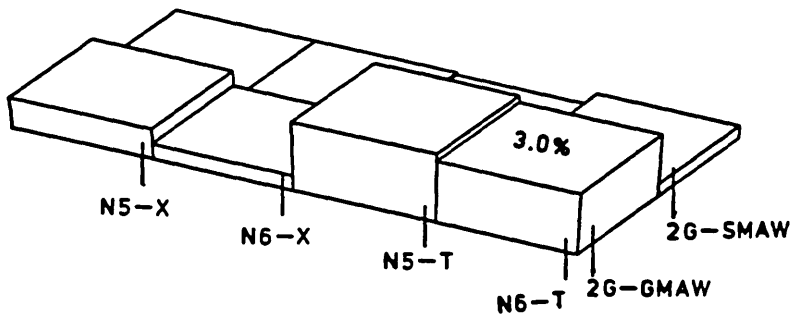


Fig. 4.5.3.5: Row Percentages for Welds Possessing 4 or more Defects

4.5.4 Defect Types

In this section analysis is undertaken of the influence of the type of welded joint (see section 3.2), welding procedure (see section 3.5) and defect type (see section 3.3) on the frequency of occurrence of defects in the zones X and Y (see section 3.6). The subset of data which is analysed were detected by ultrasonics and correspond to welds with 0% NDE after fabrication. Particular attention is given to the proportion of defects occurring in the two zones, i.e. the ratio of the numebr of defects corresponding to zone X (or Y) to the total number of defects in both zones X and Y.

Due to the fact that different welding procedures were used in plate butt welds as compared with cruciforms and tee butts, separate analyses are undertaken for these two categories of joints.

4.5.4.1 Cruciform and Tee Butt Joints

A total of 6750 defects which were found in the structure were classified according to node location (Nodes 1 to 6), position in the weld (zones X and Y), joint type (X, T), original welding procedure (W6, W8) and the type of defect which was assigned to them on detection (NF, SL, CR, IP, PO).

Because of the similarities in the construction of Nodes 1 and 4, 2 and 3, 5 and 6 and their common fabrication (see section 3.6), the data were classified according to these pairs of nodes and are shown in tables 4.5.4.1.1 to 4.5.4.1.6.

Whatever type of analysis is used, the distinction between response and explanatory variables must be made clear. In effect the choice of the response variable is not unique and by taking different response variables serves to investigate different aspects of the data, and it is not presumed that there is just one allowable choice.

Table 4.5.4.1.1 : Number of defects according to Welding Procedure, Defect Type, Type of Weld Joing and Defect Zone for Nodes 1 and 4

WELDING PROCEDURE		W6			W8		
DEFECT TYPE		NF	SL	CR	NF	SL	CR
DEFECT ZONE	WELD TYPE						
X	X	146	26	9	155	24	10
	T	79	26	10	105	11	6
Y	X	688	186	13	245	53	5
	T	353	96	7	99	25	5

Table 4.5.4.1.2 : Number of defects according to Welding Procedure, Defect Type, Type of Welded Joint and Defect Zone for Nodes 2 and 3

WELDING PROCEDURE		W6			W8		
DEFECT TYPE		NF	SL	CR	NF	SL	CR
DEFECT ZONE	WELD TYPE						
X	X	300	53	37	135	30	5
	T	172	62	26	44	7	3
Y	X	848	316	22	320	58	14
	T	469	112	8	89	14	1

Table 4.5.4.1.3 : Number of defects according to Welding Procedure, Defect Type, Type of Welded Joint and Defect Zone for Nodes 5 and 6

WELDING PROCEDURE		W6			W8		
DEFECT TYPE		NF	SL	CR	NF	SL	CR
DEFECT ZONE	WELD TYPE						
X	X	53	17	11	56	19	5
	T	56	20	12	29	14	1
Y	X	199	51	2	129	43	3
	T	155	39	1	56	12	1

Table 4.5.4.1.4 : Number of defects according to Welding Procedure, Defect Type, Type of Welded Joint and Defect Zone for Nodes 1 and 4

WELDING PROCEDURE		W6		W8	
DEFECT TYPE		IP	PO	IP	PO
DEFECT ZONE	WELD TYPE				
X	X	5	2	3	2
	T	5	2	2	0
Y	X	32	1	13	1
	T	22	7	0	0

Table 4.5.4.1.5 : Number of defects according to Welding Procedure, Defect Type, Type of Welded Joint and Defect Zone for Nodes 2 and 3

WELDING PROCEDURE		W6		W8	
DEFECT TYPE		IP	PO	IP	PO
DEFECT ZONE	WELD TYPE				
X	X	1	10	2	1
	T	0	2	0	0
Y	X	35	21	16	2
	T	12	3	2	1

Table 4.5.4.1.6 : Number of defects according to Welding Procedure, Defect Type, Type of Welded Joint and Defect Zone for Nodes 5 and 6

WELDING PROCEDURE		W6		W8	
DEFECT TYPE		IP	PO	IP	PO
DEFECT ZONE	WELD TYPE				
X	X	0	2	2	0
	T	0	3	0	0
Y	X	4	6	5	2
	T	7	2	1	0

Here, greater concern has been devoted to examining any variations in the proportions of defects in each defect zone across welding procedure, defect type and type of welded joint. Thus we study the dependance of defect zone as a response variable on the other variables as explanatory variables.

However, for some purposes it might be of direct interest to know for each defect zone, the distribution of defects according to welding procedure, weld type joint and defect type. These are shown for the main categories of defect type (NF, SL, CR), corresponding to tables 4.5.4.1.1 to 4.5.4.1.3, in tables 4.5.4.1.7 to 4.5.4.1.9 respectively, for the pairs of Nodes 1 and 4, 2 and 3, 5 and 6. It must be emphasized that such marginal tables need to be interpreted carefully. For example, the defect type classification describes the distribution of that variable alone for each type of defect zone. However, it might be possible due to association that for any particular level of welding procedure and (or) weld joint, the conditional distribution of defect type is the same for both defect zones and yet the marginal distributions may differ.

Analysis

The purpose of the analysis is to examine variations of the observed proportions in the two defect zones across welding procedure, type of welded joint and defect type, for each of the three pair locations, namely Nodes 1 and 4, 2 and 3, 5 and 6.

The first step is to calculate the proportion of defects in the X zone for each of the explanatory variables in tables 4.5.4.1.1 to 4.5.4.1.3. These proportions θ_i are shown in tables 4.5.4.1.10 to 4.5.4.1.12 respectively, for the three locations. Analysis of variance could be carried out directly on θ_i, the probability of a defect being detected in the X defect zone, but here attention is focussed on the logistic transformation $\ell n\{\theta/(1-\theta)\}$. This function is very nearly linear over the range of θ from 0.2 to 0.8 and in these data the observed proportions fall well within this range.

Table 4.5.4.1.7 : Distribution of defects according to Welding Procedure, Defect Type, and Type of Welded Joint for each Defect Zone in Nodes 1 and 4

Defect Zone	Welding Procedure		
	W6 (%)	W8 (%)	Total Number
X	48.8	51.2	607
Y	75.7	24.3	1775

Defect Zone	Defect Type			
	NF (%)	SL (%)	CR (%)	Total Number
X	79.9	14.3	5.8	607
Y	78.0	20.3	1.7	1775

Defect Zone	Welding Procedure		
	X (%)	T (%)	Total Number
X	61.0	39.0	607
Y	67.0	33.0	1775

Table 4.5.4.1.8 : Distribution of defects according to Welding Procedure, Defect Type, and Type of Welded Joint for each Defect Zone in Nodes 2 and 3

Defect Zone	Welding Procedure		
	W6 (%)	W8 (%)	Total Number
X	74.4	25.6	874
Y	78.2	21.8	2271

Defect Zone	Defect Type			
	NF (%)	SL (%)	CR (%)	Total Number
X	74.5	17.4	8.1	874
Y	76.0	22.0	2.0	2271

Defect Zone	Welding Procedure		
	X (%)	T (%)	Total Number
X	64.1	35.9	874
Y	69.5	30.5	2271

Table 4.5.4.1.9 : Distribution of defects according to Welding Procedure, Defect Type, and Type of Welded Joint for each Defect Zone in Nodes 5 and 6

Defect Zone	Welding Procedure		
	W6 (%)	W8 (%)	Total Number
X	57.7	42.3	293
Y	64.7	35.3	691

Defect Zone	Defect Type			
	NF (%)	SL (%)	CR (%)	Total Number
X	66.2	23.9	9.9	293
Y	78.0	21.0	1.0	691

Defect Zone	Welding Procedure		
	X (%)	T (%)	Total Number
X	54.9	45.1	293
Y	61.8	38.2	691

The function has been fitted separately for each weld type and node location as a linear logistic model containing only main effects and no interactions. The deviance D, i.e. $2\ell n$ (maximised likelihood), statistic and the estimated parameters with their asymptotic standard errors are given in tables 4.5.4.1.13 to 4.5.4.1.15. All calculations have been carried out using the statistical package GLIM [34] which sets the first parameter in any group to zero.

From the values of the estimated parameters it can be seen that there is an increase in the proportion of defects under the W8 as compared with the W6 welding procedure. The highest increase occurs in tee butt joints in Nodes 1 and 4, which is reflected by the parameters W6:0, W8:1.31. Thus the W8 procedure increases the ratio (defects in X zone)/(defects in Y zone) by an estimated factor of exp(1.31) = 3.7, with 95% confidence limits 5.1 and 2.7. Similar trends are observed in the three defect type categories SL, NF and CR in this order. Although the tendency for an increase in the proportions is less apparent in slag inclusion and non-fusion defects, this rise is particularly marked for crack-like defects. Note that positive values of the estimates indicate increase in the proportions whereas negative values indicate a decrease.

Making comparisons across weld types in the observed proportions given in tables 4.5.4.1.10 to 4.5.4.1.12, it can be seen that there exists a systematic increase of the proportions in tee butts as compared with those in cruciforms for each level of welding procedure. This increase is particularly noticeable in slag inclusions and crack-like defects.

The goodness of fit statistic (deviance) indicates a very good fit for the linear logistic model except in the case of cruciform joints in Nodes 2 and 3, where a full model reflecting the dependence of both defect type and welding procedure is needed. Indications of good fit are also given by the fitted proportions under the model,which are shown in tables 4.5.4.1.10 to 4.5.4.1.12 as the numbers in parenthesis.

Tables 4.5.4.1.10 to 4.5.4.1.15 also show the results of the linear logistic model containing only the defect type main effect. These are shown as the numbers in parentheses marked with an asterisk. The statistics in tables 4.5.4.1.14 and 4.5.4.1.15 corresponding to Nodes 2 and 3 and Nodes 5 and 6 indicate that although the proportions of defects in the X defect zone are numerically higher in the W8 as compared with the W6 welding procedure under each defect type level, a more parsimonious model could be considered to include only the defect type effect. The estimated parameters for each level of this effect are seen not to be different from the corresponding ones under the full model containing all main effects.

Note that the significance of the welding procedure main effect can be tested by the deviance statistic, resulting from taking the difference of the goodness of fit statistic between the full and reduced models, against the chi–squared distribution with one degree of freedom.

Table 4.5.4.1.10 : Proportions of defects in defect zone X in Nodes 1 and 4

PROCEDURE	W6			W8		
DEFECT TYPE	SL	NF	CR	SL	NF	CR
WELD TYPE						
X	0.12	0.17	0.41	0.31	0.39	0.67
	(0.13)	(0.17)	(0.40)	(0.30)	(0.39)	0.67
	(0.17)*	(0.24)*	(0.51)*	(0.17)*	(0.24)*	(0.51)*
T	0.21	0.18	0.59	0.31	0.51	0.54
	(0.17)	(0.20)	0.45	(0.44)	(0.48)	0.75
	(0.23)*	(0.29)*	(0.57)*	(0.23)*	(0.29)*	(0.57)*

Table 4.5.4.1.11 : Proportions of defects in defect zone X in Nodes 2 and 3

PROCEDURE	W6			W8		
DEFECT TYPE	SL	NF	CR	SL	NF	CR
WELD TYPE						
X	0.14	0.26	0.63	0.34	0.30	0.26
	(0.17)	(0.26)	0.52	(0.21)	(0.31)	(0.58)
	(0.18)*	(0.27)*	(0.54)*	(0.18)*	(0.27)*	(0.54)*
T	0.36	0.27	0.76	0.33	0.33	0.75
	(0.35)	(0.27)	(0.76)	(0.40)	(0.32)	(0.80)
	(0.35)*	(0.28)*	(0.76)*	(0.35)*	(0.28)*	(0.76)*

Table 4.5.4.1.12 : Proportions of defects in defect zone X in Nodes 5 and 6

PROCEDURE	W6			W8		
DEFECT TYPE	SL	NF	CR	SL	NF	CR
WELD TYPE						
X	0.25	0.21	0.85	0.31	0.30	0.62
	(0.24)	(0.22)	(0.74)	(0.32)	(0.29)	(0.80)
	(0.28)*	(0.25)*	(0.76)*	(0.28)*	(0.25)*	(0.76)*
T	0.34	0.26	0.92	0.54	0.34	0.50
	(0.37)	(0.26)	(0.86)	(0.47)	(0.35)	(0.90)
	(0.40)*	(0.29)*	(0.87)*	(0.40)*	(0.29)*	(0.87)*

Table 4.5.4.1.13 : Estimated parameters and standard errors for Cruciforms and Tee Butts in Nodes 1 and 4

DETAILS	PARAMETER	ESTIMATE	STANDARD ERROR
Cruciforms	DEFTYP SL	0 (0)*	- (-)
Deviance = 0.06	NF	0.38 (0.43)*	0.17 (0.17)
(78.68)*	CR	1.55 (1.62)*	0.38 (0.36)
D.f = 2	PROCDR W6	0 (-)*	- (-)
(3)*	W8	1.10 (-)*	0.12 (-)
Tee Butts	DEFTYP SL	0 (0)*	- (-)
Deviance = 9.15	NF	0.17 (0.29)*	0.21 (0.21)
(72.82)*	CR	1.37 (1.47)*	0.44 (0.43)
D.f = 2	PROCDR W6	0 (-)*	- (-)
(3)*	W8	1.31 (-)*	0.16 (-)

Table 4.5.4.1.14 : Estimated parameters and standard errors for Cruciforms and Tee Butts in Nodes 2 and 3

DETAILS	PARAMETER	ESTIMATE	STANDARD ERROR
Cruciforms	DEFTYP SL	0 (0)*	- (-)
Deviance = 21.18	NF	0.49 (0.52)*	0.13 (0.13)
(26.31)*	CR	1.65 (1.66)*	0.26 (0.26)
D.f = 2	PROCDR W6	0 (-)*	- (-)
(3)*	W8	0.25 (-)*	0.11 (-)
Tee Butts	DEFTYP SL	0 (0)*	- (-)
Deviance = 0.65	NF	-0.36 (-0.35)*	0.17 (0.17)
(2.13)*	CR	1.77 (1.77)*	0.41 (0.41)
D.f = 2	PROCDR W6	0 (-)*	- (-)
(3)*	W8	1.23 (-)*	0.19 (-)

Table 4.5.4.1.15 : Estimated parameters and standard errors for Cruciforms and Tee Butts in Nodes 5 and 6

DETAILS	PARAMETER	ESTIMATE	STANDARD ERROR
Cruciforms	DEFTYP SL	0 (0)*	- (-)
Deviance = 2.56	NF	-0.12 (-0.14)*	0.23 (0.22)
(6.64)*	CR	2.18 (2.12)*	0.55 (0.55)
D.f = 2	PROCDR W6	0 (-)*	- (-)
(3)*	W8	0.38 (-)*	0.19 (-)
Tee Butts	DEFTYP SL	0 (0)*	- (-)
Deviance = 3.36	NF	-0.50 (-0.50)*	0.26 (0.26)
(6.58)*	CR	2.36 (2.28)*	0.79 (0.79)
D.f = 2	PROCDR W6	0 (-)*	- (-)
(3)*	W8	1.43 (-)*	0.24 (-)

4.5.4.2 Plate Butt Joints

Because of the different welding procedures which have been used for the welding of plate butt joints, a separate analysis was undertaken for this type of welded joint.

Due to the small sample sizes for each of the three pairs of node locations, the data were merged and are shown in table 4.5.4.2.1 as a total of 646 defects. These are classified according to each level of most frequent welding procedures namely W3 and W5, and defect type namely non-fusion and slag inclusion defects.

Results from the fit of the linear logistic model with only main effects are given in tables 4.5.4.2.2 and 4.5.4.2.3. The goodness of fit statistic of 0.46 shows an excellent fit to the data. However the corresponding statistic from the fit of the model containing only the defect type main effect indicates that the overall influence of the welding procedure is statistically insignificant. Results from this latter analysis are shown in parentheses marked with an asterisk. Looking at the data it can be seen that the influence of the welding procedure affects only the occurrence of slag inclusion defects where the W3 procedure increases the proportion of defects in the X zone by a factor of 2, as compared with the W5 procedure.

The estimated parameters for the defect type are seen in table 4.5.4.2.2 to be SL : 0, NF : 0.88 in both cases. This indicates an increase in the proportion of defects in the X zone of the non-fusion type as compared with slag inclusions. This increase corresponds to a rise in the ratio (defects in X zone)/(defects in Y zone) by an estimated factor of exp(0.88)=2.4, with 95 per cent confidence limits of 3.6 and 1.6.

Table 4.5.4.2.1 : Number of defects according to Welding Procedure, Defect Type and Defect Zone in Plate Butts over all locations

PROCEDURE	W3		W5	
DEFECT TYPE	SL	NF	SL	NF
DEFECT ZONE				
X	38	120	1	5
Y	195	263	12	12

Table 4.5.4.2.2 : Estimated parameters and standard errors for Plate Butts over all locations

DETAILS	PARAMETER	ESTIMATE	STANDARD ERROR
Plate Butts	DEFTYP SL	0	-
Deviance = 0.46	NF	0.88	0.20
(0.84)*		(0.88)*	(0.20)*
	PROCDR W3	0	-
D.f = 1			
(2)*	W5	-0.38	0.47

Table 4.5.4.2.3 : Proportion of defects in Defect Zone X

PROCEDURE	W3		W5	
DEFECT TYPE	SL	NF	SL	NF
X	0.16	0.31	0.08	0.29
	(0.16)	0.31	0.13	(0.26)
	(0.16)*	(0.31)*	(0.16)*	(0.31)*

Observed (fitted) proportions in linear logistic model with only main effects.

4.6 Conclusions

The purpose of this section is to provide a summary of the main findings of the investiation on defect occurrence and to discuss their practical importance. In addition to the factors which were found to influence the occurrence and characteristics of weld defects what is of concern is the reliability of NDE data on which the current analysis has been performed. This falls into two categories namely the reliability of individual NDE operators and the reliability of computerised defect data base. These are discussed below in turn.

Reliability of Individual NDE Operators

Several hundred separate operators were used for the UT and MPI inspections, because the re-inspection had to be carried out over a relatively short period of time. With such a large number of operators, it is clear that there must be a considerable range of skill, aptitude, motivation and ability. As might be expected, with the relatively small number of welds inspected by each operator, the statistics for each operator are highly variable; but in the main this can almost certainly be attributed to the non-homogeneous nature of the welds inspected rather than to differences between operators. This conclusion is supported by the very marked and consistent differences in defect rates for different categories of weld and for different welding procedures. Had the re-NDE been associated with a large amount of operator error, it is almost certain that these differences would have been masked. One or two exceptions to the above conclusions were detected in preliminary analyses of operator performance, but a rigorous statistical analysis of the data was not undertaken.

It can also be concluded that the ability of NDE operators to detect the presence of defects was in general greater than their skill in assessing defect type. For example, in an analysis of defect type it was shown that there are very significant differences between Nodes 1 and 4 in the proportion of defective cruciform welds having linear indication defects reported. As these Nodes have very similar geometry and were fabricated by the same yards, such differences are very unlikely and result either from inspections by different groups of inspectors or from a change in what was meant by 'linear indication' over the period of the re-inspection.

Reliability of Computerised Defect Data Base

Regardless of the accuracy of the observed data, errors may have occurred in the initial recording of this information on the test record sheets and in the transcription

of these data to form the computerised data base.

There were approximately 30 million characters of information in the main computer file and it is inevitable that some of these are in error. Checks were devised and carried out for each of the main parameters used in the analysis and an appreciable number of abnormal entries were found. For example, the parameter giving the percentage of NDE undertaken immediately after fabrication showed 4,350 abnormal entries in a total of 144,761 records – an error rate of approximately 3%. However, all but one of these were due to additional alpha-numeric information being included in the data field in an unexpected fashion, and by using various techniques these data were corrected. Nevertheless, complete checking of all the data was impossible, particularly the numerical information. Range checks were included to highlight gross abnormalities where appropriate.

As a further example of data-base error, the parameter weld type joint was found to be blank in 24 out of a total of 144,761 records and to contain meaningless characters in a further 15 records. Combining these two sets gives a lower bound on the error rate of 0.027% which can be considered to be highly satisfactory. The actual error rate depends, of course, on the number of valid characters incorrectly substituted for the correct characters during the creation of the data base. However, no evidence was found to suggest that these rates might be high.

A relatively large number of factors were found to influence the occurrence and characteristics of weld defects, some in ways which might have been anticipated, otehrs in some unexpected ways. The influence of these factors is summarised below:

Influence of Amount of NDE Following Fabrication

Regarding this parameter, the following conclusions can be reached.

(1) In general, welds subjected to 100% NDE show a much lower UT defect rate than welds for which no NDE was specified, when comparisons are made between data sets which were otherwise identical.

(2) However, the reduction in defect rate which can be attributed to the specification of 100% NDE was found to be highly dependent on the particular location in the structure – i.e. it is dependent on the fabricator. Average reductions in defect rates by factors of between 1/20 and 1/80 were found in welds made by a specific fabricator for Node 1. However for Node 2

reductions by a factor of only 1/3 to 1/6 were typical, whilst in Node 6 the factors were as low as 1/1.5 to 1/4. However, regardless of the means by which it was achieved, the data for Node 1 demonstrates that a very low UT defect rate can be achieved, if 100% NDE is specified.

(3) Further information is provided by examining the statistics of average defect length and the average distance between defects for welds subjected to 0% NDE and 100% NDE. For example, for Node 1, the average defect length for welds subjected to 100% NDE is between 1/3 and 1/5 of the average distance between defects for the former is increased by a factor of between 5 and 20. This is not unexpected and shows that there is a tendency for larger and longer defects to be detected and removed (or not made in the first place).

(4) Turning now to surface-breaking defects, the apparent influence of the amount of MPI inspection undertaken immediately after fabrication is surprising: namely, the MPI defect rates for cruciform and tee butt welds are higher for welds subjected to 100% NDE than for welds with no NDE, for both main welding processes (GMAW and SMAW) and for all fabricators. Although the MPI defect rates are typically small – 1% to 2% the rates for welds subjected to 100% NDE in Japan are typically as much as a factor of 2 greater than for uninspected welds. For plate butts and fillets the differences between the two data sets are not so great. The reason for the above anomaly has been explained by looking at the average distance between defects statistics.

This distance was found to be the same for a given type of weld and welding process, irrespective of the percentage of MPI inspection. However, comparison of the average defect length statistics shows that the average defect lengths for welds subjected to 100% NDE were typically twice as great as for welds in the 0% NDE category. However, since the fact that a weld has been subjected to 100% NDE cannot be the cause of the increase in average defect length, it must be concluded that the difference is due to the selection process for welds receiving this treatment – i.e. this category of weld is more prone to having larger defects, probably because of difficulties of access during welding, and because of higher weld restraint.

Influence of Fabricator and Global Location

Overall statistics for defect rate were presented for the four main weld type joints and for the six nodal locations. However, these averages show little more than the overall proportions of defective weld that were present in the structure on arrival for

final assembly, and conceal the very significant differences that exist between fabricators and between different welding processes, different welds with different amount of NDE following fabrication. Nevertheless on average the defect rates for both embedded defects and surface-breaking defects were found to be significantly higher for Nodes 2 and 3 than for the other Nodes by a factor of about 2. These differences were particularly marked for tee butt welds but were also evident for cruciform and plate butt welds and they could not have occurred by chance. Since Nodes 2 and 3 are not radically different in structural layout from Nodes 1 and 4, these differences in defect rate can be attributed only to the use of different fabricators. Indeed the differences between fabricators became more apparent when further factors were taken into account.

Influence of Type of Welded Joint

This is one of the most important parameters in governing the occurrence of weld defects in the as-welded condition. As was shown, defect rates have been found to be highly dependent on the type of welded joint being considered. The same was also true for binary analysis and for the analysis of multiple defects. However, the true influence of the type of welded joint can only be made by taking into account the welding process, welding position and original welding procedure.

It has been shown that the overall UT defect rates were in the range of 10% - 16% for cruciform welds, 11% - 28% for tee butts and 0.5% - 4% for plate butts. The corresponding MPI defect rates were 0.17% - 1.4% for cruciforms, 0.08% - 0.52% for tee butts, 0.01% - 0.12% for plate butts and 0.01% - 0.19% for fillets. The high defect rates in tee butts as compared with cruciforms as well as the more severely affected tee butt joints in terms of multiply defective welds were found to be apparent for certain combinations of welding processes, welding position, original welding procedures and fabricators. Further details on this aspect will be given later. However as an example, the defect rates for plate butts were found to be much lower than for other weld types when the same welding process was used (SMAW and GMAW) and much lower still for the submerged-arc welding process (SAW). The latter was used only for plate butts and is associated with a defect rate which is practically zero.

Influence of Welding Process

Three main welding processes have been used, mainly:

SMAW - shielded metal arc welding

GMAW – gas metal arc welding
SAW – submerged arc welding

The welding process has been found to be an important factor which affects defect rates, the proportion of defective welds and the occurrence of multiple defects. Some conclusions concerning the influence of different types of welding process apply regardless of fabricator and weld type. Others are fabricator and weld type dependent. The major findings are summarised below.

The general conclusion was reached that the SAW process, used only for plate butt welds in the flat position, is extremely reliable, being associated with very low defect rates. For Nodes 1 and 4, there were practically no defects found for welds made by this process, either embedded or surface-breaking. In Nodes 5 and 6 there were no surface-breaking defects and the UT defect rate was low. In Nodes 2 and 3, welds known to have been fabricated by a specific fabricator had very few defects and only welds attributed to a second fabricator had an appreciable defect rate.

For the welding processes SMAW and GMAW, very much higher defect rates were found, together with significant differences between fabricators. The findings can be summarised as follows:

(1) In Nodes 5 and 6 for a common fabricator, the overall defect rates are between two and three times greater for the GMAW process than for SMAW, for both cruciform and tee butt welds. This is true for both surface and embedded defects. Examination of the data for welds subjected to 0% original NDE shows that the GMAW defect rate is about four times that for SMAW (i.e. about 8% and 35% for SMAW and GMAW respectively for UT defects; and 0.1% and 0.5% for MPI defects).

(2) Comparisons between SMAW and GMAW for plate butt welds in Nodes 5 and 6 show defect rates differing by a factor of 10.

(3) In addition, comparisons between the SMAW and GMAW processes for a single fabricator and a single welding position (horizontal) show that the odds of having multiple defects in a weld are between 3 and 7 times as great for the GMAW process as for the SMAW process for cruciform and tee butt welds in Nodes 5 and 6. This applies to both surface and embedded defects.

(4) For the other Nodes, the defect rate for the GMAW process was generally poor in comparison with the SMAW process. However, even in cases where

the defect rate was approximately the same, it was found that the chances of multiple defects occurring in a single weld are much higher for GMAW than for SMAW.

Influence of Welding Position

The general conclusion that can be drawn is that there is an increase in defect rate with increased difficulty of welding, i.e. between the flat and horizontal positions, between the horizontal and vertical positions and between the vertical and overhead positions. This general conclusion applies to both surface and embedded defects but when the data are analysed in terms of the proportion of defective welds in the multiple scale (i.e. the proportion of welds having one or more defects) rather than in terms of defect rate, welds which are made in the horizontal position are found to be more defective than vertical welds. And in addition welds made in the horizontal position using the GMAW process were found to be the most defective of all. This will be further discussed with respect to original welding procedure.

Influence of Welding Procedure

A very large number of different welding procedures were approved and used in the fabrication of the lower hull, and it was not possible to examine them all in detail because of the very small sample sizes. However comparisons have been made between some of the more commonly used procedures. The general conclusion is not altogether surprising and is that welding procedures involving a large number of passes tend to produce welds with a higher defect rate than procedures requiring only a small number of passes. This was also true in welds possessing multiple defects.

For example, in Nodes 5 and 6 cruciform welds made using the GMAW process in the horizontal (2G) position were found to have overall defect rates of about 33% when the W6–6 welding procedure was used, compared with only 19% for the W8–6 procedure. Note that the procedures W6–6 and W8–6 were the principal components of the horizontal (2G) GMAW process. Furthermore, comparisons of defective welds made by the two procedures have shown that the W6–6 procedure is much more likely to give rise to multiple defects than the W8–6 procedure. Similar results have been found for different fabricators, demonstrating the generality of these conclusions. Note that the poor performance of the 2G–GMAW position which is attributed to the W6–6 procedure was one of the main causes of higher defect rates (and more multiply defective welds) in tee butt welds as compared with cruciform welds. Although both weld type joints were made using the same welding procedures the W6–6 procedure was generally used more in tee butt than in cruciforms and gave

relatively poorer results.

Influence of Individual Welders

The computerised defect data base for the lower hull does not contain information about individual welders and therefore it has not been possible to make comparisons between welders. It is known, however, from the documentation that some of the badly defective welds in the pontoons were traced to a particular welder and it is therefore likely that some of the high local defect rates found in other parts of the structure were the result of other poorly trained or unskilled workers.

Defect Type Analysis

The frequency distributions of defects were found to be dependent on the type of welded joint (X, T, B), defect type (NF, SL, CR), defect location (zones X, Y) and sometimes on the original welding procedure (W6, W8, W3, W5).

Making comparisons between types of welded joints, it was observed that the proportion of defects in the X zone (number of defects in X zone/all defects) are systematically higher in tee butts as compared with those in cruciforms. This was true for each level of welding procedure, node location and defect type. Particularly characteristic was the increase in slag inclusions and crack-like defects.

In some locations for both cruciforms and tee butts, it was shown that the proportions of defects in the X zone are higher in the W8 procedure as compared with the W6 procedure. For intance the W8 procedure in tee butt joints in Nodes 1 and 4 increases the ratio (defects in X zone/defects in Y zone) by an estimated factor of 3.7 with 95% confidence limits 2.7 and 5.1. Furthermore, the proportions of crack-like defects in the X zone was shown to be significantly higher than the corresponding ones for slag inclusions or non-fusion defects. For example in cruciform joints in Nodes 1 and 4 under the W6 (W8) welding procedure 41% (67%) of crack-like defects were found in the X zone and as compared with 17% (39%) of non-fusion and 12% (31%) of slag inclusion defects. In some cases the effect of the welding procedure was found to be statistically insignificant.

In plate butts, it was found that the welding procedure had very little effect on the frequency of occurrence of defects in the various categories. Considering only the defect type effect over all locations, it has been shown that for NF defects in the X zone, the proportion of defects is significantly higher than the corresponding one for slag inclusion defects. This increase corresponds to a rise in the ratio (defects in X

zone/defects in Y zone) by an estimated factor of 2.4 with a 95% confidence interval of 1.6 to 3.6.

CHAPTER 5

DISTRIBUTIONS OF DEFECT SIZES

5.1 Statistical Theory

5.1.1 Choice of Distribution Models

Statistical theory offers a wide variety of models which can be used to describe variations in defect sizes but the choice of a particular model is not entirely subjective.

Theoretical justifications for using specific models do exist in many cases, because processes which govern formation mechanisms can often be modelled by algebraic equations which in turn lead to specified models. For example, if interest lies on the inter-arrival time of events which are known to occur according to a Poisson process then the exponential distribution would be the appropriate distribution as a consequence of the underlying process.

However, there are situations where the criterion for choosing a particular distribution is how well it fits the observed data in some region of interest. In such cases the choice of the distribution is made on the basis of it having a suitable shape and possibly a 'simple' mathematical form, rather than the chance of a belief that it arose from a fundamental underlying mechanism. In such cases the only practicable way is to choose a simple function, to test it empirically to see whether its c.d.f. coincides with the observed data and to adopt it if no better distribution can be found.

In this section the normal, exponential, gamma, lognormal and Weibull models are discussed within the above context.

5.1.1.1 Normal Distribution

The normal distribution is the most commonly used statistical model. Its probability density function is:

$$f(x;\mu,\sigma) = \frac{1}{\sigma\sqrt{2\pi}} \exp\left[-\frac{(x-\mu)^2}{2\sigma^2}\right]$$

$$\text{with} \quad -\infty < x < +\infty \quad , \quad -\infty < \mu < +\infty \quad , \quad \sigma > 0$$

where μ and σ are the parameters of the distribution, which can be shown to be its mean and standard deviation respectively.

The cumulative normal distribution is:

$$F(x;\mu,\sigma) = \int_{-\infty}^{x} \frac{1}{\sigma\sqrt{2\pi}} \exp\left[-\frac{(z-\mu)^2}{2\sigma^2}\right] dz$$

There is no simple expression for the above but it can be calculated using widely tabulated values of the standardised normal variable

$$y = \frac{x-\mu}{\sigma}$$

i.e.

$$F(x) = \Pr\left[X \leqslant x\right] = \Pr\left[Y \leqslant \frac{x-\mu}{\sigma}\right] = F\left[\frac{x-\mu}{\sigma}\right] = F(y) = \frac{1}{\sqrt{2\pi}} \int_{-\infty}^{y} e^{-\frac{1}{2}y^2} dy$$

The theoretical justification for the role of the normal distribution is the central limit theorem which states that the distribution of the sum of n independent observations from any distribution or even for up to n different distributions (provided that each individual variable has a small effect on the sum), approaches a normal distribution as the number of observations becomes large.

Consequently, when a r.v. represents the total effect of a process involving a large number of independent small causes none of which dominates the total, one is lead to expect the distribution governing that random variable to be normal. Examples of such physical r.v. include: instrumentation error around some specified value, scores on an intelligence test, average temperatures in a given locality, etc.

Furthermore, the normal distribution can be used as an approximation to other distributions such as gamma, binomial and Poisson under certain conditions on their parameters.

It should be emphasised that many random variables cannot be considered to result from the sum of many small effects and consequently there is no theoretical reason for assuming a normal distribution. On the other hand, if consideration is given only to the shape of the normal density and not to the possible causes for changes in the variate, it will be appreciated that the normal curve is symmetrical about the mean, that it extends from $-\infty$ to $+\infty$ and that it provides adequate approximation in the centre but it might be inadequate at one or both ends. However, the fact that the

range of the normal curve extends from $-\infty$ to $+\infty$, does not preclude its use in cases where either or both limits are fixed. After all, this is purely academic since no physical process gives rise to a measurement starting from $-\infty$ and ending at $+\infty$. When the mean is sufficiently large compared with the standard deviation ($\mu >> 3\ \sigma$) the error becomes negligible. Truncated normal distributions can also be fitted. Davis [41] has shown empirically that failure data of certain manufactured items can be represented satisfactorily with truncated normal life distributions. Further details on such models are given in Johnson and Kotz [42].

5.1.1.2 Exponential Distribution

The exponential distribution has probability density function

$$f(x;\beta) = \beta \exp(-(\beta x)) \qquad \beta > 0 \ , \ x \geq 0$$

and cumulative density function

$$F(x;\beta) = 1 - \exp(-(\beta x)) \qquad \beta > 0 \ , \ x \geq 0$$

It can be easily shown that

$$E[X] = \frac{1}{\beta}$$

$$Var[X] = \frac{1}{\beta^2}$$

The most important feature of the exponential distribution is its memoryless property which states that:

If the random variable X has an exponential distribution with parameter β, then

$$P_r[X \leq x_o + x \mid X > x_o] = P_r[X \leq x] = 1 - \exp(-(\beta x))$$
$$\text{for every } x_o > 0 \text{ and } x > 0$$

This in turn leads to the concept of constant hazard rate β. This property makes the exponential distribution particularly attractive as a distribution for the life of components which are not subject to fatigue or wear [43].

The distribution is also associated with stationary processes and arises as the distribution of inter-arrival times of events occurring according to a Poisson process,

making the model suitable in numerous situations.

The exponential model has also been used in reliability problems, justified entirely on empirical grounds. A series of examples with resistors, capacitors, electron tubes etc is given in Ref [43].

A somewhat more general form of the exponential distribution is given by

$$f(x;\beta,\mu) = \beta \exp(-\lambda(x-\mu)) \quad x \geq \mu$$

where μ is referred to as the threshold parameter.

5.1.1.3 Gamma Distribution

This is defined only for positive values of x and has density function

$$f(x;\alpha,\beta) = \frac{\beta^{\alpha}}{\Gamma(\alpha)} x^{\alpha-1} \exp(-(\beta x)) \quad x \geq 0,\ \alpha > 0,\ \beta > 0$$

where $\Gamma(\alpha)$ is the gamma function defined as

$$\Gamma(\alpha) = \int_0^{\infty} x^{\alpha-1} \exp-(x)\, dx$$

and α, β are respectively the shape and scale parameters of the distribution. If α is an integer the gamma function $\Gamma(\alpha)$ reduces to $(\alpha-1)!$ In cases where $\alpha=1$ the pdf of X reduces to

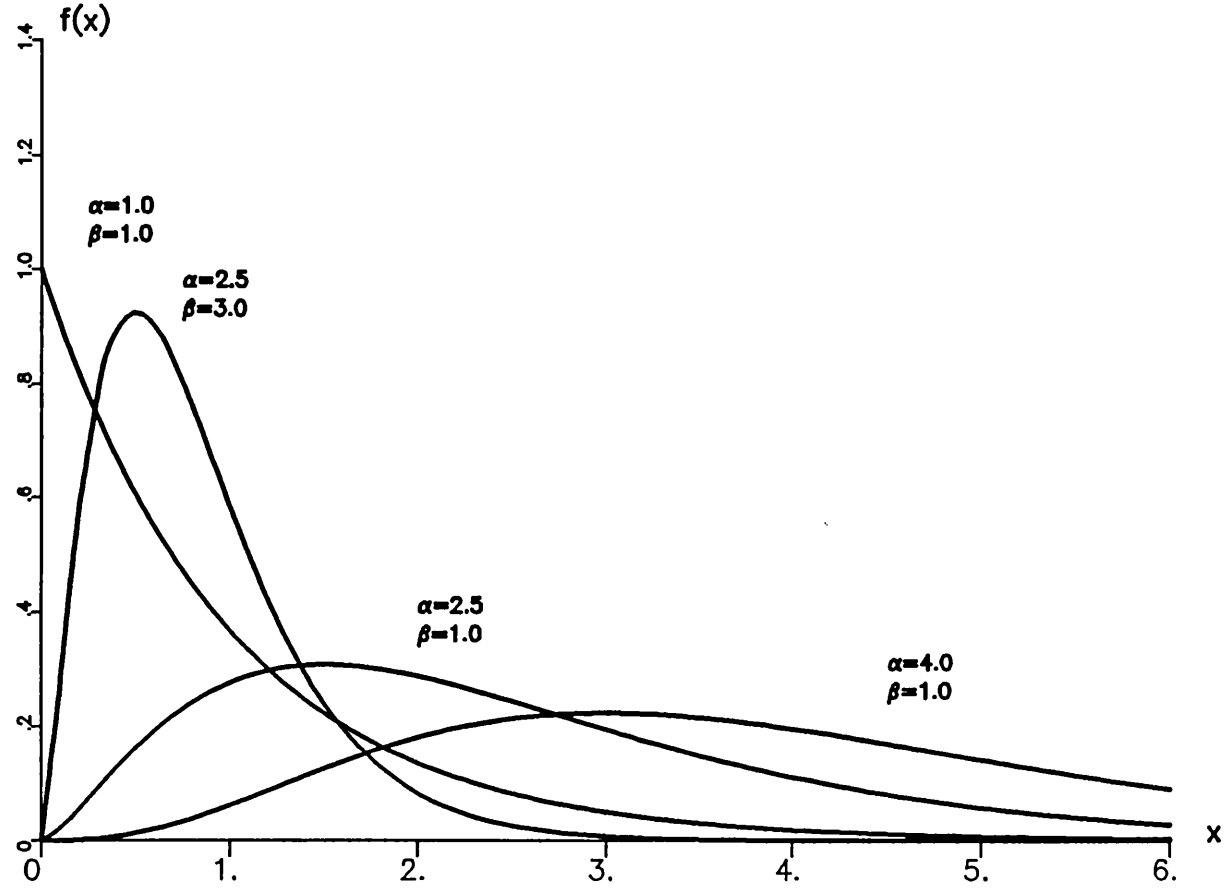
$$f(x;\beta) = \beta \exp(-(\beta x))$$

This is simply an exponential random variable with parameter β.

Figure 5.1.1.3 shows the gamma density for different values of the parameters α and β, the change of which results in a wide variety of shapes. It is seen that the distribution is limited to positive values and is highly skewed to the right. The skewness is in fact inversely proportional to the square root of the shape parameter and is given by $2/\sqrt{\alpha}$. It can also be seen that as α increases the shape of the curve becomes similar to the normal probability density curve.

The cumulative gamma distribution is given by

FIGURE 5.1.1.3 GAMMA DENSITIES FOR DIFFERENT VALUES OF α and β



$$F(x;\alpha,\beta) = \frac{\beta^{\alpha}}{\Gamma(\alpha)} \int_{0}^{x} t^{\alpha-1}\exp(-(\lambda t))\ dt \qquad x \geq 0$$

and is known as the incomplete gamma function ratio.

The mean variance of the distribution are given by

$$E[X] = \frac{\alpha}{\beta}$$

$$Var[X] = \frac{\alpha}{\beta^2}$$

The wide use of the gamma distribution is based on its derivations as the distribution of the sum of α independent and identically distributed exponential random variables with parameter β. The gamma distribution is then said to be the α–fold convolution of an exp(β) distribution [44]. This however does not restrict the use of the gamma distribution with α as non–integer.

The derivation from the exponential distribution suggests various applications in considering the time of occurrence of the event in a Poisson process. In life–testing for instance, if the time between consecutive failures of a system has an exponential distribution with parameter β then the time to the αth failure follows a gamma distribution with shape and scale parameters α and β respectively [45], or in statistical queuing theory when dealing with waiting times and servicing problems [46].

There are however other physical phenomena for which although there is no theoretical justification as gamma variables, they have been shown empirically to follow the gamma model. Such examples include family incomes, fibre measurements on wool tops [47], defect size measurements [48], depth of interval precipitation [49] and maximum stream flows and the strength of reinforced concrete members reported in [50].

5.1.1.4 Lognormal Distribution

This is a model of a random variable whose logarithm follows the normal distribution with parameters μ and σ. It is defined only for positive values of x and has probability density function

$$f(x;\mu,\sigma) = \frac{1}{\sqrt{2\pi}\,\sigma x} \exp - \frac{(\ell nx-\mu)^2}{2\sigma^2} \quad x > 0,\ \sigma > 0,\ -\infty < \mu < \infty$$

where ℓnx is the natural logarithm of the variable x.

The moments of the distribution are defined by the equation

$$E[X^r] = \exp\left[r\mu + \frac{r^2\sigma^2}{2}\right]$$

from which it follows that the mean α and variance β^2 are given by

$$\alpha = \exp\left[\mu + \frac{r^2}{2}\right] \text{ and } \beta^2 = \exp(2\mu+\sigma^2)\ (\exp\sigma^2-1)$$

The mode of the distribution is at $x = \exp(\mu-\sigma^2)$ and for q_p, the quantile of order p of the lognormal distribution the following relation exists:

$$\ell nq_p = \mu + \sigma\,\Phi^{-1}(p)$$

where $\Phi^{-1}(p)$ is the quantile of order p of the standardised unit normal distribution. From this, it follows that the median of the distribution is $q_{0.5} = \exp\mu$.

The distribution is positively skewed and the greater the value of σ^2 the greater is its skewness. The distribution has many different shapes resulting from different values of μ and σ^2 as shown in Figure 5.1.1.4.

Further properties of the distribution are given in Reference [51].

The lognormal distribution can be derived as the model of a process whose values are a result of the multiplication of small errors in a similar fashion to that of the normal distribution for the addition of errors. Galton [52] remarked that if

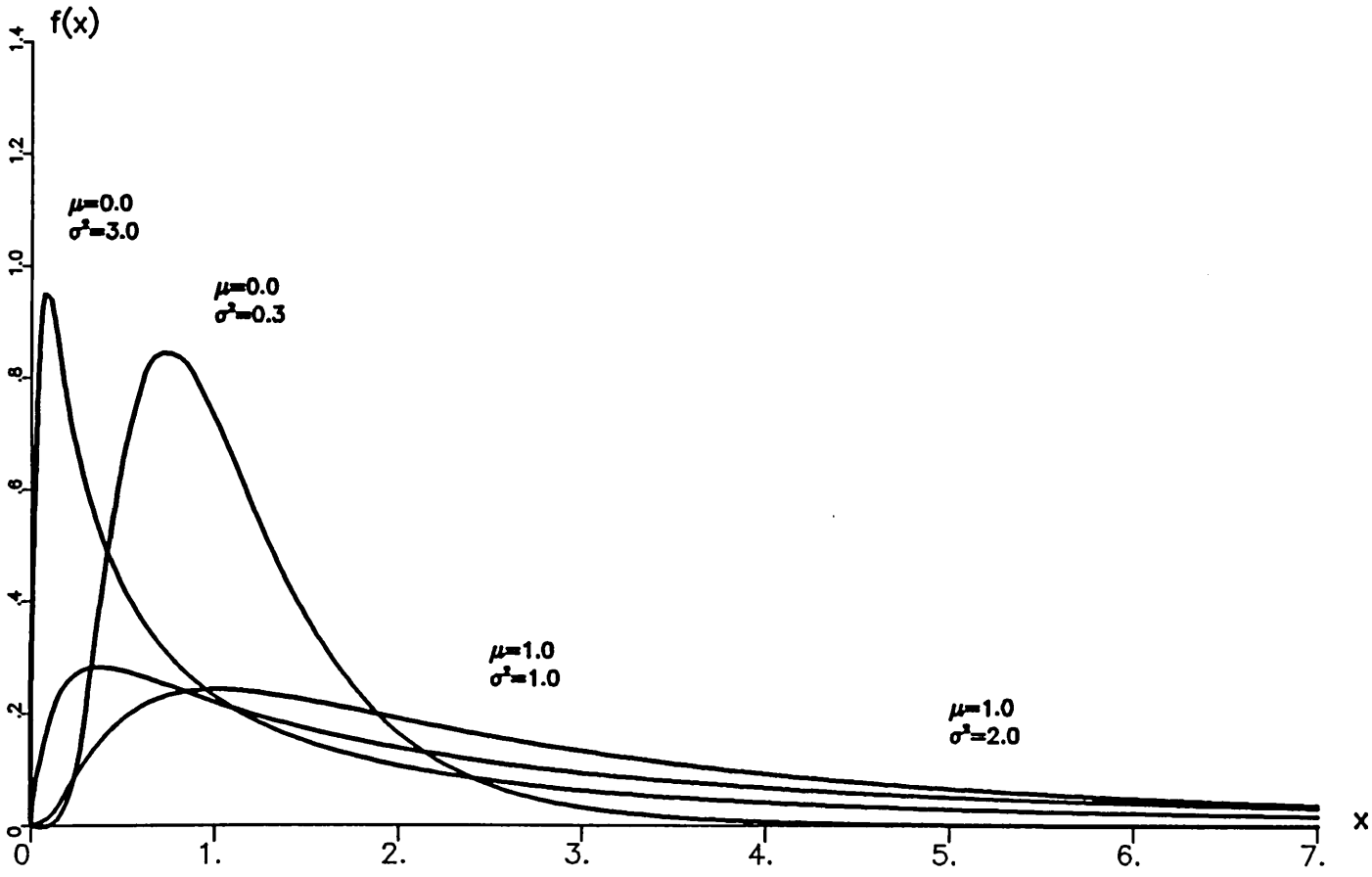
$$X_i \quad i=1,\ldots,n$$

and $$Y_n = \prod_{i=1}^{n} X_i$$

then $$\ell nY_n = \ell nX_1+\ell nX_2 + \ldots + \ell nX_n$$

would tend to a normal distribution as n tends to infinity provided that the independent r.v. ℓnX_i are such that the central limit theorem applies.

FIGURE 5.1.1.4 LOGNORMAL DENSITIES FOR DIFFERENT VALUES OF μ AND σ^2



On similar lines to the above, the distribution can be derived by considering the law of proportionate effect [51] which states that: 'A variate subject to a process of change is said to obey the law of proportionate effect if the change in the variate at any step of the process is a random proportion of the previous value of the variate'. Consequently, if the variate takes the value X_i and after n stages it reaches the final value X_n then:

$$X_i - X_{i-1} = \epsilon_i X_{i-1} \quad \text{for } i=1,\ldots, n$$

where the set $\{\epsilon_i\}$ is mutually independent and also independent of the set $\{X_i\}$.

$$\text{Thus} \quad \frac{X_i - X_{i-1}}{X_{i-1}} = \epsilon_i \quad \text{or} \quad \sum_{i=1}^{n} \epsilon_i = \sum_{i=1}^{n} \frac{X_i - X_{i-1}}{X_{i-1}}$$

Supposing $X_i - X_{i-1}$ is small at each stage of the process then

$$\sum_{i=1}^{n} \frac{X_i - X_{i-1}}{X_{i-1}} \approx \int_{X_o}^{X_n} \frac{dx}{x} = \ell n X_n - \ell n X_o$$

which gives $\ell n X_n = \ell n X_o + \epsilon_1 + \ldots + \epsilon_n$

Making use of the central limit theorem it follows that for large n $\ell n Xn$ is asymptotically distributed and therefore has a logarithmic normal distribution.

These forms of derivations which are based on technical arguments have been shown to have useful applications in economics (distribution of family incomes and bank deposits); biology (distribution of size of organisms whose growth is subject to many small causes the effect of which is proportionnal to the current size of the organism); particle physics (distribution of particle sizes obtained from breakage processes [53]); fatigue crack growth (where a proportional effect model is assumed for the growth of cracks [54]) and as time to failure model (based on the multiplicative properties of the distribution.

The dimensions of weld defects have also been shown empirically to follow the lognormal distribution (see Section 5.2). A theoretical justification for the use of the lognormal distribution in these cases can be given by considering again the law of proportionate effect and the way that certain defects are formed during the fabrication process. Reheat cracking for example (see Nichols [55]) occurs when welded joints are reheated after welding for thermal stress relief and concurrent metallurgical tempering of the welded joint, for galvanising or subsequent additional

welding or even when an as welded structure is put into high temperature service. This leads to initiation of cracking from pre-existing defects such as small hot cracks or hydrogen induced cracks for example. The mechanical factors involved in causing such defects are, among others: high residual and thermal stresses, local stress concentrations, and high brittle/ductile transition temperature. By assuming that the effects that each one of these factors have are independent and that their influence on the defect size is a random proportion of the current size of the defect then a proportional effect model may be assumed leading to a lognormal representation. Similar arguments can be put forward for delayed and other forms of cracking.

The application of the lognormal distribution has been shown to be successful on empirical observations in several other fields such as entomological concepts [56, 57], literary models [58] and in numerous other areas. For a detailed description of the use of the lognormal distribution in reliability theory the reader in referred to Reference [2].

Additional details and historical remarks can be found in [51].

5.1.1.5 Weibull Distribution

This has probability density function:

$$f(x;\alpha,\beta,\gamma) = \frac{\beta}{\alpha}\left[\frac{x-\gamma}{\alpha}\right]^{\beta-1} \exp\left[-\left[\frac{x-\gamma}{\alpha}\right]^{\beta}\right] \qquad \begin{array}{l} x \geq \gamma \\ \alpha,\ \beta > 0 \\ \gamma \geq 0 \end{array}$$

The cumulative distribution function is:

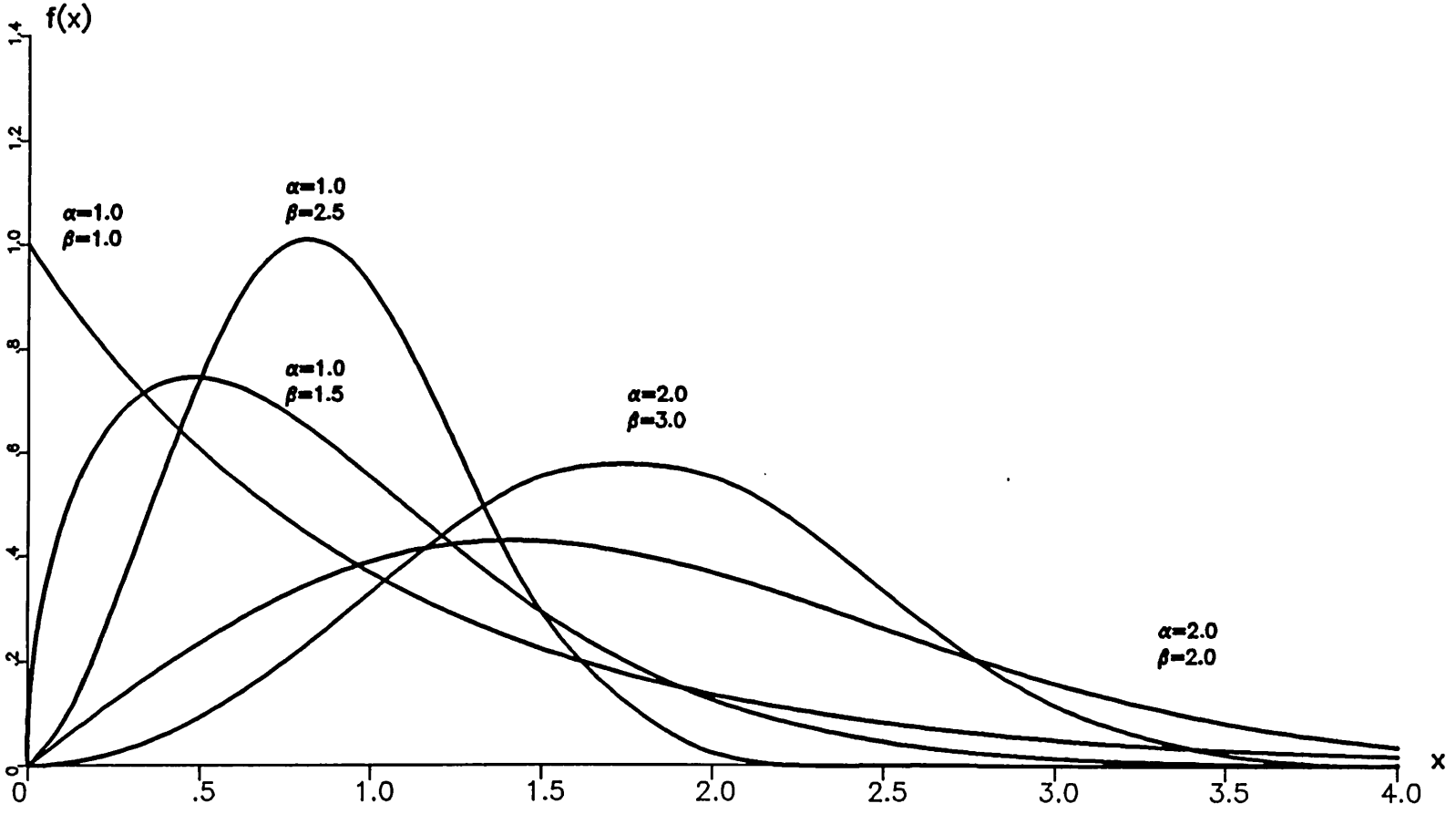
$$F(x;\alpha,\beta,\gamma) = 1 - \exp\left[-\left[\frac{x-\gamma}{\alpha}\right]^{\beta}\right]$$

where α, β, γ are, respectively, the scale, shape, and location parameters of the distribution.

It has been stated by Weibull [59] that this is the limiting distribution of the first order statistic $X_{[1]}$ for the case where the density of X is some positive non-decreasing function. This makes the distribution specifically useful in weakest link problems.

The distribution can also be derived using an appopriate hazard rate [45] which is some power function of x.

FIGURE 5.1.1.5 WEIBULL DENSITIES FOR DIFFERENT VALUES OF α and β



$$\text{i.e.} \qquad h(x) = \frac{\beta}{\alpha}\left[\frac{x-\gamma}{\alpha}\right]^{\beta-1}$$

This is in fact a decreasing (increasing) function of $x-\gamma$ if $\beta < 1$ ($\beta>1$) and is constant if $\beta=1$. In the latter case the Weibull distribution reduces to the exponential distribution. The flexibility to incorporate non-constant hazard rates makes the Weibull distribution useful in lifetime failures due to deterioration or wear where they show an increasing hazard rate.

The mean and variance of the distribution are given by the expressions:

$$E[X] = \gamma + \alpha\,\Gamma\left[\frac{\beta+1}{\beta}\right]$$

$$Var[X] = \alpha^2\left[\Gamma\left[\frac{\beta+2}{\beta}\right] - \Gamma^2\left[\frac{\beta+1}{\beta}\right]\right]$$

Weibull densities with $\gamma=0$ and different values of α and β are shown in Figure 5.1.5. Further properties of the distribution and additional remarks can be found in [45].

It must be emphasised that in most situations where the model is used there is no theoretical justification which indicates that a Weibull distribution should be used. Although this model can be derived by probabilistic arguments when the distribution is used these arguments are not usually encountered. Examples include yield strength, fatigue life and strength of cotton as is shown in [59], time of failure in electron-tubes [60, 61] and ball bearing failures [62].

Furthermore, it is generally accepted that if an exponential distribution is adequate then a Weibull distribution will provide extra flexibility to make the model sufficiently accurate.

5.1.2 Distribution Fitting

The lognormal and Weibull distributions were fitted to the dimensions defect depth, width, length and aspect ratio according to the statistical theory of sections 5.1.2.1 and 5.1.2.2.

The statistical theory of the lognormal and Weibull distributions and the methods of parameter estimation are briefly summarised below. For further details and derivation of the results the reader is referred to [2, 45, 50, 51]. The theory of distribution

fitting in general is given in [2] with emphasis on their subsequent use in reliability theory. A detailed account of the lognormal distribution is given in [51]. A similar account of the Weibull distribution can be found in [45]. Goodness-of-fit statistics are extensively explored in [50], together with appropriate probability plots.

5.1.2.1 Lognormal Distribution

If Y is a positive random variable such that $Y=\ell nX$ is normally distributed with parameters μ and σ^2 then X is said to be log-normally distributed with parameters μ and σ^2, the mean and variance of the corresponding Normal Distribution.

$$Y = \ell nX \sim N(\mu,\sigma^2) \text{ with p.d.f. } f(y;\ \mu,\sigma^2) = \frac{1}{\sigma\sqrt{2\pi}} \exp\left\{-\frac{1}{2\sigma^2}(y-\mu)^2\right\}$$

where $-\infty$, y , ∞

$$X \sim \Lambda(\mu,\sigma^2) \text{ with p.d.f. } f(x;\mu,\sigma^2) = \frac{1}{x\sigma\sqrt{2\pi}} \exp\left\{-\frac{1}{2\sigma^2}(\ell nx-\mu)^2\right\}$$

where $x>0$

Estimation of Parameters

(i) Maximum Likelihood Estimation

The Likelihood function is given by

$$L(\mu,\sigma^2;x_i) = \frac{1}{\sigma^n(2\pi)^{n/2}\prod_{i=1}^{n} x_i} \exp\left\{-\frac{1}{2\sigma^2}\sum_{i=1}^{n}(\ell nx_i - \mu)^2\right\}$$

Solution of the log-likelihood equations $\frac{\partial \ell nL}{\partial \mu} = 0$ and $\frac{\partial \ell nL}{\partial \sigma} = 0$

give $\hat{\sigma}^2 = \frac{1}{n}\sum_{i=1}^{n}(\ell nx_i-\hat{\mu})^2$ and $\hat{\mu} = \frac{1}{n}\sum_{i=1}^{n}\ell nx_i$

$\hat{\mu}$ is a consistent, minimum variance unbiased estimator with lower bound σ^2/n, and $\hat{\sigma}^2$ is a consistent, biased estimator. An unbiased estimator for σ^2 is taken to be

$\frac{1}{n-1}\sum_{i=1}^{n}(\ell nx_i - \hat{\mu})^2$. The lower bound for σ^2 is not quite attained by the standard unbiased estimate which has variance $2\sigma^4/n-1$.

Exact confidence limits for μ are given by:

$\left[\hat{\mu} \pm t_{n-1} \frac{\hat{\sigma}}{\sqrt{n}}\right]$ where t_{n-1} is the t-distribution with n-1 degrees of freedom

For large n the normal approximation can be used.

Confidence limits for σ^2 based on the chi-square distribution with n-1 d.f. are given by:

$$\left\{ \frac{\sum_{i=1}^{n} (y_i - \bar{y})^2}{\chi_1^2} , \frac{\sum_{i=1}^{n} (y_i - \bar{y})^2}{\chi_2^2} \right\}$$

where χ_1^2, χ_2^2 are appropriate percentage points for the χ^2 distribution with n-1 degrees of freedom.

(ii) Method of Moments

The r^{th} moment of the distribution is given by $M_r = E[X^r] = \exp(r\mu + \frac{1}{2}r^2\sigma^2)$. Hence solution of the equations:

$\ell nM_2 - 2\ell nM_1 = \hat{\sigma}^2$ and $2\ell nM_1 - \frac{1}{2}\ell n\, M_2 = \hat{\mu}$ give estimates for σ^2 and μ.

Their large sample variances are given by:

$$\text{Var}\ [\hat{\mu}] = \frac{1}{4n}\left[\eta^8 + 4\eta^6 - 2\eta^4 + 4\eta^2\right]$$

$$\text{Var}\ [\hat{\sigma}^2] = \frac{1}{n}\left[\eta^8 + 4\eta^6 + 2\eta^4\right]$$

where $\eta^2 = \exp(\sigma^2) - 1$.

The efficiency of the method decreases rapidly as σ^2 increases, especially for estimation of σ^2. For values of σ^2 near the neighbourhood of 0.5 the efficiency of the $\hat{\mu}$ estimator is 79% and that of $\hat{\sigma}^2$ is as low as 31%.

(iii) Method of Quantiles

The quantile of order q is given by $\xi_q = \exp(\mu + \nu_q\sigma)$, where ν_q is the corresponding quantile of the standard normal distribution. Hence solution of the equations:

$\xi_{q_1} = \exp(\hat{\mu} + \nu_{q_1}\hat{\sigma})$ and $\xi_{q_2} = \exp(\hat{\mu} + \nu_{q_2}\hat{\sigma})$ give estimates for μ and σ^2.

Maximum efficiency of the estimates is obtained when the quantiles are symmetrically placed.

Quantiles of order 27% and 73% give μ with efficiency 81%.

Quantiles of order 7% and 93% give σ^2 with 65% efficiency.

Large sample variances of $\hat{\mu}$ and $\hat{\sigma}^2$ are calculated to be:

$$\text{Var}[\hat{\mu}] = \frac{\pi\sigma^2 q e^{\nu^2}}{n} \quad \text{and} \quad \text{Var}\ [\hat{\sigma}^2] = \frac{4\pi\sigma^4 q(1-2q)e^{\nu^2}}{n\nu^2}$$

Exact confidence intervals are not available for methods (ii) and (iii). In this case approximate confidence levels can be obtained by the use of the asymptopic assumption

$$\hat{\mu} \sim N(\mu, \text{Var}\ (\hat{\mu}))$$

where σ^2 in the variance is replaced by its estimate $\hat{\sigma}^2$.
Similar remarks apply for confidence intervals of σ^2.

Estimation of Mean and Variance

(i) Maximum Likelihood Estimation

It makes use of the invariance property of maximum likelihood estimators, (MLE), ie for $\hat{\sigma}$ the MLE of θ, $g(\hat{\theta})$ is the MLE of $g(\theta)$. Hence the MLE for the mean is

$$\exp\left\{\hat{\mu} + \frac{\hat{\sigma}^2}{2}\right\}$$

The MLE for the variance is $\{(\exp(2\hat{\mu} + \hat{\sigma}^2)\}\{\exp(\hat{\sigma}^2)-1\}$.

(ii) Moment Estimators

$$\text{Mean} = \frac{1}{n}\sum_{i=1}^{n} x_i \quad \text{and Var} = \frac{1}{n}\sum_{i=1}^{n}(x_i - \bar{x})^2$$

with their asymptotic variances being:

$$\text{Var [Mean]} = \frac{\alpha^2}{n}\eta^2, \quad \text{Var[Var]} = \frac{\alpha^4}{n}(\eta^{12} + 6\eta^{10} + 15\eta^8 + 16\eta^6 + 2\eta^4)$$

where $\alpha = \exp(\mu + \sigma^2/2)$ and η^2 is defined above.

(iii) Quantile Estimators

Mean = $\exp(\hat{\mu} + \frac{1}{2}\hat{\sigma}^2)$, Variance = $\exp(2\hat{\mu} + \hat{\sigma}^2)\ [\exp[(\hat{\sigma}^2) - 1]$

Their large sample variances are:

Var [mean] = $\alpha^2\ (\text{Var}[\hat{\mu}] + \frac{1}{4}\ \text{Var}[\hat{\sigma}^2])$

Var [Var] = $\alpha^4(4\eta^4\text{Var}[\hat{\mu}] + (2\eta^2 + 1)^2\ \text{Var}\ [\hat{\sigma}^2])$

where $\hat{\mu}$ and $\hat{\sigma}$ and their variances are obtained by the method of quantiles as previously described.

Approximate confidence intervals for the mean and variance can be calculated in a similar fashion to the ones for the parameters μ and σ^2.

Goodness of fit statistics

The Kolmogovov Smirnov test or the traditional χ^2 goodness of fit statistics can be used.

Tests of the coefficient of skewness g_1 and the coefficient of kurtosis g_2 of the transformed normal variable Y can also be used, where

$$g_1 = \sum(y_i - \bar{y}\ )^3/(ns^3)$$

$$g_2 = \sum(y_i - \bar{y})^4/(ns^4) - 3$$

where s = sample standard deviation

The expected value of g_1 is zero for a symmetric distribution. The standard error of g_1 is $(6/n)^{\frac{1}{2}}$ under the assumption of normality. The ratio g_1/S.E. is a test of normality.

5.1.2.2 Weibull Distribution

The probability density function of the two parameter Weibull distribution is given by

$$f(x;\beta,\alpha) = \left[\frac{\beta}{\alpha}\right]\left[\frac{x}{\alpha}\right]^{\beta-1} \exp\left\{-\left[\frac{x}{\alpha}\right]^{\beta}\right\} \quad x \geq 0$$

$$0 \qquad\qquad x < 0$$

with the corresponding cumulative distribution function (CDF)

$$F(x;\beta,\alpha) = \begin{cases} 1-\exp\left[-\left[\frac{x}{\alpha}\right]^{\beta}\right] & x \geq 0 \\ 0 & x < 0 \end{cases}$$

where β and α are the shape and scale parameters respectively.

Estimation of Parameters

(i) Graphical method

Re-arranging the theoretical CDF and taking logarithms twice yields:

$$\ell n \ell n \left[\frac{1}{1-F(x)}\right] = \beta \ell n \frac{x}{\alpha}$$

If F(x) is replaced by the sample CDF i/n+1 after the data are ordered, standard linear regression methods can be used to estimate the parameters β and α.

(ii) Maximum Likelihood Estimation

The likelihood function is

$$L(\beta,\alpha;x_i) = \left[\frac{\beta}{\alpha}\right]^n \frac{1}{\alpha^{n(\beta-1)}} \prod_{i=1}^{n} x_i^{(\beta-1)} \exp\left[-\sum_{i=1}^{n}\left[\frac{x_i}{\alpha}\right]^{\beta}\right]$$

The long-likelihood equations are easily obtained by equating

$$\frac{\partial \ell nL}{\partial \alpha} \text{ and } \frac{\partial \ell nL}{\partial \beta} \text{ to zero}$$

Estimates for α and β can be obtained by simultaneous iterative solution of the following equations.

$$\hat{\alpha} = \left\{\frac{1}{n}\sum_{i=1}^{n} x_i^{\hat{\beta}}\right\}^{1/\hat{\beta}}$$

$$\hat{\beta} = \frac{n}{\left[\left[\frac{1}{\hat{\alpha}}\right]^{\hat{\beta}} \sum_{i=1}^{n} x_i^{\hat{\beta}} \ell n x_i - \sum_{i=1}^{n} \ell n x_i\right]}$$

(iii) Method of Moments

The r^{th} moment about the origin is given by

$$E[X^r] = \alpha^r \Gamma\left[\frac{\beta+r}{\beta}\right]$$

which yields

$$\hat{\mu} = \hat{\alpha}\Gamma\left[\frac{\hat{\beta}+1}{\hat{\beta}}\right] \text{ and } \hat{\sigma}^2 = \hat{\alpha}^2\Gamma\left[\frac{\hat{\beta}+2}{\hat{\beta}}\right] - \left\{\hat{\alpha}\Gamma\left[\frac{\hat{\beta}+1}{\hat{\beta}}\right]^2\right\}$$

where $\hat{\mu}$ and $\hat{\sigma}^2$ are the sample mean and variance of the distribution. The coefficient of variation COV is then easily obtained. A graph of the COV against the shape parameter is given in [64]. Use of the graph gives an estimate of β.

Then α can be found from the equation

$$\hat{\alpha} = \frac{\hat{\mu}}{\left[\frac{1}{\hat{\beta}} + 1\right]}$$

Confidence Intervals

Simulation results by [65] give sample sizes for which the distributions of $\hat{\beta}/\beta$ and $\hat{\alpha}/\alpha$ are asymptotically normal with known mean and standard deviation.

It is also shown that the distributions of $\hat{\beta}/\beta$ and $\hat{\beta}\ell n(\hat{\alpha}/\alpha)$ are independent of the parameters β and α.

Use of tabulated values in [65] can be made to construct confidence intervals for β and α.

The 100 $(1-\xi)$% interval for β is of the form

$$\left[\frac{\hat{\beta}}{\ell_1}, \frac{\hat{\beta}}{\ell_2}\right]$$

where ℓ_1 ℓ_2 are chosen such that $P[\ell_1 < \hat{\beta} < \ell_2] = 1 - \xi$.

For the α parameter the corresponding interval is of the form:

$(\hat{\alpha}\, e^{-t_2/\hat{\beta}}, \hat{\alpha}e^{-t_1/\hat{\beta}})$ where t_1 and t_2 are chosen such that
$P[t_1 < \hat{\beta}\ell n(\hat{\alpha}) < t_2] = 1 - \xi$

An alternative way of obtaining bounds on the shape parameter is given in [64]. The large sample variance of the COV is given by

$$\sigma^2_{COV} \approx \frac{(COV)^2}{2n}$$

Use of the Central Limit theorem gives bounds on COV as below:

$$P[\hat{COV} - Z_{(0,1)}\,\sigma(COV) < COV < \hat{COV} + Z_{(0,1)}\sigma(COV)] = 1-\xi$$

The corresponding interval for β is constructed using the relation between β and COV in [64].

For the scale parameter, bounds can be obtained by using the random variable

$$\frac{2n\hat{\alpha}^{\beta}}{\alpha^{\beta}} \sim \chi^2_{2n} \text{ as explained in [66].}$$

Upper confidence limits are given by

$$Pr\left[\alpha > \left[\frac{2n}{\chi^2_{2n(u)}}\right]^{1/\beta_{\hat{\alpha}}}\right] = 1 - \xi$$

and Lower confidence limits by

$$Pr\left[\alpha < \left[\frac{2n}{\chi^2_{2n(L)}}\right]^{1/\beta_{\hat{\alpha}}}\right] = 1 - \xi$$

where $\chi^2_{2n}(U)$ and $\chi^2_{2n}(L)$ are the upper and lower points of the chi-square distribution with 2n degrees of freedom.

5.1.2.3 Uniform Distribution

This has the probability density function

$$f(x;\theta_1,\theta_2) = \frac{1}{\theta_2-\theta_1}\, I_{[\theta_1,\theta_2]}(x_i) \qquad i=1,\ldots,n$$

where the parameters θ_1 and θ_2 satisfy $-\infty < \theta_1 < \theta_2 < \infty$.

The likelihood function is given by

$$L(\theta_1,\theta_2|x_i) = \frac{1}{(\theta_2-\theta_1)^n} \prod_{i=1}^{n} I_{[\theta_1,\theta_2]}(x_i)$$

$$= \frac{1}{(\theta_2-\theta_1)^n} \mathbb{I}_{(-\infty, X_{[1]}]}^{(\theta_1)} \mathbb{I}_{[X_{[n]}, \infty)}^{(\theta_2)}$$

Hence the MLE of the parameters θ_1 and θ_2 are given respectively by $X_{[1]}$ and $X_{[n]}$, the smallest and largest observations. The extreme observations are a pair of jointly sufficient statistics for θ_1 and θ_2 but are biased estimators. The minimum variance unbiased estimators are given by:

$$\hat{\theta}_1 = \frac{1}{n-1} (nX_{[1]} - X_{[n]})$$

$$\hat{\theta}_2 = \frac{1}{n-1} (nX_{[n]} - X_{[1]})$$

The mean and variance of the distribution are easily obtained by the method of moments and given by:

$$E[X] = \frac{\theta_1+\theta_2}{2}$$

$$Var[X] = \frac{(\theta_2-\theta_1)^2}{12}$$

A common uniform distribution is of the form

$$f(y;\theta) = \frac{1}{\theta} \mathbb{I}_{[0,\theta]}(y_i) \qquad i = 1,\ldots,n \qquad \text{and } -\infty < \theta < \infty$$

which is derived from the general form by the transformation $Y_i = X_i - \theta_1$. The MLE of θ is given by $\hat{\theta} = Y_{[n]}$, a sufficient statistic for the parameter. However, this is not an unbiased estimator. A modified unbiased estimator is easily seen to be

$$\hat{\theta}_1 = \frac{(n+1)\, Y_{[n]}}{n}$$

$$\text{with} \qquad Var(\hat{\theta}_1) = \frac{\theta^2}{n(n+2)}$$

It has been shown [67], that confidence limits, with coefficient $1 - \alpha$, for θ are t and t/ψ, where t is the sample range and ψ is given by $\psi^{n-1}\{n-(n-1)\psi\} = \alpha$.

Also confidence intervals for θ can be constructed by observing that

$$w = \frac{Y_{[n]}}{\theta} \quad \text{is a pivotal quantity with distribution } f(w) = nw^{n-1}$$

$$0 \leq w \leq 1.$$

Therefore

$$P_r \left[\frac{Y_{[n]}}{\theta} > u \right] = 1 - u^n = \alpha \qquad \text{if} \qquad u = \sqrt[n]{1-\alpha}$$

Hence $\theta < \dfrac{Y_{[n]}}{\sqrt[n]{1-\alpha}}$ is an upper confidence interval for θ.

5.1.2.4 Goodness-of-fit Statistic

The validity of a proposed distribution can be tested using the Kolmogorov Smirnov goodness-of-fit test which focuses on the deviations between the observed cumulative distribution function $F_n(x)$ and the hypothetical cumulative function $F_o(x)$.

The statistic $D_n = \sup_{-\infty < x < \infty} \left| F_n(x) - F_o(x) \right|$

has been shown to be independent of the CDF from which the sample was drawn. The exact distribution of D_n is widely tabulated – see, for example, Lindgren [68].

To test the hypothesis that the sample distribution is some specified continuous $F_o(.)$ i.e.

H_0 : $X_i \sim F_0(.)$

H_1 : X_i is other than specified

a critical value of c is calculated from table 5.1.2.4 at a prescribed significance level and H_0 is accepted if $D_n < C$.

In effect, if H_0 is false then $F_n(.)$ will tend to be near the true CDF F(.) and not near the proposed one $F_0(.)$ and consequently D_n will tend to be large.

This is called the Kolmogorov goodness-of-fit test. For further statistical details and discussion of the test the reader is referred to refs. [50, 68].

5.1.3 Correlation Coefficient

The correlation coefficient r of two random variables X and Y with expected values μ_X, μ_Y and standard deviations σ_X and σ_Y respectively, is defined by

$$r = \frac{COV[X,Y]}{\sigma_X \sigma_Y}$$

where COV [X,Y] = $E[(X-\mu_X)(Y-\mu_Y)]$ is known as the covariance of X and Y.

Sample Size (n)	Significance Level .20	.15	.10	.05	.01
1	.900	.925	.950	.975	.995
2	.684	.726	.776	.842	.929
3	.565	.597	.642	.708	.829
4	.494	.525	.564	.624	.734
5	.446	.474	.510	.563	.669
6	.410	.436	.470	.521	.618
7	.381	.405	.438	.486	.577
8	.358	.381	.411	.457	.543
9	.339	.360	.388	.432	.514
10	.322	.342	.368	.409	.486
11	.307	.326	.352	.391	.468
12	.295	.313	.338	.375	.450
13	.284	.302	.325	.361	.433
14	.274	.292	.314	.349	.418
15	.266	.283	.304	.338	.404
16	.258	.274	.295	.328	.391
17	.250	.266	.286	.318	.380
18	.244	.259	.278	.309	.370
19	.237	.252	.272	.301	.361
20	.231	.246	.264	.294	.352
25	.21	.22	.24	.264	.32
30	.21	.22	.22	.242	.29
35	.18	.19	.21	.23	.27
40				.21	.25
50				.19	.23
60				.17	.21
70				.16	.19
80				.15	.18
90				.14	
100				.14	
Asymptotic Formula:	$\frac{1.07}{\sqrt{n}}$	$\frac{1.14}{\sqrt{n}}$	$\frac{1.22}{\sqrt{n}}$	$\frac{1.36}{\sqrt{n}}$	$\frac{1.63}{\sqrt{n}}$

Table 5.1.4.1: Critical statistics for the Kolmogorov-Smirnov goodness-of-fit test [from ref 68]

The value of the correlation coefficient gives an indication of the linearity of the relationship between the two random variables (not necessarily normal). When two random variables are independent then they are uncorrelated and r=0. The converse holds when X and Y are normally distributed. The distribution of the sample correlation coefficient is not easily computable even in the case of normally distributed variables. In the general case the variance of r is an expression involving all the second-order and fourth-order moments of the population sampled.

However, for normally distributed quantities this is simplified to

$$\text{Var } (r) = \frac{(1-\rho^2)^2}{n}$$

where ρ is the true value of the correlation.

Nevertheless, this is of little value since in practice the distribution of r tends to normality very slowly if r is not close to zero, and it is not recommended for $n < 500$.

When r=0 (and the random variables are independent) it is known that the statistic

$$T = r \left[\frac{n-2}{1-r^2}\right]^{\frac{1}{2}}$$

follows a t_{n-2} distribution.

Consequently, to test the null hypothesis H_0 : r=0 against the alternative hypothesis H_1 : $r \neq 0$ at level of significance ξ, H_0 is rejected when $|T| > t_{1-\xi/2}$; n-2.

The tables by Fisher and Yates [69] allow this test to be applied directly from the value of r for samples up to 100 pairs of observations.

A more useful transformation has been proposed by Fisher [70]

$$Z = \tfrac{1}{2} \ell n \left[\frac{1+r}{1-r}\right]$$

which leads to an asymptotically normal distribution with mean

$$E\,[Z] = \tfrac{1}{2}\, \ell n \left[\frac{1+\rho}{1-\rho}\right]$$

and variance

$$V[Z] = \frac{1}{n-3}$$

Hence, approximate $100(1-\xi)\%$ Confidence Interval for r is:

$$\left\{\tanh\left[\tfrac{1}{2}\, \ell n\left[\frac{1+r}{1-r}\right] \pm \frac{Z_{1-\xi/2}}{\sqrt{n-3}}\right]\right\}$$

5.2 Literature Review

Townend [12] fitted a Weibull distribution to lack of fusion and lack of penetration defects from 1890 metres of node welds fabricated by manual metal arc in offshore structures. The parameters of the Weibull function are summarised below in table 5.2.1.

Defect Type	Defect Dimension	Distribution Parameters	
		α	β
Lack of Fusion	Depth	7.00	2.18
	Length	341	2.14
Lack of Penetration	Depth	8.13	2.76
	Length	361	3.65
Merged Data	Depth	7.38	2.39
	Length	348	2.42

Table 5.2.1 : Model Parameters of Weibull Distribution Obtained by Townend [12]

Similarly, Rogerson and Wong [71] presented results on embedded defect height from a study of 1000 metres of weld length in vertical and horizontal node joints of an offshore structure. The three parameter Weibull model was fitted to the data with parameters as shown in table 5.2.2.

Defect Type	Distribution Parameters		
	α	β	γ
Non-Planar	0.83	0.70	0.1
Planar	5.0	1.4	0.1
All Defects	3.20	0.95	1.0

Table 5.2.2 : Weibull Parameters Obtained by Rogerson and Wong [71]

These two sets of results provide the only available published information on embedded defect height in offshore structures. Comparisons between the models for the two investigations show that the cumulative probabilities fall reasonably in the same range for depths up to 15mm but there are marked variations for defects of depth larger than 15mm.

Rodrigues et al [72] also presented results from NDE programmes in offshore structures but their investigation is only on UT planar defect length. They proposed exponential and Weibull curves based on data from 250 metres of tubular node welds in four different offshore structures. Their curves indicate a marked sccatter between fabricators in both the type and the parameters of the distributions.

Turning now to surface-breaking defects, these tend to be more important from the fracture point of view because they tend to be associated with a larger stress intensity factor. Information on these defects is more widely available, especially in nuclear installations.

Nichols [73] reported 153 planar defects from 599 pressure vessel seams of 2336 metres in length but he gives no information on their dimensions, nor the method by which they have been collected.

Becher and Pedersen [74] suggested the distribution function

$$f(z) = 2.56 \exp(-2.56(z - 0.1))$$

for the crack depth z (in.) in pressure vessels. This model incorporates non-defection probabilities of the UT device and represents the distribution of defects entering service. Unfortunately it is not possible from their results to obtain separate expressions for the two functions.

Dvorak and Schwegler [75] suggested that the distribution of defect lengths of surface cracks should be lognormal and give the cumulative distribution of 10 cracks.

Bokarlud and Karlsen [76] fitted an exponential distribution with β = 0.11 mm for the depth of 325 very small surface cracks on production welds at varous shipyards. The depth of the cracks was reproduced on replicas from silicon rubber and the dimension was measured using a microscope.

Harris [77] fitted the lognormal distribution to defect sizes on base metal shop welds and field welds in pipes of various diameters and wall thicknesses which were reported by Wilson. Wilson's estimates however are based on judgement rather than data.

The lognormal function has also been used by Tank [78] to model the depth of surface cracks detected by ultrasonics. However the dimensions correspond to very small surface cracks on aluminium specimens.

In nuclear structures the most complete crack depth information is provided by Marshall [79] and Becher and Hansen [80].

Marshall [79] estimated the distribution of crack depth in PWR vessels to be exponential with parameter $1/\beta$ = 0.246 in. He indicated that in 44 vessels no defects larger than 1 in. were observed. The 12 defects found were in the range of 0.5 to 1 in.

Becher and Hansen [80] presented data from PWR vessels of defect length on slag inclusions and depth of surface breaking cracks. The 233 surface cracks were not weld defects but were due to some kind of stress corrosion. They were detected by MPI and the crack dimension was measured as the depth of grinding. They have shown that the lognormal distribution provides a good fit to the data. The parameters of the model were later estimated by Hansen [81] to be μ = 0.265 and σ = 0.818. Harris and Lim [82] modified the lognormal model to account for the impossibility of having cracks deeper than the thickness of the body. Nilson [48] has fitted a truncated gamma distribution to the crack data, with the truncation level set at 0.45 mm. This model is very similar to an exponential distribution. Weibull parameters of the same data were later obtained by Rogerson and Wong [71].

Kihara et al [83] provided information on crack depth in the form of a histogram for small (up to 5mm) surface cracks of shell plates in spherical pressure vessels, but they give no information on the way the data have been collected. Rogerson and Wong [71] obtained the Weibull parameters α = 1.62 mm, β = 1.10, γ = 0.1 mm.

With regard to the distribution of the width of embedded defects, very few data have been reported. Dufresne et al [84] evaluated this by analysing data from 338 metres of PWR and BWR shell welds inspected by ultrasonics or X-rays. They found that the probability of occurrence of long defects decreases as their width increases. Inspection of figure 10 of ref. [84] shows that for 3, 6 and 12 mm wide defects the probability of having a flaw with length smaller than 512 mm is respectively 96%, 0.14% and 0.006%.

Hansen [81] fitted the lognormal distribution to the width of slag inclusion defects in butt weld joints measured on radiographs. For a total of 131 slag inclusions in weld thickness of 25.5 mm detected in four structures he obtained the parameters

μ = 0.117 and σ = 0.748. It is also reported that width and depth below the surface are correlated but the actual degree of correlation is not mentioned.

Data on the aspect ratio defined as the ratio of surface defect length to defect depth are virtually non-existent. Harris and Lim [82] derived and discussed suitable lognormal and exponential distributions based on assumed knowledge of the proportion of cracks, p, with aspect ratio larger than 5. They concluded that a value of p of 0.01 would be assumed to be applicable.

The findings in this section will be discussed further in sections 5.3.7 and 5.4.6 of this chapter.

5.3 Surface-breaking Defects

This section contains an analysis of surface-breaking defects involving the quantities, defect depth, defect length, defect aspect ratio and appropriate defect size correlations. The defects were detected by Magnetic Particle Inspection and subsequently sized by grinding them out.

The total number of surface defects corresponding to each of the three weld type joints (X, T, B, see section 3.2) and main location (node, see section 3.1) is shown in table 5.3.1 below.

Location	Weld Type			
	X	T	B	TOTAL
Node 1	369	255	57	681
Node 2	866	467	84	1417
Node 3	286	270	71	627
Node 4	132	85	47	264
Node 5	35	40	9	84
Node 6	51	48	3	102
All Nodes	1739	1165	271	3175

Table 5.3.1 Absolute number of surface defects found by MPI

The entries in the table represent the absolute number of defects (i.e. including

multiple occurrence) as opposed to the number of defective welds.

5.3.1. Defect Location

Many imperfections result in structural discontinuities which can reduce the performance of the weld. The latter depends significantly on the orientation of the discontinuity relative to the principal stress direction. Not all discontinuities are necessarily associated with changes in the metallurgical structure of the weld.

In theory, imperfections can occur in an infinite number of locations in a joint. In this present study three defect type categories, namely CR, NF, LI (see section 3.3) were grouped into three distinct classes (see fig. 5.3.1.1):

ST and STC : Surface-breaking toe defects located in the continuous member

SW and SWC : Surface-breaking weld defects

STA : Surface-breaking toe defects located in the abutting member

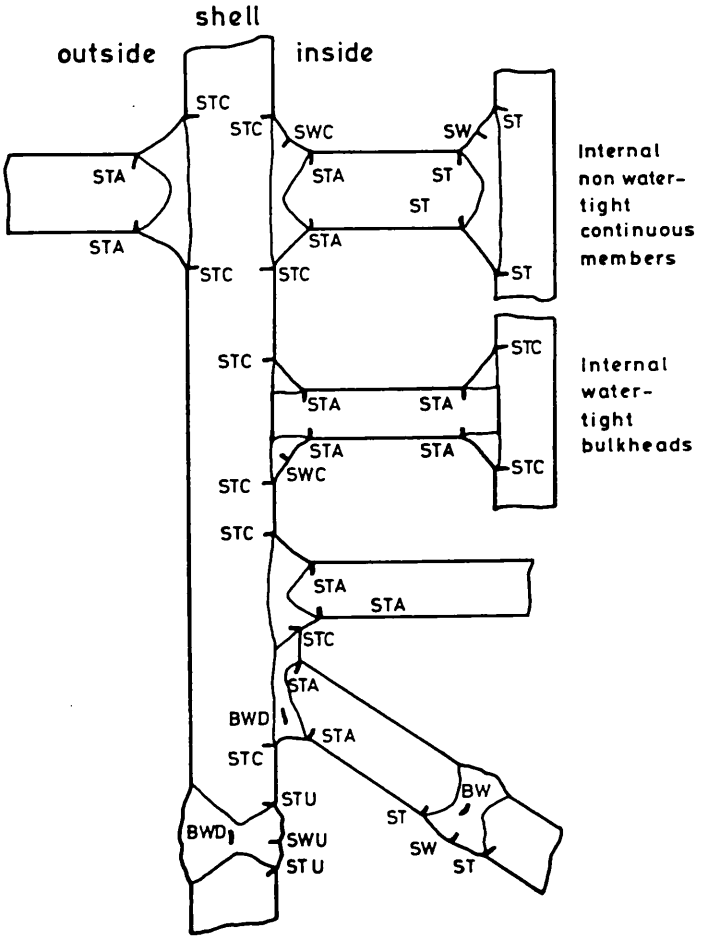


Fig. 5.3.1.1

The analysis in this report involves the dimensions defect depth and defect length, together with aspect ratio and appropriate defect size correlations.

The depth of the defects was parametrised by the dimensions L1, L3 and LW depending upon the weld type and defect location within the joint (see Fig. 5.3.1.1). These dimensions represent the depth of the defect as measured at right angles to the surface of the continuous member (L1), abutting member (L3) and weld surface (LW) (see Fig. 5.3.1.2 below)

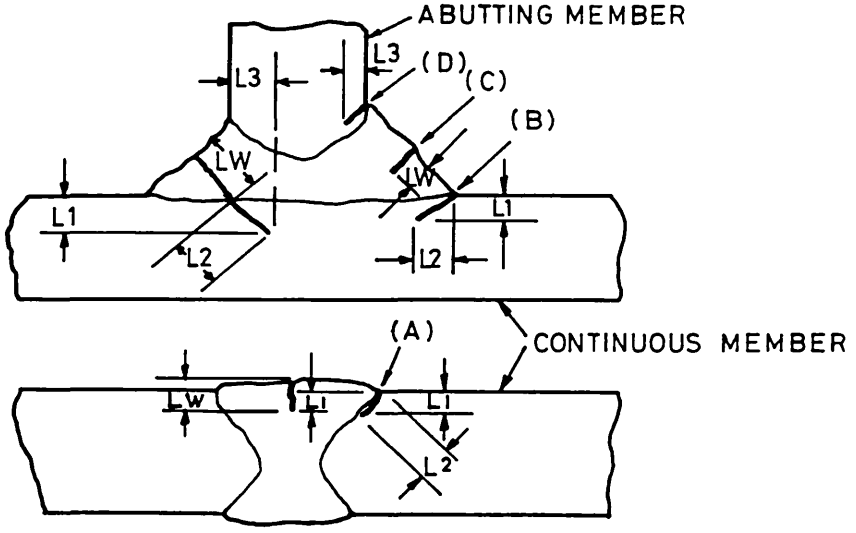


Fig. 5.3.1.2

For this classification, sufficient data were available for the following categories:

plate butt welds	: case (A)	L1 dimension of a surface-breaking toe defect (ST, STC) in a continuous member [Fig. 5.3.1.2 see (A)]
cruciforms and tee butts	: case (B)	L1 dimension of a surface-breaking toe defect (ST, STC) in a continuous member [Fig. 5.3.1.2 see (B)]
	: case (C)	LW dimension (with L2=0) of a surface-breaking weld defect (SW, SWC) [Fig. 5.3.1.2 see (C)]

: case (D) L3 dimension of a surface-breaking toe defect (STA) in an abutting member [Fig. 5.3.1.2 see (D)]

In addition, for cases (A) and (B), an analysis has been undertaken for the angle between the defect and the surface of the continuous member. Examination of Fig. 5.3.1.2 shows that the angle between the defect and the surface of the continuous member is given by $\sin^{-1}(L1/L2)$ for plate butt welds and $\tan^{-1}(L1/L2)$ for cruciform and tee butt joints.

5.3.2 Surface-breaking Toe Defects in Continuous Members

The defect characteristics which have been included in the statistical analysis are as follows:

- dimension, L1 (see Fig. 5.3.1.2)
- dimension, L2 (see Fig. 5.3.1.2)
- defect length, L (in direction of welding)
- defect aspect ratio, ϵ (taken as L/L1)
- defect surface angle, θ (see section 5.3.1)

The depth of a surface-breaking defect measured in a direction normal to the surface (dimension L1) is generally the most important parameter affecting the occurrence of fracture and is the parameter given more importance in this analysis.

Preliminary analysis of the data for the parameter L1 showed that the sample statistics for defect depth do not differ significantly between different welding processes or between different locations in the structure (for numerical results see [85]). This result is of considerable interest since the defect occurrence rate was found to be significantly different between welding processes and between different positions in the structure (see chapter 4). In addition the statistics for L1 were found to be rasonably independent of fabricator. However comparisons were difficult because of small and varying sample sizes.

The data are shown in the form of a histogram in figure 5.3.2.1 which includes defects of all types. It can be clearly seen from this that the linear indication defects tend to penetrate deeper into the member. In figure 5.3.2.2 a histogram is shown for all linear indication defects. The differences between plate butt welds and other weld types cannot be clearly distinguished.

```
    DEFECT TYPE                SYMBOL  COUNT      MEAN      ST.DEV.

 NON FUSION         (NF)         N       20        1.12        .74
 CRACK              (CR)         C       55        1.48       1.38
 LINEAR INDICATION  (LI)         L      139        3.56       2.37

INTERVAL                                         FREQUENCY PERCENTAGE
NAME       5    10   15   20   25   30   35   40  INT. CUM. INT.  CUM.
      +----+----+----+----+----+----+----+----+
  .43 +                                            0    0    .0    .0
  .86 +NNNNNNNNNCCCCCCCCCCCCCC                    23   23  10.7  10.7
 1.29 +NNNNNNCCCCCCCCCCCCCCCCCCLLLLLLLLLLLL       36   59  16.8  27.6
 1.72 +NNCCCCCCCCL                                11   70   5.1  32.7
 2.15 +NNCCCCLLLLLLLLLLLLLLLLLLLLLLLLLLLLLLLLLL+  41  111  19.2  51.9
 2.58 +NCLLLLL                                     7  118   3.3  55.1
 3.01 +NCCCCLLLLLLLLLLLLLLLLLLLLLLLLLLLLLLLLLLL+  47  165  22.0  77.1
 3.44 +                                            0  165    .0  77.1
 3.87 +CLLL                                        4  169   1.9  79.0
 4.30 +CCLLLLLLLLLLL                              13  182   6.1  85.0
 4.73 +                                            0  182    .0  85.0
 5.16 +LLLLLLLLLLL                                11  193   5.1  90.2
 5.59 +L                                           1  194    .5  90.7
 6.02 +LLLLLL                                      6  200   2.8  93.5
 6.45 +                                            0  200    .0  93.5
 6.88 +L                                           1  201    .5  93.9
 7.31 +LLL                                         3  204   1.4  95.3
 7.74 +                                            0  204    .0  95.3
 8.17 +LLL                                         3  207   1.4  96.7
 8.60 +                                            0  207    .0  96.7
 9.03 +C                                           1  208    .5  97.2
 9.46 +                                            0  208    .0  97.2
 9.89 +                                            0  208    .0  97.2
10.32 +LL                                          2  210    .9  98.1
10.75 +                                            0  210    .0  98.1
11.18 +L                                           1  211    .5  98.6
11.61 +                                            0  211    .0  98.6
12.04 +L                                           1  212    .5  99.1
12.47 +                                            0  212    .0  99.1
12.90 +                                            0  212    .0  99.1
13.33 +L                                           1  213    .5  99.5
13.76 +                                            0  213    .0  99.5
14.19 +                                            0  213    .0  99.5
14.62 +                                            0  213    .0  99.5
15.05 +L                                           1  214    .5 100.0
15.48 +                                            0  214    .0 100.0
15.91 +                                            0  214    .0 100.0
16.34 +                                            0  214    .0 100.0
      +----+----+----+----+----+----+----+----+
           5    10   15   20   25   30   35   40
```

FIGURE 5.3.2.1 : HISTOGRAM FOR L1 IN TEE BUTTS AND CRUCIFORMS
[DEFECT LOCATIONS ST AND STC]

```
    WELD TYPE                        SYMBOL  COUNT    MEAN    ST.DEV.
 PLATE BUTT WELDS            (B )      A       58     4.24     2.27
 CRUCIFORMS AND TEE BUTTS    (XT)      B      139     3.55     2.37

INTERVAL                                         FREQUENCY PERCENTAGE
NAME       5    10   15   20   25   30   35   40  INT. CUM. INT.  CUM.
      +----+----+----+----+----+----+----+----+
 1.52 +AABBBBBBBBBBBB                             14   14   7.1   7.1
 1.90 +                                            0   14    .0   7.1
 2.28 +AAAAAAAAAAAABBBBBBBBBBBBBBBBBBBBBBBBBBBB+  45   59  22.8  29.9
 2.66 +ABBBBB                                      6   65   3.0  33.0
 3.04 +AAAAAAAAAAAAABBBBBBBBBBBBBBBBBBBBBBBBBBB+  54  119  27.4  60.4
 3.42 +                                            0  119    .0  60.4
 3.80 +BBB                                         3  122   1.5  61.9
 4.18 +AAAAAAAAAAAAABBBBBBBBBBB                   24  146  12.2  74.1
 4.56 +                                            0  146    .0  74.1
 4.94 +                                            0  146    .0  74.1
 5.32 +AAAAAAAABBBBBBBBBBB                        19  165   9.6  83.8
 5.70 +B                                           1  166    .5  84.3
 6.08 +AAAAABBBBBB                                11  177   5.6  89.8
 6.46 +                                            0  177    .0  89.8
 6.84 +B                                           1  178    .5  90.4
 7.22 +AABBB                                       5  183   2.5  92.9
 7.60 +                                            0  183    .0  92.9
 7.98 +                                            0  183    .0  92.9
 8.36 +ABBB                                        4  187   2.0  94.9
 8.74 +                                            0  187    .0  94.9
 9.12 +AA                                          2  189   1.0  95.9
 9.50 +                                            0  189    .0  95.9
 9.88 +                                            0  189    .0  95.9
10.26 +ABB                                         3  192   1.5  97.5
10.64 +                                            0  192    .0  97.5
11.02 +B                                           1  193    .5  98.0
11.40 +                                            0  193    .0  98.0
11.78 +                                            0  193    .0  98.0
12.16 +B                                           1  194    .5  98.5
12.54 +                                            0  194    .0  98.5
12.92 +                                            0  194    .0  98.5
13.30 +AB                                          2  196   1.0  99.5
13.68 +                                            0  196    .0  99.5
14.06 +                                            0  196    .0  99.5
14.44 +                                            0  196    .0  99.5
14.82 +                                            0  196    .0  99.5
15.20 +B                                           1  197    .5 100.0
15.58 +                                            0  197    .0 100.0
      +----+----+----+----+----+----+----+----+
           5    10   15   20   25   30   35   40
```

FIGURE 5.3.2.2 : HISTOGRAM FOR L1 IN LINEAR INDICATION DEFECTS
[DEFECT LOCATIONS ST AND STC]

For the purpose of distribution fitting, the data have been subdivided according to defect type and according to weld type. However, data for tee butts and cruciforms have been merged because of their similarities. The lognormal and Weibull parameters together with two-sided 95% confidence intervals are shown for each of the three defect dimensions in tables 5.3.2.1 to 5.3.2.3.

Further analysis of defect dimensions has been undertaken to examine the angle at which the defect makes to the surface of the continuous member, (see fig. 5.3.1.2). Data were analysed for the cases where both dimenions L1 and L2 have been reported (somewhat smaller sample than for L1). Examination of fig. 5.3.1.2 shows that the angle between the defect and the surface of the continuous member is given by $\sin^{-1}(L1/L2)$ for plate butt joints and $\tan^{-1}(L1/L2)$ for cruciform and tee butt joints.

Histograms for the angle (in radians) for both XT and B weld joints are shown respectively in fig. 5.3.2.3 and 5.3.2.4. In the former case no differences exist between crack and non-fusion defects. The mean angles are 21° and 20° respectively, whereas in LI defects the mean angle is 29° (see fig. 5.3.2.3).

In comparison, in plate butt joints, linear indication defects have an average inclination value of 41°. The differences between the two groups of joints are shown in fig. 5.3.2.4. The two extreme values of the angle correspond to defects which are normal to the plate surface. These cannot be considered as impossible values but even if they are removed from the analysis on the basis of the range of the rest of the data, the mean angle reduces to about 38° which is well above the value of 29° in cruciform and tee butt joints.

The normal, lognormal and uniform distributions were fitted to the data and the results shown in table 5.3.2.4. The lognormal distribution appears to be non-justifiable whereas the normal distribution gives reasonably good fit to the data. The uniform distribution was chosen as an alternative distribution, although in some cases the KST value is clearly very poor to justify its use. The MLE estimates of its parameters are given in table 5.3.2.4, together with the upper 95% confidence interval for the one terminal transformed distribution.

DEFECT TYPE		SYMBOL	COUNT	MEAN	ST.DEV.
NON FUSION	(NF)	N	20	.373	.165
CRACK	(CR)	C	54	.346	.155
LINEAR INDICATION	(LI)	L	133	.503	.186

INTERVAL NAME	5 10 15 20 25 30 35 40	FREQUENCY INT.	FREQUENCY CUM.	PERCENTAGE INT.	PERCENTAGE CUM.
.060	•C	1	1	.5	.5
.080	•	0	1	.0	.5
.100	•L	1	2	.5	1.0
.120	•CLL	3	5	1.4	2.4
.140	•C	1	6	.5	2.9
.160	•NL	2	8	1.0	3.9
.180	•NNNCCCCCCCCCLL	14	22	6.8	10.6
.200	•CCCLLL	6	28	2.9	13.5
.220	•L	1	29	.5	14.0
.240	•L	1	30	.5	14.5
.260	•NNNCCCLLLLL	11	41	5.3	19.8
.280	•LLLLL	5	46	2.4	22.2
.300	•CLLL	4	50	1.9	24.2
.320	•	0	50	.0	24.2
.340	•NNCCCCCCCCCCCCLLLLLLL	21	71	10.1	34.3
.360	•CCCLLLLLL	9	80	4.3	38.6
.380	•	0	80	.0	38.6
.400	•NLLLLL	6	86	2.9	41.5
.420	•NCLLLLL	7	93	3.4	44.9
.440	•CL	2	95	1.0	45.9
.460	•	0	95	.0	45.9
.480	•NNNNNNCCCCCCCLLLLLLLLLLL	25	120	12.1	58.0
.500	•	0	120	.0	58.0
.520	•CCLLLLLL	8	128	3.9	61.8
.540	•LL	2	130	1.0	62.8
.560	•NNCCCCLLLLL	11	141	5.3	68.1
.580	•L	1	142	.5	68.6
.600	•CCLLLLLLLLLLLLL	15	157	7.2	75.8
.620	•CL	2	159	1.0	76.8
.640	•LLLLLL	6	165	2.9	79.7
.660	•CCLLLLLLLLLLL	14	179	6.8	86.5
.680	•LLLL	4	183	1.9	88.4
.700	•LL	2	185	1.0	89.4
.720	•LLLLL	5	190	2.4	91.8
.740	•	0	190	.0	91.8
.760	•LLL	3	193	1.4	93.2
.780	•	0	193	.0	93.2
.800	•NLLLLLLLLLLLL	14	207	6.8	100.0

FIGURE 5.3.2.3 : HISTOGRAM FOR DEF-SUR ANGLE IN TEE BUTTS AND CRUCIFORMS [DEFECT LOCATIONS ST AND STC]

WELD TYPE		SYMBOL	COUNT	MEAN	ST.DEV.
PLATE BUTTS	(B)	A	33	.716	.309
CRUCIFORMS AND TEE BUTTS	(XT)	B	133	.503	.186

INTERVAL NAME	5 10 15 20 25 30 35 40	FREQUENCY INT.	FREQUENCY CUM.	PERCENTAGE INT.	PERCENTAGE CUM.
.120	•BBB	3	3	1.8	1.8
.160	•B	1	4	.6	2.4
.200	•BBBBB	5	9	3.0	5.4
.240	•BB	2	11	1.2	6.6
.280	•ABBBBBBBBBB	11	22	6.6	13.3
.320	•BBB	3	25	1.8	15.1
.360	•AAABBBBBBBBBBBBB	16	41	9.6	24.7
.400	•AABBBBB	7	48	4.2	28.9
.440	•ABBBBBB	7	55	4.2	33.1
.480	•ABBBBBBBBBBB	13	68	7.8	41.0
.520	•BBBBBB	6	74	3.6	44.6
.560	•AAABBBBBBB	10	84	6.0	50.6
.600	•ABBBBBBBBBBBBB	15	99	9.0	59.6
.640	•ABBBBBBB	8	107	4.8	64.5
.680	•AAABBBBBBBBBBBBBBB	19	126	11.4	75.9
.720	•BBBBBBB	7	133	4.2	80.1
.760	•AABBB	5	138	3.0	83.1
.800	•AAABBBBBBBBBBBB	16	154	9.6	92.8
.840	•	0	154	.0	92.8
.880	•AAAAAA	6	160	3.6	96.4
.920	•	0	160	.0	96.4
.960	•A	1	161	.6	97.0
1.000	•AA	2	163	1.2	98.2
1.040	•A	1	164	.6	98.8
1.080	•	0	164	.0	98.8
1.120	•	0	164	.0	98.8
1.160	•	0	164	.0	98.8
1.200	•	0	164	.0	98.8
1.240	•	0	164	.0	98.8
1.280	•	0	164	.0	98.8
1.320	•	0	164	.0	98.8
1.360	•	0	164	.0	98.8
1.400	•	0	164	.0	98.8
1.440	•	0	164	.0	98.8
1.480	•	0	164	.0	98.8
1.520	•	0	164	.0	98.8
1.560	•	0	164	.0	98.8
1.600	•AA	2	166	1.2	100.0

FIGURE 5.3.2.4 : HISTOGRAM FOR DEF-SUR ANGLE IN LI DEFECTS [DEFECT LOCATIONS ST AND STC]

Table 5.3.2.1: Distribution results for dimension L1 for Cases (A) and (B) [defect locations ST and STC]

Lognormal Distribution

Type	μ	σ^2	C.L. (μ)	C.L. (σ^2)	KST	Size
LI (XT)	1.103	0.316	(1.009,1.196)	(0.253,0.406)	0.18	139
CR (XT)	0.130	0.471	(-0.055,0.315)	(0.334,0.714)	0.19	55
NF (XT)	-0.067	0.373	(-0.352,0.218)	(0.216,0.795)	0.25	20
ALL (XT)	0.730	0.607	(0.626,0.834)	(0.507,0.740)	0.14	217
LI (B)	1.319	0.255	(1.186,1.452)	(0.182,0.382)	0.12	58

Transformed Data (Ln)

Type	Skewness	St.Error	Kurtosis	St. Error
LI (XT)	0.280	0.208	0.320	0.415
CR (XT)	0.608	0.330	-0.040	0.661
NF (XT)	0.363	0.548	-1.286	1.095
ALL (XT)	-0.126	0.166	-0.409	0.333
LI (B)	0.024	0.322	-0.129	0.643

Weibull Distribution

Type	β	α	C.L. (β)	C.L. (α)	KST	Size
LI (XT)	1.672	4.019	(1.471,1.936)	(3.600,4.486)	0.21	139
CR (XT)	1.314	1.628	(1.024,1.597)	(1.284,2.049)	0.20	55
NF (XT)	1.692	1.272	(1.072,2.277)	(0.919,1.750)	0.19	20
ALL (XT)	1.351	3.044	(1.218,1.516)	(2.730,3.395)	0.15	217
LI (B)	2.009	4.809	(1.578,2.429)	(4.136,5.567)	0.14	58

Table 5.3.2.2: Distribution results for Defect Length for Cases (A) and (B) [defect locations ST and STC]

Lognormal Distribution

Type	μ	σ^2	C.L. (μ)	C.L. (σ^2)	KST	Size
LI (XT)	3.954	1.121	(2.125,4.130)	(0.897,1.440)	0.08	139
CR (XT)	4.012	0.899	(3.756,4.268)	(0.637,1.363)	0.08	55
NF (XT)	3.772	1.477	(3.204,4.340)	(0.854,3.150)	0.14	20
ALL (XT)	3.941	1.100	(3.801,4.080)	(0.923,1.341)	0.06	217
LI (B)	4.043	0.738	(3.817,4.269)	(0.527,1.106)	0.11	58

Transformed Data (Ln)

Type	Skewness	St.Error	Kurtosis	St. Error
LI (XT)	-0.196	0.208	0.238	0.415
CR (XT)	0.276	0.330	-0.152	0.661
NF (XT)	0.610	0.548	-0.107	1.095
ALL (XT)	-0.030	0.166	0.204	0.333
LI (B)	0.420	0.322	1.728	0.643

Weibull Distribution

Type	β	α	C.L. (β)	C.L. (α)	KST	Size
LI (XT)	0.981	87.746	(0.863,1.136)	(72,739,105.849)	0.11	139
CR (XT)	1.014	89.503	(0.790,1.232)	(65.797,120.554)	0.08	55
NF (XT)	0.765	81.425	(0.484,1.030)	(39.721,134.937)	0.17	20
ALL (XT)	0.957	86.870	(0.863,1.074)	(74.480,101.321)	0.10	217
LI (B)	0.983	88.836	(0.779,1.189)	(65.271,119.806)	0.12	58

Table 5.3.2.3: Distribution results for the Ratio (defect length)/(L1) for cases (A) and (B) [defect locations ST and STC]

Lognormal Distribution

Type	μ	σ^2	C.L. (μ)	C.L. (σ^2)	KST	Size
LI (XT)	2.852	1.474	(2.650,3.054)	(1.180,1.894)	0.08	139
CR (XT)	3.882	1.530	(3.553,4.221)	(1.085,2.320)	0.07	55
NF (XT)	3.838	2.074	(3.165,4.511)	(1.200,4.423)	0.13	20
ALL (XT)	3.211	1.749	(3.035,3.387)	(2.132,1.461)	0.06	217
LI (B)	2.723	0.812	(2.486,2.960)	(0.580,1.217)	0.08	58

Transformed Data (Ln)

Type	Skewness	St.Error	Kurtosis	St. Error
LI (XT)	-0.179	0.208	0.246	0.415
CR (XT)	0.294	0.330	-0.365	0.661
NF (XT)	0.261	0.548	-0.209	1.095
ALL (XT)	0.076	0.166	0.371	0.333
LI (B)	-0.368	0.322	0.423	0.643

Weibull Distribution

Type	β	α	C.L. (β)	C.L. (α)	KST	Size
LI (XT)	0.864	31.509	(0.760,1.000)	(25.465,38.987)	0.12	139
CR (XT)	0.788	91.054	(0.614,0.957)	(61.284,133.580)	0.12	55
NF (XT)	0.686	95.687	(0.434,0.923)	(42.982,210.241)	0.15	20
ALL (XT)	0.735	48.304	(0.663,0.825)	(39.534,59.020)	0.11	217
LI (B)	1.167	23.455	(0.917,1.411)	(18.091,30.175)	0.06	58

Table 5.3.2.4: Distribution results for defect/surface angle for Cases (A) and (B) [defect locations ST and STC]

Normal Distribution

Type	μ	σ^2	C.L. (μ)	C.L. (σ^2)	KST	Size
LI (XT)	0.502	0.035	(0.470,0.534)	(0.028,0.045)	0.12	133
CR (XT)	0.346	0.024	(0.304,0.388)	(0.017,0.036)	0.14	54
NF (XT)	0.373	0.027	(0.296,0.450)	(0.016,0.058)	0.16	20
ALL (XT)	0.449	0.036	(0.423,0.475)	(0.030,0.044)	0.09	207
LI (B)	0.716	0.096	(0.606,0.826)	(0.062,0.168)	0.12	33

Lognormal Distribution

Type	μ	σ^2	C.L. (μ)	C.L. (σ^2)	KST	Size
LI (XT)	-0.778	0.214	(-0.857,-0.699)	(0.170,0.277)	0.15	133
CR (XT)	-1.180	0.283	(-1.325,-1.034)	(0.200,0.431)	0.18	54
NF (XT)	-1.088	0.234	(-1.314,-0.862)	(0.135,0.499)	0.20	20
ALL (XT)	-0.913	0.265	(-0.983,-0.843)	(0.220,0.325)	0.15	207
LI (B)	-0.423	0.190	(-0.578,-0.268)	(0.123,0.332)	0.11	33

Skewness and Kurtosis

Type	Normal Distribution				Transformed Data (Ln)			
	Skewness	St.Error	Kurtosis	St.Error	Skewness	St.Error	Kurtosis	St.Error
LI (XT)	-0.250	0.212	-0.953	0.425	-1.163	0.212	1.190	0.425
CR (XT)	0.185	0.333	-1.052	0.667	-0.843	0.333	0.694	1.667
NF (XT)	0.433	0.548	-0.299	1.095	-0.347	0.548	-1.114	1.095
ALL (XT)	0.022	0.170	-0.997	0.340	-0.945	0.170	0.703	0.340
LI (B)	0.956	0.426	1.107	0.853	-0.180	0.426	-0.516	0.853

Uniform Distribution

Type	a	b	Range	C.L.	KST	Size
LI (XT)	0.083	0.785	0.702	0.718	0.18	133
CR (XT)	0.050	0.644	0.594	0.628	0.14	54
NF (XT)	0.142	0.785	0.644	0.748	0.35	20
ALL (XT)	0.050	0.785	0.735	0.746	0.13	207
LI (B)	0.253	1.571	1.318	1.443	0.35	33

5.3.3 Surface-breaking Weld Defects

This section contains the analysis of surface-breaking weld defects for case (C) corresponding to cruciform and tee butt joints (see section 5.3.1 and fig. 5.3.1.2).

The defect dimensions which have been considered in the analysis are as follows:

- dimension, LW (see fig. 5.3.1.2)
- defect length, L (in direction of welding)
- defect aspect ratio, ϵ (taken as L/LW)

A total of 108 defects were reported in this case. As shown in fig. 5.3.1.2, the defect dimension LW is the depth of a weld defect measured normal to the weld surface. Only very few cases were found where the defect extended into the parent plate ($L2 \neq 0$) and these have not been included in the analysis.

From the summary statistics given in [85] it became evident that no systematic differences exist between different types of welded joint, fabricators or node location. The apparent differences have been caused by other parameters such as defect type and welding process. In contrast with the surface-breaking defects (see section 5.3.2), the welding process was found to be of influence. The histogram in fig. 5.3.3.1 shows how the variations in defect depth are affected by both defect type and welding process. Whereas the overall mean value of LW for linear indication defects is 8.36 mm, it is 7.36 mm for SMAW welds and 11.50 mm for GMAW, denoting a significant difference.

Comparisons between cracks and linear indication defects show that, although the sample size for cracks is small (22), the mean depth for this type of defect is appreciably less than for linear indications.

The distribution results are shown for each welding process and each type of joint in tables 5.3.3.1 to 5.3.3.6.

WELDING PROCESS	DEFECT TYPE	SYMBOL	COUNT	MEAN	ST.DEV.
SMAW	LI	A	58	7.36	4.72
SMAW	CR	B	13	5.00	1.54
SMAW	MF	C	3	9.00	9.54
GMAW	LI	D	20	11.50	6.13
GMAW	CR	E	8	3.75	1.39
GMAW	MF	F	1	16.00	.00

INTERVAL NAME	5 10 15 20 25 30 35 40	FREQUENCY INT.	FREQUENCY CUM.	PERCENTAGE INT.	PERCENTAGE CUM.
2.01	+AAAAEE	6	6	5.8	5.8
2.68	+	0	6	.0	5.8
3.35	+AAAAAAAABCDDE	13	19	12.6	18.4
4.02	+AAAAABBBBBCDEEE	15	34	14.6	33.0
4.69	+AAA	3	37	2.9	35.9
5.36	+AAAAAAAAAABBBDE	15	52	14.6	50.5
6.03	+AAAABBDE	8	60	7.8	58.3
6.70	+	0	60	.0	58.3
7.37	+AAAAAB	6	66	5.8	64.1
8.04	+AD	2	68	1.9	66.0
8.71	+B	1	69	1.0	67.0
9.38	+DDD	3	72	2.9	69.9
10.05	+ADD	3	75	2.9	72.8
10.72	+	0	75	.0	72.8
11.39	+AA	2	77	1.9	74.8
12.06	+AAAAAA	6	83	5.8	80.6
12.73	+A	1	84	1.0	81.6
13.40	+ADD	3	87	2.9	84.5
14.07	+	0	87	.0	84.5
14.74	+	0	87	.0	84.5
15.41	+AAAD	4	91	3.9	88.3
16.08	+AADF	4	95	3.9	92.2
16.75	+	0	95	.0	92.2
17.42	+ADD	3	98	2.9	95.1
18.09	+D	1	99	1.0	96.1
18.76	+	0	99	.0	96.1
19.43	+D	1	100	1.0	97.1
20.10	+C	1	101	1.0	98.1
20.77	+	0	101	.0	98.1
21.44	+	0	101	.0	98.1
22.11	+A	1	102	1.0	99.0
22.78	+	0	102	.0	99.0
23.45	+	0	102	.0	99.0
24.12	+	0	102	.0	99.0
24.79	+	0	102	.0	99.0
25.46	+	0	102	.0	99.0
26.13	+D	1	103	1.0	100.0
26.80	+	0	103	.0	100.0
	5 10 15 20 25 30 35 40				

FIGURE 5.3.3.1 : HISTOGRAM FOR LW IN CRUCIFORMS AND TEE BUTTS (DEFECT LOCATIONS SW AND SWC)

Table 5.3.3.1: Distribution results for dimension LW (and L2 = 0) for Case (C) under SMAW [defect locations SW and SWC]

Lognormal Distribution

Type	μ	σ^2	C.L. (μ)	C.L. (σ^2)	KST	Size
LI (XT)	1.803	0.395	(1.638,1.968)	(0.282,0.592)	0.14	58
CR (XT)	1.569	0.086	(1.392,1.746)	(0.044,0.234)	0.19	13
NF (XT)	-	-	-	-	-	-
ALL (XT)	1.763	0.359	(1.624,1.902)	(0.266,0.511)	0.15	74

Transformed Data (Ln)

Type	Skewness	St.Error	Kurtosis	St.Error
LI (XT)	0.123	0.322	-0.998	0.643
CR (XT)	0.315	0.679	-0.953	1.359
NF (XT)	-	-	-	-
ALL (XT)	0.341	0.285	-0.749	0.569

Weibull Distribution

Type	β	α	C.L. (β)	C.L. (α)	KST	Size
LI (XT)	1.694	8.313	(1.331,2.048)	(6.951,9.888)	0.16	58
CR (XT)	3.501	5.549	(1.913,4.980)	(4.525,6.814)	0.16	13
NF (XT)	-	-	-	-	-	3
ALL (XT)	1.673	7.924	(1.357,1.984)	(6.759,9.251)	0.18	74

Table 5.3.3.2: Distribution results for dimension LW (and L2 = 0) for Case (C) under GMAW [defect locations SW and SWC]

Lognormal Distribution

Type	μ	σ^2	C.L. (μ)	C.L. (σ^2)	KST	Size
LI (XT)	2.281	0.385	(1.991,2.571)	(0.223,0.821)	0.15	20
CR (XT)	1.256	0.160	(0.922,1.590)	(0.070,0.663)	0.25	8
NF (XT)	-	-	-	-	-	1
ALL (XT)	2.015	0.537	(1.736,2.294)	(0.338,0.981)	0.12	29

Transformed Data (Ln)

Type	Skewness	St.Error	Kurtosis	St.Error
LT (XT)	-0.510	0.548	-0.855	1.095
CR (XT)	-3.02	0.866	-1.539	1.732
NF (XT)	-	-	-	-
ALL (XT)	-0.176	0.455	-1.253	0.910

Weibull Distribution

Type	β	α	C.L. (β)	C.L. (α)	KST	Size
LI (XT)	2.035	13.008	(1.289,2.739)	(9.932,16.961)	0.08	20
CR (XT)	3.214	4.198	(1.352,4.922)	(3.073,5.831)	0.13	8
NF (XT)	-	-	-	-	-	1
ALL (XT	1.602	10.666	(1.112,2.067)	(8.084,13.967)	0.11	29

Table 5.3.3.3: Distribution results for Defect Length for Case (C) under SMAW [defect locations SW and SWC]

Lognormal Distribution

Type	μ	σ^2	C.L. (μ)	C.L. (σ^2)	KST	Size
LI (XT)	3.710	1.004	(3.447,3.973)	(0.718,1.504)	0.10	58
CR (XT)	3.484	0.921	(2.904,4.064)	(0.473,2.512)	0.20	13
NF (XT)	-	-	-	-	-	3
ALL (XT)	3.668	0.962	(3.440,3.896)	(0.713,1.369)	0.09	74

Transformed Data (Ln)

Type	Skewness	St.Error	Kurtosis	St.Error
LT (XT)	0.119	0.322	-0.282	0.643
CR (XT)	0.223	0.679	-0.695	1.359
NF (XT)	-	-	-	-
ALL (XT)	0.157	0.285	-0.264	0.569

Weibull Distribution

Type	β	α	C.L. (β)	C.L. (α)	KST	Size
LI (XT)	1.011	67.595	(0.794,1.222)	(50,090,90.408)	0.13	58
CR (XT)	1.046	52.186	(0.572,1.488)	(26.370,103,772)	0.16	13
NF (XT)	-	-	-	-	-	3
ALL (XT)	1.020	64.313	(0.827,1.210)	(49.550,82.904)	0.13	74

Table 5.3.3.4: Distribution results for Defect Length for Case (C) under GMAW [defect locations SW and SWC]

Lognormal Distribution

Type	μ	σ^2	C.L. (μ)	C.L. (σ^2)	KST	Size
LI (XT)	3.532	2.016	(2.868,4.195)	(1.166,4.299)	0.10	20
CR (XT)	3.313	0.422	(2.771,3.855)	(0.184,1.748)	0.19	8
NF (XT)	-	-	-	-	-	1
ALL (XT)	3.350	1.899	(2.825,3.875)	(1.196,3.471)	0.11	29

Transformed Data (Ln)

Type	Skewness	St.Error	Kurtosis	St.Error
LI (XT)	0.111	0.548	-0.941	1.095
CR (XT)	-0.515	0.866	-0.965	1.732
NF (XT)	-	-	-	-
ALL (XT)	-0.153	0.455	-0.047	0.910

Weibull Distribution

Type	β	α	C.L. (β)	C.L. (α)	KST	Size
LI (XT)	0.749	68.814	(0.474,1.008)	(33.063,141.510)	0.10	20
CR (CT)	2.066	36.488	(0.869,3.164)	(22.455,60.832)	0.12	8
NF (XT)	-	-	-	-	-	1
ALL (XT)	0.769	55.709	(0.534,0.992)	(31.273,97.701)	0.11	29

Table 5.3.3.5: Distribution results for the Ratio (Defect Length)/(LW) for Case (C) under SMAW [defect locations SW and SWC]

Lognormal Distribution

Type	μ	σ^2	C.L. (μ)	C.L. (σ^2)	KST	Size
LI (XT)	1.906	1.209	(1.617,2.195)	(0.864,1.812)	0.07	58
CR (XT)	1.915	1.121	(1.250,2.555)	(0.576,3.057)	0.20	13
NF (XT)	-	-	-	-	-	3
ALL (XT)	1.905	1.183	(1.652,2.158)	(0.877,1.684)	0.06	74

Transformed Data (Ln)

Type	Skewness	St.Error	Kurtosis	St.Error
LI (XT)	0.171	0.322	-0.301	0.643
CR (XT)	0.528	0.679	0.102	1.359
NF (XT)	-	-	-	-
ALL (XT)	0.219	0.285	-0.218	0.569

Weibull Distribution

Type	β	α	C.L. (β)	C.L. (α)	KST	Size
LI (XT)	0.911	11.720	(0.716,1.102)	(8.404,16.184)	0.10	58
CR (XT)	0.868	11.612	(0.474,1.235)	(5.101,25.586)	0.20	13
NF (XT)	-	-	-	-	-	3
ALL (XT)	0.904	11.673	(0.733,1.072)	(8.697,15.546)	0.11	74

Table 5.3.3.6: Distribution results for the Ratio (Defect Length)/(LW) for Case (C) under GMAW [defect locations SW and SWC]

Lognormal Distribution

Type	μ	σ^2	C.L. (μ)	C.L. (σ^2)	KST	Size
LI (XT)	1.251	2.645	(0.491,2.011)	(1.530,5.640)	0.15	20
CR (XT)	2.057	0.837	(1.294,2.820)	(0.366,3.467)	0.20	8
NF (XT)	-	-	-	-	-	1
ALL (XT)	1.335	2.761	(0.702,1.967)	(1.739,5.046)	0.13	29

Transformed Data (Ln)

Type	Skewness	St.Error	Kurtosis	St.Error
LI (XT)	-0.105	0.548	-1.101	1.095
CR (XT)	-0.042	0.866	-1.620	1.732
NF (XT)	-	-	-	-
ALL (XT)	-0.567	0.455	-0.362	0.910

Weibull Distribution

Type	β	α	C.L. (β)	C.L. (α)	KST	Size
LI (XT)	0.700	7.632	(0.443,0.942)	(3.484,16.507)	0.13	20
CR (XT)	1.305	11.953	(0.549,1.998)	(5.542,26.848)	0.17	8
NF (XT)	-	-	-	-	-	1
ALL (XT)	0.745	8.181	(0.517,0.961)	(4.508,14.610)	0.08	29

5.3.4 Surface-breaking Toe Defects in Abutting Members

This category of defects relates to cruciform and tee butt welds and corresponds to case (D) of section 5.3.1 (see also fig. 5.3.1.2). Only 20 of these defects are reported to have been found as compared with 217 in the ST(STC) and with 108 in the SW(SWC) positions.

The defect dimensions which have been included in the analysis are as follows:

- dimension, L3 (see fig. 5.3.1.2)
- defect length, L (in direction of welding)
- defect aspect ratio, ϵ (taken as L/L3).

Defect depth here is represented by the defect dimension L3, being the depth of the toe defect measured at right angles to the surface of the abutting member (STA position, see fig. 5.3.1.2).

The sample sizes are too small to comment on differences between nodes, fabricators and welding processes but from the evidence obtained for continuous members, such differences are not to be expected. The mean values of L3 for cruciforms and tee butts are 2.10 mm and 2.20 mm respectively, which cannot be considered to be significantly different, especially as the sample sizes are small. Furthermore, classification according to defect type, although it further reduces the sample sizes, indicates no differences between the non-fusion and crack-like defects. The moment estimates of the above means for the merged sample of weld types are shown to be respectively 2.07 mm and 2.09 mm, which are well below the corresponding ones for weld defects in case (C), examined in section 5.3.3.

The distribution parameters of the lognormal and Weibull distributions on defect depth, length and defect aspect ratio are shown in tables 5.3.4.1 to 5.3.4.3.

5.3.5 Correlation between Defect Depth and Defect Length

Correlation analysis shows that a linear relationship between defect depth and defect length is virtually non-existent. Although a tendency for negative correlation exists in almost all cases, none of the regression curves appeared to be significant (see tables 5.3.5.1 to 5.3.5.4).

The largest absolute value of the correlation coefficient r, was observed in crack weld defects under the SMAW process [case (C), see table 5.3.5.3, r = 0.555] but it is

Table 5.3.4.1: Distribution results for dimension L3 for Case (D)
[defect locations STA]

Lognormal Distribution

Type	μ	σ^2	C.L. (μ)	C.L. (σ^2)	KST	Size
LI (XT)	-	-	-	-	-	1
CR (XT)	0.446	0.573	(-0.063,0.955)	(0.280,1.763)	0.27	11
NF (XT)	0.518	0.526	(-0.154,1.190)	(0.218,2.545)	0.17	7
ALL (XT)	0.528	0.551	(0.170,0.886)	(0.314,1.205)	0.18	19

Transformed Data (Ln)

Type	Skewness	St.Error	Kurtosis	St.Error
LI (XT)	-	-	-	-
CR (XT)	0.530	0.738	-0.697	1.477
NF (XT)	-0.202	0.926	-1.109	1.852
ALL (XT)	0.180	0.562	-0.864	1.124

Weibull Distribution

Type	β	α	C.L. (β)	C.L. (α)	KST	Size
LI (XT)	-	-	-	-	-	1
CR (XT)	1.285	2.285	(0.652,1.873)	(1.229,4.302)	0.21	11
NF (XT)	1.641	2.329	(0.622,2.568)	(1.177,4.827)	0.09	7
ALL (XT)	1.401	2.448	(0.874,1.896)	(1.634,3.646)	0.15	19

Table 5.3.4.2: Distribution results for Defect Length for Case (D) [defect location STA]

Lognormal Distribution

Type	μ	σ^2	C.L. (μ)	C.L. (σ^2)	KST	Size
LI (XT)	-	-	-	-	-	1
CR (XT)	3.977	2.409	(2.933,5.012)	(1.176,7.412)	0.12	11
NF (XT)	3.769	0.262	(3.295,4.243)	(0.109,1.268)	0.15	7
ALL (XT)	3.776	1.711	(3.146,4.406)	(0.977,3.742)	0.12	19

Transformed Data (Ln)

Type	Skewness	St.Error	Kurtosis	St.Error
LI (XT)	-	-	-	-
CR (XT)	0.111	0.738	-1.228	1.477
NF (XT)	0.114	0.926	-1.175	1.852
ALL (XT)	0.214	0.562	-0.384	1.124

Weibull Distribution

Type	β	α	C.L. (β)	C.L. (α)	KST	Size
LI (XT)	-	-	-	-	-	1
CR (XT)	0.702	112.625	(0.356,1.023)	(36.188,358.591)	0.12	11
NF (XT)	2.153	55.129	(0.815,3.369)	(32.769,96.080)	0.11	7
ALL (XT)	0.758	83.669	(0.473,1.026)	(39.653,174.691)	0.11	19

Table 5.3.4.3: Distribution results for the Ratio (Defect Length)/(L3) for Case (D) [defect location STA]

Lognormal Distribution

Type	μ	σ^2	C.L. (μ)	C.L. (σ^2)	KST	Size
LI (XT)	-	-	-	-	-	1
CR (XT)	3.531	3.005	(2.356,4.706)	(1.492,9.14)	0.14	11
NF (XT)	3.252	0.499	(2.598,3.906)	(0.207,2.414)	0.18	7
ALL (XT)	3.248	2.461	(2.492,4.004)	(1.405,5.382)	0.15	19

Transformed Data (Ln)

Type	Skewness	St.Error	Kurtosis	St.Error
LI (XT)	-	-	-	-
CR (XT)	0.064	0.738	-0.800	1.477
NF (XT)	0.359	0.926	-1.614	1.852
ALL (XT)	-0.002	0.562	-0.003	1.124

Weibull Distribution

Type	β	α	C.L. (β)	C.L. (α)	KST	Size
LI (XT)	-	-	-	-	-	1
CR (XT)	0.612	79.173	(0.310,0.892)	(21.528,298.887)	0.14	11
NF (XT)	1.535	36.267	(0.581,2.402)	(17.484,79.048)	0.13	7
ALL (XT)	0.645	55.432	(0.402,0.873)	(23.049.131.667)	0.14	19

Table 5.3.5.1: Correlation results for dimension L1 for Cases (A) and (B) [defect locations ST and STC]

Type	r	L1 = a_1+a_2(Def.Len)	Transformed data (Ln)		Size
			r	C.L. (r)	
LI (XT)	-0.079	L1 = 3.708-0.002DL	-0.031	(-0.196,0.136)	139
CR (XT)	-0.129	L1 = 1.622-0.002DL	-0.123	(-0.376,0.147)	55
NF (XT)	-0.131	L1 = 1.181-0.001DL	-0.151	(-0.556,0.312)	20
ALL (XT)	-0.081	L1 = 2.939-0.002DL	-0.046	(-0.179,0.089)	214
LI (B)	0.292	L1 = 3.851+0.004DL	0.208	(-0.053,0.442)	58

Table 5.3.5.2: Correlation results for dimension LW (and L2 = 0) for Case (C) under SMAW [defect locations SW and SWC]

Type	r	L1 = a_1+a_2(Def.Len)	Transformed data (Ln)		Size
			r	C.L. (r)	
LI (XT)	0.093	LW = 6.981+0.006DL	0.151	(-0.112,0.394)	58
CR (XT)	-0.296	LW = 5.371-0.007DL	-0.204	(-0.679,0.391)	13
NF (XT)	-	-	-	-	3
ALL (XT)	0.066	LW = 6.752+0.004DL	0.118	(-0.113,0.337)	74

Table 5.3.5.3: Correlation results for dimension LW (and L2 = 0) for Case (C) under GMAW [defect locations SW and SWC]

Type	r	L1 = a_1+a_2(Def.Len)	Transformed data (Ln)		Size
			r	C.L. (r)	
LI (XT)	-0.067	LW = 11.776-0.003DL	-0.138	(-0.547,0.324)	20
CR (XT)	-0.555	LW = 5.154-0.043DL	-0.492	(-0.889,0.325)	8
NF (XT)	-	-	-	-	1
ALL (XT)	0.041	LW = 9.356+0.002DL	-0.161	(-0.498,0.218)	29

Table 5.3.5.4: Correlation results for dimension L3 for Case (D)
[defect location STA]

Type	r	L1 = a_1+a_2(Def.Len)	Transformed data (Ln)		Size
			r	C.L. (r)	
LI (XT)	-	-	-	-	1
CR (XT)	-0.046	L3 = 2.146-0.0004DL	-0.031	(-0.619,0.580)	11
NF (XT)	0.332	L3 = 1.171+0.018DL	0.390	(-0.514,0.884)	7
ALL (XT)	-0.062	L3 = 2.271-0.0006DL	-0.103	(-0.532,0.368)	19

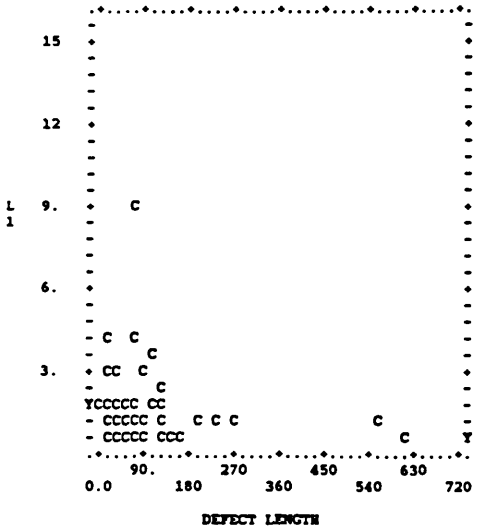


FIGURE 5.3.5.1 : CRACK DEFECT LENGTH/L1 CORRELATION
[DEFECT COCATIONS ST AND STC]

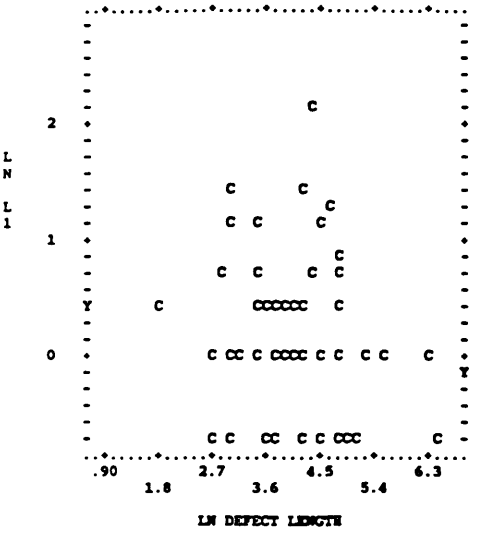


FIGURE 5.3.5.2 : TRANSFORMED DEFECT LENGTH/L1 CORRELATION
[DEFECT LOCATIONS ST AND STC]

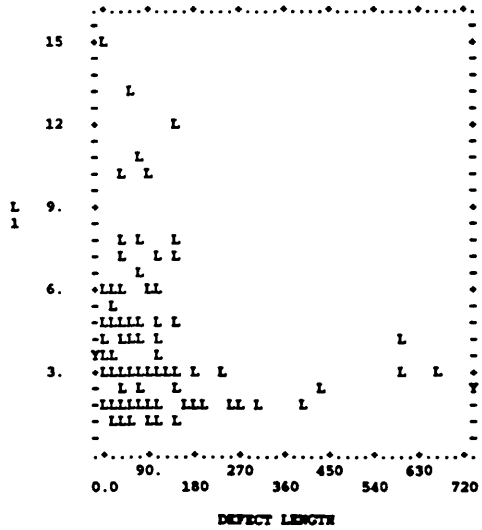


FIGURE 5.3.5.3 : LINEAR INDICATION DEFECT LENGTH/L1 CORRELATION
[DEFECT LOCATIONS ST AND STC]

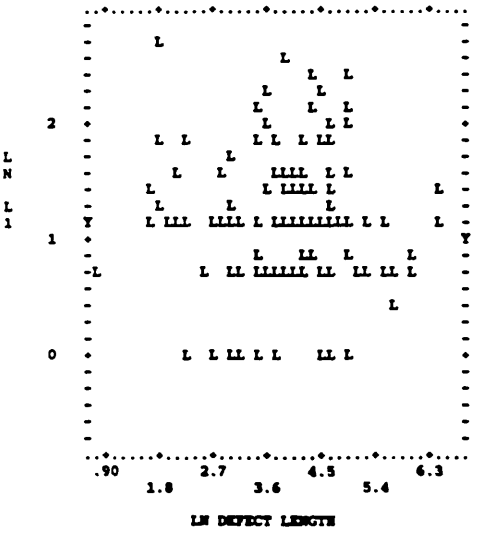


FIGURE 5.3.5.4 : TRANSFORMED DEFECT LENGTH/L1 CORRELATION
[DEFECT LOCATIONS ST AND STC]

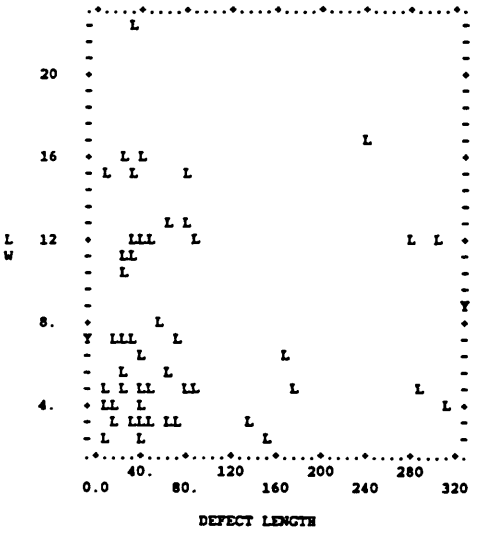


FIGURE 5.3.5.5 : LINEAR INDICATION DEFECT LENGTH/LW CORRELATION
[DEFECT LOCATIONS SW AND SWC , SMAW PROCESS]

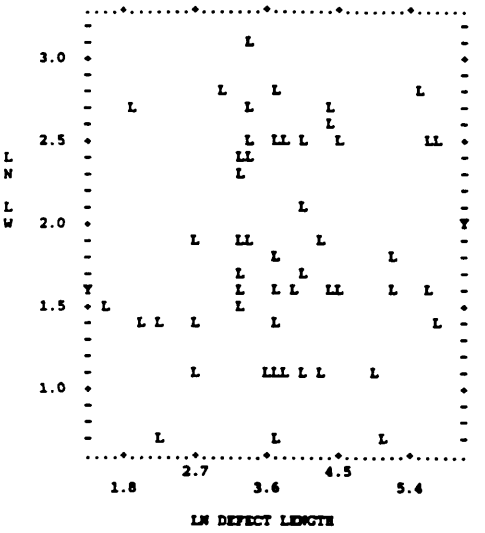


FIGURE 5.3.5.6 : TRANSFORMED DEFECT LENGTH/LW CORRELATION
[DEFECT LOCATIONS SW AND SWC , SMAW PROCESS]

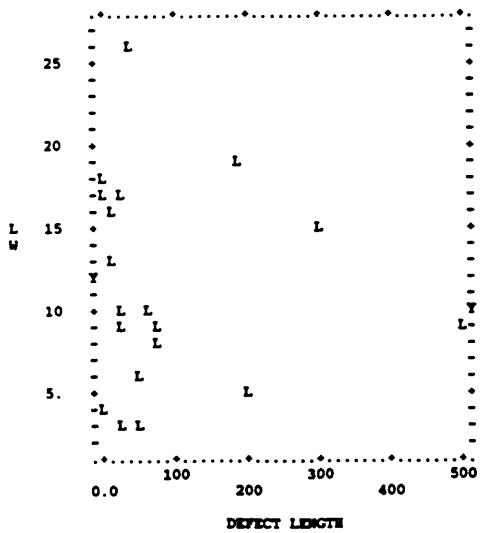


FIGURE 5.3.5.7 : LINEAR INDICATION DEFECT LENGTH/LW CORRELATION
[DEFECT LOCATIONS SW AND SWC , GMAW PROCESS]

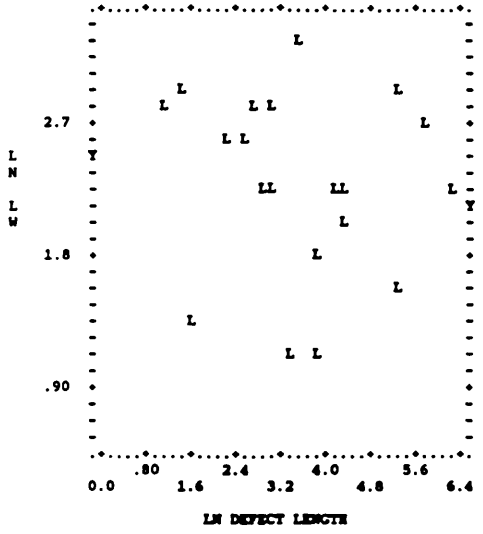


FIGURE 5.3.5.8 : TRANSFORMED DEFECT LENGTH/LW CORRELATION
[DEFECT LOCATIONS SW AND SWC , GMAW PROCESS]

statistically insignificant to support a linear relationship.

Furthermore, statistical tests on the transformed data using the T statistic (see section 5.1.3) highlight the complete independence of the logarithm of the defect length and depth variables in all cases. 95% confidence intervals for the correlation coefficient of the transformed data are shown in tables 5.3.5.1 to 5.3.5.4.

Figures 5.3.5.1 to 5.3.5.8 show selective plots of defect depth versus defect length and of their natural logarithams. The complete scatter in the data is apparent in all plots. The end points of the regressions curve are marked as Y and are shown in the two vertical scales of the plots.

5.3.6 Conclusions

The depth of surface-breaking defects has been shown to be strongly dependent on the defect type category (CR, NF, LI) and on defect location (toe defects in the continuous and abutting members and weld defects) as discussed below. Conversely, differences between cruciforms and tee butts have been found to be virtually non-existent across defect type and location. For this reason, distribution parameters were obtained for the merged sample of cruciforms and tee butts. Differences between fabricators and main node locations have also been shown to be insignificant. However, it is evident that the sample sizes were often too small to allow firm conclusions to be drawn about the influence of the other parameters such as original welding procedure and welding position .

Plate butt toe defects were found to be all of the linear indication type and showed a mean depth of 4.2mm, 0.7mm in excess of the corresponding value for cruciforms and tee butts. In the latter case, there was little variation between crack and non-fusion defects where the mean depth is about one third of the above value. Greater variations between defect types were observed in toe defect angles. Average values for CR and NF defects were about 20°, whereas in linear indications the mean angle was 29° for cruciforms and tee butts and 41° for plate butts. It should be noted that angles for all defects types in cruciforms and tee butts range from 3° to 45° while the LI flaws in plate butts cover an interval of 15° to 90°.

In most cases examined, the welding process was not found to have a significant influence and it has been shown to be influential only in defects occurring in the weld (i.e. the SW and SWC positions). The mean defect depth observed for the LI type in XT welds was 8.36mm but was found to be markedly different for the two welding processes (7.36mm for SMAW and 11.50mm for GMAW).

The sample sizes for toe defects in the abutting member were very small in comparison with those for the ST(STC) and SW(SWC) positions. The mean defect depth was nevertheless found not to be significantly different for the non-fusion and crack defects, both values being in the order of 2mm.

No significant differences in defect length were found for toe defects, between defect types, the mean values all being in the region of 85mm. Somewhat lower average values were observed for weld defects for both welding processes (about 65mm).

The differences in the values of defect depth and length exhibited the toe (ST and STC) and weld (SW and SWC) defect locations resulted in small mean aspect ratios for the latter (about 12) but appreciably for the former (about 60 in cruciforms and tee butts and 23 in plate butts).

The lognormal and Weibull distributions were the main models which were fitted to the data. The Kolmogorov-Smirnov goodness-of-fit test showed on average a better fit for the lognormal model. One of the reasons for the relatively high KST values for the depth dimension is the lumping of defect sizes into a number of discrete (rounded) values. This is an unfortunate consequence of the measuring limitations.

Finally, very little statistical evidence was found for any linear relationship between defect depth and length, and their distributions have been found to be statistically independent in all three defect locations.

5.3.7 Comparisons with other Published Data

In the light of the results of the previous sections, the following classification is introduced to make comparisons with other models direct and feasible.

CASE A1 : Surface-breaking toe defects (ST,STC) in a continuous member [cruciforms and tee butts, fig. 5.3.1.2 see (B)]

CASE A2 : Surface-breaking toe defects (STA) in an abutting member [cruciforms and tee butts, fig. 5.3.1.2 see (D)]

CASE A3 : Surface-breaking weld defects (SW,SWC) welded with the SMAW process [cruciforms and tee butts, fig. 5.3.1.2 see (C)]

CASE A4 : Surface-breaking weld defects (SW,SWC) welded with the GMAW

process [cruciforms and tee butts, fig. 5.3.1.2 see (C)]

CASE A5 : Surface-breaking toe defects (ST,STC) in a continuous member [plate butts, fig. 5.3.1.2 see (A)]

Figures 5.3.7.1 and 5.3.7.2 show the complementary lognormal cumulative distriutions respectively for defect depth and defect length for the above five cases. Fig. 5.3.7.1 shows also the Weibull probabilities obtained by Rogerson and Wong [71] from data due to Kihara et al [83]. The same figure also shows the lognormal fit by Hansen [81] to the Becher and Hansen data [80] and the Marshall distribution [79]. It is interesting to note that apart from the extrme case for the data due to Kihara et al, there is a broad similarity between the various distributions in offshore structures and in reactor vessels. However, data from various sources show that the distribution of defect size varies considerably from one application to another. For example, the distributions show that the probability of a defect exceeding a depth of 20mm varies between about 10^{-1} to 10^{-4}.

A detailed examination of fig. 5.3.7.1 shows that the complementary cumulative probabilities for weld defects under thw SMAW process obtained in the present study (fig. 5.3.7.1 case A3) are very similar to the Marshall estimates whereas the probabilities for toe defects in an abutting member (fig. 5.3.7.1 case A2) are almost identical to those obtained by Hansen. Furthermore, toe defects in a continuous member (case A1) fall mid-way between the estimates by Marshall and Hansen. The highest probabilities are seen to correspond to the surface-breaking weld defects under GMAW (case A4 of fig. 5.3.7.1) which were obtained in the present study.

FIGURE 5.3.7.1 COMPLEMENTARY CUMULATIVE DISTRIBUTIONS FOR DEFECT DEPTH

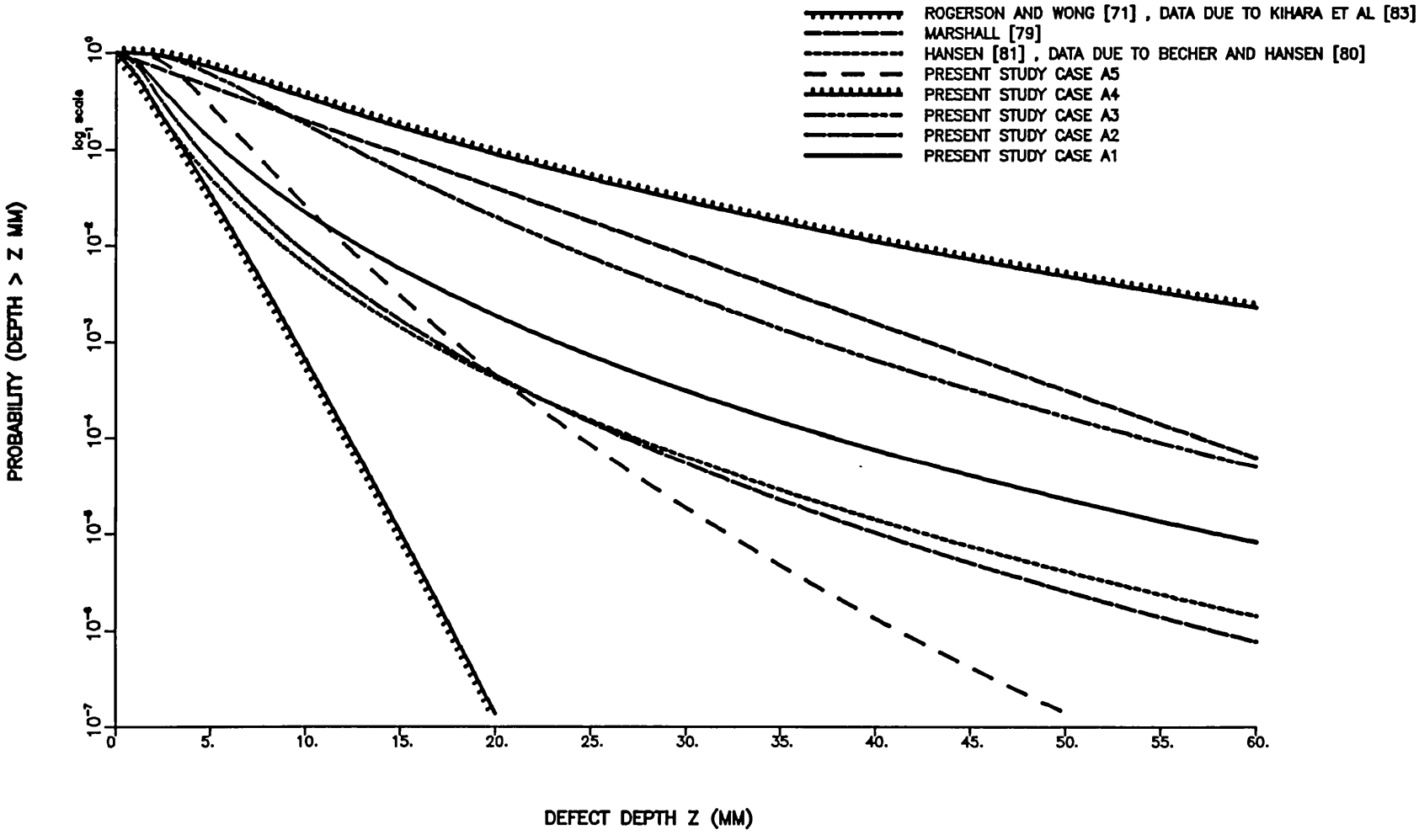
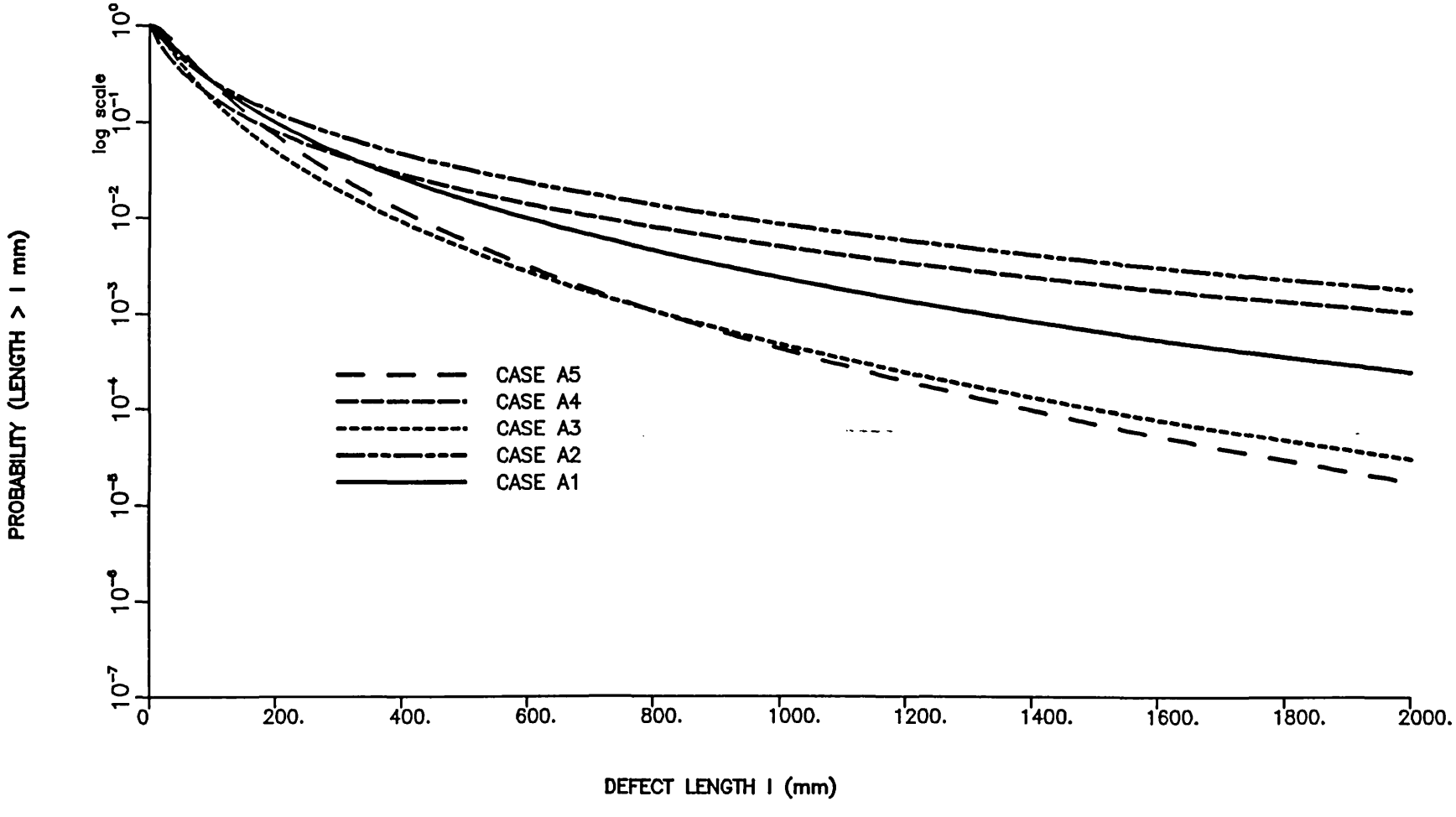


FIGURE 5.3.7.2 COMPLEMENTARY CUMULATIVE DISTRIBUTIONS FOR DEFECT LENGTH



5.4 Embedded Defects

5.4.1 Defect Characteristics

The defects which are analysed in this section were detected and subsequently sized by ultrasonice (UT).

The total number of embedded defects for each main location (node, see section 3.1) and type of welded joint (X,T,B see section 3.2) is shown below in table 5.4.1.

Location	Type of Welded Joint			
	X	T	B	TOTAL
Node 1	896	689	98	1683
Node 2	1401	685	204	2290
Node 3	922	572	232	1726
Node 4	787	497	231	1515
Node 5	333	240	29	602
Node 6	293	178	14	485
All Nodes	4632	2861	808	8301

Table 5.4.1 Number of embedded defects detected by UT

This shows the absolute number of defects detected, as opposed to the number of defective welds.

The defect characteristics which have been included in the analuysis are as follows:

- defect width, w
- defect length, L (in direction of welding)
- defect aspect ratio, ϵ (taken as L/w)

The lognormal and Weibull distributions were fitted to the data. However, greater emphasis was given to the lognormal distribution for which there is a theoretical justification for its use (see section 5.1.1).

For the purpose of distribution fitting, the data have been sub-divided according to type of welded joint (X,T,B, see section 3.2), defect type (NF, SL, CR, IP, PO, see section 3.3), welding process (SMAW, GMAW, see section 3.4), original welding procedure (W6, W8, W3, W5, see section 3.5), defect zone (X, Y, see section 3.6), location in the structure (nodes 1 to 6, see section 3.1) and fabricator (see section 3.6). The influence of each one of these parameters was carefully examined.

The three quantities, defect width, defect length and defect aspect ratio, are discussed below in turn.

5.4.2 Defect Width

Preliminary analysis of the data for the parameter w showed that the sample statistics for defect width do not differ significantly between different locations in the structure (nodes 1 to 6) or between the different defect zones X and Y. This result is of considerable interest since the defect occurrence rate was found to be significantly different for different positions in the structure (see chapter 4). It should also be noted that the frequency of occurrence of the various defect types was found in chapter 4 to depend on defect zone. In addition, to the above, the statistics for defect width were found to be reasonably independent of fabricator.

For the purpose of distribution fitting, the data have been sub-divided according to welding process, defect type and according to types of welded joint. Because the same welding procedures were used for both tee butt and cruciform joints and because of the similarities in their summary statistics for defect width, the data for tee butts (T) and cruciforms (X) have been merged (XT). Plate butts (B) have been kept and treated separately.

The data for defect width w are shown in the form of histograms in figures 5.4.2.1 and 5.4.2.2 for the SMAW welding process and in figures 5.4.2.3 and 5.4.2.4 for the GMAW welding process, and include defects of all types. Particularly important are the differences in defect width statistics for the various defect types, which apply across all types of welded joints and welding processes. Slag inclusion defects have the smallest mean w dimension with values ranging from 2.7 mm to 2.9 mm. With the exception of the incomplete penetration (IP) defects in XT joints under the SMAW process (Fig 5.4.2.1), crack-like defects (CR) have the largest mean z dimensions ranging from 8.5 mm to 10.8 mm. Comparisons between the two types of welded joint XT and B show that the mean value statistics for B Joints are consistently smaller than the corresponding ones in the XT joints for both welding processes and for all defect type categories.

	SYMBOL	COUNT	MEAN	ST.DEV.
NF	A	3497	5.805	4.812
SL	B	858	2.950	1.681
CR	C	154	10.838	6.867
IP	D	197	13.487	8.378
PO	E	44	6.295	3.130

EACH SYMBOL REPRESENTS 1 OBSERVATIONS

INTERVAL NAME	5 10 15 20 25 30 35 40	FREQUENCY INT.	FREQUENCY CUM.	PERCENTAGE INT.	PERCENTAGE CUM.
3.30000	•AAAAAAAAAAAAAAAAAAAAAAAAAAAAAAAAAAAAAAAAA°	2314	2314	48.7	48.7
4.40000	•AAAAAAAAAAAAAAAAAAAAAAAAAAAAAAAAAAAAAAAA°	623	2937	13.1	61.8
5.50000	•AAAAAAAAAAAAAAAAAAAAAAAAAAAAAAAAAAAAAAA°	357	3294	7.5	69.3
6.60000	•AAAAAAAAAAAAAAAAAAAAAAAAAAAAAAAAAAAAAAA°	258	3552	5.4	74.8
7.70000	•AAAAAAAAAAAAAAAAAAAAAAAAAAAAAAAAAAAAAA°	129	3681	2.7	77.5
8.80000	•AAAAAAAAAAAAAAAAAAAAAAAAAAAAAAAAAAAAAA°	154	3835	3.2	80.7
9.90000	•AAAAAAAAAAAAAAAAAAAAAAAAAAAAAAAAAAAAAA°	106	3941	2.2	83.0
11.0000	•AAAAAAAAAAAAAAAAAAAAAAAAAAAAAAAAAAAAAA°	229	4170	4.8	87.8
12.1000	•AAAAAAAAAAAAAAAAAAAAAAAAAAAAAAAAAAAAAA°	89	4259	1.9	89.7
13.2000	•AAAAAAAAAAAAAAAAAAAAAAAAAAAAAAAAAACCCCDD°	42	4301	.9	90.5
14.3000	•AAAAAAAAAAAAAAAAAAAAAAAAAAAAAABBCCCDDDDD°	43	4344	.9	91.5
15.4000	•AAAAAAAAAAAAAAAAAAAAAAAAAAAAAAAAAAAAAA°	77	4421	1.6	93.1
16.5000	•AAAAAAAAAAAAAAAAAAAAAAAAAAAAAAAACCCCCC°	42	4463	.9	94.0
17.6000	•AAAAAAAAAAAAAAAAAAAAAAAAAAAABCCDD	35	4498	.7	94.7
18.7000	•AAAAAAAAAAAAAAAAAAAAAAAAAAAAAABCCCC°	46	4544	1.0	95.7
19.8000	•AAAAAAACD	9	4553	.2	95.9
20.9000	•AAAAAAAAAAAAAAAAAAAAAAAAAAAAAAAAAAAAAA°	62	4615	1.3	97.2
22.0000	•AAAAAAAAAAAAAAAAACCCCCCCDDDDDDDDDDDDD°	55	4670	1.2	98.3
23.1000	•AAAACCDDDDDDDDDD	16	4686	.3	98.7
24.2000	•AAACCDDD	8	4694	.2	98.8
25.3000	•AAAAAACDDDDDDDDDDDDDDDD	24	4718	.5	99.3
26.4000	•AAAAAA	6	4724	.1	99.5
27.5000	•	0	4724	.0	99.5
28.6000	•AAAAAAAAAA	10	4734	.2	99.7
29.7000	•A	1	4735	.0	99.7
30.8000	•AAAAACDD	8	4743	.2	99.9
31.9000	•A	1	4744	.0	99.9
33.0000	•	0	4744	.0	99.9
34.1000	•	0	4744	.0	99.9
35.2000	•AA	2	4746	.0	99.9
36.3000	•	0	4746	.0	99.9
37.4000	•	0	4746	.0	99.9
38.5000	•ACC	3	4749	.1	100.0
39.6000	•	0	4749	.0	100.0
40.7000	•A	1	4750	.0	100.0
41.8000	•	0	4750	.0	100.0
42.9000	•	0	4750	.0	100.0
44.0000	•	0	4750	.0	100.0

5 10 15 20 25 30 35 40

FIGURE 5.4.2.1: HISTOGRAM FOR DEFECT WIDTH IN NT JOINTS UNDER THE SHAW PROCESS

	SYMBOL	COUNT	MEAN	ST.DEV.
NF	A	409	3.892	2.747
SL	B	254	2.770	.955
CR	C	12	8.500	6.260
IP	D	13	4.769	2.455
PO	E	5	5.200	2.049

EACH SYMBOL REPRESENTS 1 OBSERVATIONS

INTERVAL NAME	5 10 15 20 25 30 35 40	FREQUENCY INT.	FREQUENCY CUM.	PERCENTAGE INT.	PERCENTAGE CUM.
1.66000	•AAABBBBBBBBBB	13	13	1.9	1.9
2.49000	•AAAAAAAAAAAAAAAAAAAAAAAAAAAAAAAAAAAAAA°	196	209	28.3	30.2
3.32000	•AAAAAAAAAAAAAAAAAAAAAAAAAAAAAAAAAAAAAA°	281	490	40.5	70.7
4.15000	•AAAAAAAAAAAAAAAAAAAAAAAAAAAAAAAAAAAAAA°	79	569	11.4	82.1
4.98000	•	0	569	.0	82.1
5.81000	•AAAAAAAAAAAAAAAAAAAAAAAAAAAAAAAAAAAABB°	52	621	7.5	89.6
6.64000	•AAAAAAAAAAAAAABBBBBBCDD	23	644	3.3	92.9
7.47000	•AAAAAAAABCEE	12	656	1.7	94.7
8.30000	•AAAAAAC	7	663	1.0	95.7
9.13000	•AAAAD	5	668	.7	96.4
9.96000	•	0	668	.0	96.4
10.7900	•AAAAAAAAAAD	11	679	1.6	98.0
11.6200	•A	1	680	.1	98.1
12.4500	•AAAAA	5	685	.7	98.8
13.2800	•	0	685	.0	98.8
14.1100	•A	1	686	.1	99.0
14.9400	•	0	686	.0	99.0
15.7700	•C	1	687	.1	99.1
16.6000	•A	1	688	.1	99.3
17.4300	•A	1	689	.1	99.4
18.2600	•C	1	690	.1	99.6
19.0900	•	0	690	.0	99.6
19.9200	•	0	690	.0	99.6
20.7500	•	0	690	.0	99.6
21.5800	•	0	690	.0	99.6
22.4100	•AC	2	692	.3	99.9
23.2400	•	0	692	.0	99.9
24.0700	•	0	692	.0	99.9
24.9000	•	0	692	.0	99.9
25.7300	•	0	692	.0	99.9
26.5600	•	0	692	.0	99.9
27.3900	•	0	692	.0	99.9
28.2200	•	0	692	.0	99.9
29.0500	•	0	692	.0	99.9
29.8800	•	0	692	.0	99.9
30.7100	•A	1	693	.1	100.0
31.5400	•	0	693	.0	100.0
32.3700	•	0	693	.0	100.0

5 10 15 20 25 30 35 40

FIGURE 5.4.2.2 : HISTOGRAM FOR DEFECT WIDTH IN B JOINTS UNDER THE SHAW PROCESS

	SYMBOL	COUNT	MEAN	ST.DEV.
NF	A	1684	5.449	4.639
SL	B	481	2.786	1.544
CR	C	72	10.417	7.142
IP	D	55	6.527	5.786
PO	E	20	6.450	5.356

EACH SYMBOL REPRESENTS 1 OBSERVATIONS

INTERVAL NAME	5 10 15 20 25 30 35 40	FREQUENCY INT.	CUM.	PERCENTAGE INT.	CUM.
2.20000	AAAAAAAAAAAAAAAAAAAAAAAAAAAAAAAAAAAAAAAA*	583	583	25.2	25.2
3.30000	AAAAAAAAAAAAAAAAAAAAAAAAAAAAAAAAAAAAAAAA*	686	1269	29.7	54.9
4.40000	AAAAAAAAAAAAAAAAAAAAAAAAAAAAAAAAAAAAAAAA*	272	1541	11.8	66.7
5.50000	AAAAAAAAAAAAAAAAAAAAAAAAAAAAAAAAAAAAAAAA*	196	1737	8.5	75.1
6.60000	AAAAAAAAAAAAAAAAAAAAAAAAAAAAAAAAAAAAAAAA*	92	1829	4.0	79.1
7.70000	AAAAAAAAAAAAAAAAAAAAAAAAAAAAAAAAAAAAAAAA*	74	1903	3.2	82.3
8.80000	AAAAAAAAAAAAAAAAAAAAAAAAAAAAAAAAAAAAAAAA*	57	1960	2.5	84.8
9.90000	AAAAAAAAAAAAAAAAAAAAAAAAAAAAAAACCCDDE	37	1997	1.6	86.4
11.0000	AAAAAAAAAAAAAAAAAAAAAAAAAAAAAAAAAAAAAAAA*	110	2107	4.8	91.1
12.1000	AAAAAAAAAAAAAAAAAAAAAAAAAAAAAAAACCCCD	38	2145	1.6	92.8
13.2000	AAAAAAAAAAACDE	14	2159	.6	93.4
14.3000	AAAAAAAAAAAAAAAACCCD	21	2180	.9	94.3
15.4000	AAAAAAAAAAAAAAAAAAAAAAAAAAAAACCCCCCDDD	36	2216	1.6	95.8
16.5000	AAAAAAAAADEE	12	2228	.5	96.4
17.6000	AAAAACC	7	2235	.3	96.7
18.7000	AAAAAAAAAAAAAAAAAAAAAAAACE	27	2262	1.2	97.8
19.8000	AA	2	2264	.1	97.9
20.9000	AAAAAAAAAAABC	13	2277	.6	98.5
22.0000	AAAAAAB	7	2284	.3	98.8
23.1000	AACCC	5	2289	.2	99.0
24.2000	A	1	2290	.0	99.0
25.3000	AAAAACCCC	9	2299	.4	99.4
26.4000	D	1	2300	.0	99.5
27.5000		0	2300	.0	99.5
28.6000	A	1	2301	.0	99.5
29.7000	A	1	2302	.0	99.6
30.8000	AAAAD	5	2307	.2	99.8
31.9000		0	2307	.0	99.8
33.0000		0	2307	.0	99.8
34.1000	A	1	2308	.0	99.8
35.2000	AA	2	2310	.1	99.9
36.3000		0	2310	.0	99.9
37.4000	C	1	2311	.0	100.0
38.5000		0	2311	.0	100.0
39.6000		0	2311	.0	100.0
40.7000	A	1	2312	.0	100.0
41.8000		0	2312	.0	100.0
42.9000		0	2312	.0	100.0

5 10 15 20 25 30 35 40

FIGURE 5.4.2.3 : HISTOGRAM FOR DEFECT WIDTH IN NF JOINTS UNDER THE GMAW PROCESS

	SYMBOL	COUNT	MEAN	ST.DEV.
NF	A	58	3.586	2.506
SL	B	27	2.704	.724
CR	C	0	.000	.000
IP	D	0	.000	.000
PO	E	0	.000	.000

EACH SYMBOL REPRESENTS 1 OBSERVATIONS

INTERVAL NAME	5 10 15 20 25 30 35 40	FREQUENCY INT.	CUM.	PERCENTAGE INT.	CUM.
.500000		0	0	.0	.0
1.00000	A	1	1	1.2	1.2
1.50000		0	1	.0	1.2
2.00000	AAAAAAAAAAAAAAAABBBBBBBBBB	27	28	31.8	32.9
2.50000		0	28	.0	32.9
3.00000	AAAAAAAAAAAAAAAAAAAAAAAAAAAAABBBBBBBBBBBB	40	68	47.1	80.0
3.50000		0	68	.0	80.0
4.00000	AAB	3	71	3.5	83.5
4.50000		0	71	.0	83.5
5.00000	AAAAAAAAB	9	80	10.6	94.1
5.50000		0	80	.0	94.1
6.00000	A	1	81	1.2	95.3
6.50000		0	81	.0	95.3
7.00000	A	1	82	1.2	96.5
7.50000		0	82	.0	96.5
8.00000	A	1	83	1.2	97.6
8.50000		0	83	.0	97.6
9.00000		0	83	.0	97.6
9.50000		0	83	.0	97.6
10.0000	A	1	84	1.2	98.8
10.5000		0	84	.0	98.8
11.0000		0	84	.0	98.8
11.5000		0	84	.0	98.8
12.0000		0	84	.0	98.8
12.5000		0	84	.0	98.8
13.0000		0	84	.0	98.8
13.5000		0	84	.0	98.8
14.0000		0	84	.0	98.8
14.5000		0	84	.0	98.8
15.0000		0	84	.0	98.8
15.5000		0	84	.0	98.8
16.0000		0	84	.0	98.8
16.5000		0	84	.0	98.8
17.0000		0	84	.0	98.8
17.5000		0	84	.0	98.8
18.0000	A	1	85	1.2	100.0
18.5000		0	85	.0	100.0
19.0000		0	85	.0	100.0

5 10 15 20 25 30 35 40

FIGURE 5.4.2.4 : HISTOGRAM FOR DEFECT WIDTH IN B JOINTS UNDER THE GMAW PROCESS

Tables 5.4.2.1 and 5.4.2.3 show the lognormal and Weibull parameters for all defect categories. They also include two-sided 95% confidence intervals for the parameters and the corresponding goodness-of-fit statistic (KST). One of the reasons for the relatively high KST values for the width dimension is the lumping of defect sizes into a number of discrete (rounded) values. This is an unfortunate consequence of the measuring limitations. Table 5.4.2.2 shows in addition the coefficients of skewness and kurtosis, together with their standard errors, for the transformed dimension ℓn (width). These statistics can be used as tests of normality in addition to the KST values shown in table 5.4.2.1.

Figures 5.4.2.5 to 5.4.2.13 show the various complementary cumulative width distributions for the lognormal fit. These plots were grouped in a number of ways to enable comparisons to be made across all parameters which were involved in the analysis. Figures 5.4.2.5 to 5.4.2.8 contain plots of the distributions within each joint type and welding process. From these figures the importance of defect type on the defect width statistics is further highlighted. As a result of this, the complementary cumulative width probabilities for the various categories were regrouped and are shown for each defect type (NF, SL, CR, IP, PO) in figures 5.4.2.9 to 5.4.2.13. From these plots it is evident that for all widths of defect:

- The complementary cumulative probabilities are smaller in B joints as compared with XT joints across each defect type and welding process category (Figures 5.4.2.9 to 5.4.2.13),

- Slag inclusion defects are associated with the smallest probabilities and their distributions are very similar for all joint types and for both welding processes (Fig. 5.4.2.10),

- The welding process has very little effect except in the cases of incomplete penetration and porosity defects (Figures 5.4.2.12 and 5.4.2.13).

Type	Sample	$\hat{\mu}$	C.L	$\hat{\sigma}^2$	C.L	K.S.T
XT-NF-SMAW	3498	1.519	(1.497,1.541)	0.423	(0.404,0.444)	0.18
XT-SL-SMAW	858	0.994	(0.969,1.019)	0.139	(0.127,0.154)	0.26
XT-CR-SMAW	154	2.172	(2.064,2.280)	0.471	(0.381,0.597)	0.09
XT-IP-SMAW	197	2.320	(2.204,2.436)	0.694	(0.575,0.855)	0.19
XT-PO-SMAW	44	1.744	(1.615,1.873)	0.179	(0.122,0.287)	0.19
B-NF-SMAW	409	1.220	(1.173,1.267)	0.231	(0.202,0.266)	0.24
B-SL-SMAW	254	0.965	(0.925,1.005)	0.106	(0.090,0.127)	0.24
B-CR-SMAW	12	1.934	(1.527,2.341)	0.410	(0.206,0.181)	0.19
B-IP-SMAW	13	1.452	(1.162.1.742)	0.230	(0.118,0.627)	0.23
B-PO-SMAW	5	——	——	——	——	——
XT-NF-GMAW	1684	1.456	(1.425,1.487)	0.413	(0.386,0.442)	0.19
XT-SL-GMAW	481	0.948	(0.916,0.980)	0.126	(0.111,0.144)	0.27
XT-CR-GMAW	72	2.116	(1.952,2.280)	0.486	(0.359,0.696)	0.09
XT-IP-GMAW	55	1.599	(1.407,1.791)	0.506	(0.359,0.768)	0.16
XT-PO-GMAW	20	1.560	(1.193,1.927)	0.618	(0.357,1.336)	0.22
B-NF-GMAW	58	1.143	(1.019,1.267)	0.224	(0.160,0.336)	0.28
B-SL-GMAW	27	0.963	(0.863,1.063)	0.064	(0.040,0.121)	0.30

Table 5.4.2.1: Lognormal parameters – Defect Width

Type	Sample	Skewness	S.E	Kurtosis	S.E
XT-NF-SMAW	3498	0.739	0.041	-0.165	0.083
XT-SL-SMAW	858	1.578	0.084	4.073	0.167
XT-CR-SMAW	154	-0.429	1.197	-0.222	0.395
XT-IP-SMAW	197	-0.530	1.174	-1.212	0.349
XT-PO-SMAW	44	0.740	0.369	-0.228	0.738
B-NF-SMAW	409	1.088	1.121	1.789	0.242
B-SL-SMAW	254	0.066	0.154	0.857	0.307
B-CR-SMAW	12	0.596	0.707	-1.169	1.414
B-IP-SMAW	13	0.319	0.679	-1.159	1.359
B-PO-SMAW	5	——	——	——	——
XT-NF-GMAW	1684	0.819	0.060	-0.022	0.119
XT-SL-GMAW	481	1.269	0.112	4.753	0.223
XT-CR-GMAW	72	-0.099	0.289	-0.834	0.577
XT-IP-GMAW	55	0.606	0.330	-0.507	0.661
XT-PO-GMAW	20	0.405	0.548	-1.423	1.095
B-NF-GMAW	58	1.035	0.322	2.212	0.643
B-SL-GMAW	27	0.380	0.471	-0.535	0.943

Table 5.4.2.2: Coefficients of skewness and kurtosis for ℓn (Width)

Type	Sample	$\hat{\beta}$	C.L	$\hat{\alpha}$	C.L	K.S.T
XT-NF-SMAW	3498	1.392	(1.355,1.431)	6.456	(6.288, 6.628)	0.18
XT-SL-SMAW	858	1.897	(1.798,2.007)	3.335	(3.207, 3.468)	0.27
XT-CR-SMAW	154	1.674	(1.482,1.923)	12.185	(10.977,13.526)	0.09
XT-IP-SMAW	197	1.589	(1.426,1.794)	15.008	(13.617,16.541)	0.16
XT-PO-SMAW	44	2.171	(1.633.2.687)	7.148	(6.078, 8.364)	0.19
B-NF-SMAW	409	1.643	(1.522,1.785)	4.397	(4.119, 4.694)	0.22
B-SL-SMAW	254	2.929	(2.661,3.257)	3.094	(2.953, 3.241)	0.27
B-CR-SMAW	12	1.564	(0.826,2.250)	9.567	(5.915,15.573)	0.16
B-IP-SMAW	13	2.175	(1.188,3.094)	5.417	(3.901, 7.539)	0.19
B-PO-SMAW	5	——	——	——	——	——
XT-NF-GMAW	1684	1.382	(1.330,1.438)	6.045	(5.818, 6.281)	0.19
XT-SL-GMAW	481	1.909	(1.779,2.060)	3.134	(2.976, 3.301)	0.25
XT-CR-GMAW	72	1.572	(1.271,1.869)	11.674	(9.838,13.791)	0.10
XT-IP-GMAW	55	1.320	(1.029,1.604)	7.171	(5.661, 9.014)	0.15
XT-PO-GMAW	20	1.328	(0.841,1.787)	7.074	(0.623, 4.679)	0.20
B-NF-GMAW	58	1.663	(1.306,2.011)	4.054	(3.379, 4.838)	0.27
B-SL-GMAW	27	3.772	(2.580,4.905)	2.976	(2.532, 3.353)	0.25

Table 5.4.2.3 : Weibull parameters – Defect Width

FIGURE 5.4.2.5 VARIOUS COMPLEMENTARY CUMULATIVE WIDTH DISTRIBUTIONS IN XT JOINTS UNDER THE SMAW PROCESS

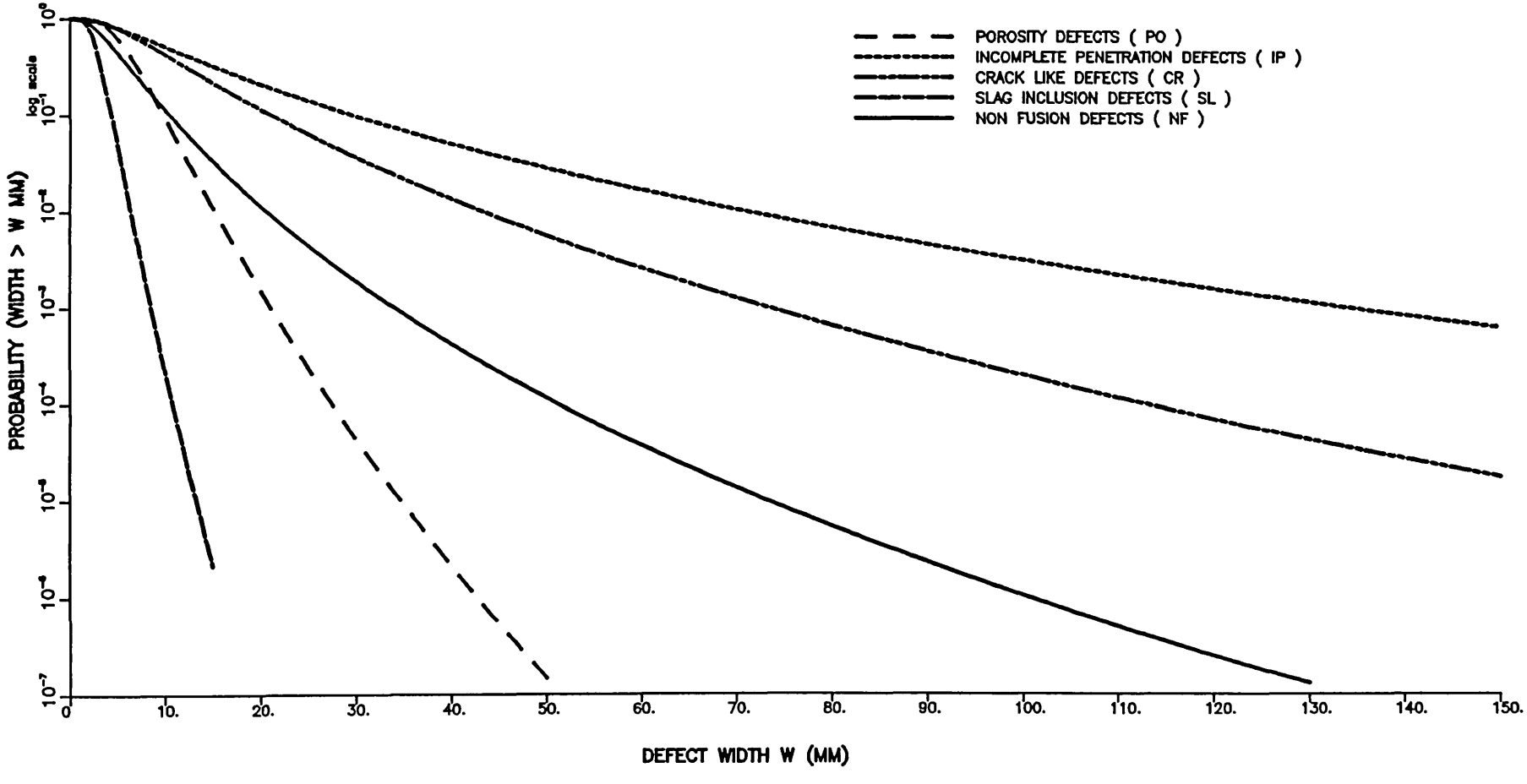


FIGURE 5.4.2.6 VARIOUS COMPLEMENTARY CUMULATIVE WIDTH DISTRIBUTIONS IN B JOINTS UNDER THE SMAW PROCESS

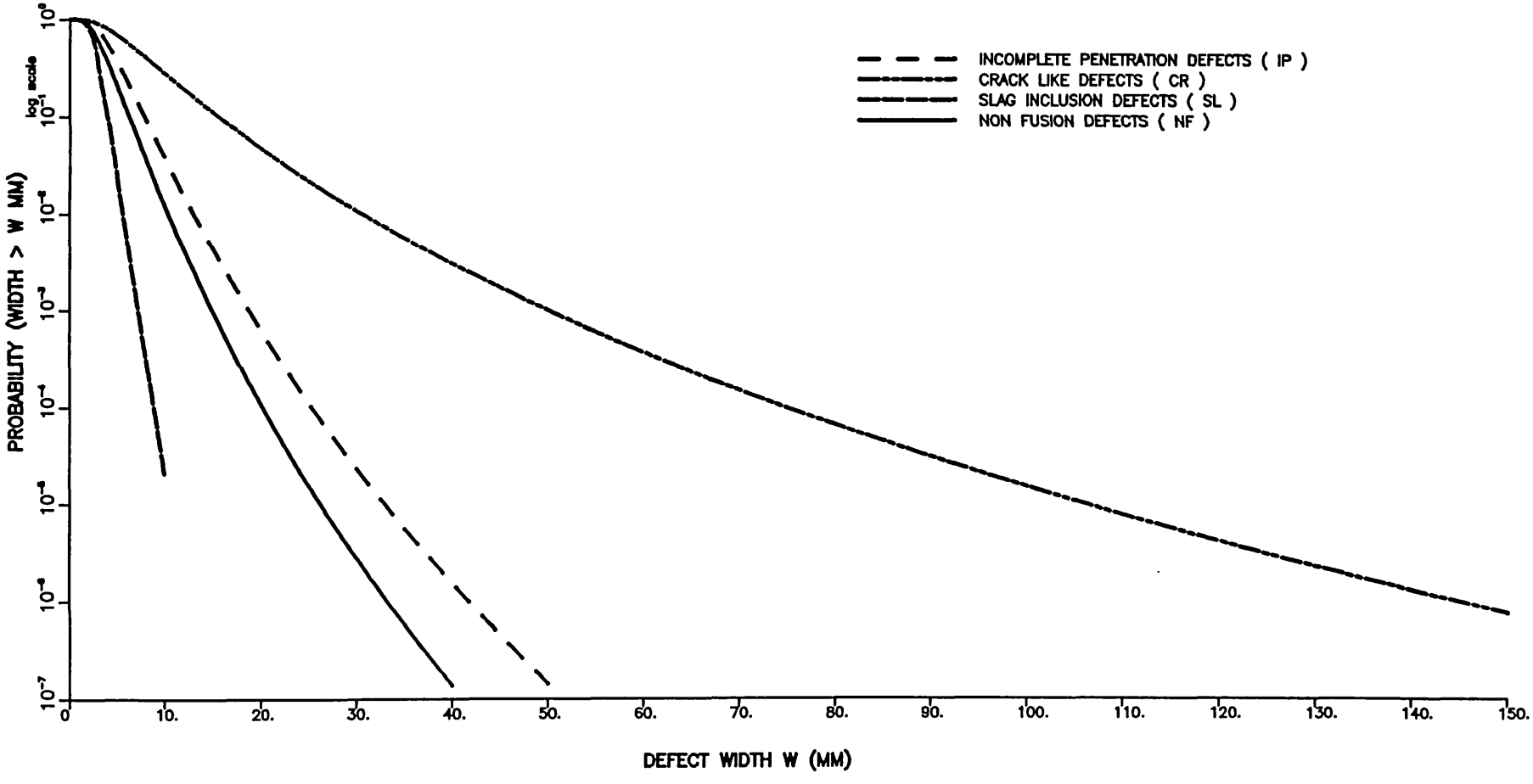


FIGURE 5.4.2.7 VARIOUS COMPLEMENTARY CUMULATIVE WIDTH DISTRIBUTIONS IN XT JOINTS UNDER THE GMAW PROCESS

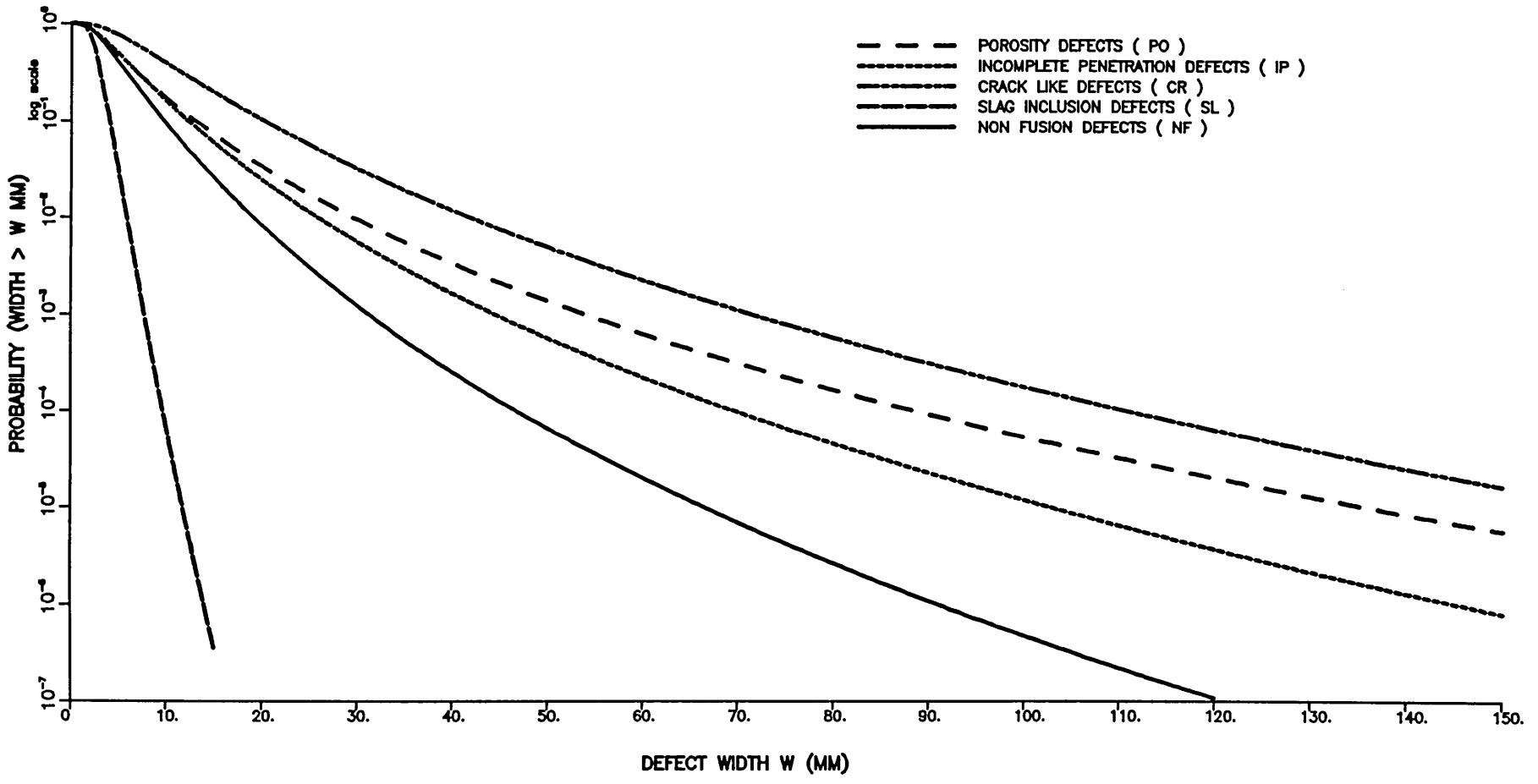


FIGURE 5.4.2.8 VARIOUS COMPLEMENTARY CUMULATIVE WIDTH DISTRIBUTIONS IN B JOINTS UNDER THE GMAW PROCESS

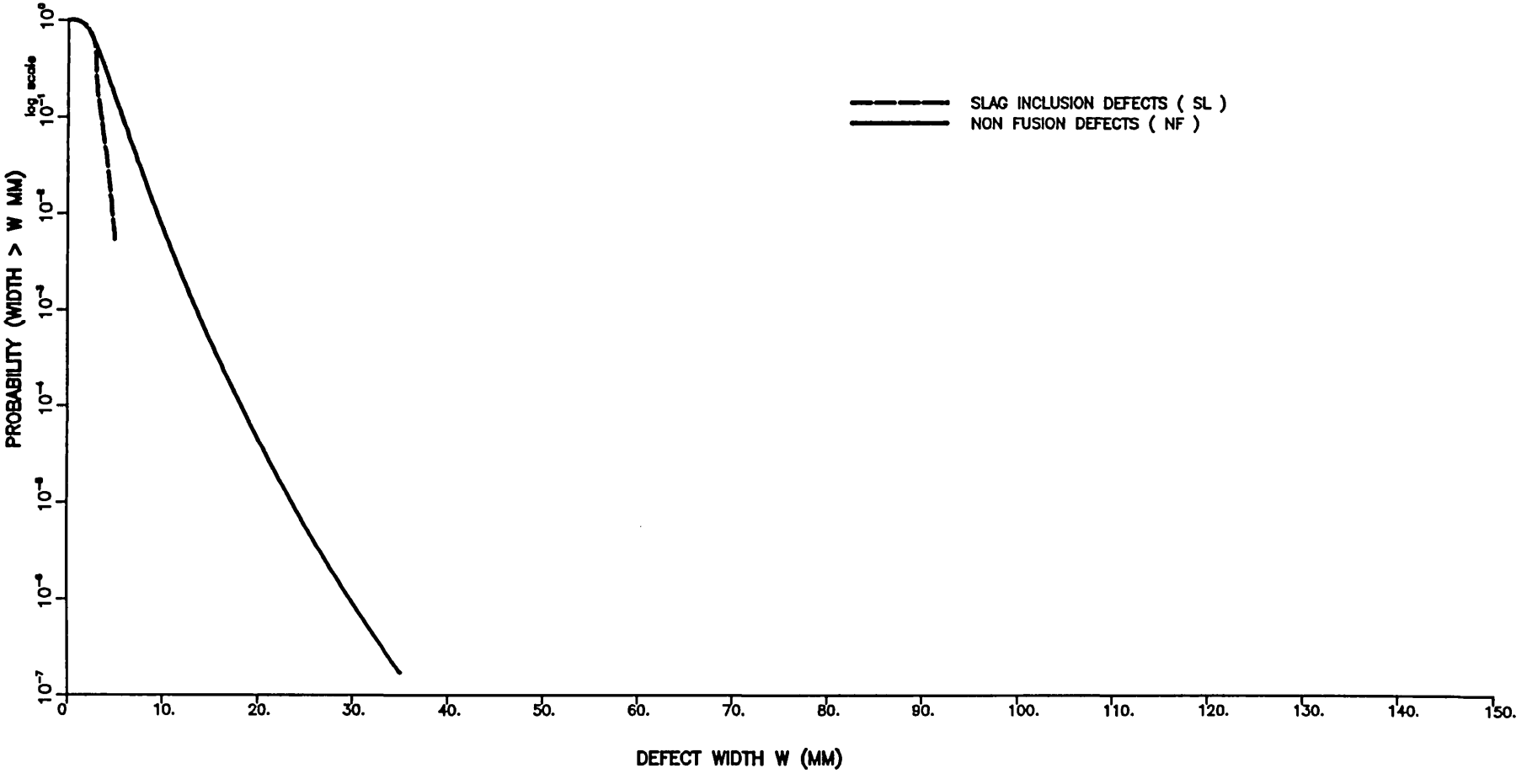


FIGURE 5.4.2.9 VARIOUS COMPLEMENTARY CUMULATIVE WIDTH DISTRIBUTIONS IN NON FUSION DEFECTS (NF)

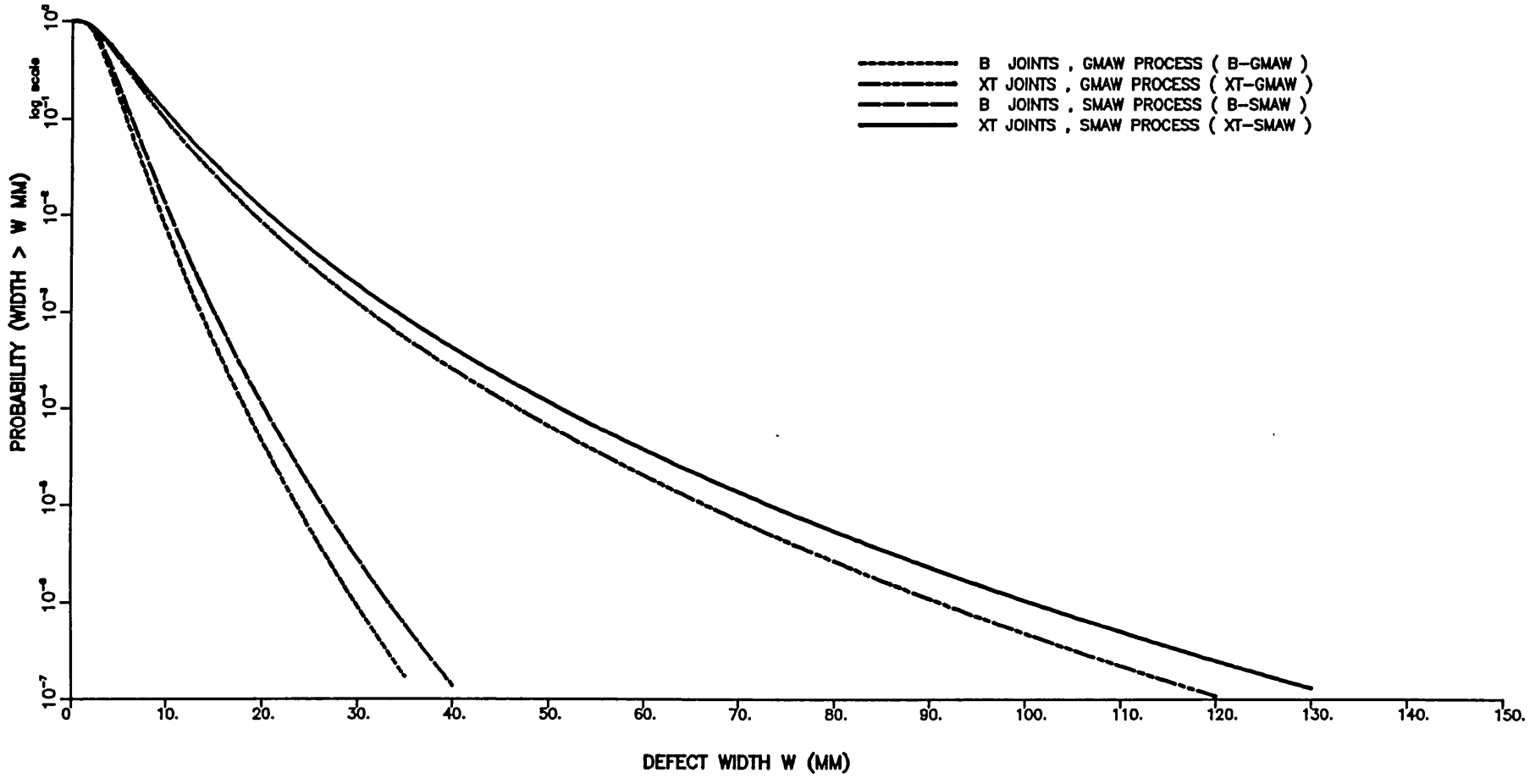


FIGURE 5.4.2.10 VARIOUS COMPLEMENTARY CUMULATIVE WIDTH DISTRIBUTIONS IN SLAG INCLUSION DEFECTS (SL)

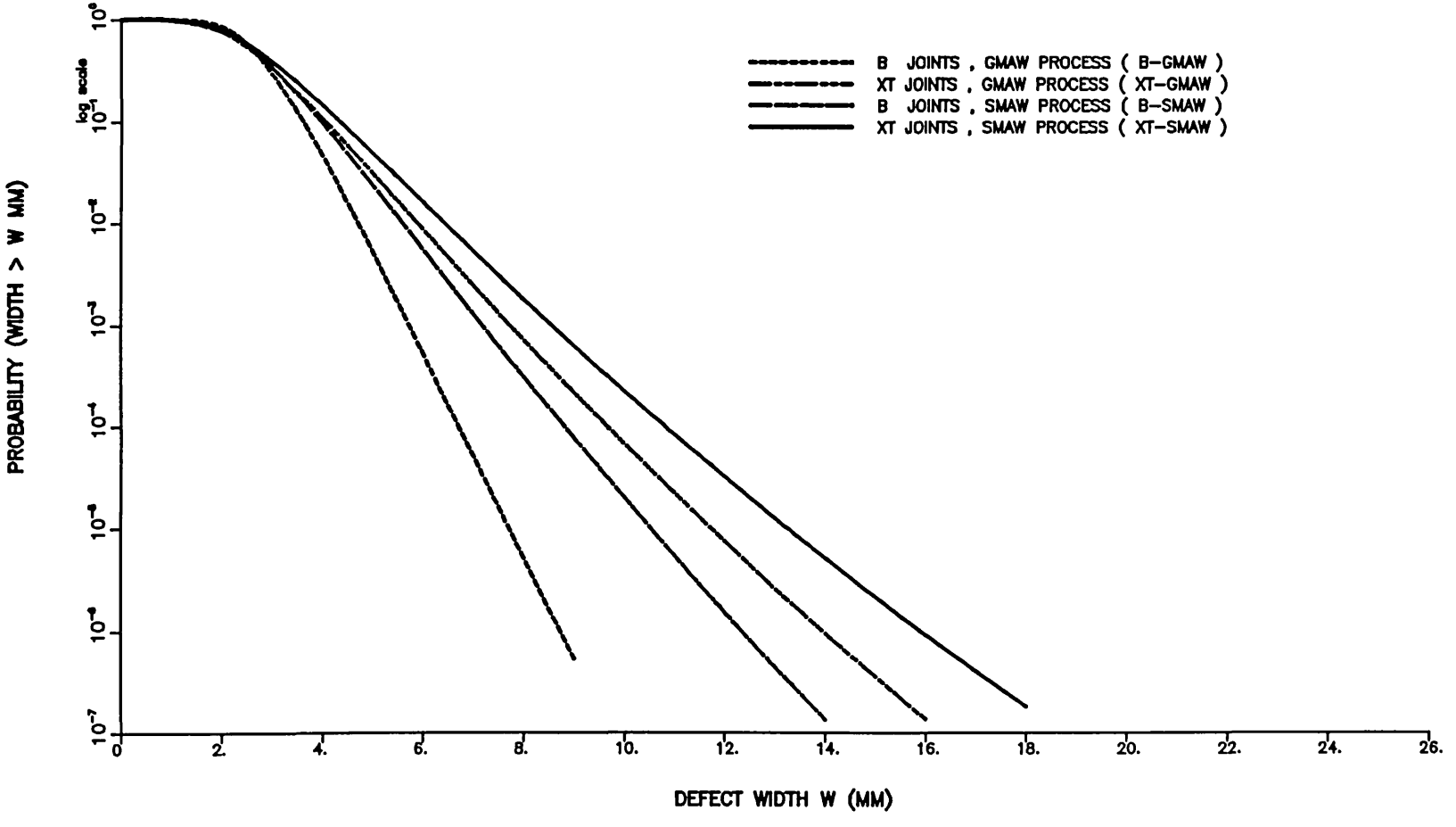


FIGURE 5.4.2.11 VARIOUS COMPLEMENTARY CUMULATIVE WIDTH DISTRIBUTIONS IN CRACK LIKE DEFECTS (CR)

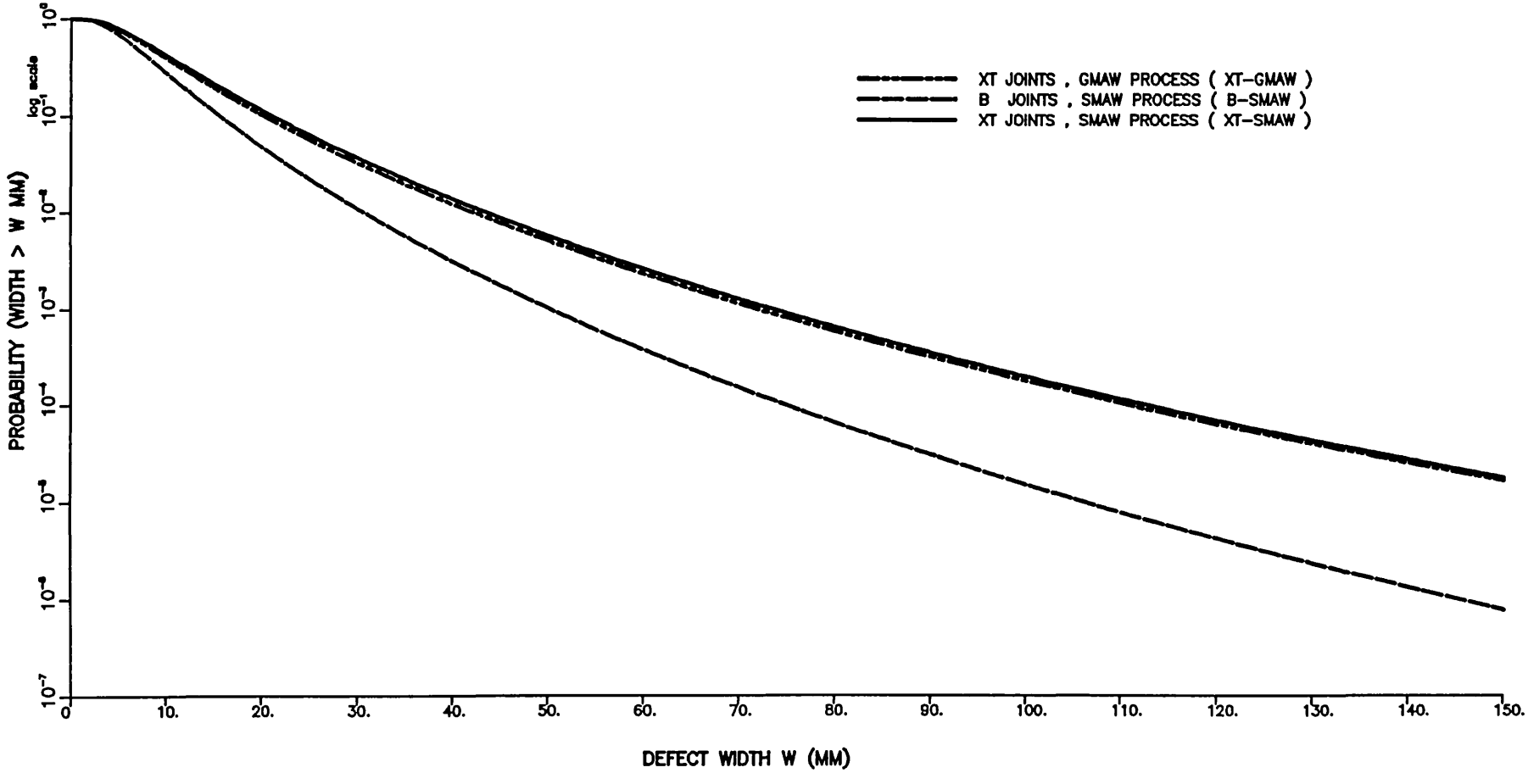


FIGURE 5.4.2.12 VARIOUS COMPLEMENTARY CUMULATIVE WIDTH DISTRIBUTIONS IN INCOMPLETE PENETRATION DEFECTS (IP)

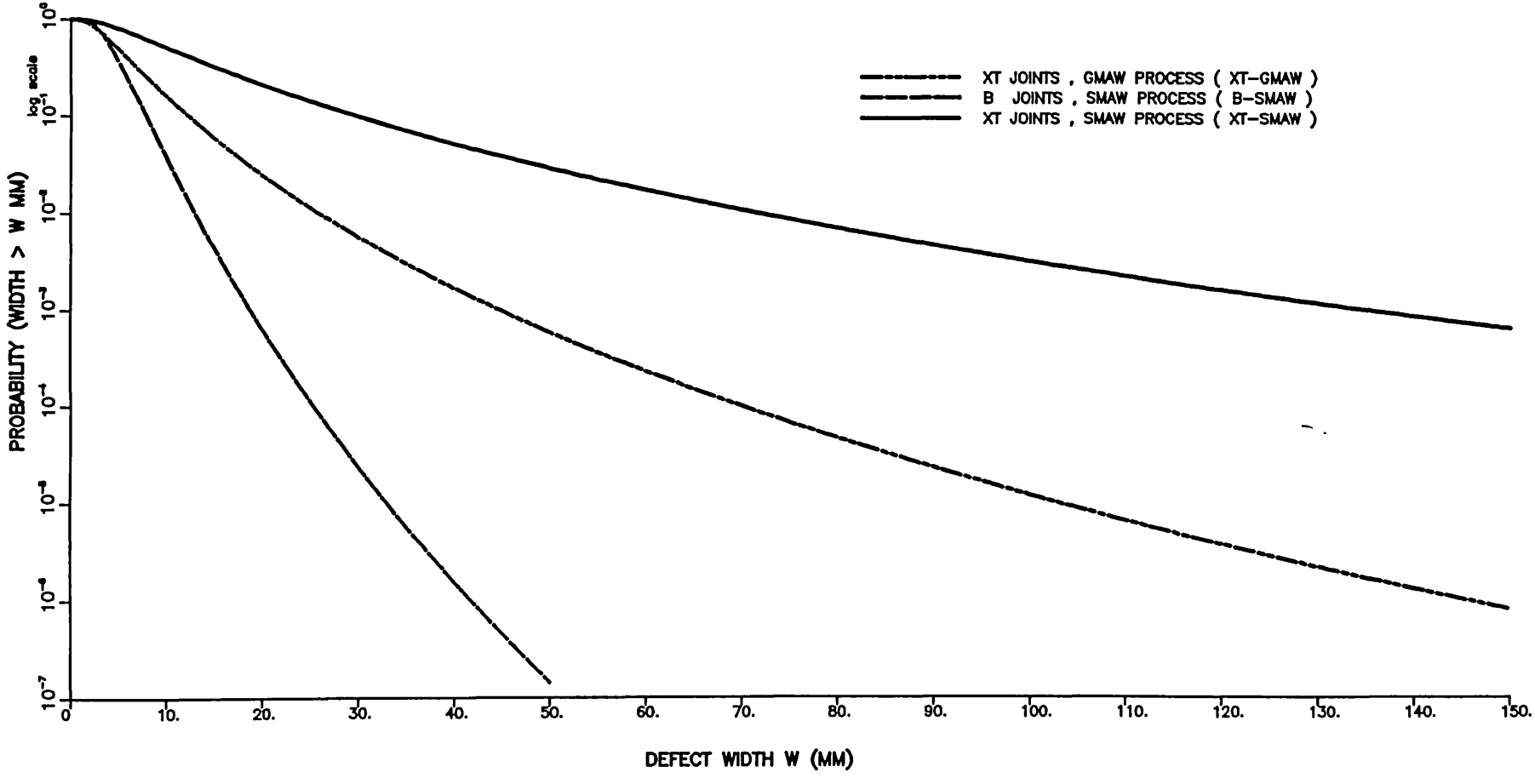
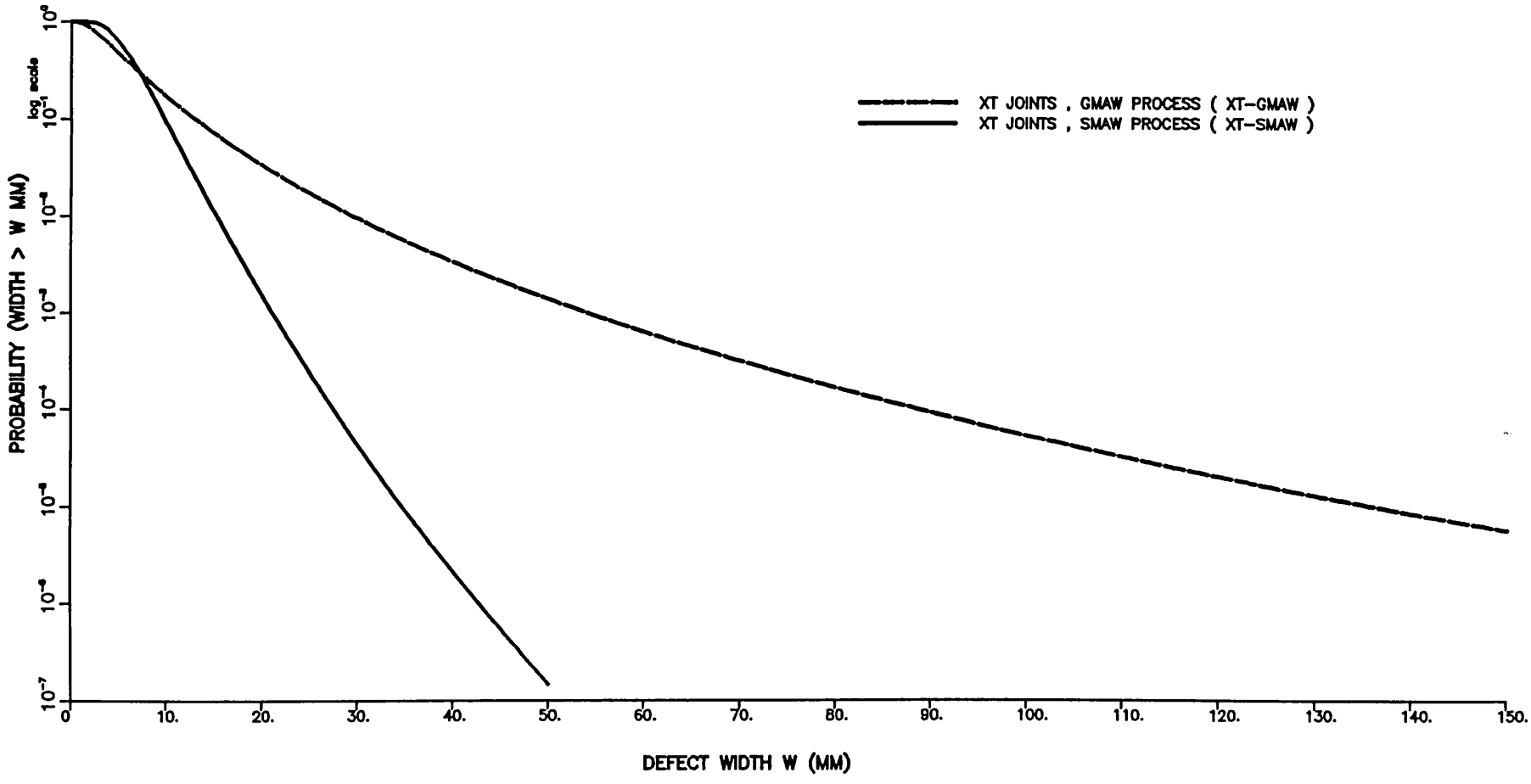


FIGURE 5.4.2.13 VARIOUS COMPLEMENTARY CUMULATIVE WIDTH DISTRIBUTIONS IN POROSITY DEFECTS (PO)



5.4.3 Defect Length

The defect length dimension was also examined for the same categories of defects as in section 5.4.2. From preliminary summary statistics it became evident, as in the case of defect width, that parameters such as the location of the defect in the structure, the defect zone and the fabricator have relatively little effect on the statistical distribution of defect length.

The data on defect length are presented in the form of histograms (Figs. 5.4.3.1 to 5.4.3.4) which involve grouping the data according to defect type, type of welded joint and welding process. From the figures it can be seen that, compared with defect width, the influence of particular parameters is less marked. The data are seen to have a wide range giving rise to high values for the standard deviations. However, slag inclusion defects are on average shorter than other defect types; porosity defects show a similar tendency. Mean values for slag inclusion defects range from 169 mm to 320 mm.

In contrast to the above, incomplete penetration and crack-like defects typically have the highest mean lengths. Mean values for the latter range from 260 mm to 414 mm.

The only questionable result is that for incomplete penetration defects in XT joints under SMAW process. This category of defects has a mean length of 1.6m and a standard deviation of about 2.1 m. Making comparisons between welding processes it can be seen that in XT joints NF, SL and CR defects appear to be longer under the GMAW as opposed to the SMAW process.

These general conclusions can also be derived from the complementary cumulative length probabilities, for the lognormal fit, which are shown in figures 5.4.3.5 to 5.4.3.13. However, care should be taken in interpreting the probability values because the plots have been extrapolated beyond the range of the data.

The estimated parameters for the lognormal and Weibull distributions, together with additional statistics, are shown in tables 5.4.3.1 to 5.4.3.3.

	SYMBOL	COUNT	MEAN	ST.DEV.
NF	A	3498	290.208	656.351
SL	B	858	227.347	316.419
CR	C	154	274.455	295.364
IP	D	197	1571.162	2154.482
PO	E	44	283.977	321.533

EACH SYMBOL REPRESENTS 1 OBSERVATIONS

INTERVAL NAME	5 10 15 20 25 30 35 40	FREQUENCY INT.	CUM.	PERCENTAGE INT.	CUM.
375.000	◆AAAAAAAAAAAAAAAAAAAAAAAAAAAAAAAAAAAAAAAAA*	3747	3747	78.9	78.9
750.000	◆AAAAAAAAAAAAAAAAAAAAAAAAAAAAAAAAAAAAAAAA*	640	4387	13.5	92.3
1125.00	◆AAAAAAAAAAAAAAAAAAAAAAAAAAAAAAAAAAAAAAA*	212	4599	4.5	96.8
1500.00	◆AAAAAAAAAAAAAAAAAAAAAAAAAAAAAAAAAAABBCCD*	42	4641	.9	97.7
1875.00	◆AAAAAAAAAAAABBB	15	4656	.3	98.0
2250.00	◆AAAAAAAAAADDDDDDDD	18	4674	.4	98.4
2625.00	◆AAAAAAAABDDDD	13	4687	.3	98.7
3000.00	◆	0	4687	.0	98.7
3375.00	◆AADDDD	6	4693	.1	98.8
3750.00	◆DDDD	4	4697	.1	98.9
4125.00	◆	0	4697	.0	98.9
4500.00	◆DDDDDDDD	8	4705	.2	99.0
4875.00	◆DDDDDD	6	4711	.1	99.2
5250.00	◆AADDDDDDDDDDDDDD	16	4727	.3	99.5
5625.00	◆	0	4727	.0	99.5
6000.00	◆ABDDD	5	4732	.1	99.6
6375.00	◆DDDDD	5	4737	.1	99.7
6750.00	◆	0	4737	.0	99.7
7125.00	◆AAD	3	4740	.1	99.8
7500.00	◆	0	4740	.0	99.8
7875.00	◆	0	4740	.0	99.8
8250.00	◆AD	2	4742	.0	99.8
8625.00	◆D	1	4743	.0	99.8
9000.00	◆	0	4743	.0	99.8
9375.00	◆	0	4743	.0	99.8
9750.00	◆	0	4743	.0	99.8
10125.0	◆A	1	4744	.0	99.9
10500.0	◆	0	4744	.0	99.9
10875.0	◆	0	4744	.0	99.9
11250.0	◆	0	4744	.0	99.9
11625.0	◆AAAD	4	4748	.1	99.9
12000.0	◆	0	4748	.0	99.9
12375.0	◆	0	4748	.0	99.9
12750.0	◆AA	2	4750	.0	100.0
13125.0	◆	0	4750	.0	100.0
13500.0	◆	0	4750	.0	100.0
13875.0	◆A	1	4751	.0	100.0
14250.0	◆	0	4751	.0	100.0

5 10 15 20 25 30 35 40

FIGURE 5.4.3.1 : HISTOGRAM FOR DEFECT LENGTH IN XT JOINTS UNDER THE SMAW PROCESS

	SYMBOL	COUNT	MEAN	ST.DEV.
NF	A	409	170.575	186.544
SL	B	254	181.224	192.556
CR	C	12	260.000	236.297
IP	D	13	311.538	240.610
PO	E	5	132.200	85.815

EACH SYMBOL REPRESENTS 1 OBSERVATIONS

INTERVAL NAME	5 10 15 20 25 30 35 40	FREQUENCY INT.	CUM.	PERCENTAGE INT.	CUM.
66.0000	◆AAAAAAAAAAAAAAAAAAAAAAAAAAAAAAAAAAAAAAAA*	256	256	36.9	36.9
99.0000	◆AAAAAAAAAAAAAAAAAAAAAAAAABBBBBBBBBBBBBBB*	50	306	7.2	44.2
132.000	◆AAAAAAAAAAAAAAAAAAAAAAAAAABBBBBBBBBBBBBB*	61	367	8.8	53.0
165.000	◆AAAAAAAAAAAAAAAAAAAAAAAAAAAAAAAAAAAAAAAA*	76	443	11.0	63.9
198.000	◆AAAAAAAAAABBBBBBBBB	20	463	2.9	66.8
231.000	◆AAAAAAAAAAAAAAAAAAAAAAAAAAAAAAAAAAAAAAAA*	51	514	7.4	74.2
264.000	◆AAAAAAAAAAAAAAAAAAAAAAAAAAAAABBBBBBBBBBBC*	43	557	6.2	80.4
297.000	◆AAABBC	6	563	.9	81.2
330.000	◆AAAAAAAAAAAABBBBBB	20	583	2.9	84.1
363.000	◆AAAAAABBBB	11	594	1.6	85.7
396.000	◆AAAAAABBBD	11	605	1.6	87.3
429.000	◆AAAAAAAAAAAABBBBBBD	20	625	2.9	90.2
462.000	◆AAAB	4	629	.6	90.8
495.000	◆B	1	630	.1	90.9
528.000	◆AAB	3	633	.4	91.3
561.000	◆BBBBBB	6	639	.9	92.2
594.000	◆	0	639	.0	92.2
627.000	◆AAAAAABBBC	10	649	1.4	93.7
660.000	◆AAAAABBBBBCCD	13	662	1.9	95.5
693.000	◆AAAABB	6	668	.9	96.4
726.000	◆AAAAAAABBBBBDD	15	683	2.2	98.6
759.000	◆AAAB	4	687	.6	99.1
792.000	◆BBB	3	690	.4	99.6
825.000	◆A	1	691	.1	99.7
858.000	◆	0	691	.0	99.7
891.000	◆	0	691	.0	99.7
924.000	◆	0	691	.0	99.7
957.000	◆	0	691	.0	99.7
990.000	◆	0	691	.0	99.7
1023.00	◆	0	691	.0	99.7
1056.00	◆	0	691	.0	99.7
1089.00	◆	0	691	.0	99.7
1122.00	◆AA	2	693	.3	100.0
1155.00	◆	0	693	.0	100.0
1188.00	◆	0	693	.0	100.0
1221.00	◆	0	693	.0	100.0
1254.00	◆	0	693	.0	100.0
1287.00	◆	0	693	.0	100.0

5 10 15 20 25 30 35 40

FIGURE 5.4.3.2 : HISTOGRAM FOR DEFECT LENGTH IN B JOINTS UNDER THE SMAW PROCESS

	SYMBOL	COUNT	MEAN	ST.DEV.
NF	A	1684	319.005	471.926
SL	B	481	319.726	475.461
CR	C	72	413.778	639.647
IP	D	55	392.818	387.655
PO	E	20	180.550	185.842

EACH SYMBOL REPRESENTS 1 OBSERVATIONS

INTERVAL NAME	5 10 15 20 25 30 35 40	FREQUENCY INT.	FREQUENCY CUM.	PERCENTAGE INT.	PERCENTAGE CUM.
88.0000	+AAAAAAAAAAAAAAAAAAAAAAAAAAAAAAAAAAAAAAAA°	654	654	28.3	28.3
176.000	+AAAAAAAAAAAAAAAAAAAAAAAAAAAAAAAAAAAAAAAA°	788	1442	34.1	62.4
264.000	+AAAAAAAAAAAAAAAAAAAAAAAAAAAAAAAAAAAAAAAA°	190	1632	8.2	70.6
352.000	+AAAAAAAAAAAAAAAAAAAAAAAAAAAAAAAAAAAAAAAA°	122	1754	5.3	75.9
440.000	+AAAAAAAAAAAAAAAAAAAAAAAAAAAAAAAAAAAAAAAA°	72	1826	3.1	79.0
528.000	+AAAAAAAAAAAAAAAAAAAABBBBBBBBBBCDDDE	38	1864	1.6	80.6
616.000	+AAAAAAAAAAAAAAAAAAAAAAAAAAAAAAAAAAAAAAAB°	46	1910	2.0	82.6
704.000	+AAAAAAAAAAAAAAAAAAAAAAAAAAAAAAABBBBBBCDE	36	1946	1.6	84.2
792.000	+AAAAAAAAAAAAAAAABBBBBBBBBBBBBBBD	33	1979	1.4	85.6
880.000	+AAAAAAAAAAAAAAAAAAAAAAAAAAAAAAAAAAAAAABBBBBB°	51	2030	2.2	87.8
968.000	+AAAAAAAAAAAAAAAAAAAAAAAAAAAAAAAAAAAAAAAA°	73	2103	3.2	91.0
1056.00	+AAAAAAAAAAAAAAAAAAAAAAAAAAAAAAAAAAAAAAAA°	78	2181	3.4	94.3
1144.00	+AAAAAAAAAAAAAAAAAD	19	2200	.8	95.2
1232.00	+AAAAAAAAAAABBD	14	2214	.6	95.8
1320.00	+AAAAAAAAAABCCD	15	2229	.6	96.4
1408.00	+AAAABBCD	8	2237	.3	96.8
1496.00	+AAAAAAAAAA	11	2248	.5	97.2
1584.00	+AAAAB	5	2253	.2	97.4
1672.00	+AABC	4	2257	.2	97.6
1760.00	+AAAAA	5	2262	.2	97.8
1848.00	+AB	2	2264	.1	97.9
1936.00	+AAB	3	2267	.1	98.1
2024.00	+A	1	2268	.0	98.1
2112.00	+AAC	3	2271	.1	98.2
2200.00	+AB	2	2273	.1	98.3
2288.00	+ABBBB	5	2278	.2	98.5
2376.00	+	0	2278	.0	98.5
2464.00	+AAABB	5	2283	.2	98.7
2552.00	+	0	2283	.0	98.7
2640.00	+AA	2	2285	.1	98.8
2728.00	+AAAAAAACC	9	2294	.4	99.2
2816.00	+ABBBC	5	2299	.2	99.4
2904.00	+	0	2299	.0	99.4
2992.00	+AAABB	5	2304	.2	99.7
3080.00	+	0	2304	.0	99.7
3168.00	+AAAAA	5	2309	.2	99.9
3256.00	+AA	2	2311	.1	100.0
3344.00	+A	1	2312	.0	100.0

5 10 15 20 25 30 35 40

FIGURE 5.4.3.3 : HISTOGRAM FOR DEFECT LENGTH IN XT JOINTS UNDER THE GMAW PROCESS

	SYMBOL	COUNT	MEAN	ST.DEV.
NF	A	58	256.690	283.155
SL	B	27	168.630	204.053
CR	C	0	.000	.000
IP	D	0	.000	.000
PO	E	0	.000	.000

EACH SYMBOL REPRESENTS 1 OBSERVATIONS

INTERVAL NAME	5 10 15 20 25 30 35 40	FREQUENCY INT.	FREQUENCY CUM.	PERCENTAGE INT.	PERCENTAGE CUM.
25.0000	+AAAAAAAAABBBB	13	13	15.3	15.3
50.0000	+AAAAAABBBB	10	23	11.8	27.1
75.0000	+AAAAAAAAAABB	12	35	14.1	41.2
100.000	+AAAAABBBBB	10	45	11.8	52.9
125.000	+AABBB	5	50	5.9	58.8
150.000	+AAAB	4	54	4.7	63.5
175.000	+B	1	55	1.2	64.7
200.000	+AAAABB	6	61	7.1	71.8
225.000	+B	1	62	1.2	72.9
250.000	+AA	2	64	2.4	75.3
275.000	+	0	64	.0	75.3
300.000	+	0	64	.0	75.3
325.000	+	0	64	.0	75.3
350.000	+	0	64	.0	75.3
375.000	+	0	64	.0	75.3
400.000	+A	1	65	1.2	76.5
425.000	+A	1	66	1.2	77.6
450.000	+B	1	67	1.2	78.8
475.000	+	0	67	.0	78.8
500.000	+	0	67	.0	78.8
525.000	+A	1	68	1.2	80.0
550.000	+	0	68	.0	80.0
575.000	+	0	68	.0	80.0
600.000	+B	1	69	1.2	81.2
625.000	+A	1	70	1.2	82.4
650.000	+AA	2	72	2.4	84.7
675.000	+B	1	73	1.2	85.9
700.000	+	0	73	.0	85.9
725.000	+A	1	74	1.2	87.1
750.000	+AAAAAAA	7	81	8.2	95.3
775.000	+B	1	82	1.2	96.5
800.000	+AAA	3	85	3.5	100.0
825.000	+	0	85	.0	100.0
850.000	+	0	85	.0	100.0
875.000	+	0	85	.0	100.0
900.000	+	0	85	.0	100.0
925.000	+	0	85	.0	100.0
950.000	+	0	85	.0	100.0

5 10 15 20 25 30 35 40

FIGURE 5.4.3.4 : HISTOGRAM FOR DEFECT LENGTH IN B JOINTS UNDER THE GMAW PROCESS

Type	Sample	$\hat{\mu}$	C.L.	$\hat{\sigma}^2$	C.L.	K.S.T.
XT-NF-SMAW	3498	5.041	(5.005,5.077)	1.191	(1.137,1.249)	0.08
XT-SL-SMAW	858	4.884	(4.812,4.596)	1.148	(1.047,1.273)	0.06
XT-CR-SMAW	154	5.060	(4.884,5.236)	1.237	(1.001,1.569)	0.08
XT-IP-SMAW	197	6.247	(6.025,6.469)	2.536	(2.100,3.124)	0.12
XT-PO-SMAW	44	5.043	(4.683,5.403)	1.400	(0.956,2.249)	0.09
B-NF-SMAW	409	4.505	(4.385,4.625)	1.539	(1.348,1.774)	0.12
B-SL-SMAW	254	4.630	(4.490,4.625)	1.290	(1.092,1.548)	0.06
B-CR-SMAW	12	5.085	(4.340,5.830)	1.374	(0.961,3.959)	0.15
B-IP-SMAW	13	5.402	(4.843,5.961)	0.856	(0.441,2.334)	0.10
B-PO-SMAW	5	-	-	-	-	-
XT-NF-GMAW	1684	4.981	(4.920,5.042)	1.612	(1.508,1.727)	0.09
XT-SL-GMAW	481	5.018	(4.910,5.126)	1.472	(1.302,1.678)	0.09
XT-CR-GMAW	72	5.133	(4.823,5.443)	1.728	(1.275,2.474)	0.20
XT-IP-GMAW	55	5.519	(5.264,5.774)	0.894	(0.634,1.357)	0.17
XT-PO-GMAW	20	4.542	(3.908,5.176)	1.839	(1.062,3.921)	0.12
B-NF-GMAW	58	4.797	(4.446,5.148)	1.786	(1.276,2.678)	0.13
B-SL-GMAW	27	4.544	(4.100,4.988)	1.252	(0.777,2.359)	0.09

Table 5.4.3.1: Lognormal Parameters – Defect Length

Type	Sample	Skewness	S.E.	Kurtosis	S.E.
XT-NF-SMAW	3498	-0.111	0.041	0.727	0.08
XT-SL-SMAW	858	-0.216	0.084	0.225	0.17
XT-CR-SMAW	154	-0.169	0.197	-0.337	0.39
XT-IP-SMAW	197	0.201	0.174	-1.094	0.35
XT-PO-SMAW	44	-0.196	0.369	-0.521	0.74
B-NF-SMAW	409	-0.295	0.121	-0.797	0.24
B-SL-SMAW	254	-0.140	0.154	-0.778	0.31
B-CR-SMAW	12	-0.753	0.707	0.137	1.41
B-IP-SMAW	13	-0.297	0.679	-1.310	1.36
B-PO-SMAW	5	-	-	-	-
XT-NF-GMAW	1684	0.060	0.060	-0.172	0.12
XT-SL-GMAW	481	0.221	0.112	-0.309	0.22
XT-CR-GMAW	72	0.437	0.289	-0.689	0.58
XT-IP-GMAW	55	0.466	0.330	-1.313	0.66
XT-PO-GMAW	20	-0.529	0.548	-0.684	1.09
B-NF-GMAW	58	-0.031	0.322	-1.189	0.64
B-SL-GMAW	27	0.056	0.471	0.678	0.94

Table 5.4.3.2: Coefficients of skewness and kurtosis for ℓn (Length)

Type	Sample	$\hat{\beta}$	C.L.	$\hat{\alpha}$	C.L.	K.S.T.
XT-NF-SMAW	3498	0.874	(0.851,0.898)	265.284	(254.381,276.054)	0.09
XT-SL-SMAW	858	0.967	(0.917,1.023)	223.450	(206.975,241.236)	0.10
XT-CR-SMAW	154	0.984	(0.871,1.130)	272.315	(227.991,325.257)	0.13
XT-IP-SMAW	197	0.666	-	1158.112	-	0.14
XT-PO-SMAW	44	0.939	(0.706,1.162)	275.151	(189.133,395.627)	0.12
B-NF-GMAW	409	0.930	(0.862,1.010)	164.688	(146.747,184.822)	0.07
B-SL-GMAW	254	0.976	(0.887,1.085)	179.167	(155.844,205.981)	0.07
B-CR-SMAW	12	1.116	(0.589,1.606)	270.805	(138.043,533.032)	0.14
B-IP-SMAW	13	1.347	(0.736,1.916)	340.284	(200.279,580.308)	0.11
B-PO-SMAW	5	-	-	-	-	-
XT-NF-GMAW	1684	0.803	(0.773,0.836)	276.123	(258.530,294.913)	0.14
XT-SL-GMAW	481	0.819	(0.763,0.884)	280.590	(248.668,316.610)	0.12
XT-CR-GMAW	72	0.747	(0.604,0.888)	334.201	(233.139,474.603)	0.21
XT-IP-GMAW	55	1.079	(0.841,1.311)	405.948	(304.012,537.062)	0.18
XT-PO-GMAW	20	0.932	(0.590,1.154)	174.800	(96.988,312.012)	0.09
B-NF-GMAW	58	0.843	(0.662,1.019)	233.902	(163.281,331.510)	0.13
B-SL-GMAW	27	0.941	(0.644,1.224)	163.399	(99.890,263.594)	0.13

Table 5.4.3.3: Weibull Parameters – Defect Length

FIGURE 5.4.3.5 VARIOUS COMPLEMENTARY CUMULATIVE LENGTH DISTRIBUTIONS IN XT JOINTS UNDER THE SMAW PROCESS

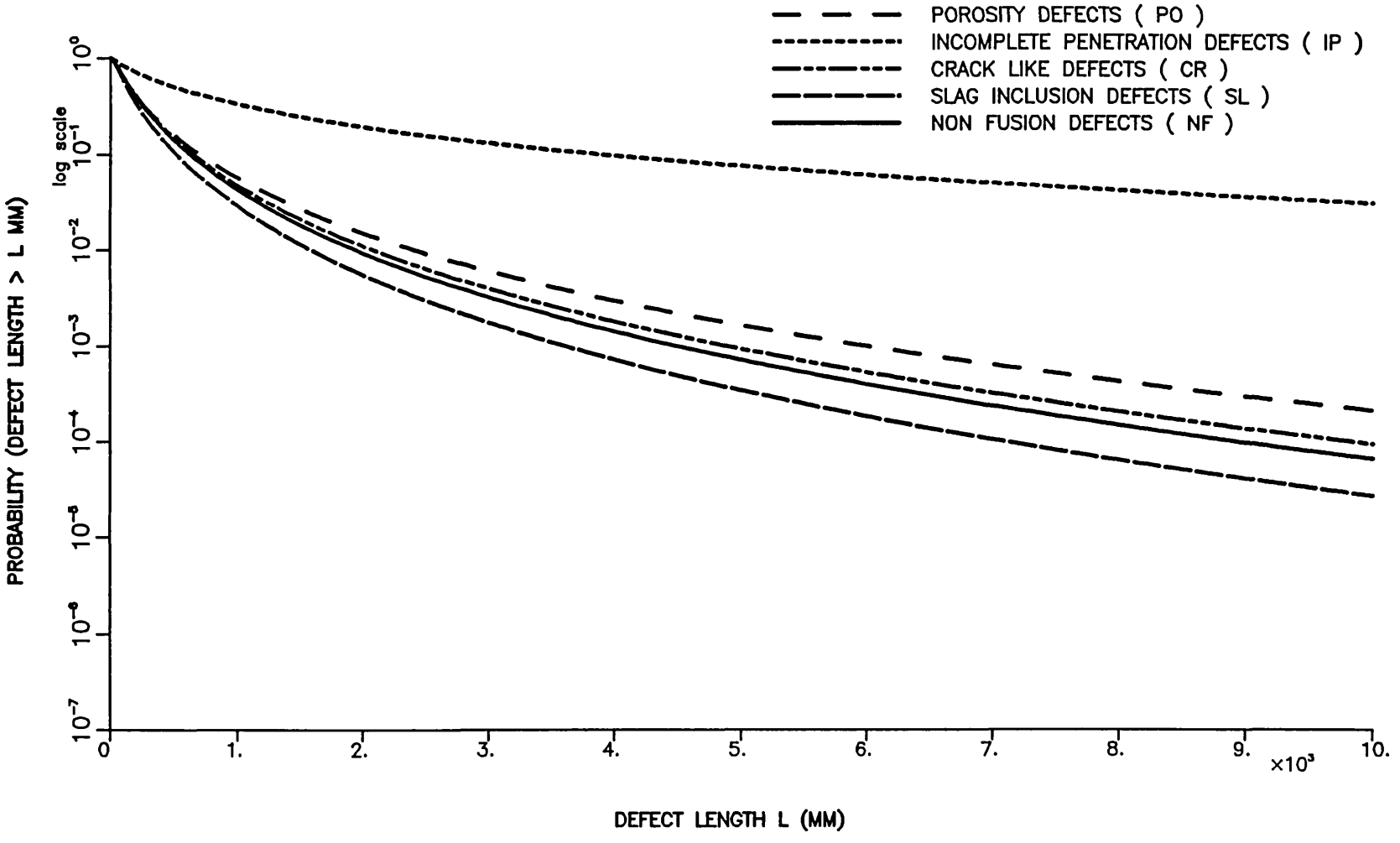


FIGURE 5.4.3.6 VARIOUS COMPLEMENTARY CUMULATIVE LENGTH DISTRIBUTIONS IN B JOINTS UNDER THE SMAW PROCESS

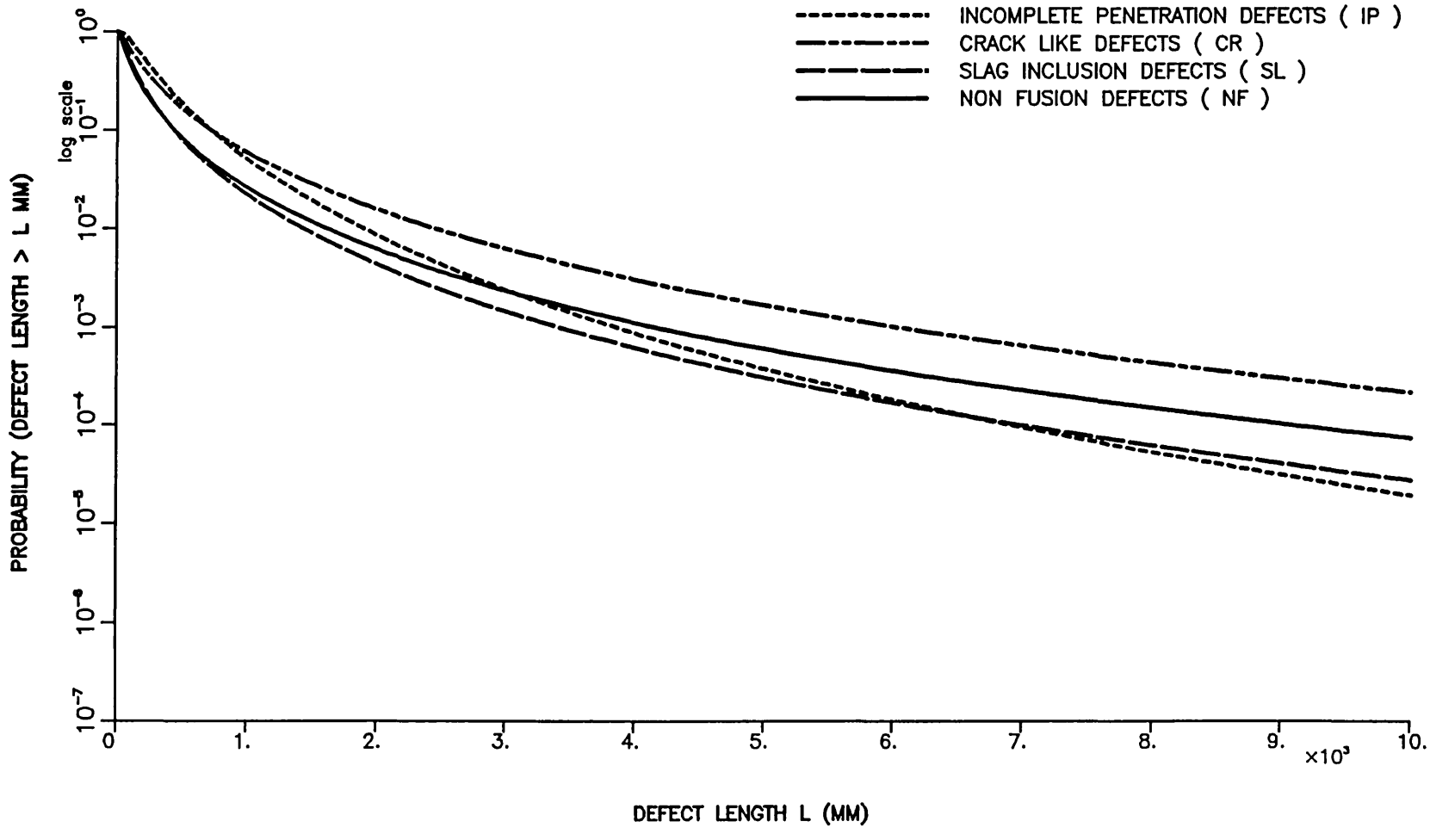


FIGURE 5.4.3.7 VARIOUS COMPLEMENTARY CUMULATIVE LENGTH DISTRIBUTIONS IN XT JOINTS UNDER THE GMAW PROCESS

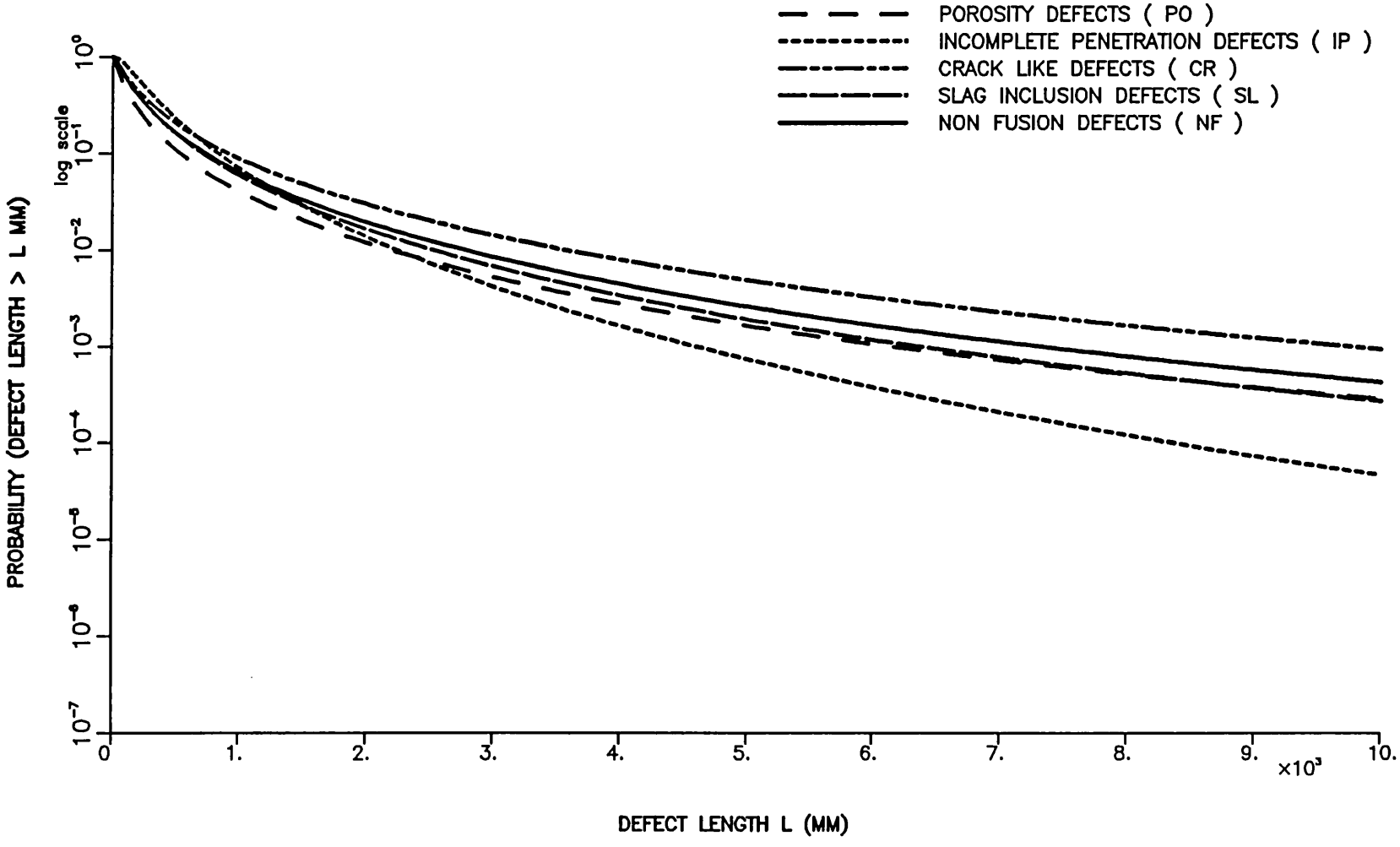


FIGURE 5.4.3.8 VARIOUS COMPLEMENTARY CUMULATIVE LENGTH DISTRIBUTIONS IN B JOINTS UNDER THE GMAW PROCESS

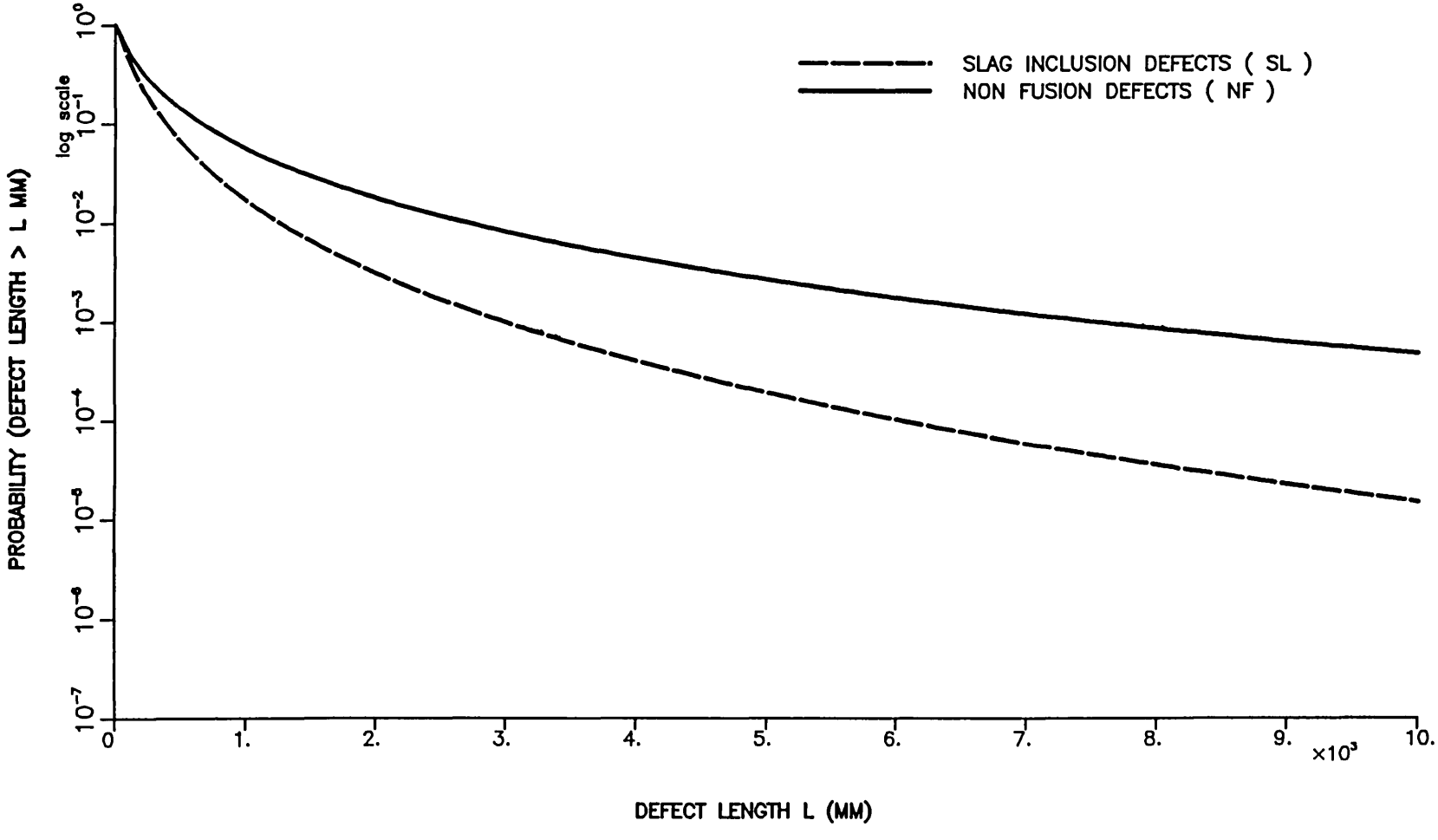


FIGURE 5.4.3.9 VARIOUS COMPLEMENTARY CUMULATIVE LENGTH DISTRIBUTIONS IN NON FUSION DEFECTS (NF)

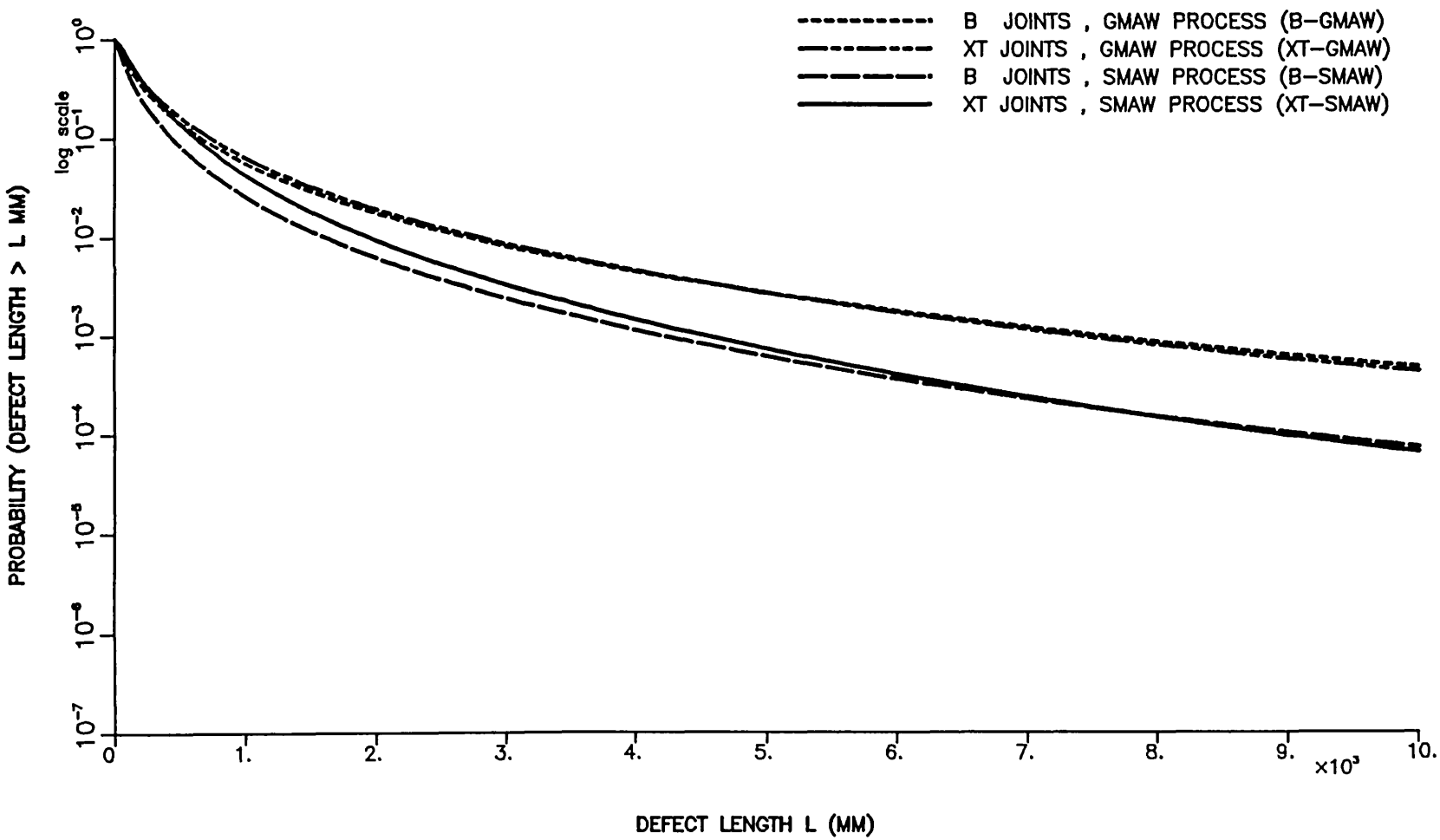


FIGURE 5.4.3.10 VARIOUS COMPLEMENTARY CUMULATIVE LENGTH DISTRIBUTIONS IN SLAG INCLUSION DEFECTS (SL)

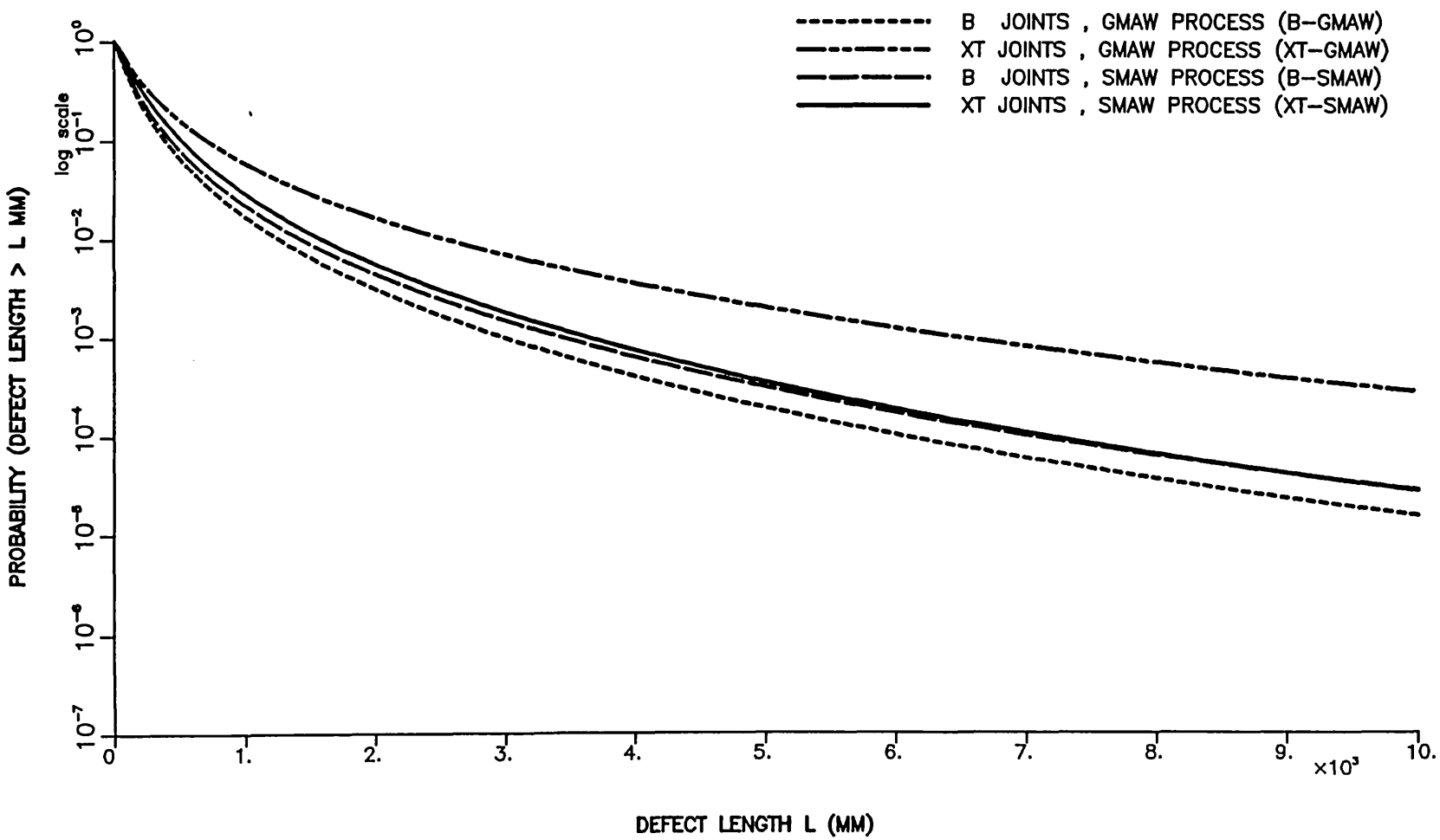


FIGURE 5.4.3.11 VARIOUS COMPLEMENTARY CUMULATIVE LENGTH DISTRIBUTIONS IN CRACK LIKE DEFECTS (CR)

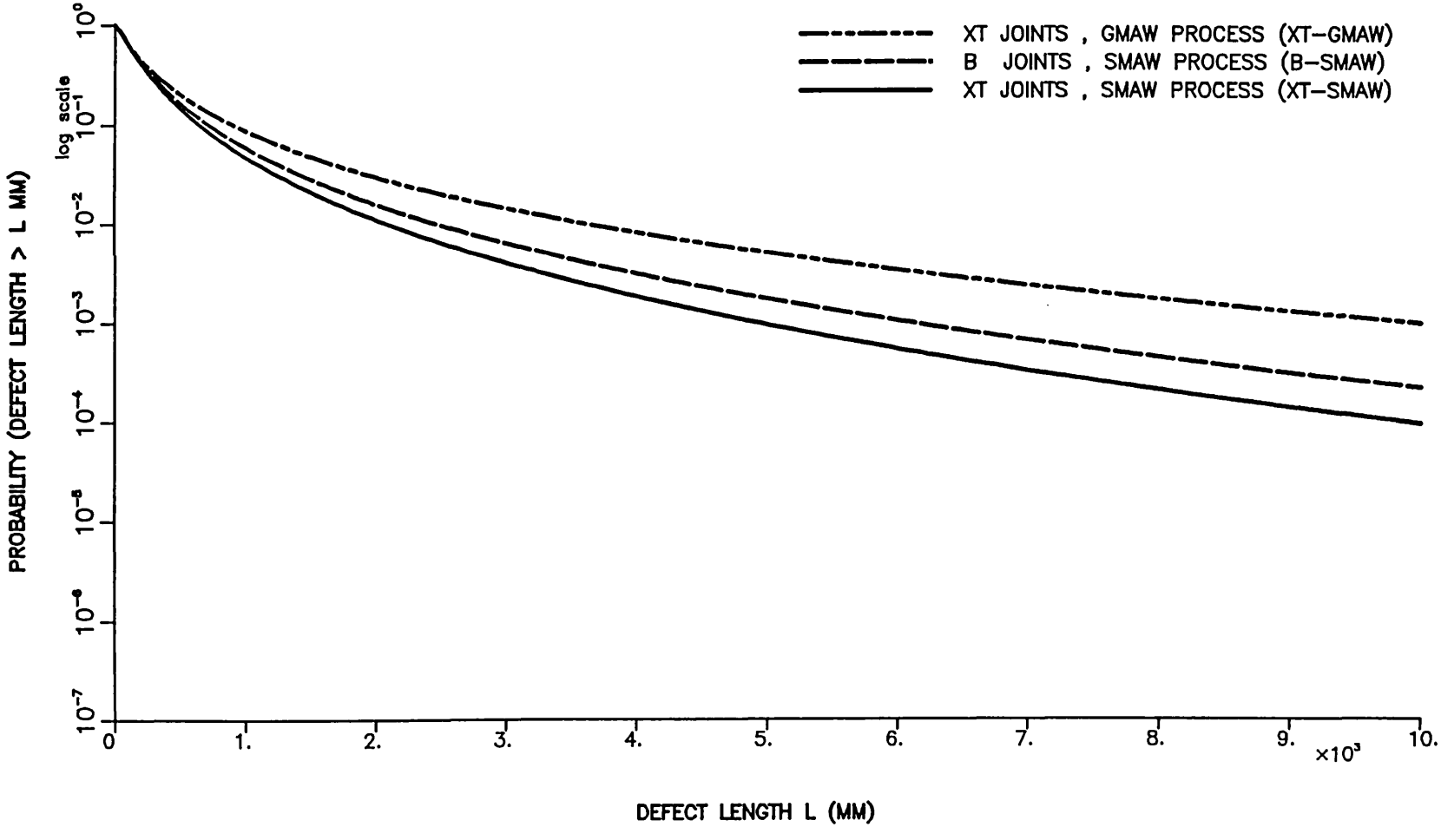


FIGURE 5.4.3.12 VARIOUS COMPLEMENTARY CUMULATIVE LENGTH DISTRIBUTIONS IN INCOMPLETE PENETRATION DEFECTS (IP)

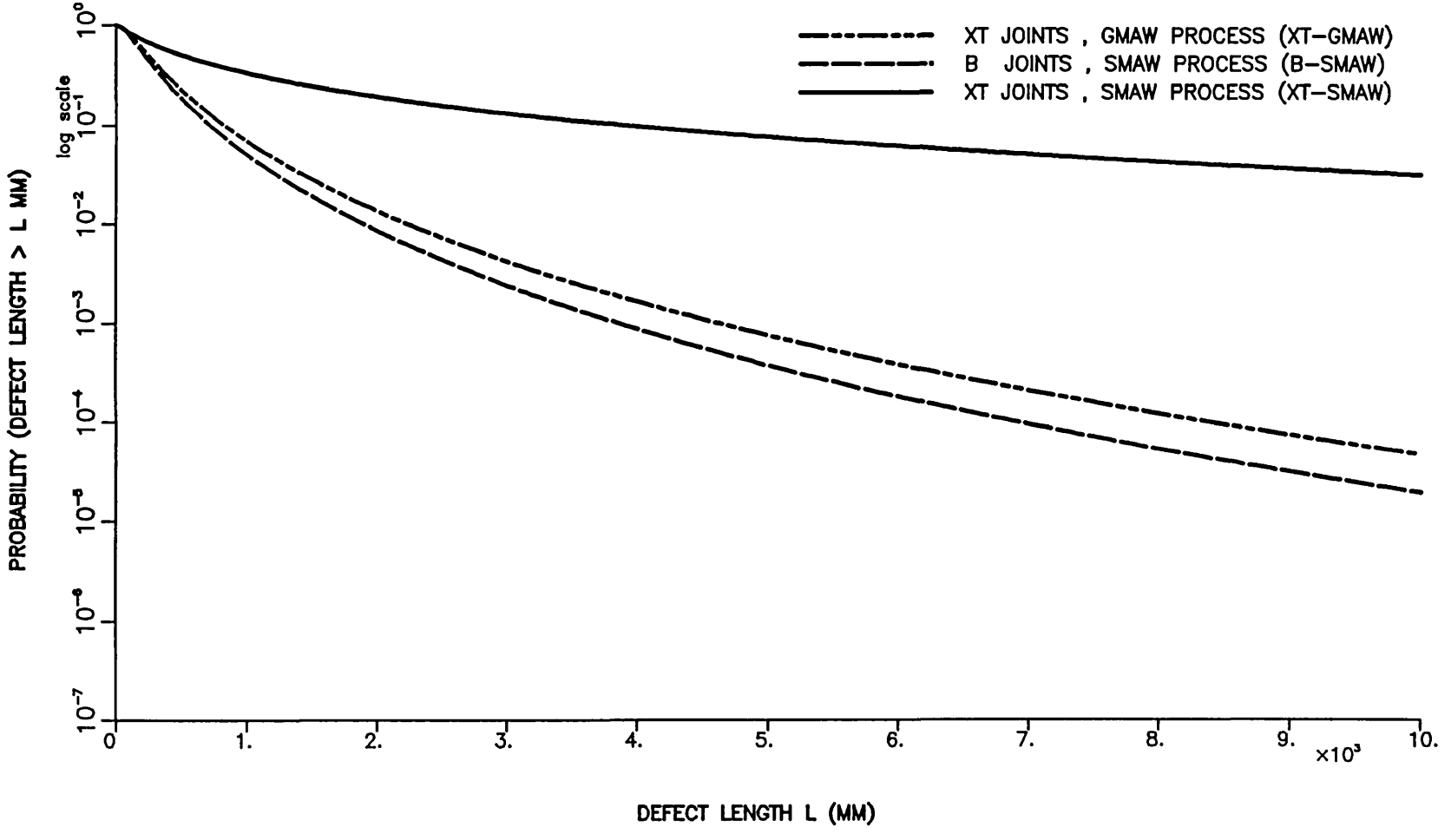
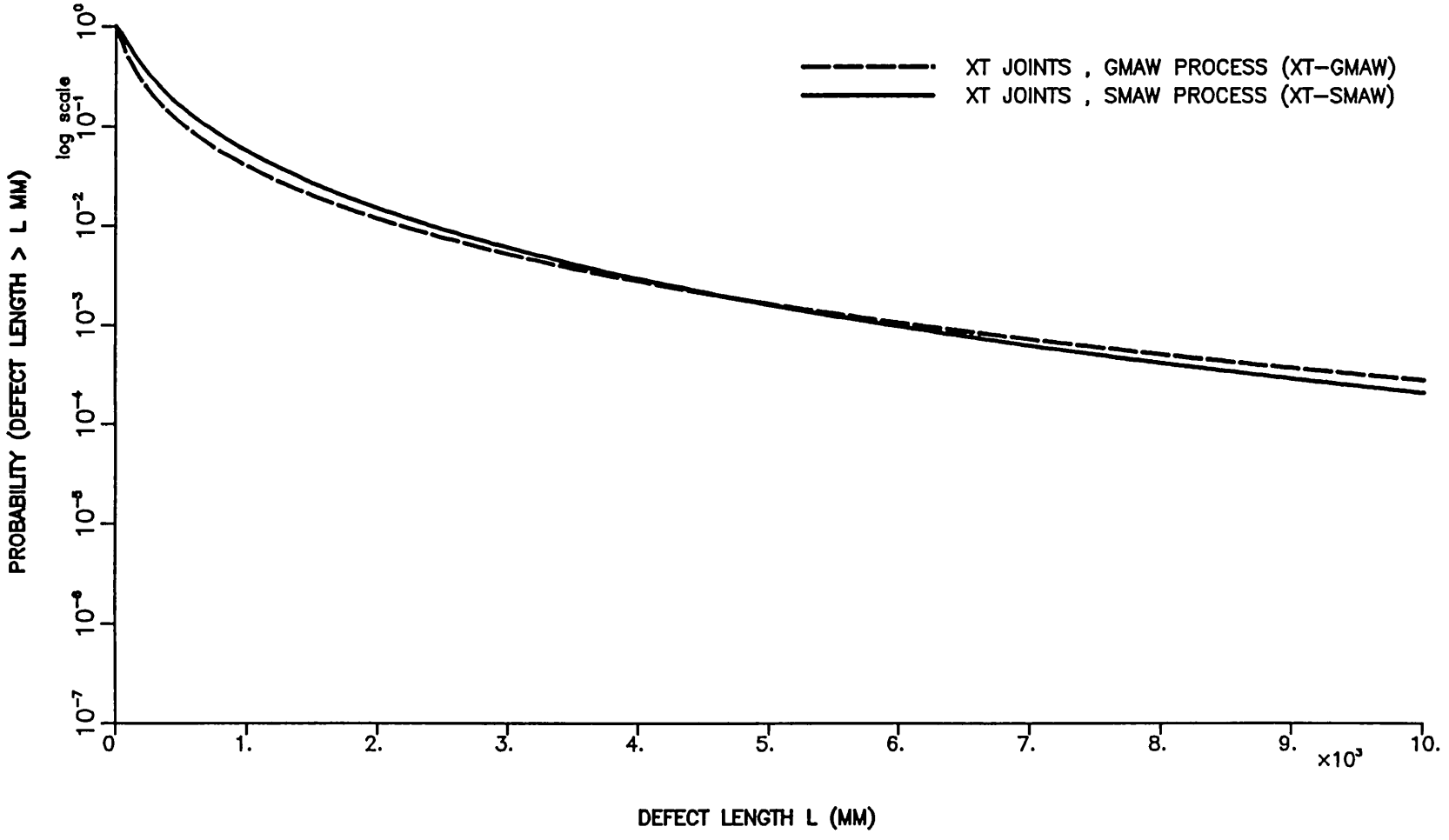


FIGURE 5.4.3.13 VARIOUS COMPLEMENTARY CUMULATIVE LENGTH DISTRIBUTIONS IN POROSITY DEFECTS (PO)



5.4.4 Defect Aspect Ratio

Figures 5.4.4.1 to 5.4.4.4 show histograms for defect aspect ratio for all categories of defect which have been examined in sections 5.4.2 and 5.4.3. The defect aspect ratio is defined as the ratio of defect length (L) to defect width (w). Mean values, together with standard deviations, are shown above each histogram. These values are seen to vary from category to category because of their dependence on both length and width. The lowest mean ratios range from 35 to 50 and are seen to be associated with crack–like defects. This is mainly due to the fact that this type of defect was found to have a larger than average width w.

The lognormal and Weibull distributions have been fitted to values of the defect aspect ratio. The superiority of the lognormal fit is shown by the relatively low KST values across all defect types and welding processes (tables 5.4.4.1 and 5.4.4.3). The good fit for the lognormal model is also demonstrated by the coefficients of skewness and kurtosis (table 5.4.4.2) which together with their standard errors provide alternative tests of normality for the natural logarithms of the data.

	SYMBOL	COUNT	MEAN	ST.DEV.
NF	A	3498	71.141	162.756
SL	B	858	85.974	114.405
CR	C	154	35.200	49.441
IP	D	197	109.263	216.613
PO	E	44	55.299	71.157

EACH SYMBOL REPRESENTS 1 OBSERVATIONS

INTERVAL NAME	5 10 15 20 25 30 35 40	FREQUENCY INT.	FREQUENCY CUM.	PERCENTAGE INT.	PERCENTAGE CUM.
113.000	+AAAAAAAAAAAAAAAAAAAAAAAAAAAAAAAAAAAAAAAAAAAAAAAA*	3911	3911	82.3	82.3
226.000	+AAAAAAAAAAAAAAAAAAAAAAAAAAAAAAAAAAAAAAAAAAAAAAAA*	556	4467	11.7	94.0
339.000	+AAAAAAAAAAAAAAAAAAAAAAAAAAAAAAAAAAAAAAAAAAAAAAAA*	175	4642	3.7	97.7
452.000	+AAAAAAAAAAAAAAAAAAAAAAAAAAAAAAAABBBBBBBBBB*	47	4689	1.0	98.7
565.000	+AAAAAAAAAAAAAAAAAAAABBBBBBB	28	4717	.6	99.3
678.000	+AAAAAAAAAABBB	13	4730	.3	99.6
791.000	+AAAAAB	6	4736	.1	99.7
904.000	+AA	2	4738	.0	99.7
1017.00	+	0	4738	.0	99.7
1130.00	+A	1	4739	.0	99.7
1243.00	+A	1	4740	.0	99.8
1356.00	+	0	4740	.0	99.8
1469.00	+A	1	4741	.0	99.8
1582.00	+	0	4741	.0	99.8
1695.00	+A	1	4742	.0	99.8
1808.00	+	0	4742	.0	99.8
1921.00	+B	1	4743	.0	99.8
2034.00	+	0	4743	.0	99.8
2147.00	+	0	4743	.0	99.8
2260.00	+	0	4743	.0	99.8
2373.00	+AAA	3	4746	.1	99.9
2486.00	+	0	4746	.0	99.9
2599.00	+A	1	4747	.0	99.9
2712.00	+	0	4747	.0	99.9
2825.00	+	0	4747	.0	99.9
2938.00	+D	1	4748	.0	99.9
3051.00	+	0	4748	.0	99.9
3164.00	+A	1	4749	.0	100.0
3277.00	+	0	4749	.0	100.0
3390.00	+	0	4749	.0	100.0
3503.00	+	0	4749	.0	100.0
3616.00	+	0	4749	.0	100.0
3729.00	+	0	4749	.0	100.0
3842.00	+	0	4749	.0	100.0
3955.00	+AA	2	4751	.0	100.0
4068.00	+	0	4751	.0	100.0
4181.00	+	0	4751	.0	100.0
4294.00	+	0	4751	.0	100.0

5 10 15 20 25 30 35 40

FIGURE 5.4.4.1 : HISTOGRAM FOR ASPECT RATIO IN XT JOINTS UNDER THE SMAW PROCESS

	SYMBOL	COUNT	MEAN	ST.DEV.
NF	A	409	52.107	57.476
SL	B	254	75.310	90.745
CR	C	12	46.189	55.896
IP	D	13	87.942	100.795
PO	E	5	38.983	49.036

EACH SYMBOL REPRESENTS 1 OBSERVATIONS

INTERVAL NAME	5 10 15 20 25 30 35 40	FREQUENCY INT.	FREQUENCY CUM.	PERCENTAGE INT.	PERCENTAGE CUM.
28.0000	+AAAAAAAAAAAAAAAAAAAAAAAAAAAAAAAAAAAAAAAA*	308	308	44.4	44.4
42.0000	+AAAAAAAAAAAAAAAAAAAAAAAAAAAAAAAAAAAAAAAA*	77	385	11.1	55.6
56.0000	+AAAAAAAAAAAAAAAAAAAAAAAAAAAAAAAAAAAAAAAA*	69	454	10.0	65.5
70.0000	+AAAAAAAAAAAAAAAAAAAAAAAAAAAAAAAABBBBBBBBB*	45	499	6.5	72.0
84.0000	+AAAAAAAAAAAAAAAABBBBBBBBBBBBBBBBBBBBCD	39	538	5.6	77.6
98.0000	+AAAAAAAABBBBBBBB	16	554	2.3	79.9
112.000	+AAAAAAAAAAAABBBBBBBB	21	575	3.0	83.0
126.000	+AAAAAAAAAAAABBBBBBBE	21	596	3.0	86.0
140.000	+AAAAAAAAAABBBBB	15	611	2.2	88.2
154.000	+AAAAAABBCD	10	621	1.4	89.6
168.000	+AAAAABBC	8	629	1.2	90.8
182.000	+AAAABBB	7	636	1.0	91.8
196.000	+AAAABB	6	642	.9	92.6
210.000	+AAAAAAAABBBBB	14	656	2.0	94.7
224.000	+ABBBB	5	661	.7	95.4
238.000	+ABBBBBB	7	668	1.0	96.4
252.000	+AAAAAABBD	9	677	1.3	97.7
266.000	+BB	2	679	.3	98.0
280.000	+	0	679	.0	98.0
294.000	+	0	679	.0	98.0
308.000	+BB	2	681	.3	98.3
322.000	+BB	2	683	.3	98.6
336.000	+BB	2	685	.3	98.8
350.000	+ABD	3	688	.4	99.3
364.000	+	0	688	.0	99.3
378.000	+	0	688	.0	99.3
392.000	+B	1	689	.1	99.4
406.000	+BB	2	691	.3	99.7
420.000	+B	1	692	.1	99.9
434.000	+	0	692	.0	99.9
448.000	+	0	692	.0	99.9
462.000	+	0	692	.0	99.9
476.000	+	0	692	.0	99.9
490.000	+	0	692	.0	99.9
504.000	+	0	692	.0	99.9
518.000	+	0	692	.0	99.9
532.000	+	0	692	.0	99.9
546.000	+B	1	693	.1	100.0

5 10 15 20 25 30 35 40

FIGURE 5.4.4.2 : HISTOGRAM FOR ASPECT RATIO IN B JOINTS UNDER THE SMAW PROCESS

	SYMBOL	COUNT	MEAN	ST.DEV.
NF	A	1684	87.413	150.630
SL	B	481	126.581	176.919
CR	C	72	48.565	82.022
IP	D	55	88.048	96.889
PO	E	20	37.104	54.208

EACH SYMBOL REPRESENTS 1 OBSERVATIONS

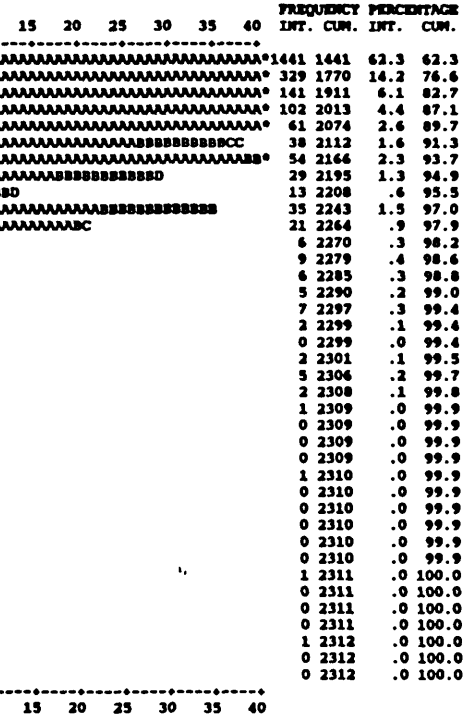


FIGURE 5.4.4.3 : HISTOGRAM FOR ASPECT RATIO IN XY JOINTS UNDER THE GMAW PROCESS

	SYMBOL	COUNT	MEAN	ST.DEV.
NF	A	58	91.530	117.854
SL	B	27	70.864	92.278
CR	C	0	.000	.000
IP	D	0	.000	.000
PO	E	0	.000	.000

EACH SYMBOL REPRESENTS 1 OBSERVATIONS

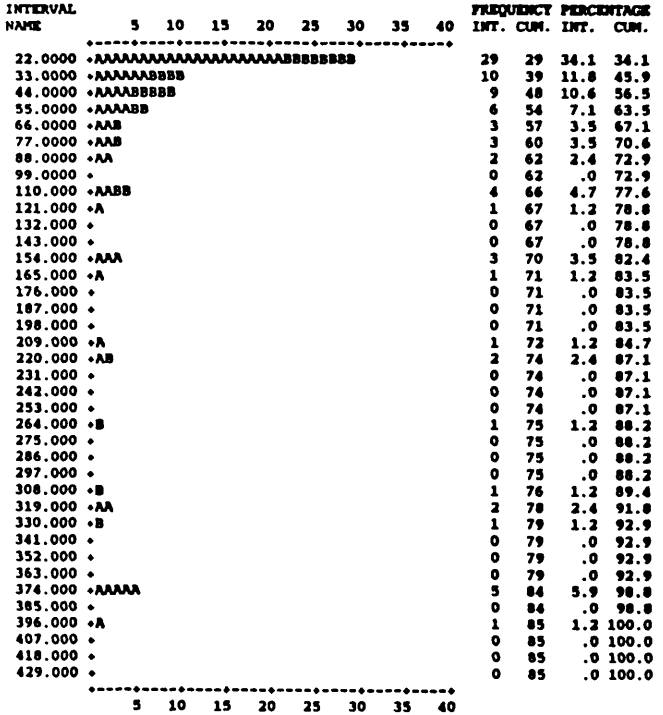


FIGURE 5.4.4.4 : HISTOGRAM FOR DEFECT ASPECT RATIO IN B JOINTS UNDER THE GMAW PROCESS

Type	Sample	$\hat{\mu}$	C.L.	$\hat{\sigma}^2$	C.L.	K.S.T.
XT-NF-SMAW	3498	3.522	(3.483,3.561)	1.401	(1.338,1.469)	0.02
XT-SL-SMAW	858	3.889	(3.815,3.963)	1.236	(1.127,1.371)	0.04
XT-CR-SMAW	154	2.888	(2.701,3.074)	1.395	(1.128,1.769	0.06
XT-IP-SMAW	197	3.927	(3.740,4.114)	1.789	(1.482,2.204)	0.09
XT-PO-SMAW	44	3.299	(2.923,3.675)	1.521	(1.038,2.443)	0.10
B-NF-SMAW	409	3.285	(3.161,3.409)	1.635	(1.432,1.885)	0.09
B-SL-SMAW	254	3.665	(3.217,3.813)	1.440	(1.219,1.728)	0.05
B-CR-SMAW	12	3.151	(2.350,3.952)	1.590	(0.799,4.578	0.13
B-IP-SMAW	13	3.951	(3.299,4.603)	1.162	(0.598,3.169)	0.13
B-PO-SMAW	5	-	-	-	-	-
XT-NF-GMAW	1684	3.525	(3.458,3.591)	1.939	(1.814,2.077)	0.04
XT-SL-GMAW	481	4.070	(3.959,4.181)	1.535	(1.358,1.749)	0.07
XT-CR-GMAW	72	3.018	(2.699,3.337)	1.835	(1.354,2.628)	0.06
XT-IP-GMAW	55	3.920	(3.610,4.230)	1.318	(0.934,2.000)	0.14
XT-PO-GMAW	20	2.983	(2.450,3.515)	1.302	(0.752,2.776)	0.11
B-NF-GMAW	58	3.653	(3.283,4.023)	1.985	(1.419,2.976)	0.07
B-SL-GMAW	27	3.581	(3.102,4.060)	1.459	(0.905,2.749)	0.11

Table 5.4.4.1: Lognormal Parameters - Length to Width Ratio

Type	Sample	Skewness	S.E.	Kurtosis	S.E.
XT-NF-SMAW	3498	0.103	0.041	0.033	0.083
XT-SL-SMAW	858	-0.308	0.084	0.367	0.167
XT-CR-SMAW	154	-0.022	0.197	0.027	0.395
XT-IP-SMAW	197	-0.275	0.174	-0.791	0.349
XT-PO-SMAW	44	0.153	0.369	-0.905	0.738
B-NF-SMAW	409	-0.296	0.121	-0.784	0.242
B-SL-SMAW	254	-0.013	0.154	-0.801	0.307
B-CR-SMAW	12	0.107	0.707	-1.250	1.414
B-IP-SMAW	13	0.121	0.679	-1.015	1.359
B-PO-SMAW	5	-	-	-	-
XT-NF-GMAW	1684	0.069	0.060	-0.066	0.119
XT-SL-GMAW	481	0.146	0.112	-0.424	0.223
XT-CR-GMAW	72	-0.026	0.289	-0.243	0.572
XT-IP-GMAW	55	-0.336	0.330	-0.346	0.661
XT-PO-GMAW	20	0.161	0.548	-0.703	1.095
B-NF-GMAW	58	0.050	0.322	-1.094	0.643
B-SL-GMAW	27	0.070	0.471	-0.591	0.943

Table 5.4.4.2: Coefficients of skewness and kurtosis for ℓn (Ratio)

Type	Sample	$\hat{\beta}$	C.L.	$\hat{\alpha}$	C.L.	K.S.T
XT-NF-SMAW	3498	0.814	(0.793,0.837)	61.398	(58.693,64.228)	0.08
XT-SL-SMAW	858	0.956	(0.906,1.011)	84.006	(77.744,90.773)	0.08
XT-CR-SMAW	154	0.869	(0.769,0.998)	32.377	(26.477,39.591)	0.10
XT-IP-SMAW	197	0.821		96.427		0.06
XT-PO-SMAW	44	0.850	(0.640,1.052)	50.256	(33.215,75.061)	0.15
B-NF-SMAW	409	0.904	(0.837,0.982)	49.551	(44.007,55.794)	0.06
B-SL-SMAW	254	0.895	(0.813,0.995)	70.924	(60.918,82.514)	0.06
B-CR-SMAW	12	0.877	(0.463,1.262)	42.967	(18.228,102.443)	0.14
B-IP-SMAW	13	0.996	(0.544,1.417)	87.780	(42.861,180.679)	0.13
B-PO-SMAW	5	-	-	-	-	-
XT-NF-GMAW	1684	0.727	(0.700,0.757)	68.567	(63.758,73.739)	0.10
XT-SL-GMAW	481	0.819	(0.763,0.884)	109.698	(92.219,123.281)	0.11
XT-CR-GMAW	72	0.763	(0.617,0.907)	40.031	(28.137,56.432)	0.10
XT-IP-GMAW	55	0.984	(0.767,1.196)	87.397	(63.649,118.792)	0.10
XT-PO-GMAW	20	0.892	(0.365,1.200)	34.687	(18.744,63.545)	0.08
B-NF-GMAW	58	0.772	(0.606,0.933)	77.705	(52,480,113.721)	0.10
B-SL-GMAW	27	0.868	(0.594,1.129	65.270	(38.287,109.614)	0.14

Table 5.4.4.3: Weibull parameters – Length to Width Ratio

5.4.5. Correlations between Defect Width and Defect Length

Correlation analysis shows that there is almost no linear relationship between defect width and defect length. There is generally a tendency for positive correlation but this must be interpreted very carefully because of the large sample sizes.

Of particular importance are the statistical tests on the transformed data using the T statistic (see section 5.1.3). These were performed at the 95% level and those values found to be statistically significant are marked with an asterisk in table 5.4.5. The T statistic, however, is very sensitive to the sample size N, and care should be taken in interpreting the significance of these values from the practical point of view. Due to the large sample sizes, it would be a too strong conclusion that the two distributions are indeed correlated. From the practical point of view, it can be stated that there is a tendency for positive correlation which needs to be investigated by examining further sets of data from other structures.

Two cases that deserve special mention are the ones belonging to the categories XT-IP-SMAW and XT-PO-GMAW. In these cases the correlation between the variables defect width and defect length exceeds the value of 50%, but it is not clear whether this is due to the defect type (IP,PO) or the welding process (SMAW,GMAW).

Figures 5.4.5.1 to 5.4.5.8 show selective plots of defect width versus defect length and of their natural logarithms. All the plots show a wide scatter. The end points of the regression curves are marked with Y and are shown on the two vertical scales of the plots.

5.4.6 Comparisons and Conclusions

The statistical distribution of the parameters defect width w, defect Length L, and aspect ratio ϵ were found to be reasonably independent of factors such as original fabricator, general position in the structure and the position of the defect within the weld. In addition, very close similarities were found between the probability distributions for the dimensions of defects in cruciform (X) and tee butt (T) welds; and as a result, data from these two sources were merged into one category (XT).

The effect of different welding processes on the width of embedded defects has been found to be relatively unimportant. In contrast, defect type and weld joint type have been found to be the main governing factors. The narrowest defects were the slag inclusion defects with mean values for w ranging from 2.7mm to 2.9mm. Crack-like

Type	r	$W=a_1+a_2(Def.Len)$	Transformed Data (Ln)		Size
			r	C.L. (r)	
XT-NF-SMAW	0.032	$W=5.75 + 24 \times 10^{-6}DL$	0.150*	(0.117,0.182)	3498
XT-SL-SMAW	0.054	$W=2.88 + 29 \times 10^{-6}DL$	0.064	(-0.003,0.130)	858
XT-CR-SMAW	0.281	W=9.05 + 0.006 DL	0.205*	(0.048,0.352)	154
XT-IP-SMAW	0.586	W=9.91 + 0.002 DL	0.543*	(0.436,0.635)	197
XT-PO-SMAW	-0.160	W=6.74 -0.001 DL	0.057	(-0.244,0.348)	44
B-NF-SMAW	0.157	W=3.49 + 0.002 DL	0.113*	(0.016,0.208)	409
B-SL-SMAW	-0.086	$W=2.84 - 43 \times 10^{-6}DL$	-0.060	(-0.182,0.064)	254
B-CR-SMAW	-0.203	W=9.89 - 0.005 DL	0.130	(-0.480,0.655)	12
B-IP-SMAW	-0.049	$W=4.93 - 50 \times 10^{-6}DL$	-0.086	(-0.608,0.488)	13
B-PO-SMAW	-0.643	W=7.23 - 0.015 DL	0.568	(-0.966,0.630)	5
XT-NF-GMAW	-0.026	$W=5.53 - 25 \times 10^{-6}DL$	0.052*	(0.004,0.099)	1684
XT-SL-GMAW	0.058	$W=2.72 + 19 \times 10^{-6}DL$	0.072	(-0.017,0.160)	481
XT-CR-GMAW	0.228	W=9.36 + 0.002 DL	0.207	(-0.026,0.419)	72
XT-IP-GMAW	0.086	W=6.02 + 0.001 DL	0.061	(-0.208,0.321)	55
XT-PO-GMAW	0.399	W=4.37 + 0.011 DL	0.542*	(0.131,0.794)	20
B-NF-GMAW	-0.016	$W=3.62 - 14 \times 10^{-6}DL$	0.020	(-0.239,0.277)	58
B-SL-GMAW	-0.248	$W=2.85 - 88 \times 10^{-6}DL$	-0.253	(-0.577,0.140)	27

Table 5.4.5 : Results for Correlation between Defect Width and Defect Length

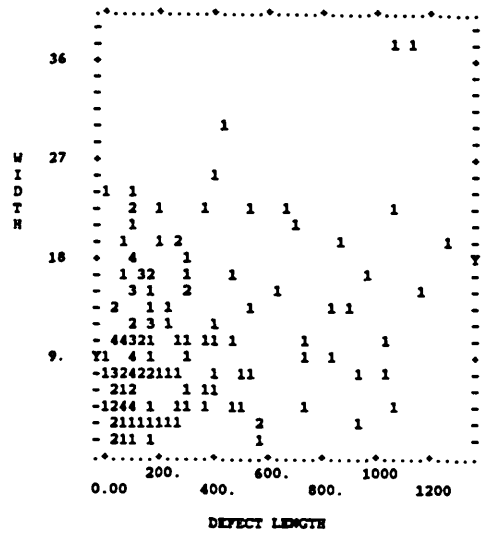


FIGURE 5.4.5.1 : DEFECT LENGTH/WIDTH CORRELATION FOR CR DEFECTS IN XT JOINTS UNDER THE SMAW PROCESS

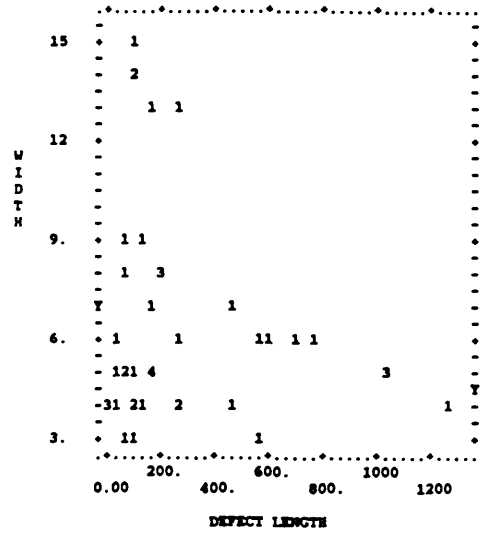


FIGURE 5.4.5.2 : DEFECT LENGTH/WIDTH CORRELATION FOR PO DEFECTS IN XT JOINTS UNDER THE SMAW PROCESS

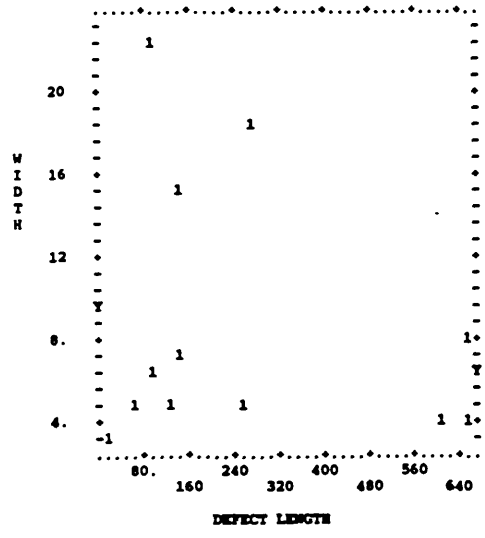


FIGURE 5.4.5.3 : DEFECT LENGTH/WIDTH CORRELATION FOR CR DEFECTS IN B JOINTS UNDER THE SMAW PROCESS

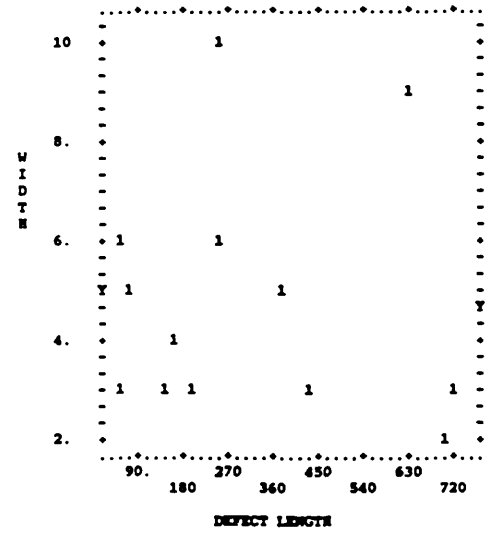


FIGURE 5.4.5.4 : DEFECT LENGTH/WIDTH CORRELATION FOR IP DEFECTS IN B JOINTS UNDER THE SMAW PROCESS

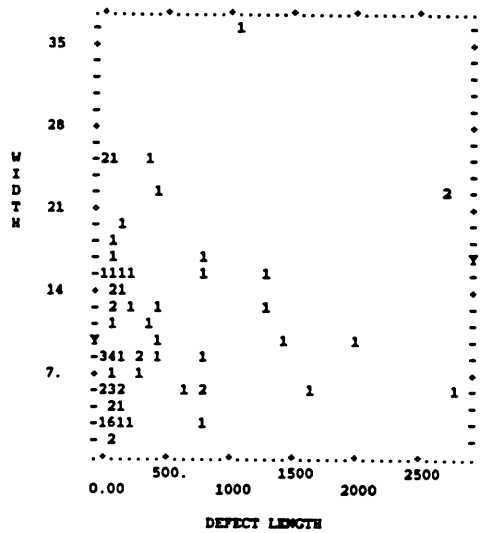


FIGURE 5.4.5.5 : DEFECT LENGTH/WIDTH CORRELATION FOR CR DEFECTS IN XT JOINTS UNDER THE GMAW PROCESS

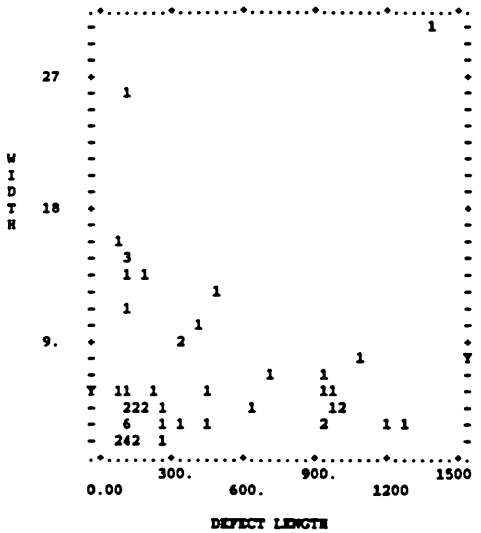


FIGURE 5.4.5.6 : DEFECT LENGTH/WIDTH CORRELATION FOR IP DEFECTS IN XT JOINTS UNDER THE GMAW PROCESS

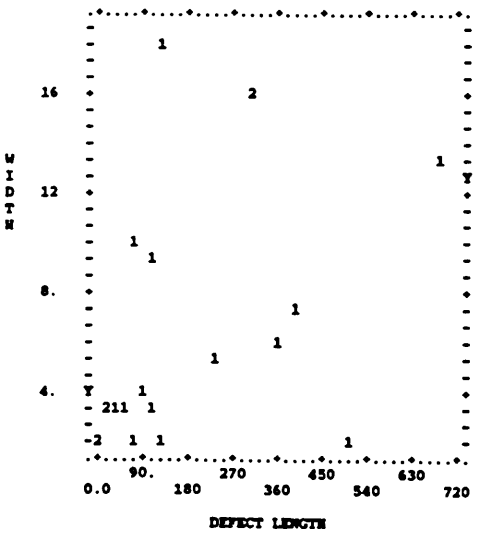


FIGURE 5.4.5.7 : DEFECT LENGTH/WIDTH CORRELATION FOR PO DEFECTS IN XT JOINTS UNDER THE GMAW PROCESS

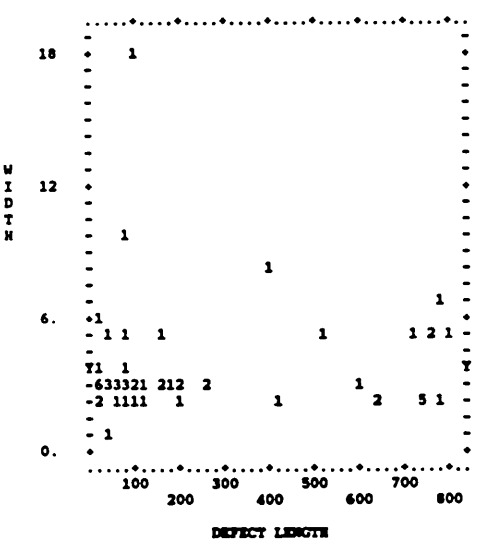


FIGURE 5.4.5.8 : DEFECT LENGTH/WIDTH CORRELATION FOR MF DEFECTS IN B JOINTS UNDER THE GMAW PROCESS

defects were found to have the largest widths, with mean values of w ranging from 8.5mm to 10.8mm. Comparisons between types of welded joint have shown that defects in plate butts were consistently narrower than in cruciforms and tee butts (category XT) These differences were found for both welding processes, SMAW and GMAW, and for all defect types.

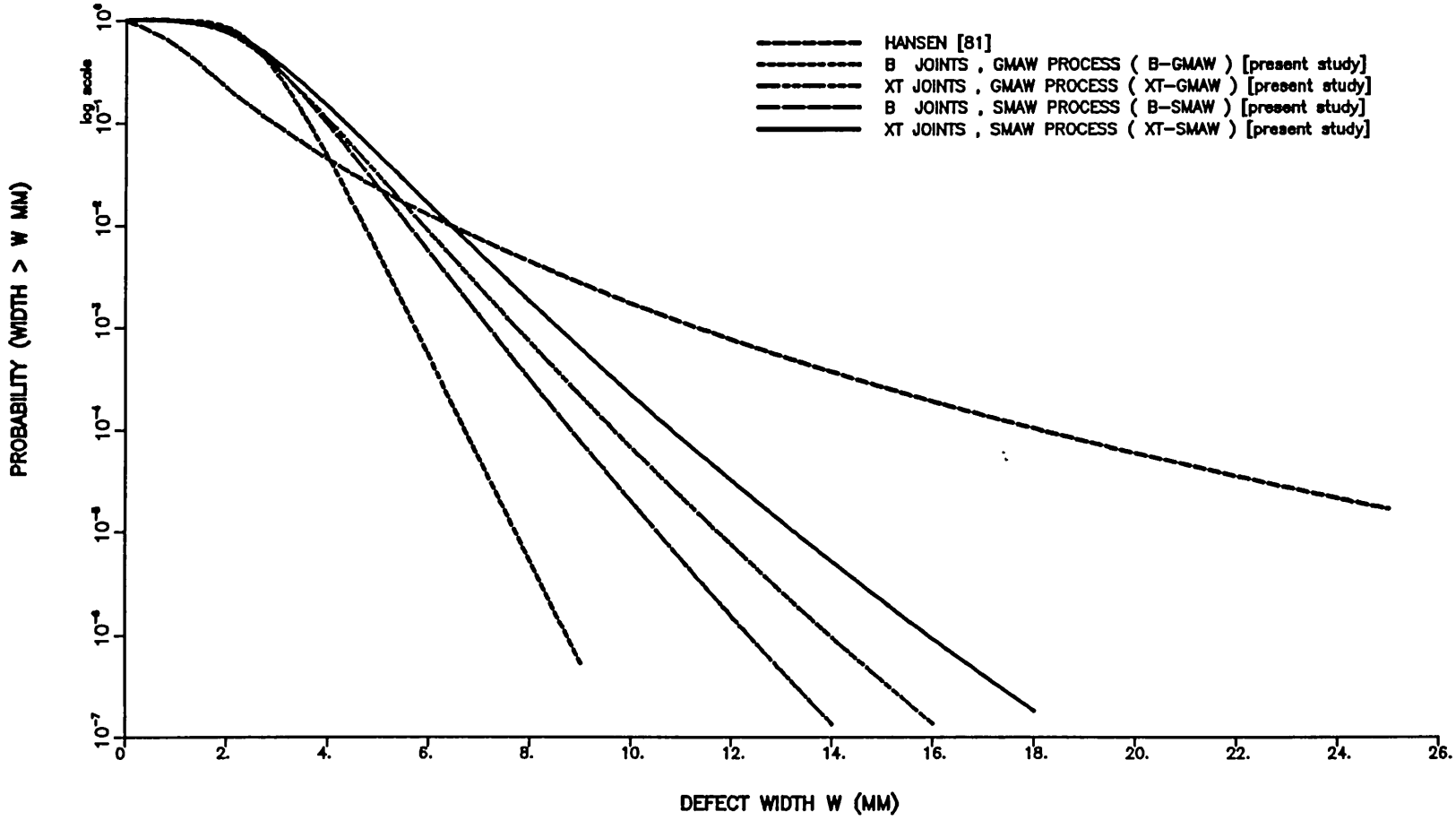
In the case of the defect length parameter L, greater variations were found between the various defect type categories than in the case of the parameter w. In general, slag inclusion defects were found to be shorter than other defect types. A similar trend was found for porosity defects. Mean values for L for slag inclusions ranged from 169mm to 320mm. In contrast, the mean lengths of crack-like defects varied between 260mm and 414mm, with incomplete penetration defects having similar characteristics.

Turning now to the defect aspect ratio ϵ(=L/w), this was found to vary considerably. However, the smallest values of L were found in crack-like defects, with mean values ranging from 35 to 50. The main reason for this was the larger values of w found in this class of defects.

Finally, tests on the correlation between defect length and defect width have been performed for each category of defect. These have shown that there is a tendency for positive correlation (i.e. long defects tend to be wider than short defects, and vice-versa), but there are large variations and this finding is not of practical significance.

Unfortunately there are very few data on defect width in the literature to enable comparisons to be made with the findings in this study. Hansen [81] fitted the lognormal distribution to the width of slag inclusion efects in butt weld joints measured on radiographs. For a total of 131 slag defects in welds of 25.4mm thickness from four different structures he obtained the parameters μ = 0.117 and σ = 0.748. These correspond to a mean value of 1.5mm estimated by maximum likelihood. This is lower than 2.8mm, the midpoint for the range of mean values observed for slag inclusion defects in this study. Figure 5.4.6.1 shows the complementary cumulative width distributions for slag inclusions due to Hansen [81] and the various estimates in the present study. It can be seen that because of the high value of the parameter σ in the former case, the probabilities of exceeding a value of about 6mm are much higher in Hansen's case than in all cases of the present study, whereas the reverse is true for defects with widths smaller than 6mm. A possible explanation for this is that the Hansen data were non-honogeneous.

FIGURE 5.4.6.1 COMPLEMENTARY CUMULATIVE DISTRIBUTIONS FOR DEFECT WIDTH IN SLAG INCLUSION DEFECTS (SL)



Another source of information on the width of weld defects is due to Dufresne et al [84]. By analysing data from 338m of PWR and shell welds, inspected by ultrasonics or X-rays, they found that the probability of occurrence of long defects increases as the width increases. Examination of fig. 10 of ref [84] shows that for 3, 6 and 12mm wide defects, the probabilities of having a flaw of length smaller than 512mm are 96%, 0.14% and 0.005% respectively. This conclusion implies a degree of correlation between the two dimensions L and w which was indirectly revealed in the present study.

CHAPTER 6

PROBABILISTIC MODELS FOR DEFECT DETECTION AND SIZING

6.1 Statistical Theory

The problem of modelling detection efficiencies deserves special attention because the basic observations are proportions for which the form of random variations is very likely to be binomial.

In a non-destructive examination programme a number of specimens containing n_i defects of size x_i are subjected to test and a count is made of the number of defects which have been detected. Such data give rise to many difficulties like non-constant variance and non-normal distributions to allow standard statistical methods to be used, as discussed in Section 6.2.3.

Non-linear relationships are also another problem because regression curves of the observed proportion r_i/n_i against the defect sizes are very unlikely to be linear since any changes in the defect sizes at the lowest or highest values of x_i do not usually produce much change in the proportion. Graphs of 'sigmoidal' shape are in fact very likely to be found. In order to linearise the observed proportions several types of transformations are used which have very similar effects. Such transformations are very well known in statistical theory and have been used extensively in biological assay and many other fields for a number of years. The standard textbook on binary data by Cox [31] provides valuable information on their properties and applications. Also the book by McCullagh and Nelder [86] describes the theory of linear models and gives detailed descriptions of fitting algorithms. Finally the book by Cox and Snell [85] contains applications of linear models with numerous examples.

6.1.1 Binomial Distribution

Suppose that the response from the outcome of an experiment is measured on an attribute basis, where the random variable Y is defined as:

$$Y = \begin{cases} 1 & \text{if the response is present (e.g. a real defect is detected} \\ 0 & \text{if the response is absent (e.g. a real defect is not detected} \end{cases}$$

If there are n independent identically distributed random variables (i.i.d.r.v.) with $\pi = \Pr[Y = 1]$ then the r.v. R denoting the number of outcomes with the attribute present has a binomial distribution:

$$R \sim B(n,\pi) \quad \text{i.e. } Pr[R = r] = \binom{n}{r}\pi^r (1 - \pi)^{n-r} \quad r = 0, 1, \ldots, n$$

with $E[R] = n\pi$ and $Var(R) = n\pi (1-\pi)$

The sample proportion P can be identified with the sample mean of Y and it can be easily shown

$$E[P] = \pi \text{ and } Var[P] = \frac{\pi(1-\pi)}{n}$$

For probability calculations the analytical approach can be used when n is small or use may be made of readily tabulated values [87].

When n is large, use of the normal distribution N $(n\pi, n\pi(1-\pi))$ can be made. To calculate the probability $Pr(R \geq r_o)$ we can use the area under the approximate normal curve over the range (r_o, ∞)

$$\text{i.e.} \qquad 1 - \Phi \left[\frac{r_o - n\pi}{\sqrt{n\pi(1-\pi)}} \right]$$

A better approximation is obtained by integrating over the range $(r_o - 1/2, \infty)$

$$\text{i.e.} \qquad 1 - \Phi \left[\frac{r_o - 1/2 - n\pi}{\sqrt{n\pi(1-\pi)}} \right]$$

The correction of 1/2 is usually called the continuity correction and its effect becomes negligible as n increases. The accuracy of the normal approximation is a function of the parameters n, and the range of R used for integration. The accuracy improves as n becomes large and π tends to 0.5. For a discussion of the use of the normal distribution as an approximation to the binomial see Wetherill [88].

Confidence intervals for π can be obtained in a number of ways. For a sample size of n, if the number of outcomes with the attribute present is r then π will obviously be close to r/n. A two-sided confidence interval for π is (π_L, π_H) where

$$Pr[R \geq r \mid \pi = \pi_L] = Pr[R \leq r \mid \pi = \pi_H] = \alpha/2$$

with $1-\alpha$ the size of the confidence level and $\pi_L(\pi_H)$ the lowest (highest) value of π that we are prepared to consider, given any value of R, namely R=r. If $r > n\pi$ and the probability in the binary distribution with parameters π and n are $P_o, P_1, \ldots, P_n$

the values of π_L and π_H are given by:

$$\pi_H = P_r + P_{r+1} + \ldots + P_n$$

$$\pi_L = P_{r'} + P_{r'-1} + \ldots + P_o$$

where $r' = 2n\pi - r$ if this is an integer and the highest integer less than this quantity otherwise.

Furthermore, the use of the normal approximation gives:

$$Z = \frac{r - n\pi}{\sqrt{n\pi(1-\pi)}} \sim N(0,1)$$

which leads to

$$Pr\left[- Z_{\alpha/2} < \frac{r - n\pi}{\sqrt{n\pi(1-\pi)}} < Z_{\alpha/2} \right] = 1 - \alpha$$

i.e.

$$Pr\left[\frac{r - Z_{\alpha/2}\sqrt{n\pi(1-\pi)}}{n} \leq \pi \leq \frac{r + Z_{\alpha/2}\sqrt{n\pi(1-\pi)}}{n} \right] = 1-\alpha$$

The solution of the above equation is quadratic in π; nevertheless a simple solution is to replace π in the variance by $\hat{\pi} = r/n$. This is not a too drastic step as $\hat{\pi}(1-\hat{\pi})$ changes relatively slowly with changes in $\hat{\pi}$ especially for values of $\hat{\pi}$ close to 1/2. The introduction of the continuity correction for confidence intervals is done in a similar fashion as in the calculation of probabilities previously investigated.

6.1.2 Binary Regression Models

Consider again the responses $r_1 \ldots, r_n$ which correspond to the independent r.v. $R_1, \ldots R_n$ associated with the number of outcomes with the attribute present in N different groups. Suppose further that the probability π depends on the covariate vector x_j ; j=1,...,k with the relation

$$g(\pi_i) = \sum_{j=1}^{k} x_{ij}\,\beta_j \qquad i=1,\ldots,N$$

The function $g(\pi)$ could take several forms, the most common of which are:

Logit $$g_1(\pi) = \ell n\left[\frac{\pi}{1-\pi}\right] \qquad 6.1.2.1$$

Probit $$g_2(\pi) = \Phi^{-1}(\pi) \qquad 6.1.2.2$$

Complementary log-log $\quad g_3(\pi) = \ell n\,[-\ell n(1-\pi)]$ 6.1.2.3

As an important additional remark, the transformation

$$Z_i = \ell n\left[\frac{r_i}{n_i - r_i}\right]$$

called the empirical logistic transformation (Cox [31]) gives a variable Z, with variance approximately equal to

$$\mathrm{Var}(Z_i) = \frac{1}{n_i \pi_i (1-\pi_i)}$$

an estimate of which is taken to be

$$\frac{n_i}{r_i(n_i - r_i)} = \frac{1}{r_i} + \frac{1}{n_i - r_i}$$

The approximation is improved (if r_i=0 or n_i, for then π_i=0 or 1 and Z_i=$-\infty$ or ∞ respectively) by taking the modified transformation

$$Z_i = \ell n \frac{r_i + 1/2}{n_i - r_i + 1/2}$$

and an estimate of variance

$$\mathrm{Var}[Z_i] = \frac{(n_i+1)(n_i+2)}{n_i(r_i+1)(n_i - r_i+1)}$$

which gives an almost unbiased estimate of Var[Z_i]. Plots of Z_i against the covariate vectors are preliminary essentials in investigating the suitability of the logistic model. Further details and important applications of this transformation are given by Cox [31].

For any form of $g(\pi)$ the log-likelihood is

$$L(\underline{\pi}\ ;\ \underline{r}) = \sum_{i=1}^{N} \left[r_i \ell n\left[\frac{\pi_i}{1-\pi_i}\right] + n_i \ell n\,(1-\pi_i) + \ell n\binom{n_i}{r_i}\right] \qquad 6.1.2.4$$

Considering the case where the relationship between the binomial probabilities and the covariate vectors takes the form of 6.1.2.4,

i.e.

$$g(\pi_i) = \ell n\left[\frac{\pi_i}{1-\pi_i}\right] = \sum_{i=1}^{k} x_{ij}\beta_j \qquad i=1,\ldots,N$$

the log-likelihood function 6.1.2.4 becomes

$$L(\underline{\beta}\ ;\ \underline{r}) = \sum_i \sum_j r_i x_{ij}\beta_j - \left[\sum_i n_i \ell n(1+\exp\sum_j x_{ij}\beta_j)\right] + \text{const}$$

where the probabilities $\underline{\pi}$ are expressed in terms of the parameters $\underline{\beta}$.

The maximum likelihood estimate $\hat{\underline{\beta}}$ satisfies the equation

$$\left[\frac{\partial L}{\partial \beta_j}\right]_{\underline{\beta}=\hat{\underline{\beta}}} = 0$$

which for the linear logistic model yields:

$$\sum_i (r_i - n_i\hat{\pi}_i)\, x_{ij} = 0 \qquad j=1,\ldots,k \qquad\qquad 6.1.2.5$$

with

$$\hat{\pi}_i = \frac{\exp \sum_j x_{ij}\,\hat{\beta}_j}{1+\exp \sum_j x_{ij}\,\hat{\beta}_j}$$

Estimation of $\hat{\underline{\beta}}$ is obtained via the solution of 6.1.2.5. This can be done by using the Newton-Raphson method and solving the weighted equations at each iteration with weights $w_i = \pi_i(1-\pi_i)/n_i$. The calculations can be performed using the statistical package GLIM [34] with binomial errors, logit-link. Similarly, fits can be obtained for the other two models. For details of the fitting algorithm see McCullagh and Nelder [86].

To measure the goodness of fit of the model, if $\hat{\underline{\beta}}$ are the maximum likelihood estimators of the parameters $\underline{\beta}$, the deviance D is of the form:

$$D(\underline{r}\ ;\ \hat{\underline{r}}) = 2 \sum_{i=1}^{N} \left\{ r_i \ell n\left[\frac{r_i}{\hat{r}_i}\right] + (n_i - r_i)\ \ell n\left[\frac{n_i - r_i}{n_i - \hat{r}_i}\right] \right\}$$

For a model which involves k independent parameters, the fit of the model is assessed by comparing D with the critical values of the χ^2_{N-k} distribution.

To test the adequacy of the proposed model, the standard residuals

$$d_i = \frac{O_i - E_i}{(E_i(1-E_i)/n_i)^{1/2}}$$

which have approximately zero mean and unit variance can be used for diagnostic checks. O_i and E_i denote respectively the observed proportions and the proportions estimated from the data. The distribution of d_i is however far from normal. For more complicated residuals which are nearly normally distributed and give almost linear plots on probability paper; see Cox and Snell [89].

In the simplest case where one concomitant variable is involved the three models reduce to:

$$\pi = \frac{\exp(\alpha+\beta x)}{1+\exp(\alpha+\beta x)} \qquad \text{Logit Model}$$

$$\pi = \Phi(\alpha+\beta x) \qquad \text{Probit Model}$$

$$\pi = 1-\exp[-\exp(\alpha+\beta x)] \qquad \text{Complementary Log-Log Model}$$

The complementary log-log function is the inverse of the cumulative distribution of the extreme value distribution and unlike the two other models it is not symmetric about
$\pi = 0.5$. The latter functions for most purposes agree closely over the whole range. The only exception is when attention focuses to the regions where the probability π is either very small or very near to one. For small π the complementary log-log function is very similar to the logit but as π approaches one, it approaches infinity more slowly than either of the other two models.

6.2 Defection Efficiencies

Several national and international test programmes have been conducted on welded samples containing various flaws for the purpose of determining the reliability of non-destructive examination with respect to the detection, sizing and positioning of defects.

However, these programmes were concerned mostly with artificially induced defects rather than natural ones, and it must be emphasised that the response from artificial defects may differ from that of natural defects because of shape variations, orientation and microscopic roughness, as investigated by Allen and Brandford [90]. Such differences have been found to be highly marked in the data from aircraft specimens reported by Norris, especially with ultrasonic testing (Figures 8 and 9 of Ref. 91). The importance of examining realistic defects was appreciated by several teams and recently a new programme, PISC III, was initiated [92] to evaluate the NDE reliability by considering not only real flaws but real flaws in typical surroundings.

Although modelling the detection efficiency of an NDE device is not easy due to the large number of uncertainties involved, in addition to the defect dimensions themselves, a variety of mathematical models have previously been proposed. In some cases, numerical values have been given for detection probabilities for different defect categories. A review of previous work is given below in Section 6.2.1.

6.2.1 Literature Review

Thomas and Kloster [93] compared the reliability of magnetic rubber, magnetic particle and ultrasonic techniques in the detection of very small induced flaws on forged steel. An 85% detection probability is reported for a 0.76mm long flaw with the magnetic techniques. For ultrasonic testing, the same probability corresponds to a flaw area of 2.49mm^2.

Becher and Pedersen [74] suggested a model in conjunction with the initial crack size distribution entering service under which the probability of detecting a crack of depth 20mm is 90%.

O'Neill and Jordan [94] suggested that the probability of missing a potentially dangerous defect by ultrasonics is somewhere between 1 and 0.01.

Tank [78] derived the model:

$$P_{DN}(z) = \begin{cases} 0 & z \leqslant 0 \\ 5z & 0 \leqslant z \leqslant 0.02\text{in.} \\ 9z-0.08 & 0.02\text{ in.} \leqslant z \leqslant 0.12\text{in.} \\ 1.0 & z \geqslant 0.12\text{in.} \end{cases} \qquad 6.2.1.1$$

based on ultrasonic data from aluminium specimens.

Rummel *et al* [95] published data on small tight cracks on aluminium alloy specimens. The specimens were between 1.52mm to 5.32mm in thickness and contained fatigue cracks ranging from 0.18mm to 12.7mm long and 0.03mm to 4.51mm deep. For the ultrasonic inspection Fig. 9 of Ref. [95] reveals that cracks of depths 0.13mm and 0.76mm have probabilities of detection of 50% and 90% respectively.

Kauppinen and Aaltio [96] and Forsten and Aaltio [97] reported results reflecting the dependence of the detection efficiency on the defect size, type and location as well as on the inspection time used by the UT operator. Lack of fusion defects exceeding a length of 40mm are reported to have 100% detection probability, whereas for smaller defects the probability reduced to 75%. Slag inclusions in general gave stronger indications. In butt-welded plate seams, defects 50mm long had a 100% detection probability whereas in tee joints the corresponding detection efficiency was clearly less than 100%. The average detection probability for 10-30mm long defects in more complex geometries was recorded as being about 50%. Root area defects were shown to be more difficult to detect. A root area defect of length 35mm was detected with 30% probability. The importance of inspection time was found to be distinct. An increase from one hour to two hours resulted in an 18% increase in detection probability.

Packman *et al* [98, 99] reported data on artificially induced surface elliptical fatigue cracks inspected by aluminium penetrant, titanium penetrant and magnetic particle methods. They assessed the NDE reliability by assuming a binomial distribution and suggested a test programme for obtaining detection probabilities.

Marshall [79] tried to estimate the detection function by means of a questionaire sent out to independent experienced ultrasonic operators asking each individual operator for his estimate of the efficiency with which he would detect defects of specified size and location. The overall detection efficiency was estimated by averaging overall detection probabilities for each defect size and location.

The function:

$$P_{ND}(z) = \epsilon + (1-\epsilon)\ \exp-(\mu z) \qquad 6.2.1.2$$

with $\epsilon = 0.005$

$\mu = 2.88\ in^{-1}$

was suggested as representing the largest average probability values for not detecting a defect of depth z.

Marriot and Hudson [100] assumed a general exponential model in their work for predicting the failure risk in pressure vessels. The model was treated theoretically with general defect dimension C and parameters α and β to be estimated from the data. The function is of the form:

$$P_{DN}(c) = \alpha + (1-\alpha)\ \exp-(\beta c) \qquad 6.2.1.3$$

and its form is seen to be identical to that suggested by Marshall [79].

Harris [77] suggested the use of the lognormal model:

$$P_{ND}(z) = \frac{1}{2}\ \mathrm{erfc}\ \left[\upsilon\ \ell n\ \frac{z}{z^*}\right] \qquad 6.2.1.4$$

where z^* is the crack depth in inches for which $P_{ND} = 0.5$ and erfc is the complementary error function.

The above model was fitted to the UT data reported by Tank [78]. The data are in the range $z < 0.1$ in. (2.5mm) for 3in. (7.62cm) OD tubes of 0.25in. (6.4mm) wall thickness. The calculated values for the parameters were $\upsilon = 1.33$, $z^* = 0.063$in. (1.6mm). He also obtained a least squares fit for the models:

$$\text{Weibull}\quad P_{ND}(z) = \exp-(z/\gamma)^{\eta}\ ,\ z^* = \gamma(\ell n 2)^{1/\eta} \qquad 6.2.1.5$$

$$\text{Gamma}\quad P_{ND}(z) = \exp-(\mu z) \sum_{n=0}^{k-1} \frac{(\mu z)^n}{n!} \qquad 6.2.1.6$$

with parameters estimated from the data:

Weibull $\gamma = 0.07$in. , $\eta = 2$
Gamma $\mu = 74\text{in.}^{-1}$, $k = 5$

Although the three models fit the data well within the range reported, the behaviour of the models at larger values of z differ significantly. For z = 1/4in. (6.35mm) the non- detection probabilities are:

Lognormal : 4.6×10^{-3}
Weibull : 2.9×10^{-6}
Gamma : 6.5×10^{-5}

The Plate Inspection Steering Committee (PISC I) [101] published results of an NDE programme on test blocks containing various welding defects. It was reported that for small volumetric defects ranging from 1 to 10mm there is almost no correlation between detection probability and crack depth. For defects perpendicular to the inspection surface and of depth greater than 10mm the correlation is very high, and it can be confidently stated that for cracks greater than 50mm the detection probability is higher than 95%. For cluster defects grouped together by the ASME XI proximity rules the detection probability was significantly lower and ranged between 0 and 50%.

Townend [12] modelled and compared the performance of the PVRC [102] and PISC I [101] programmes by least square fit of the models:

$$P_{DN}(z) = 1-\exp-(z/57) \text{ for PISC I} \qquad 6.2.1.7$$

$$P_{DN}(z) = 1-\exp-(z/6.3) \text{ for PVRC} \qquad 6.2.1.8$$

where z is the depth of the defects in mm.

Harris and Lim [103] incorporated the area A of the crack into the non-detection function. They suggested the lognormal model:

$$P_{ND}(z) = \epsilon + \frac{1}{2}\left[1-\epsilon\right] \operatorname{erfc}\left[\upsilon \ell n \frac{A}{A^*}\right] \qquad 6.2.1.9$$

They assumed part-circumferential cracks and evaluated the area from $A = \pi/4 D_B z$.

The beam diameter D_B was assumed to be 1in. (25.4mm) and to be always smaller than the defect length. A* corresponds to a depth of z* having a detection probability of 50%. With values of $\epsilon = 0$, $\upsilon = 1.60$ and $A^* = 0.98\text{in.}^2$ (622.3mm^2) corresponding to z* = 1.25in. (31.75mm) the model predicts much smaller detection probabilities than any previously suggested function and assumes that a crack would have to be half way through the wall thickness before it would have a 50% probability of being detected.

Dufresne [104] argued that the detection probability increases with the length of the defect because of the greater number of upcrossings of the ultrasonic transducer. He modelled this idea mathematically suggesting the expression:

$$P_{Dn} = 1-(1-P_{D1})^{2b/D_b} \qquad 6.2.1.10$$

Where P_{Dn} = the detection probability after n crossings
P_{D1} = the detection probability at each crossing
D_b = the beam diameter
2b = the length of the defect

By pooling data from different trial programmes he plotted the detection probability as a function of crack length for various crack depths. His Figure 2 (page 521 of Ref. [104]) is reproduced here as Fig. 6.2.1 for further reference. The beam diameter was taken to be 40mm and the 50% detection probability to correspond to a 9mm long defect.

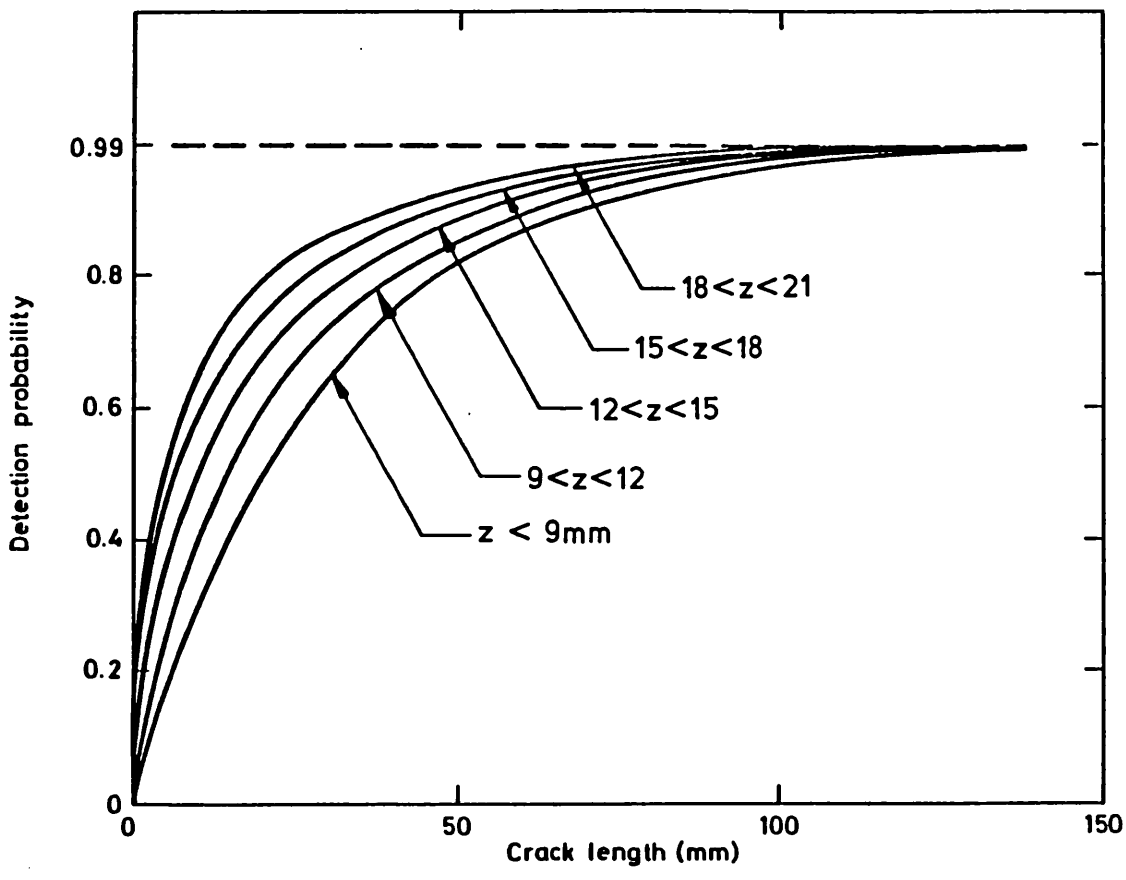


Fig. 6.2.1 : Defect Detection Probability as a function of crack length for various crack depths (Dufresne [104])

Temple [105] analysed data obtained by ultrasonics and liquid penetrant techniques on aluminium alloy. The depth and length of the defect were treated separately and three models were fitted by minimising the least square error. Models 6.2.1.12 and 6.2.1.13 are identical to those suggested by Harris [77].

$$P_{ND}(x) = \frac{1+\exp(-\alpha x^*)}{1+\exp(\alpha(x-x^*)} \qquad 6.2.1.11$$

$$P_{ND}(x) = \frac{1}{2}\,\mathrm{erfc}\left[\upsilon \ell n \frac{x}{x^*}\right] \qquad 6.2.1.12$$

$$P_{ND}(x) = \exp\left[-\left[\frac{x}{\gamma}\right]^{\eta}\right] \qquad 6.2.1.13$$

where x denotes the dimension of interest in mm and α, x^*, υ, γ, η the model parameters estimated from the data. The values of the parameters for the ultrasonic inspection as extracted from Table IV, page 262 of Ref. [105] are shown below in Table 6.2.2.

UT Dimension	Equation 3.1.11		Equation 3.1.12		Equation 3.1.13	
	α	x^*	υ	x^*	γ	η
Depth	1.773	0.012	0.585	0.251	0.533	8.69
Length	0.262	0.149	0.512	1.437	2.762	8.86

Table 6.2.2 : Model parameters obtained by Temple [105]

He also proposed the more general empirical model:

$$P_{ND}(x) = \frac{1+\exp\left[-\sum_i \alpha_i x_i^*\right]}{1+\exp\left[\sum_i \alpha_i \left[x_i - x_i^*\right]\right]} \qquad 6.2.1.14$$

with 2n constants α_i and x_i^*, and x_i a vector of n size-related variables.

Berens and Hovey [106] fitted a variety of models on surface cracks on aircraft data tested by eddy current inspections. By performing transformations to the detection probabilities and minimising the least square error of the regression curve the best fit was obtained by the logistic model:

$$P_{DN}(a) = \frac{\exp(\alpha+\beta\ell na)}{1+\exp(\alpha+\beta\ell na)} \qquad 6.2.1.15$$

where α and β are the model parameters and a is the crack length. The parameters α and β are not specified but a crack length of 25mm is reported to have a 90% chance of being detected. This model will be discussed further in Section 6.2.2.

Woo and Simonen [107] fitted a model based on the normal distribution function for data on ferritic and stainless steel. They applied the model separately on the results which were obtained for each material type and according to three teams identified as poor, good and advanced teams. It is not however clear whether this classification is based on team performance under identical UT procedures. The function is dependent on the crack depth to pipe wall thickness ratio z/t and is of the form:

$$P_{DN}(x) = \Phi(x) = \int_{-\infty}^{x} \frac{1}{\sqrt{2\pi}} e^{-t^2/2} \, dt \qquad 6.2.1.16$$

$$\text{with } x = \alpha + \beta\ell n \left[\frac{z}{t}\right]$$

The parameters α and β are given in Table 6.2.3 below

Team	Material	
	Ferritic Steel	Stainless Steel
Poor	a = 0.432 β = 0.163	α = 0.240 β = 1.485
Good	α = 1.750 β = 0.583	α = 1.526 β = 0.533
Advanced	α = 3.630 β = 1.106	α = 3.630 β = 1.106

Table 6.2.3: Model Parameters Obtained by Woo and Simonen [107]

Bokalrud and Karlsen [76] suggested the use of the normal distribution in relation to the echo height. From work involving the ultrasonic examination of 70m of steel butt welds by twelve operators, they observed that the logarithms of the echo height for the same defect size are normally distributed with σ = 0.693 (6 DB). By

assuming that the echo amplitude increases linearly with the height of the defect they proposed a detection model as a function of the reference level:

$$Pr[E>Eo] = \int_{\ell nE_o}^{\infty} \frac{1}{\sigma\sqrt{2\pi}} \exp - \left\{ [\ell nE_o - (\ell nx + \ell n\mu)]^2 / 2\sigma^2 \right\} \qquad 6.2.1.17$$

where E_o = reference level

x = defect size corresponding to the echo height E

μ = constant ; $E = \mu x$

Differences in detection efficiencies within defect types and operators are also highlighted in the acceptance curves (probability of non-detection) presented by Forli and Pettersen [108,109]. In particular, Figure 8 of Ref. [109] reveals a roughly constant 60% difference in detection efficiency between operators over all defect heights.

The plate inspection steering committee (PISC) has recently published results of a more detailed programme (Phase 2) [110] in which the influences of several factors such as: recording level, scanning surface, defect category, defect orientation, complex and advanced testing procedures in addition to those in the spirit of ASME XI [111] are investigated. The results of this study are given and discussed in detail in the PISC II Report No. 5 [110]. A range of conclusions were reached of which the most important are:

- Reduction of the recording threshold from 50% to 20% DAC increases the detection rate by as much as 25% [Fig. 5.7, Ref. [110]] but no significant improvement is observed by a further reduction.

- Procedures in the spirit of ASME XI appear to perform better if a 70% longitudinal angle probe is added, either in the simple echo technique or with dual beam.

- Defect category was the most important parameter which dominated the performance of the NDE programme. Smooth cracks with sharp edges (fatigue cracks) were the most difficult to detect whereas small volumetric defects (slag inclusions and porosity) gave on average stronger indications. Figs. 9.10 and 9.11 of Ref. [110] contain plots for the regression curves of defect detection probabilities versus defect height for the two categories with ranges from 10 to 30mm for the former and up to 5mm for the latter. The slopes of the two

lines estimated from the figures were found to be $0.025mm^{-1}$ and $0.25mm^{-1}$ respectively, using the best results from each team (Fig. 9.10) and $0.025mm^{-1}$, $0.043mm^{-1}$ for the group of procedures in the spirit of ASME with 20% DAC (Fig. 9.11).

- Inspection through the unclad surface showed that defects near to the clad side are difficult to detect. The most difficult case for detection was the fatigue crack defect category of depth 25mm or more, situated near to the internal surface.

The results of these programmes are discussed further in Section 6.2.2.

6.2.2 Applications of Binary Regression Models

The results from the various non-destructive examination programmes reviewed in Section 6.2.1 revealed many of the factors which influence the performance of non-destructive examination techniques. These factors are obviously not exhaustive, but the influence of several of them has been well established. The performance of the various programmes in terms of detection probabilities has been shown to vary, and the same models when applied on separate occasions give significantly different results (see Section 6.2.1).

The logistic, probit and complementary log-log models have been applied to two main categories of defect data, mainly on aluminium (see Temple [105]) and steel specimens (see PVRC [102], PISC I [101], and PISC II [110]).

The modelling and performance of the PVRC and PISC I programmes have been discussed extensively by Townend [12]. The results from these programmes together with the most recent findings of the PISC II project are used here again to fit the models of Section 6.1.2. The model parameters estimated by the method of M.L.E. together with their standard errors are shown in Tables 6.2.2.1 to 6.2.2.4. The deviance from each fit when compared with the appropriate chi-squared distribution shows that none of the models can be rejected. Closer fits were obtained when the defect depth is replaced by its natural logarithm (modified models), with the exception of the PISC II results where the statistic is lower for the non-transformed depth. The detection probabilities from the modified models are plotted as a function of defect depth and are shown respectively in Figs. 6.2.2.1 to 6.2.2.3.

Comparison of Figs. 6.2.2.1 and 6.2.2.2 shows that the logistic and probit detection models are closely similar for each of the four data sets. However, the

FIGURE 6.2.2.1 THE LOGISTIC AND OTHER DETECTION MODELS

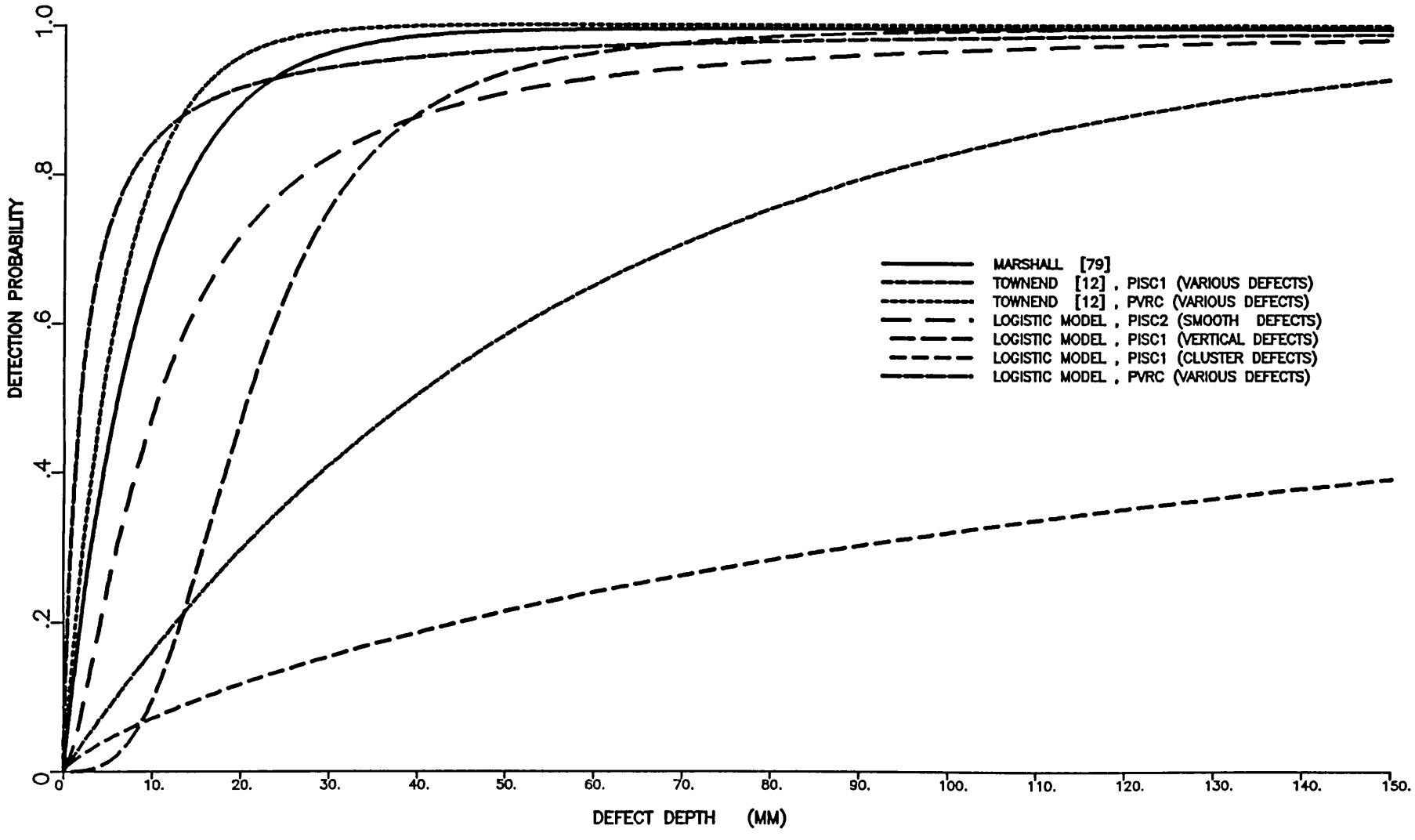


FIGURE 6.2.2.2 THE PROBIT AND OTHER DETECTION MODELS

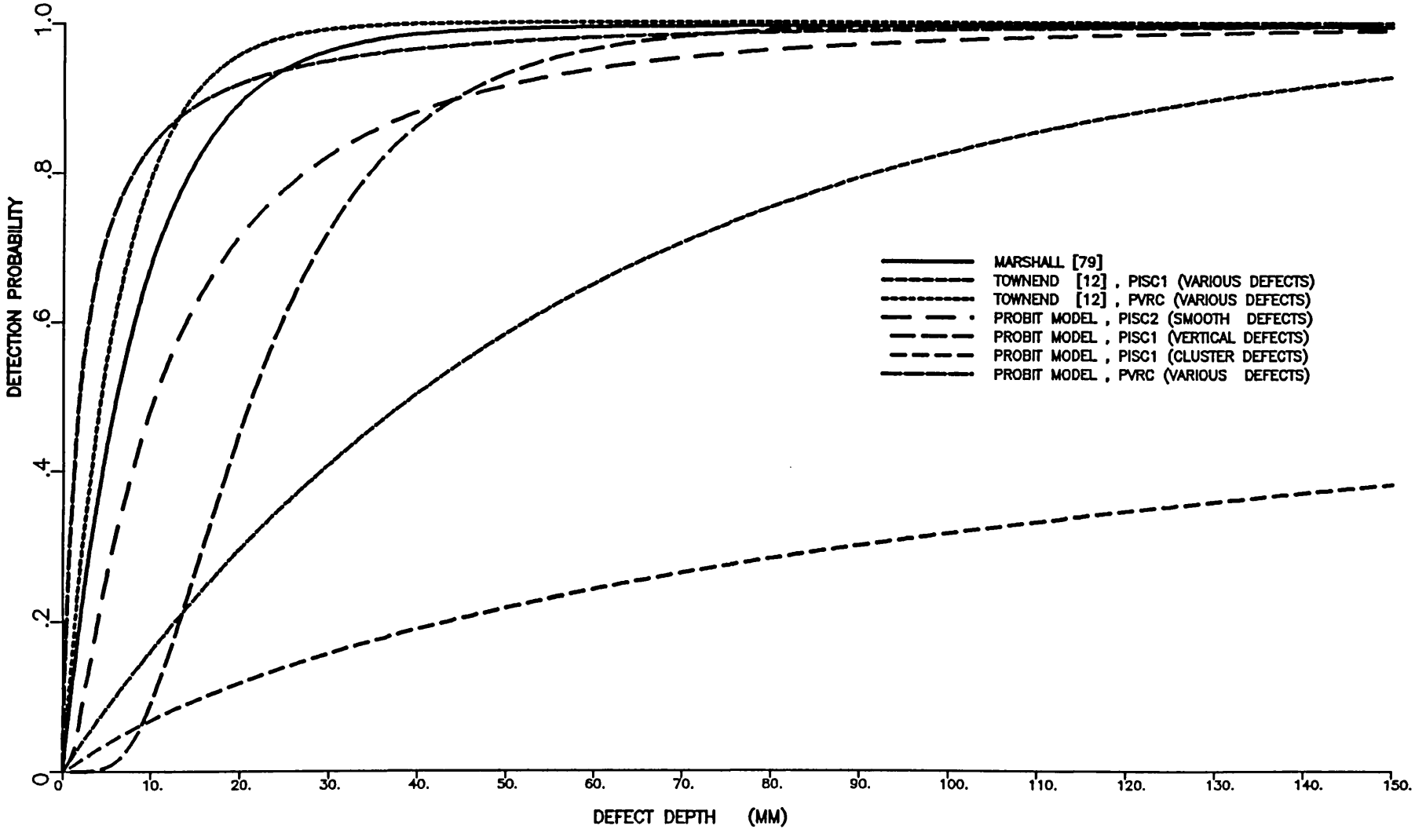
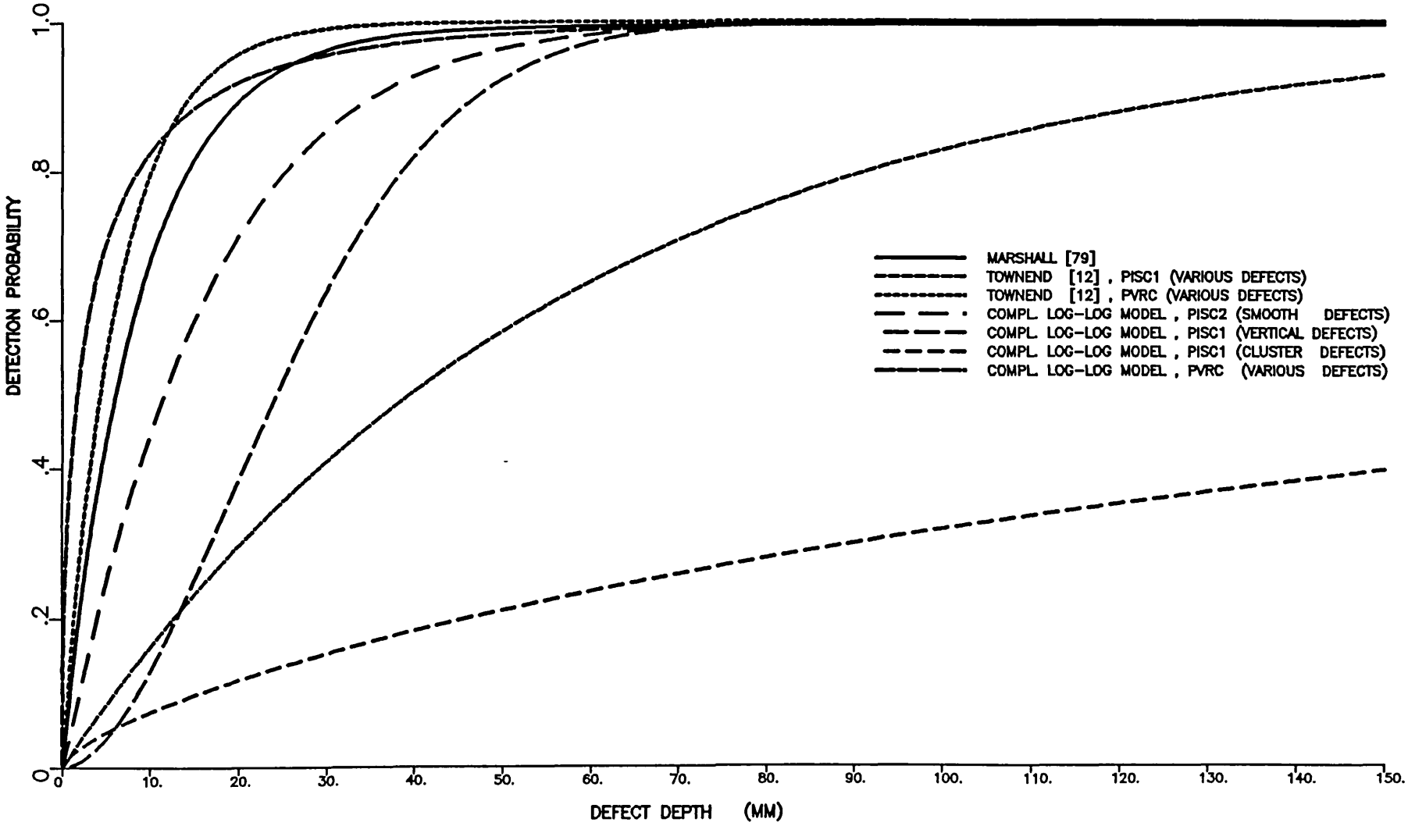


FIGURE 6.2.2.3 THE COMPLEMENTARY LOG–LOG AND OTHER DETECTION MODELS



complementary log-log model (Figs 6.2.2.3) shows the detection probability approaching the value of 1.0 more rapidly that the other models for two of the data sets.

These figures also show the exponential models suggested by Marshall (see Section 6.2.1, Eqn. 6.2.1.2) and Townend (see Section 6.2.1, Eqns. 6.2.1.7 and 6.2.1.8). It can be seen that for the PVRC data the models proposed in this report predict somewhat higher detection probabilities for small defects (about 10mm deep) as compared with the exponential model proposed by Townend. For higher values of defect depth this trend reverses. It can also be seen that the lowest detection probabilities of all are observed for the cluster defects of the PISC I programme. Vertical defects from the same programme are comparatively easy to detect. Townend has merged these data from the PISC I programme into one inhomogeneous category. His detection model for this data lies, not unexpectedly, between the other two curves.

Data from the PISC II programme for fatigue cracks (the type of defect which was the most difficult to detect) show higher detection probabilities than the most easily detected defects in the PISC I programme (vertical defects). Finally, it can be seen that the detection probabilities predicted by the Marshall model are in reasonably close agreement with those from the PVRC programme.

Temple [105] reports some data on defect depth and length from ultrasonic inspection of aluminium alloy specimens. The results are reported to be due to Magistrali *et al* and be quite old, but are used here as an illustration.

The logistic, probit and complementary log-log models were fitted to both dimensions. The model parameters together with estimates of their standard errors are given in Tables 6.2.2.5 and 6.2.2.6. The deviance of each fit when compared with the chi-squared distribution on 6 d.f. shows that the modified models provide the best fit to the data. The only exception is with the complementary log-log model which can only be accepted at the 0.001 significance level. The predicted detection probabilities under the models are plotted against defect depth and length and are shown in Figures 6.2.2.4 and 6.2.2.5 respectively. The same figures also show Temple's function (see Section 6.2.1, Eqn. 6.2.1.7), and the log-normal (see Section 6.2.1, Eqn. 6.2.1.12) and Weibull (see Section 6.2.1 Eqn. 6.2.1.13) models proposed by Harris [77] and fitted by Temple [105]. From both figures it can be seen that the modified logistic, probit and complementary log-log models agree very closely over the entire range, whereas the rest of the models differ significantly. Particularly important is the behaviour of the Weibull model, which in both cases changes very slowly for very small values of the defect dimension, rising abruptly over a short

FIGURE 6.2.2.4 COMPARISON OF VARIOUS DETECTION MODELS BASED ON DATA REPORTED BY TEMPLE [105]

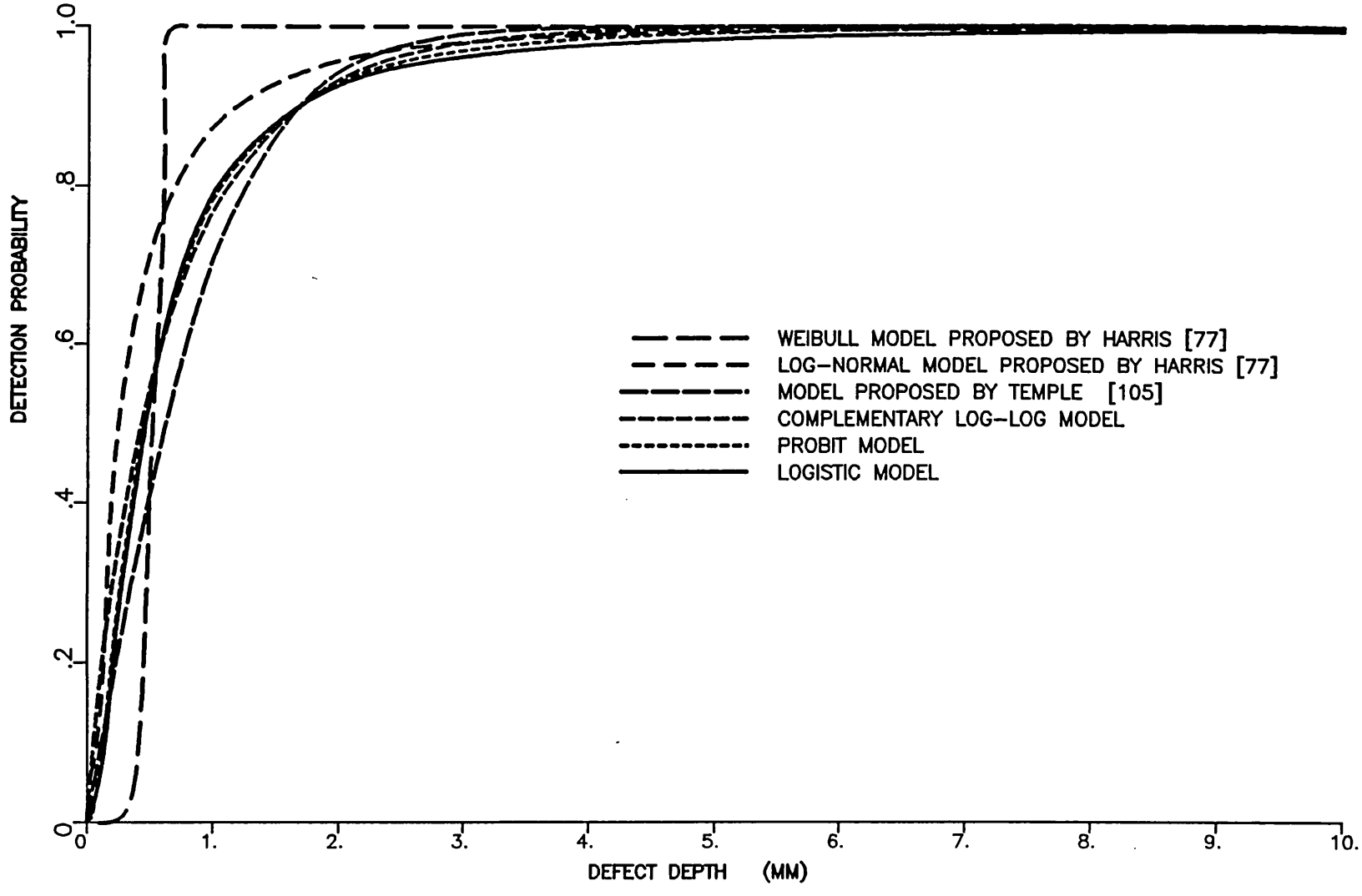
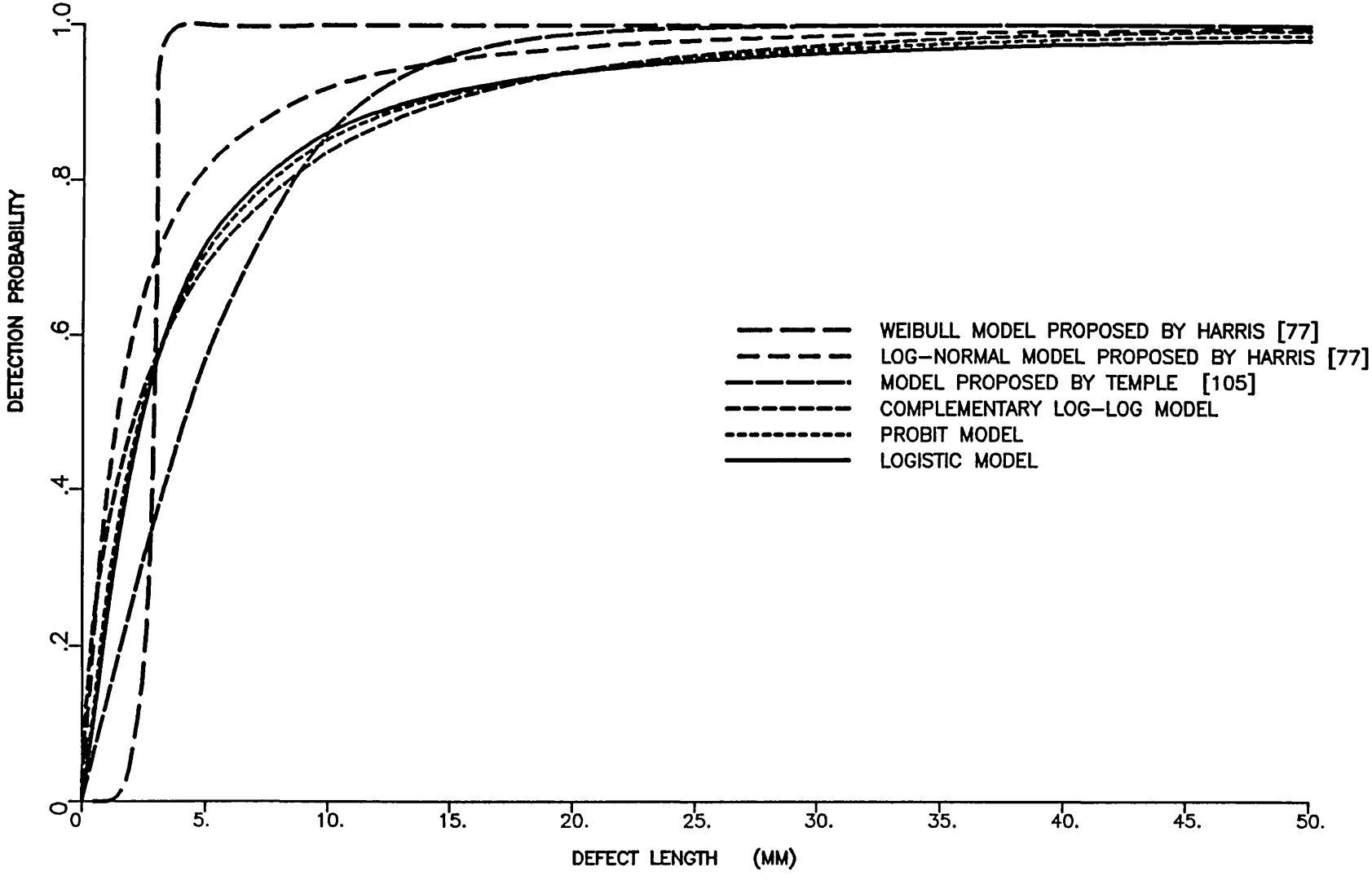


FIGURE 6.2.2.5 COMPARISON OF VARIOUS DETECTION MODELS BASED ON DATA REPORTED BY TEMPLE [105]



range to reach the value of 1.0 quite rapidly.

There are very few examples of sets of data which give more than one characterising variable for each defect, or to more than one inspection technique. The data reported by PISC I provide information on the three defect dimensions x, y, z. [The defect dimension y corresponds to the size of the defect in the through thickness direction; the other two dimensions were taken parallel to the sides of the plate]. The generalised forms of the functions 6.1.2.1, 6.1.2.2 and 6.1.2.3 were fitted by M.L.E. in a stepwise manner and the goodness of fit statistic has shown no significant improvement by the introduction of the additional parameters x and y. It is important to mention, however, that the statistics have shown greater influence of the y rather than the x dimension but the additional contribution of this parameter was still found to be statistically insignificant. Detailed results are presented in Tables 6.2.2.7 to 6.2.2.12.

This particular analysis reinforces the usefulness of the generalised models in modelling detection efficiencies but some of the findings are not particularly surprising. It is reasonable to assume that the chance of detecting a defect of given size (z) will also depend on the other dimensions of the defect, since these will affect the chances of the ultrasound beam being reflected. However, in the case of the data examined, all the defects were relatively long and hence small changes in length are relatively unimportant.

Finally, in this section, mention should be made of the characteristics of the new detection probability models when fitted to previous data sets (e.g. Figures 3.2.4.1 to 3.2.4.5) when compared with earlier models. From Figure 3.2.4.5 it can be seen that for medium length defects (e.g. 20mm) the probability of non-detection predicted by the models is not insignificant. The other figures show similar trends. Since these new models have been shown to fit the data better than previous models, it must be concluded that previous models may be unconservative in their predictions for the probability of detection of defects of a moderate size. This could have important practical implications.

6.2.3 Discussion

The simplest function that one could consider in modelling detection efficiencies is of the form:

$$\pi_i = \sum_{j=1}^{k} x_{ij}\,\beta_j \qquad i=1,\ldots,N \qquad 6.2.3.1$$

where the relevant probabilities are estimated by the observed proportions $p_i=r_i/n_i$. Under this model the observed data are assumed to be linearly related to the concomitant variable x_{ij}.

Application of ordinary least squares (OLS) is in most cases the convenient way of estimating the unknown parameters β. However, this approach is valid only under the strong assumption that the independent random variables p_i are normally distributed with constant variance; but the variance of our observations r_i/n_i is not constant and varies with the mean π, being zero at $\pi=0$ or 1 and rising to a maximum at $\pi=0.5$, (see Section 6.1.1). Another drawback, probably the most serious, arises from the restriction that the condition

$$0 \leqslant \pi_i \leqslant 1 \qquad 6.2.3.2$$

imposes on the predicted values. In fact, it is very likely that the least squares estimates, obtained by minimising the sum of squares, could lead to fitted values which do not comply with the restrictions of 6.2.3.2. An approximate solution could be obtained by using weighted regression in which each value of p_i is weighted in inverse proportion to its variance.
An even more accurate method is to use maximum likelihood estimation, the basis of generalised linear models (see Cox [31], McCullagh and Nelder [86] which allows problems to be tackled where variances of observations are functions of the means. Further advantages of such methods are that M.L.E. can be performed even when there is a single response i.e. $n_i=1$ for each parameter combination $x_{ij}\beta_j$. Also goodness of fit statistics are readily available and for the binomial distribution the log-likelihood ratio statistic D is completely determined. This enables the assessment of the overall goodness of fit of the model as well as the assessment of the relative contributions from various parameters. Finally, residuals can be calculated to check for outlying observations and so on.

In addition to the problem of non constant variance is the question of linearity. As was pointed out in the introduction to Section 6.1 , linear relations are very unlikely to occur since the proportions range between the value of 0 and 1 and changes in any of the concominant variables at the extreme ends are unlikely to produce much change in the proportion. The inclusion of polynomials in one or more variables (see PISC I [101]) could be an alternative approach, provided allowances are made for the above problems, but such considerations lack interpretation and restrict the validity of the model to other situations. The three models which have been proposed have the purpose of linearising the observed proportions but with no effect in stabilising the variance. For example, the logistic model has approximate variance

$$\frac{1}{n_i \pi_i (1-\pi_i)}$$

and application of the ordinary least squares to the transformed proportions for estimating the unkown parameters is clearly incorrect.

The probit and/or the logistic models as a function of one variable (depth or length) have been suggested by several authors, see for example Berens and Hovey [106], Woo and Simonen [107], Harris [77]. Berens and Hovey report that in addition they have fitted the Weibull and modified Weibull functions but it is not obvious whether their model is the one proposed by Harris [77] or the complementary log-log model (Eqn. 6.1.2.3, Section 6.1.2).

It must be emphasised that in addition to the correct method of estimating the parameters, the three models which have been proposed are new with respect to possible generalisations. The vector $\underline{x}$, for example, may include a number of independent covariate variables both quantitative or qualitative such as NDE operator, DAC, defect type, specimen thickness, length, depth, width, area, ultrasonic beam diameter etc. The only other general model which has been proposed is that due to Temple [105]. Furthermore, it must be pointed out that presenting such generalised models does not imply loss of the parsimony of the function since it has been demonstrated experimentally (see Section 6.2.1) that the efficiency of defect detection is indeed a function of a number of variables, the influence of some can be controlled. This has been clearly established. In addition to such demonstrations, Duffresne [104] has shown mathematically that there exists a high association between detection probability and both defect depth and length (see Section 6.2.1, Fig. 6.2.1). The modelling of these trends by any of the general modes which have been proposed is novel.

Table 6.2.2.1 : Model parameters for PISC I data [101] Vertical Defects

Defect Dimension	Model	α	β	s e (α)	s e (β)	D_4	Notes
z	I	-2.721	0.105	0.427	0.018	3.68	Depth of six vertical defects ranging from 11 to 236mm. Ultrasonic inspection with probe angles 45° and 60°, frequency 2MHz to 3MHz and recording level 50% DAC, scanning from one side.
	II	-1.612	0.060	0.234	0.009	3.28	
	III	-2.241	0.062	0.330	0.009	3.93	
ℓnz	I	-9.317	3.067	1.401	0.483	2.51	
	II	-5.374	1.754	0.700	0.235	2.09	
	III	-6.177	1.820	0.793	0.230	2.44	

Table 6.2.2.2 : Model Parameters for PISC I data [101] Cluster Defects

Defect Dimension	Model	α	β	s e (α)	s e (β)	D_4	Notes
z	I	-2.189	0.012	0.319	0.004	3.00	Depth of six cluster defects ranging from 11 to 148mm. Ultrasonic inspection with probe angles 45° and 60°, frequency 2MHz to 3MHz and recording level 50% DAC, scanning from one side.
	II	-1.302	0.007	0.173	0.002	2.90	
	III	-2.212	0.011	0.293	0.003	3.11	
ℓnz	I	-4.365	0.783	0.953	0.243	2.56	
	II	-2.503	0.440	0.525	0.138	2.69	
	III	-4.153	0.692	0.842	0.208	2.51	

Table 6.2.2.3 : Model parameters for data published by PVRC [102]

Defect Dimension	Model	α	β	s e (α)	s e (β)	D_5	Notes
z	I	-0.007	0.131	0.586	0.088	6.99	Specimen 201 unclad plate scanned both sides by ultrasonics. Seven defects of several defect types ranging from 0.76 to 20.32 deep. Probes had operating frequencies of 2.25 MHz, scanning was done at 45° and recording level was set at 10% DAC
	II	0.056	0.067	0.345	0.045	7.22	
	III	-0.211	0.053	0.340	0.036	7.55	
ℓnz	I	-0.670	1.021	0.741	0.466	4.10	
	II	-0.382	0.594	0.437	0.262	4.23	
	III	-0.670	0.533	0.492	0.263	4.72	

Table 6.2.2.4 : Model parameters for data published by PISC II [110]

Smooth cracks with sharp edges (fatigue cracks)

Defect Dimension	Model	α	β	s e (α)	s e (β)	D_5	Notes
z	I	-1.674	0.124	0.441	0.024	5.93	Seven smooth cracks with sharp edges ranging from 3 to 29mm on plate no.3. Ultrasonic inspection as defined in ASME Section V, Article 4, with the recording level set at 20% of the DAC curve
	II	-1.013	0.075	0.261	0.014	6.05	
	III	-1.491	0.078	0.332	0.015	6.65	
ℓnz	I	-3.529	1.489	0.874	0.319	8.29	
	II	-2.063	0.879	0.486	0.177	8.49	
	III	-3.002	1.077	0.668	0.227	6.93	

Table 6.2.2.5 : Model parameters for data reported by Temple [105]

Defect Dimension	Model	α	β	s e (α)	s e (β)	D_6	Notes
a	I	-0.573	1.654	0.189	0.163	8.98	Depth of eight defects on aluminium alloy detected by ultrasonics. Various defect types ranging from 0.2 to 3.5mm deep
	II	-.0225	0.869	0.109	0.084	13.60	
	III	-0.383	0.670	0.100	0.068	21.47	
ℓnz	I	1.335	1.730	0.089	0.155	5.97	
	II	0.786	0.994	0.050	0.086	4.82	
	III	0.382	0.885	0.046	0.080	4.71	

Table 6.2.2.6 : Model parameters for data reported by Temple [105]

Defect Dimension	Model	α	β	s e (α)	s e (β)	D_6	Notes
a	I	-0.081	0.147	0.145	0.015	57.34	Length of eight defects on aluminium alloy detected by ultrasonics. Various defect types ranging from 0.5 to 37.5mm long.
	II	0.088	0.070	0.083	0.007	70.39	
	III	-0.099	0.050	0.075	0.005	85.28	
ℓna	I	-1.177	1.311	0.203	0.102	10.75	
	II	-0.640	0.736	0.119	0.055	13.72	
	III	-0.855	0.632	0.127	0.053	21.68	

Table 6.2.2.7 : Model parameters of the LOGIT function for the PISC I Data [Vertical Defects]

Terms (T)	α	β	γ	δ	s.e.(α)	s.e.(β)	s.e.(γ)	s.e.(δ)	D_{6-T-1}
X_1	-0.647	0.060	-	-	0.227	0.011	-	-	78.55
Y_1	-1.085	0.013	-	-	0.297	0.004	-	-	52.83
Z_1	-2.721	0.105	-	-	0.427	0.018	-	-	3.68
Y_1+Z_1	-2.777	0.002	0.101	-	0.481	0.005	0.019	-	3.38
X_1+Z_1	-2.720	-0.004	0.105	-	0.464	0.026	0.108	-	3.68
$X_1+Y_1+Z_1$	-2.685	-0.023	0.005	0.096	0.559	0.041	0.009	0.021	3.05
ℓnX_1	-0.733	0.554	-	-	0.279	0.118	-	-	100.20
ℓnY_1	-6.719	1.618	-	-	1.282	0.311	-	-	61.71
ℓnZ_1	-9.317	3.067	-	-	1.401	0.483	-	-	2.51
$\ell nY_1+\ell Z_1$	-10.37	0.360	2.932	-	2.305	0.544	0.521	-	2.01
$\ell nX_1+\ell nZ_1$	-9.428	0.072	3.069	-	1.472	0.221	0.491	-	2.40
$\ell nX_1+\ell nY_1+\ell nZ_1$	-11.75	-0.280	0.963	2.718	3.844	0.483	1.270	0.618	1.66

Table 6.2.2.8 : Model parameters of the Probit function for the PISC I Data [Vertical Defects]

Terms (T)	α	β	γ	δ	s.e.(α)	s.e.(β)	s.e.(γ)	s.e.(δ)	D_{6-T-1}
X_1	-0.405	0.038	-	-	0.139	0.006	-	-	76.74
Y_1	-0.644	0.007	-	-	0.170	0.002	-	-	52.08
Z_1	-1.612	0.060	-	-	0.234	0.009	-	-	3.28
Y_1+Z_1	-1.629	0.0008	0.059	-	0.253	0.002	0.010	-	3.13
X_1+Z_1	-1.608	-0.0006	0.060	-	0.252	0.014	0.009	-	3.28
$X_1+Y_1+Z_1$	-1.575	-0.011	0.002	0.056	0.292	0.022	0.004	0.011	2.90
ℓnX_1	-0.468	0.351	-	-	0.173	0.070	-	-	99.55
ℓnY_1	-4.055	0.975	-	-	0.689	0.164	-	-	59.97
ℓnZ_1	-5.374	1.754	-	-	0.700	0.235	-	-	2.09
$\ell nY_1+\ell Z_1$	-5.922	0.188	1.683	-	1.142	0.276	0.263	-	1.58
$\ell nX_1+\ell nZ_1$	-5.437	0.042	1.755	-	0.733	0.121	0.240	-	1.97
$\ell nX_1+\ell nY_1+\ell nZ_1$	-6.519	-0.138	0.460	1.582	1.789	0.253	0.607	0.318	1.29

Table 6.2.2.9 : Model parameters of the complementary log-log function for the PISC I data [Vertical Defects]

Terms (T)	α	β	γ	δ	s.e.(α)	s.e.(β)	s.e.(γ)	s.e.(δ)	D_{6-T-1}
X_1	-0.898	0.042	-	-	0.176	0.006	-	-	71.45
Y_1	-1.051	0.007	-	-	0.191	0.001	-	-	50.76
Z_1	-2.241	0.062	-	-	0.330	0.009	-	-	3.93
Y_1+Z_1	-2.241	0.00003	0.062	-	0.332	0.002	0.009	-	3.93
X_1+Z_1	-2.210	-0.004	0.062	-	0.332	0.015	0.008	-	3.87
$X_1+Y_1+Z_1$	-2.148	-0.016	0.001	0.059	0.384	0.034	0.003	0.011	3.70
ℓnX_1	-0.976	0.407	-	-	0.215	0.074	-	-	96.94
$\ell nY1$	-4.541	0.984	-	-	0.694	0.156	-	-	56.49
ℓnY_1	-6.177	1.820	-	-	0.793	0.230	-	-	2.44
$\ell nY_1+\ell Z_1$	-6.516	0.125	1.766	-	1.091	0.247	0.261	-	2.15
$\ell nX_1+\ell nZ_1$	-6.241	0.049	1.819	-	0.824	0.137	0.237	-	2.32
$\ell nX_1+\ell nY_1+\ell nZ_1$	-6.825	-0.116	0.299	1.690	1.516	0.353	0.590	0.345	2.04

Table 6.2.2.10 : Model Parameters of the Logit Function for the PISC I Data (Cluster Defects]

Terms (T)	α	β	γ	δ	s.e.(α)	s.e.(β)	s.e.(γ)	s.e.(δ)	D_{6-T-1}
X_1	-2.748	0.047	-	-	0.519	0.016	-	-	3.57
Y_1	-2.659	0.020	-	-	0.496	0.007	-	-	6.10
Z_1	-2.189	0.012	-	-	0.319	0.004	-	-	3.00
Y_1+Z_1	-1.325	-0.030	0.028	-	0.740	0.024	0.013	-	1.47
X_1+Z_1	-2.536	0.023	0.008	-	0.514	0.025	0.006	-	2.10
$X_1+Y_1+Z_1$	-1.565	0.007	-0.026	0.024	1.280	0.031	0.031	0.021	1.41
ℓnX_1	-3.081	0.535	-	-	0.818	0.253	-	-	7.23
ℓnY_1	-6.490	1.261	-	-	1.989	0.492	-	-	6.87
ℓnZ_1	-4.365	0.783	-	-	0.953	0.243	-	-	2.56
$\ell nY_1+\ell Z_1$	-3.652	-0.304	0.915	-	2.255	0.877	0.459	-	2.44
$\ell nX_1+\ell nZ_1$	-4.369	0.044	0.749	-	0.956	0.294	0.332	-	2.53
$\ell nX_1+\ell nY_1+\ell nZ_1$	-3.645	-0.002	-0.306	0.918	2.506	0.327	0.988	0.646	2.44

Table 6.2.2.11 : Model Parameters of the Probit Function for the PISC I Data (Cluster Defects]

Terms (T)	α	β	γ	δ	s.e.(α)	s.e.(β)	s.e.(γ)	s.e.(δ)	D_{6-T-1}
X_1	-1.551	0.025	-	-	0.263	0.009	-	-	3.94
Y_1	-1.563	0.012	-	-	0.278	0.004	-	-	6.19
Z_1	-1.302	0.007	-	-	0.173	0.002	-	-	2.90
Y_1+Z_1	-0.843	-0.016	0.015	-	0.421	0.013	0.007	-	1.51
X_1+Z_1	-1.459	0.011	0.005	-	0.261	0.013	0.004	-	2.15
$X_1+Y_1+Z_1$	-0.937	0.003	-0.014	0.014	0.683	0.017	0.017	0.011	1.48
ℓnX_1	-1.692	0.270	-	-	0.401	0.127	-	-	8.03
ℓnY_1	-3.706	0.710	-	-	1.139	0.285	-	-	7.01
ℓnZ_1	-2.503	0.440	-	-	0.525	0.138	-	-	2.69
$\ell nY_1+\ell Z_1$	-2.279	-0.090	0.476	-	1.289	0.479	0.240	-	2.66
$\ell nX_1+\ell nZ_1$	-2.503	0.021	0.424	-	0.525	0.155	0.186	-	2.68
$\ell nX_1+\ell nY_1+\ell nZ_1$	-2.311	0.010	-0.077	0.463	1.395	0.170	0.526	0.329	2.65

Table 6.2.2.12 : Model Parameters of the Complementary Log-Log Function for the PISC I Data [Cluster Defects]

Terms (T)	α	β	γ	δ	s.e.(α)	s.e.(β)	s.e.(γ)	s.e.(δ)	D_{6-T-1}
X_1	-2.778	0.044	-	-	0.489	0.015	-	-	3.33
Y_1	-2.638	0.108	-	-	0.442	0.006	-	-	6.03
Z_1	-2.212	0.011	-	-	0.293	0.003	-	-	3.11
Y_1+Z_1	-1.397	-0.029	0.025	-	0.661	0.002	0.012	-	1.46
X_1+Z_1	-2.568	0.023	0.006	-	0.489	0.023	0.005	-	2.09
$X_1+Y_1+Z_1$	-1.667	0.008	-0.024	0.021	1.195	0.029	0.029	0.020	1.39
ℓnX_1	-3.126	0.513	-	-	0.785	0.240	-	-	7.54
ℓnY_1	-6.096	1.133	-	-	1.725	0.421	-	-	6.74
ℓnZ_1	-4.153	0.692	-	-	0.842	0.208	-	-	2.51
$\ell nY_1+\ell Z_1$	-3.345	-0.357	0.856	-	1.972	0.795	0.426	-	2.31
$\ell nX_1+\ell nZ_1$	-4.166	0.050	0.655	-	0.849	0.275	0.289	-	2.47
$\ell nX_1+\ell nY_1+\ell nZ_1$	-3.317	-0.008	-0.368	0.867	2.241	0.309	0.909	0.608	2.31

6.3 Defect Sizing

The measurement of defect dimensions by a non-destructive examination device requires skill and is governed by a large number of uncertainties and limitations, some of which have been discussed in previous sections. Probe movement techniques [112] such as 6DB drop, 20DB, maximum amplitude, etc. are extensively employed for sizing flaws. Accuracies by which such measurements are made are valid only for particular categories of defect, but nevertheless information about the tendency to undersize or oversize defects can be obtained by examining trends between measured and actual sizes or means and standard deviations of sizing errors (measured size - actual size), when data are available.

Sizing errors can have serious consequences since, if insignificant defects are overestimated, this could result in unnecessary repairs causing financial losses and possibly lead to the introduction of further defects by the repair process. Conversely, if insignificant defects are overlooked this could have serious effects on overall structural integrity.

6.3.1 Literature Review

Based on surface cracks detected and sized by ultrasonics on aluminum specimens, Tank [78] suggested the calibration curve

$$E[\text{Actual depth}|\text{measured depth}] = 0.0592 + 0.839\ \text{Measured depth}$$

for defect sizes up to 0.2in., with a normally distributed calibration error of zero mean and s.d. of 0.0342in.. Depth measurements were made by longitudinally scanning and observing the position at which the amplitude of the reflected signal dropped off to 50% of the maximum amplitude attained in passing the defect.

On 50% DAC the results from the PISC I program showed that on average small volumetric defects of depth from 1-10mm were overestimated whereas planar defects ranging from 11-236mm in size were underestimated. These conclusions were based on mean values for the ratio of the measured to actual size of 1.38 and 0.49 respectively.

Burdekin and Townend [113] have also noted that ultrasonic sizing errors (with 6DB drop) for defect height ranging from 4-47mm in steel railway rail are dependent on the actual defect size. They observed that small defects were overestimated and large defects underestimated with a changeover at about 25mm. They modelled this trend

with a linear regression curve of sizing error versus actual defect sizes:

Error = 13.86 -0.54 Actual depth

Errors about this line were normally distributed with a s.d. of 6.3mm.

Based on a program carried out at the Welding Institute [114, 115, 116] Mudge and Williams [117] observed that UT sizing errors were also normally distributed but independent of the actual defect size. They noted that the depth of planar defects could be underestimated by as much as 5 to 6mm and non-planar defects by 7 to 8mm. For a 20DB drop sizing technique under laboratory conditions, the mean error for planar defects was -1.7mm and non-planar defects -2.3mm. The corresponding s.d. for these values were calculated to be 1.9mm and 2.6mm respectively. Measurements were undertaken on defect sizes ranging from 1.5mm to 12mm and 1mm to 7mm respectively for planar and non-planar defects.

The UKAEA Defect Detection Trials [118, 119, 120] using several probe movement techniques were reported by Bowker *et al* [119] to show a mean sizing error of -1.0mm and s.d. of 2.5mm.

Kato *et al* [121] estimated on a 6DB drop a mean error of +0.5mm with a s.d. of 3.2mm. Their evaluation was made on butt welds in splices containing several defect categories ranging from about 2 to 20mm in depth (Fig. 7, Ref. [121]).

The results from the PISC II project [110] showed systematic trends for undersizing of planar defects and oversizing volumetric defects. These trends were characteristic of the dependence of sizing errors on the defect depth where small defects were generally oversized and large defects were on average undersized. The s.d. of the mean sizing errors as a function of defect size range for the ASME 20% DAC procedure are shown below in Table 6.3.1.1, and were extracted from Figure 9.6 and Table 9.3 of Ref. [110].

Table 6.3.1.1 : Mean sizing errors and s.d. for categories of defects in plate no. 3 from Ref. [110]

Defect Category	Mean Error (mm)	St. Dev. (mm)
From 3 to 10mm	+12	7
From 105 to 25mm	-1	7
From 25.5 to 80mm	-4	11

6.3.2 Analysis of Data on Fatigue Cracks in Tubular Welded Joints

The Department of Energy has published data on fatigue cracks obtained from four typical tubular welded joints [122]. The dimensions of the cracks are presented here in Table 6.3.2.1 and were extracted from Table 2, Section 6.4 and Table 4, Section 7.2.2 of Ref. [122].

Table 6.3.2.1: Actual and predicted dimensions of fatigue cracks from Ref. [122]

Actual Depth (mm) (Sectioning)	Predicted Depth (mm) (Ultrasonics)	Actual Length (mm) (Sectioning)	Predicted Length (mm) (Ultrasonics)
8.7	8.8	222.5	255
5.6	5.7	215	226
9.2	9.3	177.5	238
5.7	7.2	228.5	224
18.6	14.5	174.5	172
19.3	15.5	188.5	195
9.3	4.5*	54.5	57
7.5	7.0	56	61
12.7	12.7	366.5	95
4.2	6.0	92	365
6.7	6.1	424.5	57*

FIGURE 6.3.2.1 PREDICTED AND ACTUAL CRACK DEPTH

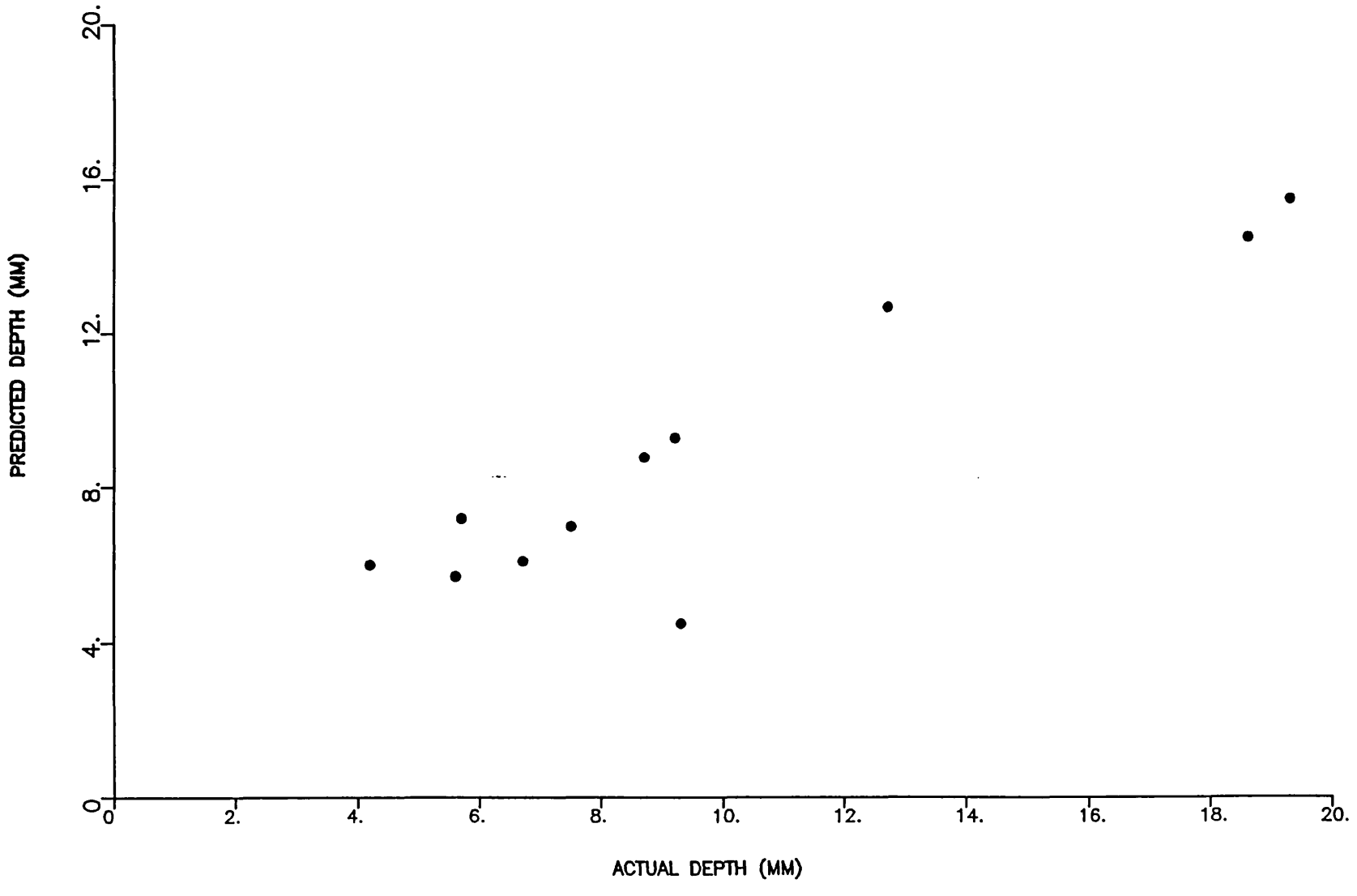


FIGURE 6.3.2.2 PREDICTED AND ACTUAL CRACK LENGTH

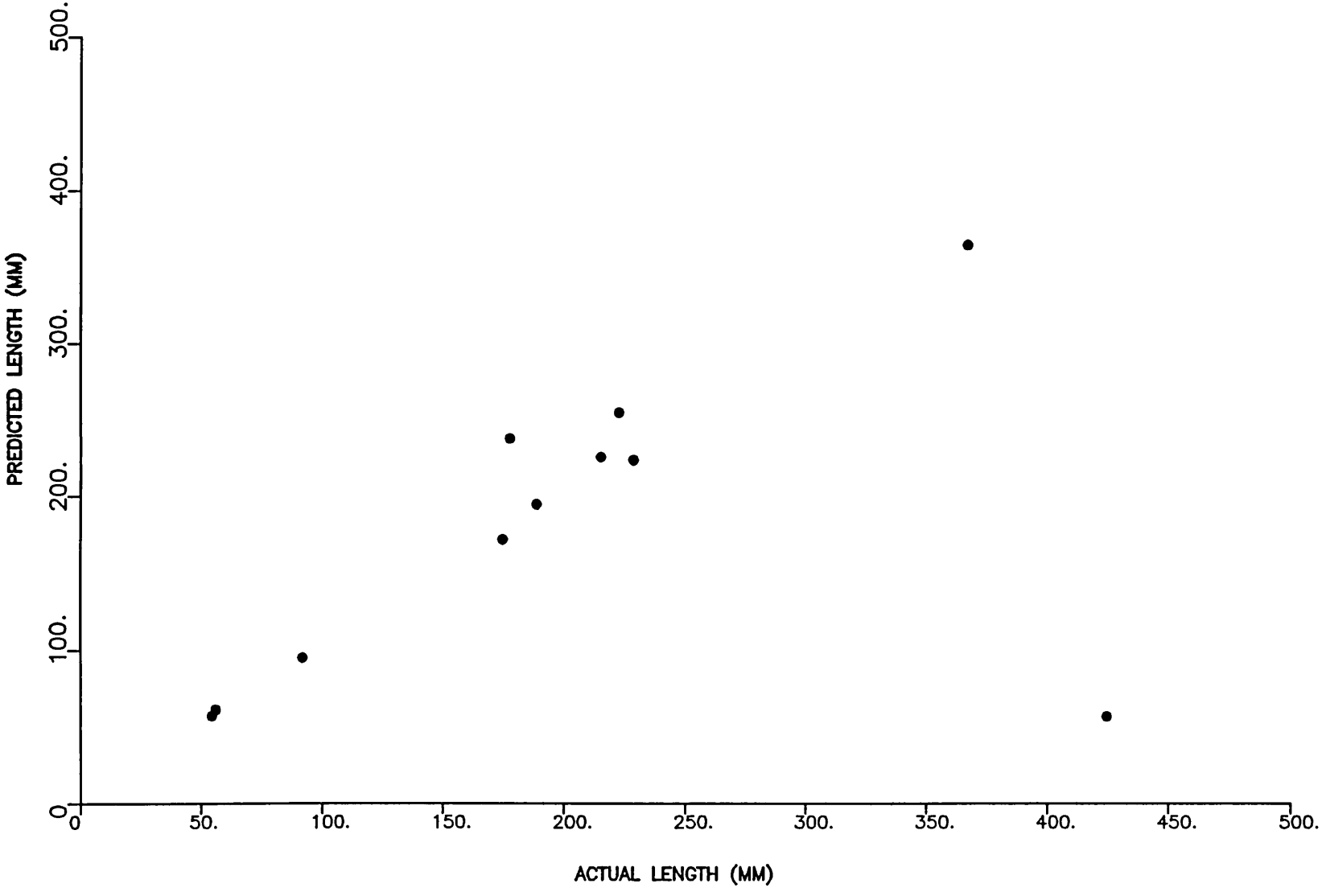


Table 6.3.2.2 : Calibration details for data of Table 6.3.2.1 Ref [65]

Regression	r.m.s	Calibration	Error mean (mm)	Error s.d. (mm)
$d_m = 2.24 + 0.68d_t$	2.64	$d_t = -3.29 + 1.47d_m$	-0.93	2.26
$\ell_m = 102.84 + 0.37\ell_t$	8964.70	$\ell_t = -277.95 + 2.70\ell_m$	-23.18	115.80
$d_m^* = 2.72 + 0.67d_t^*$	0.74*	$d_t^* = -4.06 + 1.49d_m^*$	-0.54*	1.96*
$\ell_m^* = 10.66 + \ell_t^*$	460.28*	$\ell_t^* = -10.66 + \ell_m^*$	11.25*	20.23*

It can been seen that for the case of defect depth in both cases (including and excluding the extreme observation) sizing errors are dependent on the actual defect size. Defects of depth up to about 7mm are seen to be overestimated whereas defects greater than this value to be underestimated. In the case of defect length, the most reliable case is the one which excludes the extreme observations and it is seen that in this case defects are usually overestimated.

6.3.3 Discussion

It follows from Sections 6.3.1 and 6.3.2 that there are large differences in the outcome of various experimental programmes set up to examine the reliability of techniques for sizing defects. These differences in performance are due to the fact that the data from each exercise are not directly comparable, in that different test procedures have been followed

and different material thicknesses or weld types have been studied.

Sizing errors are governed not only by the characteristics of the flaw detector and the defects themselves but also on the competence of the operator and the methods used to derive information about the defect from the signals obtained.

Comparison of the data from the various programmes show that:

- The range of defects which have been examined in each programme are different.
- Reporting levels differ between programmes.
- The number of operators used are either different or not specified.

- Various defect positions and geometries result in particular sizing problems.

- In some cases testing was done from one side of the plate and in other cases from both sides. Very often this information is not included in the description.

The data published by the Department of Energy are totally incompatible with the rest of the data since the cracks induced are all surface-breaking defects which have been detected by MPI and subsequently sized by ultrasonics. Furthermore, the definition of defect depth differs from that given in the other programmes.

Although the work details and results differ from programme to programme it can be stated that the size of small defects is usually overestimated, whereas large defects are usually underestimated (Burdekin and Townend, PISC I, PISC II). The Welding Institute study, however, showed that the size of both small planar and non-planar defects is usually underestimated.

Finally, it must be emphasised that most of these programmes were performed on artificially induced defects. Application of the results to naturally occurring defects must therefore be undertaken with care.

CHAPTER 7

CONCLUSIONS

Throughout this work conclusions or relevant discussions have been presented at the end of each chapter. They represent a rather complex pattern of effects which cannot easily be condensed further, and the reader is referred to the summary or conclusions of each relevant section for detailed information. Here only main features will be given.

General Remarks

The major part of this work has been devoted to the analysis of weld defect data base of the Hutton TLP structure.

The Hutton TLP is unusual in a number of respect. It was the first structure of the tension leg type and was therefore very much a prototype. The detailed construction of the hull of the TLP is radically different from that of the conventional type of jacket structure involving a complex arrangement of steel plating and stiffening, especially in the six nodes. The simpler pontoon sections are rather similar to the cross-section of a ship, with bulkheads, and longitudinal stiffening between cross-frames. For speed of construction the lower hull was fabricated in a number of different yards, all working to the same specifications.

Other unusual factors in the construction were the events which led up to the extensive re-NDE of the lower hull, which are briefly described in [40]. It is now clear that not only were there inadequacies in the original welding but also in the standards of the NDE which was carried out immediately following fabrication. The re-NDE which was undertaken by the main contractor at a very late stage in the construction therefore covered: some welds which had never been inspected before, other than visually, some welds which had had partial NDE, and the remaining welds which should all have received full NDE following fabrication.

An additional comment which must be made concerns the classification of defect types. Because of the very large number of NDE operators who carried out the re-examination of the lower hull, it is unlikely that there would have been complete consistency in the classification of defects. In particular, the term 'linear indication' was used to describe any defect of initially unknown origin which showed up as a linear trace on the surface of the metal during MPI. Whereas it might be expected that such indications might relate to defects of a minor nature, it has been found in

the analysis that these defects are typically deeper than those originally identified as 'cracks ' and 'non-fusion' defects. Some thought has been given to the classification of defects by Groves and Connell [24]. As far as the TLP data analysis is concerned the linear indication defects have been treated separately from the others since they have been separately identified and have different statistical characteristics.

Defect Occurrence

(1) Defect rates for welds of the same type (e.g. cruciform, tee butt, plate butt and fillet) varied considerably between different fabricators, even when other factors were apparently the same (i.e. welding process, welding position, welding procedure and percentage of weld subjected to original NDE).

(2) The influence of the amount of weld subjected to original NDE varied considerably between fabricators - in some cases the defect rate being reduced by a factor of about 100, in others hardly at all.

(3) Extremely low defect rates can be, but are not always, achieved when welds are subjected to 100% UT and MPI NDE. It is not known, however, whether this is the result of

- more careful preparation and welding in the first place, or
- the same standard of preparation and welding as for other areas, followed by effective NDE and subsequent repair, or
- a combination of these two factors.

(4) The defect rates for surface-breaking defects are typically only 10% of those for embedded defects, for welds of the same type produced using the same welding process, position and procedure.

(5) Defect rates depend significantly on the type of welded joint; and for the Hutton Lower Hull could be clearly ranked in order of decreasing defect rate as follows: cruciform and/or tee butt, plate butt and fillet welds. The defect rates for plate butt and fillet welds are typically only 10% of those for tee butt and cruciform welds.

(6) Defect rates depend significantly on the welding process used. In the analysis of the Hutton data, the automatic submerged arc welding process (SAW), used mainly for plate butt welds welded in the flat position, was found to give welds which were practically defect free. The manual shielded metal arc process

(SMAW) showed significant defect rates, particularly for tee butt and cruciform welds, but varying according to the other factors mentioned in (1) to (5) above. The gas metal arc process (GMAW) on average showed even higher defect rates than the SMAW process, typically 2–4 times as great. The GMAW process was also found to be associated with the occurrence of multiple defects.

(7) Significant differences in defect rate can occur between welds made in the flat, horizontal, vertical and overhead positions, but which are otherwise similar. Defect rates between the flat and overhead positions were typically found to differ by a factor of about five. However, in terms of multiple defects, welds made in the horizontal position, especially with the GMAW process, were most likely to be associated with multiple defects.

(8) Defect rates have also been shown to differ according to welding procedure, when other factors are the same. Welding procedures involving a large number of passes are likely to have a higher defect rate than welds made under the same conditions with a smaller number of passes. The same applies with multiply defective welds. However, this effect is much less significant than the other factors mentioned above.

(9) Clearly, defect rates also depend to a certain extent on the skills of individual welders, but no data were available to enable this effect to be quantified.

(10) Although some structural details may be somewhat more prone to weld defects than others, the analysis of the Hutton data showed that when the above have been taken into account, the defects were fairly evenly distributed between all the details that were examined.

Defect Sizes

(1) Lengths and depths for surface-breaking defects and lengths and widths for embedded defects were found to be only weakly correlated and for most practical purposes they can be considered to be independent variables.

(2) The lognormal and Weibull distributions were the main models which were fitted to the lengths, depths and aspect ratios for defects found by magnetic particle inspection and lengths, widths and aspect ratios for defects found by ultrasonic testing. The Kolmogorov-Smirnov goodness-of-fit test showed on average a better fit for the lognormal model. One of the reasons for the

relatively high KST values for the depth of surface-breaking defects and widths of embedded defects is the lumping of defect sizes into a number of discrete values (i.e. measurements rounded to the nearest mm). This is an unfortunate consequence of the measuring limitations.

(3) A number of strong conclusions were drawn from the analysis of the surface-breaking defect data in the following areas: the dependence of defect size on defect type, on the position of the defect in the welded joint and, in some joints, on the type of joint itself; the lack of dependence of defect size on the type of welding process used, except for defects occurring in the weld metal itself, and on the particular yard in which the welding was carried out; and the dependence of the orientation of planar defects to the surface on the type of welded joint. The depth of defects has been shown to be strongly dependent not only on the type of defect (CR, NF, LI) but also on the position of the defect in the welded joint. Defects classified as 'linear indications' were found to be consistently deeper than 'cracks' and non-fusion defects, but the actual depth depended on the position of the defect in the welded joint. Surface-breaking defects in the weld metal were found to be deeper on average than weld toe defects.

(4) For embedded defects, the defect width, length and aspect ratio were found to be strongly dependent on the various defect type categories. For example, slag inclusions defects were found to be the narrowest among all other defect types. The above dimensions however were found to be independent of defect location in the joint, overall node location, original welding procedure and fabricator.

(5) From the detailed results it was seen that, at least for the structure which has been studied, weld defects vary considerably in size, but more importantly the statistics which control the distribution of size (e.g. mean and standard deviation) are themselves dependent on other parameters such as defect type, type of welded joint etc. The fact that the structure was fabricated under conditions typical for large steel structures, especially ships, means that the results are likely to be of general validity. However, it should be stressed that, depending on the type of defect being considered, the probability of exceeding a defect size of, say z mm, may vary by several orders of magnitude.

(6) The results obtained are suitable for use in typical probabilistic fracture mechanics analyses of structures but generally, it will be necessary to model not only the distribution of defect size, but also the defect occurrence rate. As it was also shown, this latter quantity is also highly variable, depending on the

various welding parameters and the standards and extent of subsequent NDE and repair.

Reliability of Non-Destructive Evaluation

(1) Published data from several national and international programmes set up to determine the reliability of NDE procedures for the detection of weld defects have been reviewed. Functions currently used in industry to model the probability of non-detection have been critically examined and new generalised models have been proposed. The proposed models can be used to update the defect occurrence and defect size distributions obtained from raw data.

(2) The functions currently used for modelling detection efficiencies have been shown to be incorrectly fitted by the application of an ordinary least squares approach. This approach is incorrect because the basic observations are proportions for which the form of random variables is very likely to be binomial. The variance of such observations is not constant but varies with the mean. This gives rise to the problem of non-constant variance which can be tackled either by using weighted regression in which each value of the proportion is weighted in inverse proportion to its variance, or by using maximum likelihood estimation.

(3) Three new generalised models of sigmoidal shape have been proposed for modelling detection effeciencies which have the capability of accommodating a large number of variables such as defect length, defect depth, defect width, defect areas, plate thickness, recording level, etc. The three models are based on the binomial distribution and the methods of estimating the parameters are based on maximum likelihood estimation, for which the goodness-of-fit statistic (deviance) is completely determined. These models have been applied and compared with existing models currently in use, by using data derived from presssure vessel reliability programmes.

(4) Sizing errors using magnetic particle inspection have been assessed using data from surface-breaking fatigue cracks in tubular joints typical of offshore structures.

(5) The suitability of various probability distributions for modelling various defect parameters have been reviewed and compared. In particular, distributions for defect depth in surface-breaking defects in offshore structures were found to be very similar to the distributions found for other steel structures, mainly

pressurised water reactors.

(6) Various distribution functions for modelling variations of defect sizes have been reviewed on the basis of the criteria for choosing one particular function rather than another. Theoretical criteria for using the lognormal distribution for weld defects have been proposed. These are based on the law of proportionate effect and the way that certain defects are formed during the fabrication process.

Future Work

Several areas were found during the present work, where additional research is needed to confirm, improve or extend the applicability of the conclusions reached in the present analysis. These areas are briefly summarised below:

(1) Further data are required on defect sizes for both surface-breaking defects and embedded defects from additional sources in either the nuclear or offshore industry to confirm the generality of both defect size distributions and defect size correlations derived in the present work.

(2) The conclusions reached on the occurrence of defects in welds are based on a large non-destructive evaluation programme carried out on a single offshore structure and it is therefore unique. Similar programmes from large NDE exercises in other steel structures would be of great value in confirming the generality of the conclusions in the present analysis. In particular, additional information on the performance of NDE operators and individual welders is needed to evaluate their influence on the overall occurrence of defects. If such programmes are not available because of the high financial costs involved, the best plan for the future would be Bayesian updating using the results from the present study as Bayesian priors.

(3) The data on non-destructive examination for detection and sizing of defects are very few and vary from one detection programme to another. Further work in this area, especially on naturally occurring defects, is required to assess the reliability of the various non-destructive examination procedures. It is hoped that when the results from the recently devised PISC III project - on real defects and surroundings - become available, they will provide valuable input for the latter analysis.

(4) Bayesian reliability analysis coupled with fracture mechanics formulations is

needed for devising quality control schemes for future inspections. These analyses should be based on both the initial defect size and occurrence distributions which have been derived in the present analysis.

REFERENCES

[1] Central Electricity Generating Board, R/H/R6
'Assessment of the Integrity of Structures Containing Defects',
Revision 1 : 1977
Revision 2 : 1980
Revision 3 : 1985

[2] Thoft–Christensen, P. and Baker, M.J.
Structural Reliability Theory and Its Applications, Springer–Verlag, 1982

[3] Madsen, H.O., Krenk, S. and Lind, N.
Methods of Structural Safety, Prentice Hall, 1986.

[4] Wirshing, P.H.
'Fatigue Damage Assessment Models for Offshore Structures', Earthquake Behaviour and Safety of Oil Gas Storage Failures', PVP–Vol. 77, ASME, 1983.

[5] Manners, W.
Reliability Analysis of the Fatigue Resistance of Offshore Structures, Ph.D Thesis, Imperial College of Science and Technology, University of London, Sept. 1983.

[6] Karadeniz, H., Vrouwenvelder, A. and Bouma, A.C.
'Stochastic Fatigue Analysis of Jacket Type Offshore Structures', NATO ASI on Reliability Theory and Applications in Structural and Soil Mechanics, 1982, Martinus Nijhoff, 1983, pp. 613–642.

[7] Baker, M.J.
'Probabilistic Fracture Mechanics Analysis of Typical Lower Hull Welded Joints', April 1984, Appendix E, Final Conoco Engineering Review Team Report.

[8] Baker, M.J., Kountouris, I.S. and Etemad, M.R.
TLP Study, Assessment of Fabrication Defect Data, Report to Conoco (UK) Ltd., Volume B, Procedures for the Assessment of Weld Defects, Dept. of Civil Eng., Imperial College, 1987.

[9] Jessop, T.J.
'Non-Destructive Testing of Welded Joints', in Quality Assurance of Welded Construction, N.T. Burgess (Ed.), Applied Science Publishers, 1983, pp. 151-166.

[10] Krautkramer, J., Krautkramer, H., Grabendorfer, W. and Niklas, L.
Ultrasonic Testing of Materials, Springer Verlag, 1969.

[11] United Kingdom Atomic Energy Authority (UKAEA)
'An Assessment of the Integrity of PWR Pressure Vessels', Second Report of a Study Group Under the Chairmanship of Dr. W. Marshall, HMSO, 1982.

[12] Townend, P.H.
'Statistical Aspects of Fracture of Welded Defects in the Node Joints of Tubular Steel Offshore Structures', Ph.D. Thesis, University of Manchester, 1981.

[13] Hedden, O.F.
'On Developing New Rules for Ultrasonic Examination of Welds in Nuclear Vessels', in Periodic Inspection of Pressurised Components, Institution of Mechanical Engineers, 1974, pp. 7-11.

[14] Wustenberg, H. and Mundry, E.
'Limiting Influences on the Reliability of Ultrasonic In-Service Inspection Methods', in Periodic Inspection of Pressurised Components, Institution of Mechanical Engineers, 1974, pp. 108-113.

[15] Bush, S.J.
'The Impact of In-Service Inspection on the Reliability of Pressure Vessels and Piping', in Reliability Engineering in Pressure Vessels and Piping, The Second National Congress on Pressure Vessels and Piping, A.C. Gangadharan (Ed.), San Francisco, 1975, pp. 108-113.

[16] Silk, M.J.
'Developments in Ultrasonics for Sizing and Flaw Characterisation', in Developments in Pressure Vessel Technology, Inspection and Testing, Vol. 2, R.W. Nichols (Ed.), 1979, pp. 101-139.

[17] Mudge, P.J. and Williams, S.
'Statistical Aspects of Defect Sizing Using Ultrasonics', in Proc. Int. Conf. Non-Destructive Testing in the Fitness-For-Purpose Assessment of Welded Constructions, The Welding Institute, 1985, pp. 135-143.

[18] Rogerson, J.H.
'Welding Defects and their Elimination', in Developments in Pressure Vessel Technology, Materials and Fabrication, R.W. Nichols (Ed.), Vol. 3, 1979, pp. 237-355.

[19] Hanstock, R.F.
'Inspection', in Pressure Vessel Engineering Technology, R.W. Nichols (Ed.), 1971, pp. 351-401.

[20] Coffey, J.M. and Whittle, M.J.
'Developments in the Industrial Application of Ultrasonic Testing', in Developments in Pressure Vessel Technology, Inspection and Testing, Vol. 2, R.W. Nichols (Ed.), 1979, pp, 35-70.

[21] Murgatroyd, R.
'The Reliability of Defect Detection, Sizing and Occurrence Distributions', in Reliability Methods in Fatigue Fracture and NDT, The Welding Institute, 1987.

[22] British Standards Institution, BS 6513
'Magnetic Particle Flaw Detection, a Guide to the Principles and Practice of Applying Magnetic Particle Flaw Detection in Accordance with BS 6072 British Standards Institution, London, UK, 1985.

[23] Lumb, R.F. and Winship, P.
'Magnetic Particle Crack Detection, Parts 1 and 2', Metal Construction, Vol. 7, 1977, pp. 293-296 and 331-334.

[24] Groves, D. and Connel, D.
'Offshore Structure Fabrication Experience with Magnetic Particle Inspection', NDT International, Vol. 18, 1985, pp. 85-88.

[25] Baker, M.J., Kountouris, I.S. and Etemad, M.R.
TLP Study, Assessment of Fabrication Defect Data, Report to Conoco (UK) Ltd.,
Volume I , Statistical Tables Relating to Node 1

Volume II, Statistical Tables Relating to Node 2
Volume III, Statistical Tables Relating to Node 3
Volume IV, Statistical Tables Relating to Node 4
Volume V, Statistical Tables Relating to Node 5
Volume VI, Statistical Tables Relating to Node 6

[26] International Institute of Welding
'Classification of Welding Defects in Metallic Fusion Welds with Explanations', Welding in the World, Vol. 7, 1969, pp. 200–210.

[27] International Institute of Welding
'Parameter Characterising Defects in Metallic Fusion Welds', Welding in the World, Vol. 9, 1971, pp. 92–111.

[28] Rogerson, J.H.
'Defects in Welds – Their Prevention and Their Significance', in Quality Assurance of Welded Construction, N.T. Burgess (Ed.), Applied Science Publishers, 1983, pp. 115–133.

[29] Welding Handbook
Section 2, 6th Ed., Miami: American Welding Society, 1969.

[30] British Standards Institution, BS 639
Covered Electrodes for the Manual Metal–Arc Welding of Carbon and Carbon Manganese Steels, 1976.

[31] Cox, D.R.
The Analysis of Binary Data, Methuen, 1970.

[32] Armitage, P.
Statistical Methods in Medical Research, London, 1970.

[33] Cox, D.R. and Snell, E.J.
Applied Statistics, Chapman and Hall, London, 1981.

[34] General Linear Interactive Modelling (GLIM)
Manual Release 3, Numerical Algorithms Group, Royal Statistical Society, 1977.

[35] Statistical Software BMDP
University of California Press, Berkeley, 1983.

[36] Clayton, D.G.
'Some Odds-Ratio Statistics for the Analysis of Ordered Categorical Data', Biometrica, Vol. 61, 1974, pp. 525-531.

[37] McCullagh, P.
'Analysis of Ordered Categorical Data', Technical Report No. 62, Department of Statistics, University of Chicago, 1978.

[38] McCullagh, P.
'Regression Models for Ordinal Data', Journal of the Royal Statistical Society, Series B, Vol. 42, 1980, pp. 109-142.

[39] Maxwell, A.E.
Analysing Qualitative Data, Chapman and Hall, London 1961.

[40] Baker, M.J., Kountouris, I.S. and Etemad, M.R.
TLP Study, Assessment of Fabrication Defect Data, Report to Conoco (UK) Ltd., Volume A, Statistical Analysis of Hutton TLP Weld Defect Data, Dept. of Civil Eng., Imperial College, 1987.

[41] Davis, D.J.
'An Analysis of Some Failure Data', Journal of the American Statistical Association, Vol. 47, 1952, pp. 113-150.

[42] Johnson, N.L. and Kotz, S.
Distributions in Statistics, Continuous Univariate Distributions-1, John Wiley and Sons, 1970.

[43] Barlow, R.E. and Proshan, F.
Statistical Theory of Reliability and Life Testing, To Begin With, Silver - Spring, 1981.

[44] Feller, W.
An Introduction to Probability Theory and its Applications, 2nd Edition, John Wiley and Sons, 1965.

[45] Mann, N.R., Shafer, R.E. and Singpurwalla, N.D.
Methods for Statistical Analysis of Reliability and Life Data, John Wiley and Sons, 1974.

[46] Cox, D.R. and Smith, W.L.
Queues, John Wiley and Sons, 1961.

[47] Jackson, D.A.Y.
'Fitting a Gamma or Lognormal Distribution to Fibre-Diameter Measurements on Wool Tops', Applied Statistics, Vol. 18, 1969, pp. 70–75.

[48] Nilson, F.
'A Model for Fracture Mechanical Estimation of the Failure Probability of Reactor Pressure Vessels', in Third International Conference on Pressure Vessel Technology, Part 2, Materials and Fabrication, American Society of Mechanical Engineers, 1977, pp. 593–601.

[49] Kotz, S. and Newman, J.
'On the Distribution of Precipitation Amounts for Periods of Increasing Length, Journal of Geophysical Research, Vol. 68, 1963, pp. 3635–3640.

[50] Benjamin, J.R. and Cornell, C.A.
Probability, Statistics and Decision for Civil Engineers, McGraw-Hill Inc., 1970.

[51] Aitchison, J. and Brown, J.A.C.
The Lognormal Distribution, Cambridge University Press, 1957.

[52] Galton, F.
'The Geometric Mean in Vital and Social Statistics', Proceedings of the Royal Society of London, Vol. 29, 1879, pp. 365–367.

[53] Epstein, B.
'The Mathematical Description of Certain Breakage Mechanisms Leading to the Logarithmico-Normal Distribution', Journal of the Franklin Institute, Vol. 244, 1947, pp. 471–477.

[54] Kao, J.H.K.
'Statistical Model in Mechanical Reliability', Proceedings of the Eleventh National Symposium on Reliability and Quality Control, 1965, pp. 240–247.

[55] Nichols, R.W.
'Reheat Cracking in Welded Structures', Welding in the World, Vol. 7, 1969, pp. 244–261.

[56] Gurundy, P.M.
'The Expected Frequencies in a Sample of an Animal Population in which the Abundances of Species are Log-Normally Distributed, Part 1', Biometrica, Vol. 38, 1951, pp. 427-434.

[57] Williams, C.B.
'The Use of Logarithms in the Interpretation of Certain Entomological Problems', Annals of Applied Biology, Vol. 24, 1937, pp. 404-414.

[58] Williams, C.B.
'A Note on the Statistical Analysis of Sentence-Length as a Criterion of Literary Style', Biometrica, Vol. 31, 1941, pp. 356-361.

[59] Weibull, W.
'A Statistical Distribution Function of Wide Applicability', Journal of Applied Mechanics, Vol. 18, 1951, pp. 293-297.

[60] Kao, J.H.K.
'A Graphical Estimation of Mixed Weibull Parameters in Life-Testing of Electron Tubes', Technometrics, Vol. 1, 1959, pp. 389-407.

[61] Kao, J.H.K.
'A New Life-Quality Measure for Electron Tubes, Institute of Radio Engineers Transactions on Reliability and Quality Control, PGRQC-7, 1957, pp. 1-11.

[62] Lieblein, J. and Zelen, M.
'Statistical Investigation of the Fatigue Life of Deep-Groove Ball Bearings', Journal of Research of the National Bureau of Standards, Vol. 57, 1956, pp. 273-316.

[63] Kendal, M.J. and Stuart, A.
The Advanced Theory of Statistics, Vol. 2, Third Edition, Griffin, 1973.

[64] Cohen, C.A.
'Maximum Likelihood Estimation in the Weibull Distribution Based on Complete and Censored Samples', Technometrics, Vol. 7, 1965, pp. 579-588.

[65] Thoman, D.R., Bain, L.J. and Antle, C.E.
'Inferences on the Parameters of the Weibull Distribution', Technometrics, Vol. 11, 1969, pp. 445-460.

[66] Harter, H.L. and Moore, A.H.
'Point and Interval Estimators Based on the M–Orded Statistics for the Scale Parameter of a Weibull Distribution with Known Shape Parameter', Technometrics, Vol. 7, 1965, pp. 405–422.

[67] Wilks, S.S.
'Fiducial Distributions in Fiducial Inference', Ann. Math. Statistics, Vol. 9, 1938, pp. 272–280.

[68] Lindgren, B.W.
Statistical Theory, Macmillan Company, New York, 1962.

[69] Fisher, R.A. and Yates, F.
Statistical Tables for Biological, Agricultural and Medical Research, Fourth Edition, Oliver and Boyd, 1953.

[70] Fisher, R.A.
'Statistical Methods for Research Workers', Twelfth Edition, Oliver and Boyd, 1954.

[71] Rogerson, J.H. and Wong, W.K.
'Weld Defect Distributions in Offshore Structures and their Influence on Structural Reliability', 14th Offshore Technology Conference, Houston, USA. 1982, Paper OTC 4237.

[72] Rodrigues, P.E.L.B., Wong, W.K. and Rogerson, J.H.
'Weld Defect Distributions in Offshore Platforms and their Relevance to Reliability Studies, Quality Control and In–Service Inspection', 12th Offshore Technology Conference, Houston, USA, 1980, Paper OTC 3693.

[73] Nichols, R.W.
'The Uses of Welded Materials in Nuclear Power Engineering', Welding Journal, Vol. 54, 1975, Welding Research Supplement, pp. 417s–432s.

[74] Becher, P.E. and Pedersen, A.
'Applications of Statistical Linear Elastic Fracture Mechanics to Pressure Vessel Reliability Analysis', Nuclear Enginereing and Design, Vol. 27, 1974, pp. 413–425.

[75] Dvorac, H.R. and Schwegler, E.C.
'Statistical Distribution of Flaw Sizes', International Journal of Fracture Mechanics, Vol. 8, 1972, pp. 110–111.

[76] Bokalrud, T. and Karlsen, A.
'Probabilistic Fracture Mechanics Evaluation of Fatigue Failure from Weld Defects in Butt Welded Joints', in International Conference on Fitness for Purpose Validation of Welded Constructions, The Welding Institute, 1982, Paper 28.

[77] Harris, D.O.
'A Means of Assessing the Effects of NDE on the Reliability of Cyclically Loaded Structures', Materials Evaluation, Vol. 35, 1977, pp. 57–65.

[78] Tang, W.H.
'Probabilistic Updating of Flaw Information', Journal of Testing and Evaluation, Vol. 1, 1973, pp. 459–467.

[79] United Kingdom Atomic Energy Authority (UKAEA)
'An Assessment of the Integrity of PWR Pressure Vessels', Report of a Study Group Under the Chairmanship of Dr. W. Marshall, HMSO, London, 1976.

[80] Becher, P.E. and Hansen, B.
'Statistical Evaluation of Defects in Welds and Design Implications', Danish Welding Institute, 1974.

[81] Hansen, B.
'A Study of Inspection Systems for Welded Products, Part 2: The Occurrence of Defects in Welds', The Danish Welding Institute', 1978.

[82] Harris, D.O. and Lim. E.Y.
'Applications of a Probabilistic Fracture Mechanics Model to the Influence of In–Service Inspection on Structural Reliability', Probabilistic Fracture Mechanics and Fatigue Methods : Applications for Structural Design and Maintenance, ASTM STP 798, 1982, pp. 19–41.

[83] Kihara, H., Oba, H. and Susei, S.
'Precautions for Avoidance of Fracture of Pressure Vessels', Int. Conference on Practical Application of Fracture Mechanics to Pressure Vessel Technology, Inst. Mech. Eng., London, 1971, pp. 183–189.

[84] Dufresne et al
'PWR Rector Pressure Vessel Fracture Probabilities', in 4th International Conference in Pressure Vessel Technology, Institution of Mechanical Engineers,London, 1980, Paper C13/80.

[85] Cox, D.R. and Snell, E.J.
Applied Statistics Principles and Examples, Chapman and Hall, 1981.

[86] McCullagh, P. and Nelder, J.A.
Generalised Linear Models, Chapman and Hall, 1983.

[87] Murdoch, J. and Barnes, J.A.
'Statistical Tables for Science, Engineering, Management and Business Studies', Second Edition, MacMillan, 1974.

[88] Wetherill, G.B.
Elementary Statistical Methods, Methuen, 1969.

[89] Cox, D.R. and Snell, E.J.
'A General Definition of Residuals (with Discussion)', Journal of Royal Statistical Society, Series B, Vol. 30, 1968, pp. 248-275.

[90] Allen, D.J. and Blandford, P.J.
'Manufacture of Deliberate Welding Defects for NDT Research', in International Conference on Non-Destructive Testing in the Fitness-for-Purpose Assessment of Welded Constructions', the Welding Institute, 1985, pp. 153-157.

[91] Norriss, T.H.
'The Role of Non-Destructive Testing in Relation to Damage-Tolerant Aircraft Design', British Journal of NDT, Vol. 27, 1975, pp. 345-350.

[92] Crutzen, S., Jehenson, P., Nichols, R. and Stephens, M.
'The PISC 2 Project : Initial Conclusions Regarding the Procedures used in the Round-Robin Tests', NDT International, Vol. 18, 1985, pp. 243-249.

[93] Thomas, E.F. and Kloster, W.E.
'Can You Trust Your NDT?', Tooling and Production, Vol. 39, 1973, pp. 37-40.

[94] O'Neill, R. and Jordan, G.M.
'Safety and Reliability Requirements for Periodic Inspection of Pressure Vessels in the Nuclear Industry', in Conference on Periodic Inspection of Pressure Vessels, Institution of Mechanicsl Engineers, 1972, pp. 140–146.

[95] Rummel, W.D., Todd, P.H., Rathke, R.H. and Castner, W.L.
'The Detection of Fatigue Cracks by Non–Destructive Test Methods', Materials Evaluation, Vol. 32, 1974, pp. 205–212.

[96] Altio, M.A. and Kauppinen, K.P.
'Reliability and Defect Sizing', in Conference on Periodic Inspection of Pressurised Components, Institution of Mechanical Engineers, London, 1982, pp. 283–294.

[97] Forsten, J. and Aaltio, M.
'On the Detection of Weld Defects by X–Ray and Ultrasonic Examination', British Journal of NDT, Vol. 24, 1982, pp. 33–36.

[98] Packman, P.F., Malpani, J.K., Wells, F. and Yee, B.W.E.
'Reliability of Defect Detection in Welded Structures', in Reliability Engineering in Pressure Vessels and Piping, Second National Congress on Pressure Vessels and Piping, Gangadharan, A.C. (Ed.), California, 1975, pp. 15–28.

[99] Packman, P.F., Klima, S.J., Davies, R.L., Maplpani, J., Moyzis, J., Walker, W., Yee, B.G.W. and Johnson, D.P.
'Reliability of Flaw Detection by Non–Destrictive Inspection', Metals Handbook, Vol. 11, 1975, pp. 414–424.

[100] Marriot, D.L. and Hudson, J.M.
'Prediction of Failure Risk in A Pressure Vessel Due to a Manufacturing Defect', in Reliability Problems of Reactor Pressure Components, Proceedings of a Symposium, Vienna, Vol. 2, 1977, pp. 95–115.

[101] Plate Inspection Steering Committee (PISC I)
'Euratom Report EUR 6371 EN', Vol. 6, 1979.

[102] Pressure Vessel Research Committee (PVRC)'Non–Destructive Examination of PVRC Weld Specimen 201', Welding Research Supplement, 1971, pp. 529s–538s.

[103] Harris, D.O. and Lim, E.Y.
'Applications of a Fracture Mechanics Model of Structural Reliability to the Effects of Seismic Events on Reactor Piping', Progress in Nuclear Energy, Vol. 10, 1982, --.125-159.

[104] Dufresne, J.
'Probabilistic Applications of Fracture Mechanics, in Proceedings of the Fifth International Conference on Fracture, Cannes, 1981, pp. 517-532.

[105] Temple, J.A.G.
'The Reliability of Non-Destructive Detection and Sizing', Paper presented in the Conference of Periodic Inspection of Pressurised Components, Institution of Mechanical Engineers, London, 1982.

[106] Berens, A.P. and Hovey, P.W.
'Statistical Methods for Estimating Crack Detection Probabilities', in Probabilistic Fracture Mechanics and Fatigue Methods : Applications for Structural Design and Maintenance, Bloom, J.M. and Akvall, J.C. (Eds.), ASTM STP 798, 1983, pp. 79-94.

[107] Woo, H.H. and Simonen, F.A.
'The Impact of In-Service Inspection on the Reliability of Nuclear Piping', in Advances in Probabilistic Fracture Mechanics, Sundararajan, C., PVP, Vol. 92, 1984, pp. 153-176.

[108] Forli, O. and Pettersen, B.
'The Performance of Conventional Ultrasonic and Radiographic Weld Examination', British Journal of NDT, Vol. 27, 1975, pp. 364-366.

[109] Forli, O. and Pettersen, B.
'The Performance of Conventional Ultrasonic and Radiographic Weld Examination'. British Journal of NDT, Vol. 27, 1985, pp. 364-366.

[110] Plate Inspection Steering Committee (PISC II)
'Evaluation of the PISC II Trials Results, PISC 2 Report No. 5 - September 1986.

[111] ASME Section XI
'Rules for In-Service Inspection of Nuclear Plant', ASME Boiler and Pressure Vessel Code Section.

[112] British Standard, BS 3923
'Methods for Ultrasonic Examination of Welds', Part 1, Manual Examination of Fusion Welds in Ferritic Steels, British Standards Institution, London, 1978.

[113] Burdekin, F.M. and Townend, P.H.
'Reliability Aspects of Fracture on Stress Concentration Regions in Offshore Structures', in Second International Symposium Integrity of Offshore Structures, D. Faulkner, M.J. Cowling, and P.A. Frieze (Eds.), 1981, pp. 269-286.

[114] Jessop, T.J. and Mudge, P.J.
'Size Measurement and Characterisation of Weld Defects by Ultrasonic Testing', Part 1 : Non-planar Defects in Ferritic Steels, Welding Institute, 1979.

[115] Jessop, T.J. and Mudge, P.J.
'Size Measurement and Characterisation of Weld Defects by Ultrasonic Testing', Part 2 : Planar Defects in Ferritic Steels, Welding Institute, 1982.

[116] Mudge, P.J.
'Size Measurement and Characterisation of Weld Defects by Ultrasonic Testing', Part 3 : The Effect of Metallurgical Features in Ferritic Steels, Welding Institute, 1982.

[117] Mudge, P.J. and Williams, S.
'Performance of Ultrasonic Non-Destructive Methods for Defect Assessment in Relation to Fracture Mechanics Requirements', in International Conference on Fitness-for-Purpose Validation of Welded Constructions, The Welding Institute, 1982, Paper 44.

[118] Watkins, B., Cowburn, K.J., Ervine, R.W. and Latham, F.G.
'Results Obtained from the Inspection of Test Plates 1 and 2 of the Defects Detection Trials', British Journal of NDT, Vol. 25, 1983, pp. 186-192.

[119] Bowker, K.J., Coffey, J.M., Hanstock, D.J., Owen, R.C. and Wrigley, J.M.
'CEGB Inspection of Plates 1 and 2 in UKAEA Defect Detection Trials'. British Journal of NDT, Voil. 25, 1983, pp. 186-192.

[120] Watkins, B., Lock, D., Cowburn, K.J. and Ervine, R.W.
'The UKAEA Defect Detection Trials on Test Pieces 3 and 4', British Journal of NDT, Vol. 26, 1984, pp. 97–105.

[121] Kato, B., Morita, K. and Furuzawa, H.
'Estimatkon of Weld Defects Through Ultrasonic Testing', Welding Journal, Vol. 55, 1976, pp. 946–953.

[122] Department of Energy
'Study of Calibration Procedures for Accurately Quantifying Crack Sizes in Welded Tubular Joints', Offshore Technology Report, OTH 87 263, University College London, 1987.